WADC TECHNICAL REPORT 58-264
ASTIA DOCUMENT NO. 155-596

THE BEHAVIOR OF FUELS AND LUBRICANTS IN DYNAMIC TEST EQUIPMENT OPERATING IN THE PRESENCE OF GAMMA RADIATION

M. Z. EAINMAN
M. E. KRASNOW
E. D. KAUFMAN
O. P. REYNOLDS
R. L. THISTLETHWAITE
O. C. WOLFORD

COOK ELECTRIC COMPANY
INLAND TESTING LABORATORIES DIVISION

31 MARCH 1958

PROPULSION LABORATORY
CONTRACT NO. AF 33(616)-3865
PROJECT NO. 3115
TASK NO. 30385

WRIGHT AIR DEVELOPMENT CENTER
AIR RESEARCH AND DEVELOPMENT COMMAND
UNITED STATES AIR FORCE
WRIGHT-PATTERSON AIR FORCE BASE, OHIO

McGregor & Werner Midwest Corp., Dayton, O.
13-338-300-1-5-59

FOREWORD

This report was prepared by Cook Electric Company, Inland Testing Laboratories Division, Morton Grove, Illinois, on Air Force Contract No. AF 33(616)-3865. This contract was initiated under Project no. 3115 - "(U) Chemical Propulsion Subsystems," Tasks Nos. 30385 - "Lubricants for Propulsion Subsystems 125A" and 3086 - "Fuels for Propulsion Subsystems 125A". The work was administered under the direction of the Propulsion Laboratory, Directorate of Laboratories, Wright Air Development Center, Wright-Patterson Air Force Base, Ohio. For the period of this report, Lt. J. H. Way and then Lt. J. T. Edwards were project engineers. Lt. E. N. Cart, WCLPF-2 is the present project engineer.

This report includes work from the inception of the program on 1 October 1956 to the period ending 31 March 1958.

We wish to acknowledge the help and cooperation of L. S. Ackermann, R. N. Cooper, E. P. Dallafior, D. M. Hattori, E. G. Kreppert, N. F. Offenberg, C. A. Rogalski, M. A. Schmutzer, and R. E. Simpson of the Inland Testing Laboratories; of C. R. Memhardt, E. R. Rathbun, and E. T. Stepke of the Cook Research Laboratories; and of L. W. Haaker of Nucledyne Corporation who was in charge of the design and construction of the radiation facility.

ABSTRACT

This report summarizes work conducted on a program designed to evaluate fuels, hydraulic fluids, and lubricants for use in a nuclear-powered aircraft. During the performance period ending March 1958, 79 fuels and 41 lubricants were investigated. Results obtained clearly indicate that it is necessary to assess the effects of mechanical, thermal, and radiation stresses simultaneously. It has been observed that mechanical tests in a radiation environment often affect materials more drastically and at lower doses of radiation than the same tests conducted with statically irradiated samples without attendant radiation. Relative ratings of ten of the most promising fuels and six lubricants with the best performance characteristics are given. These ratings are based on performance in dynamic test machinery operated in a radiation environment.

FUELS

Fuel properties show little change with static radiation up to doses of 10^8 ergs/gram carbon. However, with doses beyond 10^9 ergs/gram carbon changes in some parameters such as flash point, initial boiling point, gum, and viscosity at -30°F become evident. Individual fuels behave differently, but at higher doses the flash point, initial boiling point, and viscosity at -30°F will usually decrease, while the gum content will increase.

Relative performance of fuels under normal conditions and in a radiation environment were determined with the CFR Fuel Coker. Many fuels were also preirradiated and tested in a conventional environment. This preirradiation and subsequent mechanical evaluation often indicated an improvement or no change in the relative fuel rating. The same evaluation conducted in a radiation environment indicated a decrease in goodness rating or a rapid failure. For some fuels, these failures in the CFR Fuel Coker in a radiation environment have been associated with observed precipitate formation during or after static irradiation. Comparison of the results of mechanical evaluation with specification tests at various dose levels indicate that determining the effect of radiation alone on fuel properties is not sufficient to predict future performance. Additional work to obtain better correlation is suggested.

Ten fuels were selected from those available which will probably perform well in conjunction with an airborne reactor. These fuels with pertinent performance data are given as follows.

RELATIVE RATING OF FUELS BASED ON RADIATION STABILITY IN THE CFR FUEL COKER

Relative Rating in Fuel Type	Fuel Designation ANPF No.	Fuel Type	Test Temperature °F	ΔP, inches Hg at 300 min.		Maximum Preheater Deposits CRC Code	
				No Radiation	10^8 ergs/gmC (approximate)	No Radiation	10^8 ergs/gmC (approximate)
1*	57-95	JP-4	300/400	0.08	0.15	0	1
2	57-112	JP-4	300/400	0.0	4.60	0	1
1**	57-120	JP-5	400/500	0.0	0.0	1	2
2	57-107	JP-5	400/500	0.0	0.0	1	2
3	57-51	JP-5	400/500	0.9	0.0	1	2
4	57-105	JP-5	400/500	0.2	0.0	0	2
5	57-56	JP-5	400/500	0.1	0.0	2	2
6	57-102	JP-5	400/500	0.6	0.15	1	0
7	57-57	JP-5	400/500	11.15	0.6	2	0
1***	57-96	Thermally Stable	400/500	0.15	9.4	0	2

* Specification test data included in Tables IV and V
** Specification test data included in Tables VI and VII
*** Specification test data included in Tables VIII and IX

Relative behavior was assessed at 10^8 ergs/gram carbon since this represents the average accumulated dose obtained without extensive preirradiation of the fuel samples. Additional tests with preirradiation indicate that these fuels should perform satisfactorily up to doses of 10^{10} ergs/gram carbon.

LUBRICANTS

Lubricants show no significant changes in physical properties upon static radiation until a dose of about 10^9 ergs/gram carbon is reached. When this gamma dose is exceeded, the flash point and viscosity will generally decrease, while the neutralization number, the tendency toward metal corrosion, and the deposit forming tendency will usually increase.

Lubricants were mechanically evaluated with the Model C Panel Coker and the WADC Deposition Tester, both with and without the presence of gamma radiation. Results of preirradiation and subsequent mechanical evaluation generally indicated less coke and sludge formation than observed with comparable runs in a radiation environment. Specification tests at various gamma doses indicate a possible correlation with mechanical evaluation results, however, considerable work will be necessary to establish this. The mechanical evaluation in a radiation environment revealed no general behavior trend: however, individual lubricants yield definite repeatable behavior patterns when test data are examined. With additional work, it may be possible to predict engine performance from specification and mechanical test data.

Six lubricants were selected which performed well in a radiation environment. Their performance data are listed on the following page. Relative performance is at a radiation dose of 10^8 ergs/gram carbon, since that is the dose on the WADC Deposition Tester without preirradiation. Additional tests on preirradiated lubricant samples indicate these materials should be satisfactory at doses approaching 10^{10} ergs/gram carbon.

PUBLICATION REVIEW

This report has been reviewed and is approved.

FOR THE COMMANDER:

Webster W. Round Lt. Col. USAF
for

JOSEPH M. SILK
Colonel, USAF
Chief Propulsion Laboratory

RELATIVE RATING OF LUBRICATING OILS

Relative Rating	Designation ANP No.	Oil Type	Unirradiated Results: Panel Coker 600°F	Unirradiated Results: Panel Coker 700°F	Unirradiated Results: Deposition Test	Radiated Results (approx. 10^8 ergs/gmC): Panel Coker 600°F	Radiated Results (approx. 10^8 ergs/gmC): Panel Coker 700°F	Radiated Results (approx. 10^8 ergs/gmC): Deposition Test
1*	80	Ester	10.7	22.6	3.61	4.3	28.3	1.31
2*	79	Ester	15.7	55.6	1.69	15.1	221.2	1.86
3*	78	Ester	16.7	22.6	0.80	22.6	28.3	2.54
4**	70	Poly-glycol	-	37.5	2.20	-	126.2	2.63
5*	76	Ester	46.7	39.8	4.74	30.0	67.2****	3.24
6***	61	Olefin Poly-mer (Poly Butene)	2.7	-	2.55	87.7	-	4.47

* Specification test data included in Table XI and XII

** Specification test data included in Table XIII

*** Specification test data included in Table XI

**** Approximately 10^9 ergs/gmC

TABLE OF CONTENTS

TABLE OF CONTENTS (cont'd)

LIST OF ILLUSTRATIONS

LIST OF ILLUSTRATIONS (cont'd)

LIST OF ILLUSTRATIONS (cont'd)

LIST OF TABLES

LIST OF TABLES (cont'd)

LIST OF TABLES (cont'd)

LIST OF TABLES (cont'd)

SECTION I

INTRODUCTION

The increasing use of nuclear reactors as mobile power sources presents many new and challenging problems. Foremost among these problems is radiation-induced damage to organic materials. This damage may be minimized with adequate shielding. However, the high cost of this shielding, together with attendant weight penalties, requires the development of materials which perform well in a radiation environment.

Reactors, both stationary and mobile, require hydraulic fluids and lubricants which are not adversely affected by radiation. In addition, nuclear-powered aircraft will require support fuels. Programs to develop these materials supplement each other by supplying information needed for the design of nuclear-powered equipment from the submarine below the sea to the satellite in space.

In particular, the Air Force has requirements for fuels and lubricants that must operate in the combined environments of radiation and high temperature.[24] As a consequence, these substances must be considered as engineering materials since they influence the design of the components and machinery in which they are to function. This, in turn, means that engineering data for these materials in a radiation environment must be obtained for presently available specimens and also for new samples as they are developed.

Considerable data already exist on the behavior of organic materials applicable for use in a nuclear-powered aircraft.[14] A number of materials have been statically irradiated and then evaluated in bench tests and in rigs.[19, 20, 22] Preliminary experiments with dynamic equipment operating in a radiation environment point out limitations in predicting service life from the behavior of materials with static irradiation.[11, 12, 21] It is thus becoming more apparent that there is a need for a detailed and systematic study of fuel and lubricant behavior in machinery operating in a radiation field. The following paragraphs outline the procedures used in

---

Manuscript released by the author September 1958 for publication as a WADC Technical Report.

this program to conduct a study aimed at choosing materials suitable for use in a radiation environment.

Gamma radiation provided by Cobalt 60 was chosen to simulate that of a reactor. The energy peaks of 1.17 and 1.33 Mev are representative of a nuclear reactor output and are among the most difficult to shield in practice. In addition, there seems to be little difference in the effect produced by various kinds of radiation.(8) Fifty thousand curies of Cobalt 60 were used to provide an intense, high energy radiation source which promotes damage to organic materials without the attendant hazards of residual radioactivity.

The mechanical test machines chosen for this study are those which have been useful in predicting the performance of fuels and lubricants. Although some modifications were necessary to obtain maximum and uniform radiation exposure and also to permit remote handling, such changes were kept to a minimum to maintain correlations with machines in other laboratories. Duplicate machinery was used, one in the laboratory and the other in the radiation environment. In this way, the effects of radiation were assessed separately.

Fuels and lubricants submitted by Wright Air Development Center were evaluated according to the appropriate specification tests listed in Table I. If the fuels or lubricants were found satisfactory after specification tests, they were tested in the applicable mechanical equipment, Table II. Where performance was adequate in the laboratory, they were run in the duplicate rig in the radiation cell. Bench tests were used to evaluate radiation-induced damage in the materials, both with static irradiation alone, and also after dynamic tests performed with and without radiation.

To date, the program has shown that static irradiation causes changes in some properties at doses as low as 10^8 ergs/gm carbon, but gross changes in many materials occur only above 10^{10} ergs/gm carbon. Further, it is shown that mechanical tests used in this study can evaluate gross differences in performance between different fuels and different lubricants, as well as ascertain the effects of additives. Preirradiation of the materials under investigation affect behavior in the test machines, either improving or impairing performance. Mechanical evaluation in a radiation environment shows greater interactions than tests using the environments separately. With a test such as the CFR Fuel Coker, trends are actually altered from those obtained by preirradiation and subsequent mechanical evaluation.

The evaluation of fuels and lubricants in dynamic test machinery operated in a radiation environment has shown that many materials will

TABLE I

SPECIFICATIONS FOR FUELS, HYDRAULIC FLUIDS AND LUBRICANTS

Specification	Title
MIL-F-5624C	Fuels, Aircraft Turbine and Jet Engine Grades JP-3, JP-4, JP-5
MIL-F-25656	Grade JP-6 Turbojet Fuel
MIL-F-25558	Ramjet Fuel
MIL-F-25576	Rocket Fuel RP-1
MIL-G-3278	Greases: Aircraft and Instruments (For Low and High Temperature)
MIL-G-25013A	Grease, Ball and Roller Bearing, Extreme High Temperature
MIL-H-8446	Hydraulic Fluid, Nonpetroleum Base, Aircraft
MIL-O-6081B	Oil, Lubricating, Jet Engine
MIL-L-6082B	Lubricating Oil, Aircraft Reciprocating Engine
MIL-L-7808C	Lubricating Oil, Aircraft Turbine Engine Synthetic Base
MIL-L-9236A	Lubricating Oil, Aircraft Turbine Engine, High Temperature
MIL-L-25336	Lubricating Oil, Aircraft Turbine Engine, High Film Strength, Synthetic Base
MIL-H-5606A	Hydraulic Fluid, Petroleum Base, Aircraft and Ordnance

TABLE II

DYNAMIC TEST EQUIPMENT

Machine	Purpose of Test	Design Modifications
Erdco Universal Tester	To evaluate performance of fluid lubricants in gears or in bearings.	The front bearing and metal from the housing was removed. The seals were replaced with graphite and with metal bellows. Lead shielding was added behind the test head to reduce radiation damage to supporting equipment.
CRC Grease Tester	To evaluate the performance of a grease in a bearing at high speed and at high temperature.	Metal removed from around the test bearing, cover reduced in length, and all openings moved to pulley end. Belt tension device revised. Mounted on portable stand and controlled remotely.
CFR Fuel Coker	To evaluate deposit forming tendency of fuels.	The preheater-filter section and manometer mounted on a portable rack. Remainder outside the cell for remote control.
WADC Deposition Tester	To evaluate stability, corrosivity, and sludging tendency of oil.	The complete oil test loop is mounted on a portable rack in the test cell. The teflon seals are replaced with silicone seals. Instrumentation is outside the cell for remote control.
Model C Panel Coker	To evaluate coking tendency of fluid lubricants.	The motor is shielded with lead against radiation damage. The operation is controlled remotely outside the cell.

perform satisfactorily. In some instances there are actually benefits that can be ascribed to radiation. The reasons for fuel or lubricant failure in the test machines are often discernible, and a systematic evaluation of both satisfactory and unsatisfactory samples in a combined mechanical and radiation environment should point out the requirements for good performance in each type of test machine. This eventually should lead to the modification of bench tests which are able to better predict radiation damage.

Following is the detailed account of the entire program with test procedures, results, and evaluation.

SECTION II

EXPERIMENTAL FACILITIES AND PROCEDURE

A. Facilities

The investigation of the behavior of fuels and lubricants in a radiation environment was conducted in a modern facility specifically designed and constructed for this purpose. This modern chemistry and petroleum laboratory (Appendix I), staffed and equipped to perform the tests required by the specifications listed in Table I, is illustrated in Figure 1.

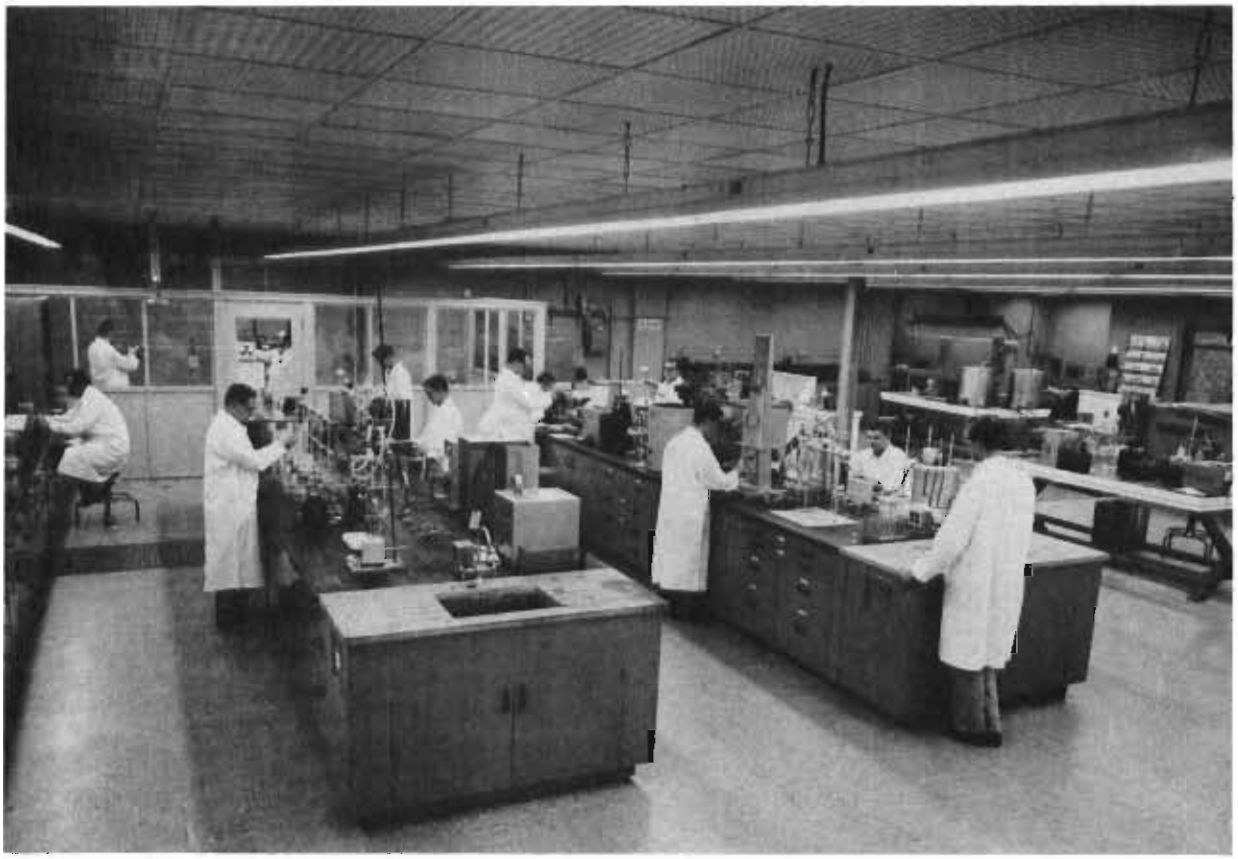

Figure 1. Interior of the Chemistry and Petroleum Laboratory

The radiation facility containing the 50,145 curie Cobalt 60 source consists of two structures, an inner structure housing the hot cell and an outer structure containing a laboratory and service area (Appendix II). An

aerial view of the building, Figure 2, shows the radiation facility and laboratory in the small building in the foreground. The chemistry and petroleum laboratory is located in the large building adjacent to it. The actual cell is shown in Figure 3.

B. Laboratory Evaluation

The laboratory evaluations of fuels and lubricants were conducted in accordance with appropriate specifications. The applicable test methods are listed in Appendix III, together with the appropriate references or descriptions of the test methods.

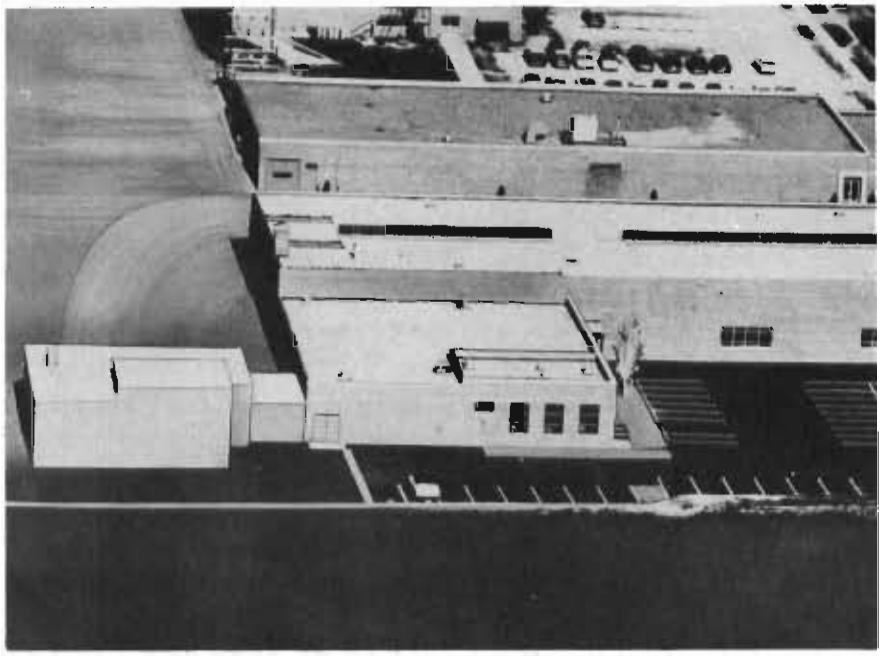

Figure 2. Aerial View of Laboratory and Radiation Facility

C. Mechanical Evaluation

The mechanical test systems used in the evaluation of fuels and lubricants were: (1) the CFR Fuel Coker; (2) the WADC Deposition Tester; (3) the Model C Panel Coker; (4) the WADC High Temperature Bearing Tester; and (5) the CRC Grease Tester. Two of each of the above machines were used (see Appendix IV).

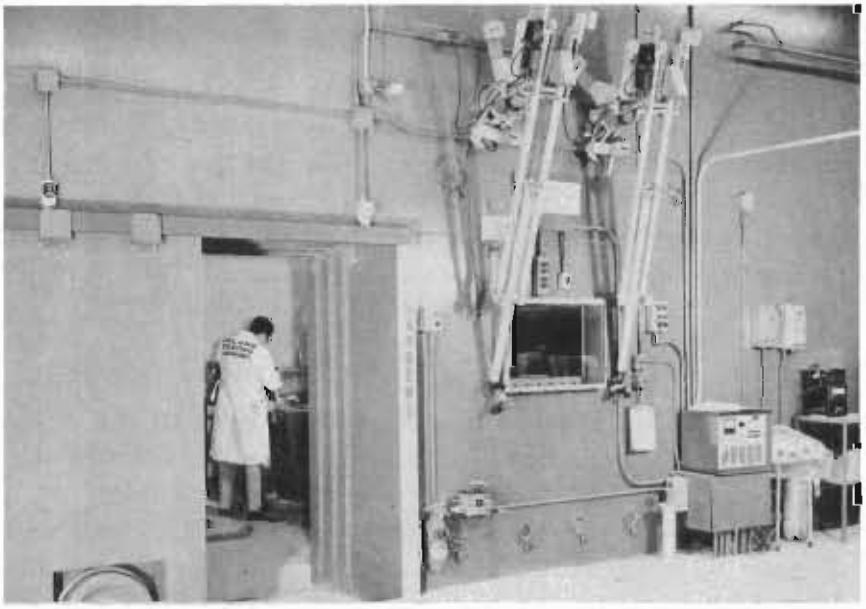

Figure 3. Radiation Cell

Wherever possible, the modifications of test systems were kept to a minimum as governed by the desired radiation levels and the need to maintain correlation with other investigators. Where the test section was altered, as in the WADC High Temperature Bearing Tester, both machines were modified. The basic modifications in each of the mechanical systems will be discussed.

The CFR Fuel Coker test section was not modified. It was necessary, however, to alter the flow pattern in the Coker by positioning the flow sensing equipment after the test section, rather than in its conventional location before the test section. Test results were obtained by the procedure described in FTMS 791, Method No. 3464T.

The WADC Deposition Tester was modified by mounting the air saturator on the test section rack. The heat exchanger was mounted horizontally to reduce the over-all height of the test section. The lengths of connecting tubing were kept as nearly standard as possible. It was further necessary to replace the teflon gaskets in the test section with more radiation resistant silicone rubber gaskets (Appendix IV-C). The Deposition Tester was operated according to the procedure described in the "Detailed Handbook."[28]

The only modification made in the Model "C" Panel Coker was to increase the reservoir capacity to one liter. This was necessary due to the high rate of consumption of many lubricants. The test procedure outlined in the "Detailed Handbook"[28] was used in obtaining the "Coking Tendency" data for lubricants.

The WADC High Temperature Bearing Tester was modified by reducing metal components around, and in front of, the test bearing. Minor modifications were also made in the plumbing arrangement of the drive and support sections. One entire assembly was placed permanently in the radiation cell. The Bearing Tester was operated in accordance with the procedure outlined in the WADC High Temperature Bearing Test Cooperative Program Number Two.

The CRC Grease Tester was modified by mounting the motor, cradle, and spindle on a steel plate, rather than in the conventional "over and under" arrangement. Excess metal was removed from the volume surrounding the test bearing, and the oven size was decreased. The latter modifications were necessary to minimize radiation shielding and scattering. The Grease Tester was operated according to the procedure described in FTMS 791, Method No. 333T.

D. Dosimetry

The investigation of fuels and lubricants in a radiation environment required the performance of accurate dosimetry measurements. Dosimetry involves the measurement of radiant energy emitted by a source as well as the calculation of the radiation energy absorbed by a medium. The radiation emitted by the decay of Cobalt 60 consists of an 0.3 Mev beta particle followed by two gamma photons of energy 1.33 Mev and 1.17 Mev in cascade. The basic dosimetry instrument for the Inland Testing Laboratories Cobalt 60 facility is an Oak Ridge type graphite CO_2 ionization chamber, modified specifically for the energy range of Cobalt 60 gamma and designed to obey Bragg-Gray principles as discussed in Appendix V-A.

All dosimetry measurements were based on absorbed energy in terms of ergs per gram carbon. The roentgen is equivalent to 87.1 ergs per gram carbon.

Before measurements could be made on the modified ionization chamber, it was necessary to know the photon energy limitation, operational characteristics, and the calibration constant for the chamber. The range of photon energies, with respect to the absorbed energy of graphite corresponding to one roentgen, was found to be essentially equivalent to that for air over an energy range of 0.1 to 2.0 Mev (Appendix V-B). This is well within the energy range of Cobalt 60 gammas. The chamber operational characteristics were determined by theoretical calculations and were verified by experimental studies. It was demonstrated that the chamber approaches the ideal saturation current within 99.8 percent (Appendix V-C). The chamber constant (i.e., the expression of gamma dose rate in terms of ionization current equivalent to 1 R/hr) was obtained by theoretical calculations and confirmed by calibration with a standard kilocurie Cobalt 60 source. The measured ionization current from the standard source agrees within 5.7 percent with the calculated values (Appendix V-D).

Ferrous-ferric chemical dosimetry methods were selected to supplement the ionization chamber after several methods of chemical dosimetry were studied (Appendix V-E). The comparison between the ionization chamber values and the ferrous-ferric dosimetry values is given in Table III and shows the close agreement of the methods.

The effect of the shielding material on albedo and background within the cell was studied (Appendix VI-B). The shielding was found to be effective in reducing normal background activity by a factor of two.

TABLE III

COMPARISON OF DOSE RATE

Iron and Ion Chamber

Dosimeter	Dose Rate (ergs/gm carbon/hr) x 10^{-3}					
Ionization Chamber	2.09	1.50	1.46	1.44	1.31	0.45
Iron Dosimeter	2.10	1.55	1.45	1.41	1.39	0.44

The design and configuration of the source container entailed an extensive study to determine the optimum configuration based on the geometry of the source elements (Appendix VI-B). To obtain a large area for placement of equipment and the maximum uniform dose, the configuration chosen was a hollow cylinder of three source element slugs thick, 25.0 inches outside diameter, 20.50 inches inside diameter, and a height of 14.75 inches.

The element slugs were assayed at the time of loading the source container. The total activity was found to be 50,145 curies (Appendix VI-C).

Isodose maps of the cell were made for reference purposes (Figure 4 and Appendix VI-D). The placement of heavy test machinery in the cell altered the isodose lines so that dose rate values of the empty cell are valid only within 1 foot from the outside of the source. The greatest dose rate is 9.6×10^7 ergs per gram carbon at a point 2 inches from the inside wall of the source cylinder at the midplane. An aluminum platform insert was designed for use in the center of the source to utilize this high dose rate for static irradiation of materials.

The dose rates on the dynamic test equipment was determined using both the graphite ionization chamber and the ferric-ferrous method. The details of the measurements are discussed in Appendix VI-E.

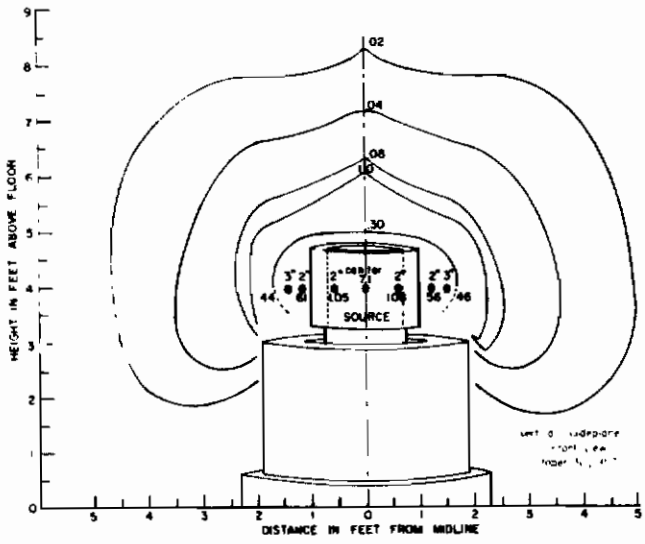

Figure 4. Isodose Plot of Cobalt 60 Source, Megaroentgens/Hour

SECTION III

EXPERIMENTAL RESULTS

The previous section has discussed the facility, apparatus, and procedures used to obtain the experimental results of the program. This section summarizes the results obtained during the performance period for:

(1) Fuels

(2) Lubricants

(3) Greases

Each of these material classes is discussed in the following way. The specification tests describing the physical properties are listed first. Following this are found the results of the mechanical evaluation tests on the fuel, lubricant, etc. The summary of the mechanical evaluation tests contains both the result of screening tests (run in a nonradiation environment) and, also, the results of dynamic tests run in a radiation environment.

A. Fuels

The experimental results are for fuels tested according to the following specifications:

MIL-F-5624C (Grade JP-4)

MIL-F-5624C (Grade JP-5)

MIL-F-25656 (Grade JP-6)

MIL-F-25558A (Grade RJ-1)

MIL-F-25576A (Grade RP-1)

MIL-F-25524A (Thermally Stable Fuels)

Miscellaneous Fuels

The results of mechanical evaluation tests in the CFR Fuel Coker follow the specification test data, with the exception of the miscellaneous

fuels which were not subjected to any mechanical evaluation tests. Data on fuels are summarized in Tables IV through X inclusive.

Under the heading "Fuel Sample" in Tables V, VII, and IX are the terms Base, Static, and Dynamic. These refer respectively to the fluid as received, the fuel taken from the reservoir at the end of the run, and the fuel taken from the discharge at different times.

To interpret the fuel data, an evaluation of repeatability was made. The data for the fuel designated ANPF 57-2 may be used as an indication of the repeatability of the goodness ratings obtained with the CFR Fuel Coker. A series of determinations gave results ranging from 532 to 775, with an average deviation of ± 89. The maximum deviation from the mean was 25 percent and the average deviation was 15 percent.

B. Lubricants

The experimental results for lubricants were obtained by using the procedures given in the following specifications:

MIL-L-7808C

MIL-L-9236A

MIL-O-6081B

MIL-L-6082B

The large number of lubricants submitted and the lack of time to evaluate all of them necessitated the establishment of an order of priority for testing. The first two groups of lubricants, MIL-L-7808C and MIL-L-9236A, were considered to have the highest priority, and, as a result, mechanical evaluation tests on MIL-O-6081B and MIL-L-6082B type lubricants were not undertaken. The mechanical evaluation tests for lubricants consist of Model "C" Panel Coker tests and WADC Deposition tests. The Panel Coker tests on specific lubricants, besides providing engineering data, served as screening tests for both the Deposition and Bearing Tester. Results of Model C Panel Coker tests are presented following the specification test data. This is followed by tables giving the results on the WADC Deposition Tester. Data on lubricants are summarized in Tables XI through XVII inclusive.

Under the heading "Lubricant Sample" in Tables XIV and XV are the terms Base, Static, and Dynamic. These refer respectively to the lubricant

TABLE IV

PHYSICAL PROPERTIES OF FUELS ACCORDING TO MIL-F-5624C, GRADE JP-4

Fuel Designation	Gamma Dose, ergs/gm Carbon	Distillation Temperature, °F at: Initial B.P.	10% Evap.	20% Evap.	50% Evap.	90% Evap.	End Point	Evap. at 400°F, %	Residue, Vol. %	Distillation Loss, %	Gravity, °API	Gum, mg/100ml Existent	Potential	Sulfur, % Total	Mercaptan	Reid Vapor Pressure, PSI	Freezing Point, °F	Composition, Vol. % Aromatics	Olefins	Corrosion	Water Reaction	Thermal Value: Heat of Combustion, BTU/lb Gross	Aniline Gravity Product	Smoke Point, mm	Smoke Volatility Index
56-6	0	161	249	265	295	360	421	99.0	1.1	1.0	53.5	0.7	4.7	0.0340	0.0001	2.95	-80	10.1	1.3	Pass 1B	Pass	-	6991	30.5	72.1
56-6A	2.61×10^9	179	245	265	297	363	422	98.0	1.1	0.4	51.4	2.1	-	0.0251	0.0002	2.71	-73	11.9	0.9	Pass 1A	Pass	-	6600	26.7	42.2
57-85	0	147	223	245	293	415	481	86.0	0.5	0.5	56.7	4.8	-	0.0221	0.0080	3.00	-76	6.6	1.6	Pass 1A	Pass	-	8260	40.5	76.6
57-86	0	154	212	-	-	-	454	87.5	1.0	1.0	52.1	1.4	5.8	0.0250	0.0010	2.30	-76	10.0	3.0	Pass 1A	Pass	18692	7164	29.5	66.3
57-87	0	142	204	-	-	-	410	98.0	1.0	0.0	54.9	1.0	14.4	0.0220	0.0010	2.90	-80	16.9	1.1	Pass 1A	Pass	18622	6588	33.0	74.6
57-88	0	-	-	287	375	465	-	60.8	1.1	0.8	48.1	0.6	2.6	0.2300	0.0006	2.90	-74	12.3	0.7	Pass 1B	Pass	18651	6670	27.3	51.1
57-95	0	-	199	217	253	330	362	-	1.0	-	53.2	0.8	3.2	0.0100	0.0010	2.80	-80	19.5	0.7	Pass 1A	Pass	18563	5932	29.0	-
57-110	0	150	232	260	309	400	468	89.5	1.5	0.5	56.6	2.0	-	0.0188	0.0007	3.30	<-75	9.7	1.0	Pass 1A	Pass	18788	8150	38.9	76.5
57-112	0	155	209	230	277	365	401	98.5	1.3	0.2	56.3	0.6	1.4	0.0210	0.0001	2.80	<-75	7.5	0.8	Pass 1B	Pass	-	7540	36.5	77.7
57-114	0	148	219	240	280	357	429	94.5	1.8	0.2	55.6	3.5	-	0.0310	0.0021	2.10	<-75	10.1	1.2	Pass 1B	Pass	18709	7320	30.9	71.2

TABLE V

EVALUATION OF JP-4 TYPE FUELS IN THE CFR FUEL COKER

Fuel Designation, ANPF No	Run No	Gamma Dose, ergs/gm Carbon		Test Condition	Goodness Rating	Preheater Deposits		Fuel Sample	Gamma Dose on Fuel Sample, ergs/gm Carbon	Viscosity at -30°F, cs.	Flash Point, °F	Gravity, °API	Index of Refraction, n_d^{25}
		Static	CFR Coker Tube			Max.	Av						
56-6								Base		2.36	<76	53.5	1.4265
	14	0	0	300/400/6	744	2	0.31						
	34	1.47×10^8	5.75×10^6	300/400/6	40	0	0.00						
	11	0	0	350/450/6	50	0	0.00						
	12	0	0	350/450/6	58	0	0.00						
57-86								Base		2.55	<76	52.1	1.4336
	68	0	0	300/400/6	875	2	1.22	Dynamic	0			51.8	1.4325
	174	8.79×10^7	0	300/400/6	120	3	1.47	Static	8.79×10^7	2.66	<75	51.6	1.4328
								Dynamic	8.79×10^7	2.64	<75	51.6	1.4330
	167	8.71×10^7	1.81×10^8	300/400/6	337	2	0.85	Static	3.47×10^8	3.36	<75	51.3	1.4336
								Dynamic	1.22×10^8	3.06	<75	51.5	1.4347
								Dynamic	1.66×10^8	2.64	<75	51.4	1.4335
57-87								Base		1.88	<76	54.9	1.4245
	69	0	0	300/400/6	81	0	0.00	Dynamic	0			54.7	1.4248
	84	7.81×10^7	4.42×10^7	300/400/6	310	2	0.23	Static	1.37×10^8	1.70	<74	54.4	1.4244
								Dynamic	1.07×10^8	1.68	<72	54.4	1.4241
57-88								Base		3.89	<76	48.1	1.4430
	196	0	0	300/400/6	840	1	1.00	Dynamic	0	4.41		47.9	1.4420
57-95								Base		1.55	<72	53.2	1.4273
	76	0	0	300/400/6	900	0	0.00	Dynamic	0	1.61	<80	52.8	1.4268
	135	0	0	300/400/6	841	0	0.00						
	166	8.71×10^7	1.81×10^8	300/400/6	842	1	0.46	Static	2.97×10^8	1.75	<78	52.1	1.4269
								Dynamic	1.22×10^8	1.68	<75	52.4	1.4280
								Dynamic	1.74×10^8	1.65	<75	52.4	1.4275
								Dynamic	2.45×10^8	2.86	<75	52.2	1.4265
	169	1.08×10^9	2.03×10^8	300/400/6	213	3	1.62						
57-110								Base		2.48	<76	56.6	1.4227
	52	0	0	300/400/6	900	0	0.00						
	178	8.71×10^7	2.03×10^8	300/400/6	240	2	0.54	Static	1.74×10^8	2.58	<78	56.3	1.4254
								Dynamic	1.19×10^8	2.58	<78	56.3	1.4226
								Dynamic	1.39×10^8	2.56	<76	56.3	

TABLE V (cont'd)

EVALUATION OF JP-4 TYPE FUELS IN THE CFR FUEL COKER

Fuel Designation, ANPF No	Run No	Gamma Dose, ergs/gm Carbon		Test Condition	Goodness Rating	Preheater Deposits		Fuel Sample	Gamma Dose on Fuel Sample, ergs/gm Carbon	Viscosity at -30°F, cs	Flash Point, °F	Gravity, °API	Index of Refraction, n_D^{25}
		Static	CFR Coker Tube			Max	Av						
57-112								Base		1.92	< 76	56.3	1.4216
	54	0	0	300/400/6	900	0	0.00						
	96	7.81×10^7	1.52×10^8	300/400/6	578	1	0.54	Static	1.76×10^8	2.17	< 77	55.4	1.4211
								Dynamic	9.76×10^7	2.16	< 76	55.6	1.4226
	173	9.75×10^8	2.03×10^8	300/400/6	300	3	1.23	Static	1.05×10^9	2.10	116	55.8	1.4213
								Dynamic	1.03×10^9	1.90	< 75	55.8	1.4226
								Dynamic	1.05×10^9	2.09	< 75	55.8	1.4228
	194	1.04×10^9	0	300/400/6	390	1	0.32	Static	1.04×10^9	2.13	< 78	55.8	1.4209
								Dynamic	1.04×10^9	2.10	< 78	55.9	1.4218
57-114								Base		2.06	< 76	55.6	1.4250
	56	0	0	300/400/6	210	4	1.70						

TABLE VI

PHYSICAL PROPERTIES OF FUELS ACCORDING TO MIL-F-5624C, GRADE JP-5

Fuel Designation, AMPP No.	Gamma Dose, ergs/gm Carbon	Distillation, Temperature, °F At: Initial B.P	10% Evap.	20% Evap	50% Evap.	90% Evap	End Point	Residue, Vol %	Distillation Loss, Vol %	Gravity, °API	Gum, mg/100ml: Existent	Potential	Sulfur, %: Total	Mercaptan	Freezing Point, °F	Viscosity, at -30°F cs	Composition, Vol %: Aromatics	Olefins	Explosiveness, %	Flash Point, °F	Corrosion	Water Reaction	Thermal value, Heat Of Combustion, BTU/lb Gross	Aniline Gravity Product	Smoke Point, mm
57-4	0	331	341	346	355	382	404	1.1	0.8	46.9	1.1	2.7	0.0013	0.0010	-50	4.90	11.1	1.26	15.0	120	Pass1B	Pass	-	6547	28.1
57-2A	2.61×10^9	330	344	346	355	382	422	0.8	0.4	46.9	-	-	0.0001	0.0001	<-75	4.54	10.0	1.2	15.0	116	Pass1A	Pass	-	6620	27.7
57-50	0	538	551	555	560	577	606	1.5	0.5	30.8	2.0	2.0	0.0100	0.0001	-65	884.4*	100.0	0.0	15.0	245	Pass1B	Pass	19,198	-	13.1
57-51	0	235	300	332	478	553	587	1.0	0.5	43.2	3.0	6.1	0.0100	0.0001	<-75	23.06	50.0	1.0	>100.0	82	Pass1B	Pass	-	5120	20.1
57-52	0	324	378	387	407	446	478	1.0	0.5	32.6	1.6	15.0	0.0010	0.0001	<-112	10.85	88.0	4.0	30.0	120	Pass1A	Pass	19,020	-	10.6
57-53	0	403	419	425	440	470	497	1.1	0.3	47.9	3.8	-	0.0017	0.0001	-30	13.34**	1.5	0.7	5.0	176	Fail 2C	Pass	-	8520	40.8
57-54	0	415	420	424	441	471	480	1.1	0.4	47.8	0.8	1.2	0.0010	0.0001	-30	13.32**	1.5	0.7	5.0	176	Fail 2C	Pass	-	8513	41.8
57-55	0	306	340	350	371	474	576	1.4	0.6	53.3	4.2	7.8	0.0025	0.0001	<-75	10.14	-	-	7.3	45.0	102	Pass1B	Fail	-	9870	37.8
57-56	0	318	327	330	337	360	395	0.8	0.2	47.4	0.4	6.0	0.0020	0.0001	<-76	3.72	17.3	2.0	10.0	110	Pass1A	Pass	-	6140	24.9
57-57	0	332	401	419	454	505	533	0.8	0.2	40.1	1.2	3.9	0.0390	0.0001	-35	15.32	9.4	7.1	10.0	138	Pass1A	Fail	-	6040	21.4
57-58	0	317	356	366	397	458	508	1.2	0.2	44.2	1.0	4.1	0.0190	0.0007	-55	7.18	15.3	2.0	40.0	118	Pass1A	Pass	-	6290	24.5
	2.61×10^9	332	357	366	394	459	514	1.2	0.5	44.0	3.5	8.0	0.0230	0.0006	-60	7.16	-	-	40.0	110	Fail 2C	Pass	-	6260	23.8
57-59	0	317	356	366	-	458	514	0.9	0.2	44.1	1.5	2.0	0.0219	0.0007	-55	7.39	16.2	2.5	45.0	118	Pass1A	Pass	-	6280	23.5
	8.71×10^8	174	353	367	395	455	510	0.8	0.2	43.9	1.5	-	0.0228	0.0002	-60	6.80	15.3	1.4	>100.0	74	Pass1A	Pass	-	6180	23.7
57-60	0	344	352	360	394	458	516	0.9	0.2	44.1	1.5	2.9	0.0239	0.0007	-60	7.16	15.9	2.7	40.0	116	Pass1A	Pass	-	6250	24.0
	8.71×10^8	-	-	-	-	-	-	-	-	43.8	-	-	-	-	-	6.64	-	-	-	80	-	-	-	-	-
57-61	0	344	354	363	394	456	512	1.0	0.3	44.1	1.0	1.9	0.0175	0.0008	-60	7.20	15.4	2.2	40.0	118	Pass1A	Pass	-	6260	23.5
	8.71×10^8	-	-	-	-	-	-	-	-	43.9	-	-	-	-	-	6.63	-	-	-	108	-	-	-	-	-
57-62	0	342	354	364	396	458	518	0.9	0.1	44.1	1.5	1.5	0.0144	0.0012	-65	7.14	15.9	2.8	45.0	118	Pass1A	Pass	-	6230	23.5
57-63	0	332	356	366	396	460	517	1.0	0.2	44.1	<0.2	0.4	0.0189	0.0012	-50	7.19	15.5	3.2	45.0	118	Pass1A	Pass	-	6240	24.5
57-76	0	354	380	392	427	476	505	1.4	0.3	40.7	0.8	-	0.6280	0.0138	-50	10.26	-	-	5.0	140	Pass1A	Pass	-	5700	22.6
57-77	0	378	404	409	427	465	490	1.1	0.6	41.3	0.2	-	0.0882	0.0041	-50	10.30	-	-	0.0	160	Pass1A	Pass	-	5840	24.1
57-78	0	390	422	436	458	500	528	1.0	0.7	27.7	24.6	-	0.5760	0.0112	-35	14.92	-	-	5.0	172	Pass1A	Fail	18,754	-	12.2
57-79	0	408	431	439	458	504	533	1.1	0.4	28.7	0.8	-	0.0490	0.0030	-30	17.14**	-	-	0.0	192	Pass1A	Fail	18,802	-	11.8
57-80	0	340	378	387	422	478	507	1.2	0.6	47.7	0.2	-	0.0790	0.0146	-25	8.68**	-	-	5.0	136	Pass1A	Pass	-	7750	40.3
57-81	0	361	386	397	431	483	508	1.1	0.7	32.8	0.5	-	0.0510	0.0073	-35	15.79	-	-	0.0	144	Pass1A	Pass	19,376	4330	16.7
57-89	0	-	-	-	-	-	-	-	-	42.3	-	-	-	0.0001	-	8.93	-	-	5.0	148	-	-	18,590	6130	-
57-90	0	-	-	-	-	-	-	-	-	41.8	-	-	-	0.0001	-	9.66	-	-	5.0	148	-	-	18,584	6220	-

*Crystals Present
**Sharp Formation of Crystals

TABLE VI (cont'd)

PHYSICAL PROPERTIES OF FUELS ACCORDING TO MIL-F-5624C, GRADE JP-5

Fuel Designation, AMPF No.	Gamma Dose, ergs/gm Carbon	Distillation Temperature, °F At: Initial B P	10% Evap.	20% Evap	50% Evap	90% Evap	End Point	Residue, Vol %	Distillation Loss, Vol %	Gravity, °API	Gum, mg/100ml Existent	Potential	Sulfur, % Total	Mercaptan	Freezing Point, °F	Viscosity, at -30°F cs	Composition, Vol % Aromatics	Olefins	Explosiveness, %	Flash Point, °F	Corrosion	Water Reaction	Thermal Value, Heat Of Combustion, BTU/lb Gross	Aniline Gravity Product	Smoke Point, mm
57-93	0	-	-	-	-	-	-	-	-	41.2	-	-	-	0.0001	-	10.50	-	-	5.0	156	-	-	18,565	-	-
57-94	0	-	-	-	-	-	-	-	-	41.0	-	-	-	0.0001	-	10.23	-	-	-	156	-	-	18,568	-	-
57-97	0	338	367	376	402	450	493	0.4	0.1	45.1	1.9	-	0.0179	0.0001	-55	7.54	11.4	2.2	20.0	120	Pass 1B	Pass	-	6680	27.3
57-98	0	336	366	376	401	446	495	0.4	0.2	47.9	1.0	-	0.0036	0.0001	-45	7.51	2.8	0.8	20.0	124	Pass 1B	Pass	-	7790	39.5
	8.71×10^8	-	-	-	-	-	-	-	-	47.8	-	-	-	-	<-75	4.91	-	-	-	114	-	-	-	-	-
	1.56×10^8	-	-	-	-	-	-	-	-	47.8	-	-	-	-	-	6.90	-	-	-	112	-	-	-	-	-
57-99	0	331	364	373	399	448	494	0.3	0.2	45.1	10.5	-	0.0006	0.0001	-50	7.45	13.5	0.9	25.0	120	Pass 1A	Pass	-	6650	26.7
	7.81×10^7	-	-	-	-	-	-	-	-	47.9	-	-	-	-	-	6.77	-	-	-	76	-	-	-	-	-
57-100	0	365	389	401	428	479	514	1.2	0.3	43.7	5.3	-	0.0691	0.0010	-40	10.01	-	-	15.0	144	-	Pass	-	6770	26.0
57-102	0	344	350	351	357	372	402	1.3	0.2	55.8	0.3	0	0.0001	0.0001	<-75	6.67	-	-	10.0	122	Pass 1B	Pass	-	10350	50.0
57-104	0	373	393	402	427	480	512	1.3	0.2	43.7	-	-	-	0.0001	-45	9.77	-	-	15.0	146	Pass 1A	Pass	-	6720	26.5
57-111	0	348	375	386	420	487	533	1.0	0.5	46.0	-	-	0.0900	0.0002	-40	8.71	-	-	15.0	134	Pass 1B	Pass	18,681	7050	28.9
57-113	0	322	372	388	427	483	515	1.2	0.3	43.0	5.0	0	0.1200	0.0001	-40	10.22	10.7	4.7	5.0	138	Pass 1A	Pass	-	6420	24.8
57-115	0	336	371	382	410	465	508	1.3	0.2	45.0	10.2	42.5	0.0007	0.0001	-40	6.58	13.3	0.6	35.0	122	Pass 1B	Fail	-	6642	28.5
57-120	0	358	370	374	392	481	558	1.3	0.2	53.1	1.8	-	0.0010	0.0001	-65	13.84	2.5	3.6	10.0	130	Pass 1A	Pass	-	10100	50.0
57-121	0	344	398	410	436	495	532	1.5	0.5	42.6	1.9	-	0.0090	0.0003	-35	12.07	18.2	3.6	80.0	98	Pass 1A	Pass	-	6360	24.8

TABLE VII

EVALUATION OF JP-5 TYPE FUELS IN THE CFR FUEL COKER

Fuel Designation, ANPF No	Run No	Gamma Dose, ergs/gm Carbon		Test Condition	Goodness Rating	Preheater Deposits		Fuel Sample	Gamma Dose on Fuel Sample, ergs/gm Carbon	Viscosity at -30°F, cs	Flash Point, °F	Gravity, °API	Index of Refraction, n_d^{25}
		Static	CFR Coker Tube			Max.	Av.						
57-2								Base		4.90	120	46.9	
	9	0	0	350/450/6	775								
	10	0	0	350/450/6	765	1	0.38						
	21	0	0	350/450/6	758	0	0.00						
	24	1.34×10^7	3.49×10^7	350/450/6	272	0	0.00						
	17	0	0	400/500/6	70	0	0.00						
	18	0	0	400/500/6	420	2	0.46						
57-50								Base		884.4*	245	30.8	1.4861
	43	0	0	300/400/6	742	1	0.62						
	192	0	0	400/500/6	750	2	0.62	Dynamic	0	999.2	172	31.0	1.4856
	195	8.71×10^7	2.03×10^8	400/500/6	840	4	2.54	Static	2.84×10^8	1072.0	238	30.9	1.4860
								Dynamic	1.23×10^8	922.3	120	31.1	1.4856
								Dynamic	1.77×10^8	1017.0	222	31.0	1.4858
								Dynamic	2.49×10^8	1088.0	234	31.0	1.4864
57-51								Base		23.06	82	43.2	1.4539
	44	0	0	300/400/6	900	1	0.15						
	185	0	0	400/500/6	715	1	0.46	Dynamic	0	27.47	76	43.1	1.4534
	190	8.71×10^7	2.03×10^8	400/500/6	900	2	0.94	Static	3.10×10^8	30.14	82	42.2	1.4547
								Dynamic	1.23×10^8	24.34	74	43.2	1.4339
								Dynamic	1.77×10^8	24.44	74	43.1	1.4331
								Dynamic	2.45×10^8	28.57	74	43.0	1.4324
57-52								Base		10.85	120	32.6	1.4834
	45	0	0	300/400/6	875	0	0.00						
	165	0	0	400/500/6	900	1	0.46	Dynamic	0	10.01	100	32.7	1.4875
	176	8.71×10^7	2.03×10^8	400/500/6	900	4	2.00	Static	2.59×10^8	12.60	110	32.7	1.4834
								Dynamic	1.55×10^8	12.68	108	32.7	1.4831
								Dynamic	1.87×10^8	12.49	110	32.7	1.4835
								Dynamic	2.41×10^8	12.45	114	32.6	1.4830
57-53								Base		13.34	176	47.9	1.4380
	46	0	0	300/400/6	522	1	0.15						
	158	0	0	400/500/6	653	2	0.77	Dynamic	0	-	-	47.9	1.4350
	184	8.71×10^7	2.03×10^8	400/500/6	900	3	2.17	Static	2.63×10^8	Solid	166	47.9	1.4354
								Dynamic	1.23×10^8	Solid	106	48.0	1.4354
								Dynamic	1.77×10^8	Solid	142	48.0	1.4354
								Dynamic	2.45×10^8	Solid	154	47.9	1.4354

*Crystals present

TABLE VII (cont'd)

EVALUATION OF JP-5 TYPE FUELS IN THE CFR FUEL COKER

Fuel Designation, ANPF No	Run No	Gamma Dose, ergs/gm Carbon		Test Condition	Goodness Rating	Preheater Deposits		Fuel Sample	Gamma Dose on Fuel Sample, ergs/gm Carbon	Viscosity at -30°F, cs	Flash Point, °F	Gravity, °API	Index of Refraction, n_d^{25}
		Static	CFR Coker Tube			Max.	Av.						
57-54								Base		13.32	176	47.8	1.4350
	47	0	0	300/400/6	773	1	0.69						
	49	0	0	400/500/6	782	2	1.32						
	136	1.12×10^9	1.18×10^8	400/500/6	856	1	0.46	Static	1.23×10^9	11.36	166	47.8	1.4355
								Dynamic	1.21×10^9	11.50	114	47.8	1.4355
								Dynamic	1.22×10^9	11.71	141	47.8	1.4355
								Dynamic	1.23×10^9	12.05	144	47.8	1.4355
	99	3.71×10^8	9.84×10^7	400/500/6	420	1	0.80	Static	4.67×10^8	Solid	172	47.8	-
								Dynamic	3.90×10^8	14.36	154	47.8	1.4355
	104	2.71×10^9	1.31×10^8	400/500/6	900	2	1.52	Static	2.60×10^9	11.83	170	47.6	1.4363
								Dynamic	2.74×10^9	Solid	150	47.7	1.4365
	177	1.02×10^{10}	2.03×10^8	400/500/6	803	1	1.00	Static	1.04×10^{10}	14.32	150	46.8	1.4369
								Dynamic	1.02×10^{10}	14.53	94	47.0	1.4367
								Dynamic	1.03×10^{10}	15.25	114	46.9	1.4363
								Dynamic	1.04×10^{10}	13.86	130	46.9	1.4367
57-55								Base		10.14	102	53.3	1.4248
	48	0	0	400/500/6	765	2	0.93						
	101	7.81×10^7	1.04×10^8	400/500/6	592	4	1.15	Static	1.96×10^8	9.09	98	53.3	1.4256
								Dynamic	8.17×10^7	8.45	82	55.0	1.4260
	138	1.07×10^9	1.81×10^8	400/500/6	750	4	2.23	Static	1.17×10^9	8.28	99	53.4	1.4245
								Dynamic	1.09×10^9	8.88	80	53.4	1.4253
								Dynamic	1.11×10^9	8.85	82	53.5	1.4253
								Dynamic	1.16×10^9	8.90	88	53.4	1.4254
57-56								Base		3.72	110	47.4	1.4375
	50	0	0	400/500/6	857	2	0.93						
	100	7.81×10^7	1.04×10^8	400/500/6	900	2	0.63	Static	1.76×10^8	3.87	100	47.4	1.4376
								Dynamic	9.58×10^7	3.84	98	47.4	1.4376
	140	2.93×10^9	1.81×10^8	400/500/6	900	4	2.23	Static	3.03×10^9	3.37	104	47.2	1.4385
								Dynamic	2.95×10^9	3.51	87	47.3	1.4382
								Dynamic	2.98×10^9	3.49	99	47.2	1.4382
								Dynamic	3.02×10^9	3.45	100	47.2	1.4383

TABLE VII (cont'd)

EVALUATION OF JP-5 TYPE FUELS IN THE CFR FUEL COKER

Fuel Designation, ANPF No	Run No	Gamma Dose, ergs/gm Carbon		Test Condition	Goodness Rating	Preheater Deposits		Fuel Sample	Gamma Dose on Fuel Sample, ergs/gm Carbon	Viscosity at -30°F, cs	Flash Point, °F	Gravity, °API	Index of Refraction, n_d^{25}
		Static	CFR Coker Tube			Max	Av						
57-57								Base		15.32	138	40.1	1.4548
	51	0	0	400/500/6	500	2	1.83						
	102	7.81×10^7	1.04×10^8	400/500/6	750	0	0.00	Static	1.96×10^8	14.06	-	40.1	1.4564
								Dynamic	8.17×10^7	13.27	114	40.2	1.4564
	143	1.49×10^9	1.81×10^8	400/500/6	827	3	1.77	Static	1.59×10^9	14.18	135	39.9	1.4556
								Dynamic	1.51×10^9	13.92	112	40.0	1.4557
								Dynamic	1.54×10^9	12.83	123	40.0	1.4557
								Dynamic	1.58×10^9	13.18	125	40.0	1.4558
57-58								Base		7.18	118	44.2	1.4459
	20	0	0	300/400/6	900	1	0.78						
	26	1.34×10^7	6.37×10^7	300/400/6	340	2	1.04						
	35	0	0	400/500/6	49	3	2.03						
57-59								Base		7.39	118	44.1	1.4461
	23	0	0	300/400/6	900	0	0.00						
	28	1.48×10^7	4.36×10^7	300/400/6	303	2	1.80						
	36	0	0	400/500/6	900	4	1.54						
57-60								Base		7.16	116	44.1	1.4465
	25	0	0	300/400/6	802	2	0.62						
	193	2.83×10^9	2.03×10^8	300/400/6	555	4	2.30	Static	3.05×10^9	9.06	114	43.6	1.4466
								Dynamic	2.87×10^9	9.09	96	43.7	1.4467
								Dynamic	2.93×10^9	8.66	108	43.6	1.4466
								Dynamic	3.00×10^9	8.25	110	43.6	1.4474
	37	0	0	400/500/6	900	3	1.57						
	60	3.90×10^7	4.47×10^7	400/500/6	310	3	2.00	Dynamic	7.82×10^7	6.64	98	43.9	1.4465
57-61								Base		7.20	118	44.1	1.4462
	27	0	0	300/400/6	900	1	0.38						
	38	0	0	400/500/6	900	3	1.70						
	61	8.80×10^7	9.06×10^6	400/500/6	72	2	1.38						
57-62								Base		7.14	118	44.1	1.4464
	29	0	0	300/400/6	900	1	0.23						
	38a	0	0	400/500/6	900	1	0.69						
	63	8.80×10^7	3.14×10^7	400/500/6	230	4	2.45	Static	1.08×10^8	6.74	110	44.0	1.4465
								Dynamic	9.53×10^7	6.30	82	43.2	1.4456

TABLE VII (cont'd)

EVALUATION OF JP-5 TYPE FUELS IN THE CFR FUEL COKER

Fuel Designation, ANPF No	Run No	Gamma Dose, ergs/gm Carbon		Test Condition	Goodness Rating	Preheater Deposits		Fuel Sample	Gamma Dose on Fuel Sample, ergs/gm Carbon	Viscosity at -30°F, cs	Flash Point, °F	Gravity, °API	Index of Refraction, n_d^{25}
		Static	CFR Coker Tube			Max.	Av.						
57-63								Base		7.19	118	44.1	1.4253
	30	0	0	300/400/6	900	1	0.23						
	39	0	0	400/500/6	98	3	1.76						
	64	8.80×10^7	2.45×10^6	400/500/6	38	2	1.38	Static	1.17×10^8	6.57	98	44.0	1.4463
								Dynamic	8.80×10^7	5.97	< 75	43.1	1.4452
57-76								Base		10.26	140	40.7	1.4543
	62	0	0	400/500/6	92	1	1.00	Dynamic	0	9.54	106	40.4	1.4542
	142	0	0	400/500/6	327	1	0.23	Dynamic	0	-	-	-	1.4544
	187	7.23×10^7	0	400/500/6	137	3	1.38	Static	7.23×10^7	-	-	40.7	-
								Dynamic	7.23×10^7	13.05	110	40.7	1.4545
	106	7.81×10^7	6.28×10^7	400/500/6	297	2	1.23	Static	2.07×10^8	9.33	130	40.7	1.4553
								Dynamic	8.17×10^7	9.65	116	40.8	1.4553
57-77								Base		10.30	160	41.3	1.5034
	78	0	0	400/500/6	507	3	0.85	Dynamic	0	9.94	134	41.4	1.4525
	97	8.71×10^7	6.01×10^7	400/500/6	390	3	2.00	Static	1.96×10^8	9.26	152	41.3	1.4535
								Dynamic	9.66×10^7	6.02	148	41.4	1.4528
	108	7.81×10^7	1.09×10^8	400/500/6	721	4	2.15	Static	1.93×10^8	9.18	142	41.4	1.4535
								Dynamic	8.17×10^7	10.10	140	41.3	1.4538
	200	2.02×10^8	0	400/500/6	324	4	1.46	Static	2.02×10^8	12.82	146	41.5	1.4529
								Dynamic	2.02×10^8	12.36	110	41.5	1.4535
	157	1.98×10^9	1.81×10^8	400/500/6	570	4	2.00	Static	2.16×10^9	9.97	154	41.4	1.4591
								Dynamic	2.01×10^9	9.79	140	41.4	1.4585
								Dynamic	2.07×10^9	10.02	156	41.4	1.4589
								Dynamic	2.14×10^9	10.48	158	41.4	1.4591
57-78								Base		14.92	172	27.7	1.5048
	79	0	0	400/500/6	405	4	2.93	Dynamic	0	15.24	142	27.8	1.5043
	109	7.81×10^7	6.89×10^7	400/500/6	320	4	2.69	Static	1.96×10^8	14.89	146	27.7	1.5047
								Dynamic	8.12×10^7	14.75	136	27.8	1.5045
	188	1.27×10^8	0	400/500/6	541	4	2.38	Dynamic	1.27×10^8	Solid	166	27.7	1.5027
57-79								Base		17.14	192	28.7	1.4990
	80	0	0	400/500/6	100	3	1.30	Dynamic	0	16.05	136	28.9	1.4985
	110	7.81×10^7	2.61×10^7	400/500/6	134	2	1.00	Static	1.96×10^8	15.68	168	28.7	1.4989
								Dynamic	8.17×10^7	15.16	160	29.1	1.4993

TABLE VII (cont'd)

EVALUATION OF JP-5 TYPE FUELS IN THE CFR FUEL COKER

Fuel Designation, ANPF No	Run No	Gamma Dose, ergs/gm Carbon		Test Condition	Goodness Rating	Preheater Deposits		Fuel Sample	Gamma Dose on Fuel Sample, ergs/gm Carbon	Viscosity at -30°F, cs	Flash Point, °F	Gravity, °API	Index of Refraction, n_D^{25}
		Static	CFR Coker Tube			Max.	Av						
57-80								Base		8.68	136	47.7	1.4385
	82	0	0	400/500/6	485	0	0.00	Dynamic	0	8.44	102	47.6	1.4385
	111	5.88×10^7	1.09×10^8	400/500/6	660	3	1.85	Static	1.57×10^8	Solid	136	47.5	1.4389
								Dynamic	7.80×10^7	Solid	139	47.7	1.4385
	175	8.01×10^7	0	400/500/6	235	4	1.92	Static	8.01×10^7	Solid	132	47.6	1.4385
								Dynamic	8.01×10^7	Solid	116	47.6	1.4388
	155	8.90×10^8	0	400/500/6	95	2	1.77	Dynamic	8.90×10^8	Solid	136	-	1.4385
	152	9.87×10^8	1.81×10^8	400/500/6	98	4	1.77	Static	1.03×10^9	Solid	136	47.6	1.4386
								Dynamic	9.95×10^8	8.18	114	47.6	1.4388
57-81								Base		15.79	144	32.8	1.4696
	137	0	0	400/500/6	484	4	1.22				144		1.4694
	114	4.36×10^7	1.09×10^8	400/500/6	900	2	1.33	Static	1.37×10^8	14.47	144	32.8	1.4695
								Dynamic	5.27×10^7	14.40	132	33.0	1.4697
	154	1.26×10^9	1.81×10^8	400/500/6	826	3	1.52	Static	1.36×10^9	16.03	148	32.8	1.4699
								Dynamic	1.28×10^9	15.17	118	32.9	1.4703
								Dynamic	1.31×10^9	15.26	138	32.9	1.4761
								Dynamic	1.35×10^9	14.89	144	32.8	1.4706
57-84								Base		9.56	148	41.9	1.4506
	98	0	0	400/500/6	703	1	0.08						
	197	8.71×10^7	2.03×10^8	400/500/6	272	3	1.54	Static	2.02×10^8	10.79	140	42.0	1.4505
								Dynamic	1.23×10^8	10.13	108	42.0	1.4505
								Dynamic	1.74×10^8	10.28	126	42.0	1.4506
57-89								Base		8.93	148	42.3	1.4494
	70	0	0	400/500/6	857	1	0.23	Dynamic	0	8.88	134	42.3	1.4494
	183	8.71×10^7	2.03×10^8		900	3	1.25	Static	2.70×10^8	10.29	142	42.2	1.4495
								Dynamic	1.23×10^8	10.18	106	42.3	1.4492
								Dynamic	1.74×10^8	10.24	130	42.3	1.4496
								Dynamic	2.41×10^8	10.28	136	42.2	1.4497
57-90								Base		9.66	148	41.8	1.4505
	71	0	0	400/500/6	477	3	1.00	Dynamic	0	9.18	< 80	41.9	1.4505
	171	8.71×10^7	2.03×10^8	400/500/6	353	3	1.77	Static	2.37×10^8	4.33	124	41.9	1.4505
								Dynamic	1.22×10^8	9.50	106	42.0	1.4506
								Dynamic	1.76×10^8	9.50	116	41.9	1.4509

TABLE VII (cont'd)

EVALUATION OF JP-5 TYPE FUELS IN THE CFR FUEL COKER

Fuel Designation, ANPF No	Run No	Gamma Dose, ergs/gm Carbon		Test Condition	Goodness Rating	Preheater Deposits		Fuel Sample	Gamma Dose on Fuel Sample, ergs/gm Carbon	Viscosity at -30°F, cs.	Flash Point, °F	Gravity, °API	Index of Refraction, n_d^{25}
		Static	CFR Coker Tube			Max	Av						
57-93								Base		10.50	156	41.2	1.4520
	74	0	0	400/500/6	826	2	0.46	Dynamic	0	9.62	98	41.3	-
	180	8.71×10^7	2.03×10^8	400/500/6	765	4	2.60	Static	2.73×10^8	11.79	134	41.2	1.4520
								Dynamic	1.22×10^8	11.60	120	41.3	1.4516
								Dynamic	1.77×10^8	11.71	128	41.2	1.4518
								Dynamic	2.49×10^8	11.73	140	41.2	1.4520
57-94								Base		10.23	156	41.0	1.4526
	75	0	0	400/500/6	165	3	1.16	Dynamic	0	10.35	138	41.0	-
	134	0	0	400/500/6	92	1	0.32						
	151	8.71×10^7	1.81×10^8	400/500/6	257	4	2.15	Static	1.45×10^8	10.42	142	40.9	1.4576
								Dynamic	1.10×10^8	10.09	126	41.0	1.4576
								Dynamic	1.31×10^8	9.87	128	40.8	1.4524
57-97								Base		7.54	120	45.1	1.4430
	139	0	0	300/400/6	485	1	0.77	Dynamic	0	9.16	118	45.1	1.4432
	40	0	0	400/500/6	534	4	1.85						
	67	3.45×10^8	5.40×10^6	400/500/6	45	2	1.61	Static	3.84×10^8	7.14	130	44.7	-
								Dynamic	3.50×10^8	6.72	< 84	44.8	-
57-98								Base		7.51	124	47.9	1.4430
	41	0	0	400/500/6	855	1	0.38						
	81	1.56×10^8	2.70×10^7	400/500/6	200	3	1.46	Static	2.43×10^8	5.70	126	47.8	1.4344
								Dynamic	1.62×10^8	5.36	90	47.9	1.4344
	92	1.17×10^8	7.40×10^7	400/500/6	900	3	1.32						
57-99								Base		7.45	120	45.1	1.4436
	42	0	0	300/400/6	900	1	0.38						
	88	7.81×10^7	7.36×10^7	300/400/6	578	2	0.32	Static	1.76×10^8	5.44	120	45.0	1.4435
								Dynamic	8.79×10^7	5.36	94	45.1	1.4432
	144	0	0	400/500/6	55	2	0.45	Dynamic	0	Solid	118	45.0	1.4434
	66	0	0	400/500/6	130	2	0.32	Dynamic	0	-	124	45.1	1.4430

TABLE VII (cont'd)

EVALUATION OF JP-5 TYPE FUELS IN THE CFR FUEL COKER

Fuel Designation, ANPF No	Run No	Gamma Dose, ergs/gm Carbon		Test Condition	Goodness Rating	Preheater Deposits		Fuel Sample	Gamma Dose on Fuel Sample, ergs/gm Carbon	Viscosity at -30°F, cs	Flash Point, °F	Gravity, °API	Index of Refraction, n_d^{25}
		Static	CFR Coker Tube			Max	Av						
57-100								Base		10.01	144	43.7	1.4479
	153	0	0	400/500/6	670	3	1.54	Dynamic	0	9.64	118	43.7	1.4486
	93	7.81×10^7	7.36×10^7	400/500/6	814	3	2.23	Static	1.76×10^8	9.92	146	43.7	1.4473
								Dynamic	8.09×10^7	7.62	120	43.7	1.4472
	168	1.35×10^9	2.03×10^8	400/500/6	708	3	1.77	Static	1.72×10^9	10.35	128	43.7	1.4475
								Dynamic	1.38×10^9	10.03	112	43.7	1.4473
								Dynamic	1.44×10^9	10.55	122	43.7	1.4480
								Dynamic	1.51×10^9	9.91	134	43.6	1.4476
57-101								Base		11.38	112	44.9	1.4425
	117	0	0	400/500/6	900	2	0.54	Dynamic	0	9.36	106	45.1	1.4427
	116	7.81×10^7	1.09×10^8	400/500/6	827	4	2.15	Static	1.86×10^8	9.13	118	45.1	1.4427
								Dynamic	8.17×10^7	8.95	98	45.1	1.4427
	145	1.35×10^9	1.81×10^8	400/500/6	103	2	0.77	Static	1.40×10^9	9.56	119	44.9	1.4428
								Dynamic	1.36×10^9	8.66	87	44.9	1.4428
	148	1.40×10^9	1.81×10^8	400/500/6	81	2	0.77	Static	1.43×10^9	9.83	108	44.9	1.4476
								Dynamic	1.41×10^9	9.87	114	44.9	1.4471
57-102								Base		6.67	122	55.8	1.4200
	147	0	0	400/500/6	752	1	0.61						
	94	7.81×10^7	7.36×10^7	400/500/6	842	0	0.00	Static	1.76×10^8	7.83	122	55.8	1.4205
57-103								Base		12.43	151	43.6	1.4475
	118	0	0	400/500/6	654	0	0.00						
	119	7.84×10^7	1.09×10^8	400/500/6	900	3	1.93	Static	2.29×10^8	10.18	142	43.5	1.4479
								Dynamic	9.80×10^7	10.39	128	43.6	1.4479
	179	1.17×10^9	2.03×10^8	400/500/6	900	3	2.00	Static	1.29×10^9	12.58	144	43.4	1.4478
								Dynamic	1.21×10^9	12.33	100	43.5	1.4478
								Dynamic	1.26×10^9	12.40	128	43.5	1.4479
								Dynamic	1.29×10^9	12.49	136	43.5	1.4476
57-104								Base		9.77	146	43.7	1.4472
	146	0	0	400/500/6	532	2	1.08						
	95	7.80×10^7	1.09×10^8	400/500/6	457	4	1.23	Static	1.76×10^8	11.44	-	-	-

TABLE VII (cont'd)

EVALUATION OF JP-5 TYPE FUELS IN THE CFR FUEL COKER

Fuel Designation, ANPF No	Run No	Gamma Dose, ergs/gm Carbon		Test Condition	Goodness Rating	Preheater Deposits		Fuel Sample	Gamma Dose on Fuel Sample, ergs/gm Carbon	Viscosity at -30°F, cs	Flash Point, °F	Gravity, °API	Index of Refraction, n_D^{25}
		Static	CFR Coker Tube			Max	Av						
57-105								Base		6.40	124	41.6	1.4545
	120	0	0	400/500/6	827	0	0.00	Dynamic	0	6.60	108	41.7	1.4530
	122	8.42×10^7	1.09×10^8	400/500/6	900	2	0.85	Static	2.07×10^8	6.61	130	41.5	1.4534
								Dynamic	1.20×10^8	6.38	124	41.6	1.4534
	159	1.04×10^9	1.81×10^8	400/500/6	826	4	2.23	Static	1.26×10^9	6.44	132	41.5	1.4550
								Dynamic	1.08×10^9	6.81	110	41.6	1.4557
								Dynamic	1.13×10^9	7.09	116	41.5	1.4557
								Dynamic	1.21×10^9	7.03	116	41.7	1.4554
57-106								Base		12.27	148	43.5	1.4476
	121	0	0	400/500/6	900	4	1.08						
	127	8.62×10^7	1.81×10^8	400/500/6	900	4	2.00	Static	1.84×10^8	12.06	102	43.7	1.4477
								Dynamic	8.85×10^7	12.13	130	43.6	1.4480
57-107								Base		12.17	146	43.5	1.4477
	123	0	0	400/500/6	900	1	0.63						
	124	7.84×10^7	1.09×10^8	400/500/6	900	2	1.30	Static	2.07×10^8	13.42	116	43.5	1.4479
								Dynamic	7.96×10^7	9.90	128	43.6	1.4479
	162	2.02×10^9	1.81×10^8	400/500/6	900	4	2.30	Static	2.25×10^9	10.25	146	43.5	1.4495
								Dynamic	2.09×10^9	10.60	118	43.6	1.4481
								Dynamic	2.14×10^9	9.92	128	43.5	1.4490
								Dynamic	2.21×10^9	10.85	132	43/4	1.4490
57-108								Base		12.48	150	43.5	1.4475
	125	0	0	400/500/6	815	1	0.23						
	128	7.80×10^7	1.81×10^8	400/500/6	900	3	1.54	Static	1.47×10^8	-	-	43.5	-
								Dynamic	9.75×10^7	9.70	144	43.5	1.4479
								Dynamic	1.27×10^8	10.17	148	43.5	1.4476
	164	2.05×10^9	1.81×10^8	400/500/6	765	4	2.23	Static	2.40×10^9	10.31	150	43.4	1.4487
								Dynamic	2.09×10^9	13.53	126	43.5	1.4474
								Dynamic	2.14×10^9	10.21	140	43.5	1.4488
								Dynamic	2.21×10^9	11.65	146	43.5	1.4485
57-109								Base		12.26	138	43.4	1.4476
	129	0	0	400/500/6	825	1	0.32						
	130	1.05×10^8	1.81×10^8	400/500/6	665	4	2.15	Static	2.08×10^8	11.44	148	43.5	1.4481
								Dynamic	1.11×10^8	11.92	124	43.6	1.4481
	172	2.06×10^9	2.03×10^8	400/500/6	900	3	1.69	Static	2.29×10^9	-	146	43.4	1.4478
								Dynamic	2.09×10^9	10.75	120	43.4	1.4479
								Dynamic	2.15×10^9	7.50	126	43.5	1.4477
								Dynamic	2.22×10^9	5.00	136	43.5	1.4509

TABLE VII (cont'd)

EVALUATION OF JP-5 TYPE FUELS IN THE CFR FUEL COKER

Fuel Designation, AMPF No	Run No	Gamma Dose, ergs/gm Carbon		Test Condition	Goodness Rating	Preheater Deposits		Fuel Sample	Gamma Dose on Fuel Sample, ergs/gm Carbon	Viscosity at -30°F, cs	Flash Point, °F	Gravity, °API	Index of Refraction, n_D^{25}
		Static	CFR Coker Tube			Max.	Av						
57-111								Base		8.71	134	46.0	1.4225
	53	0	0	400/500/6	187	2	0.69						
57-113								Base		10.22	138	43.0	1.4486
	55	0	0	300/400/6	520	0	0.00						
	181	8.71×10^7	2.03×10^8	300/400/6	543	3	1.46	Static	2.48×10^8	10.86	114	43.0	1.4436
								Dynamic	1.23×10^8	10.54	94	43.0	1.4431
								Dynamic	1.77×10^8	10.68	102	43.0	1.4436
								Dynamic	2.41×10^8	10.82	110	43.0	1.4432
57-115								Base		6.58	122	45.0	1.4439
	112	0	0	400/500/6	900	2	0.54	Dynamic	0	9.06	122	44.7	1.4435
	141	8.71×10^7	1.81×10^8	400/500/6	900	3	1.24	Static	1.80×10^8	6.49	121	45.0	1.4435
								Dynamic	1.07×10^8	6.67	97	45.1	1.4435
								Dynamic	1.36×10^8	6.44	111	45.0	1.4435
								Dynamic	1.75×10^8	6.45	114	45.0	1.4439
	156	1.09×10^9	1.81×10^8	400/500/6	900	4	2.32	Static	1.24×10^9	6.34	132	44.9	1.4453
								Dynamic	1.12×10^9	6.90	108	45.0	1.4451
								Dynamic	1.17×10^9	7.23	120	44.9	1.4446
								Dynamic	1.23×10^9	6.90	126	44.9	1.4455
	182	9.06×10^9	2.03×10^8	400/500/6	440	3	2.32	Static	9.31×10^9	8.69	120	44.6	1.4442
								Dynamic	9.10×10^9	8.41	<78	44.8	1.4442
								Dynamic	9.14×10^9	5.61	82	44.8	1.4444
								Dynamic	9.21×10^9	-	80	44.7	1.4441
57-120								Base		13.84	130	53.1	1.4255
	198	0	0	400/500/6	900	1	0.69	Dynamic	0	14.89	116	53.3	1.4254
	199	8.71×10^7	2.03×10^8	400/500/6	900	2	1.23	Static	2.81×10^8	14.95	130	53.1	1.4256
								Dynamic	1.23×10^8	14.30	80	53.1	1.4256
								Dynamic	1.68×10^8	14.16	96	53.1	1.4256
								Dynamic	2.48×10^8	16.08	108	53.1	1.4255
57-121								Base		12.07	98	42.6	1.4501
	65	7.81×10^7	2.89×10^7	400/500/6	213	3	1.92	Static	1.56×10^8	11.24	112	42.4	1.4513
								Dynamic	8.10×10^7	10.89	98	42.3	1.4509

TABLE VIII

PHYSICAL PROPERTIES OF FUELS ACCORDING TO MIL-F-25656 (JP-6), MIL-F-2558A (RJ-1), MIL-F-25576A (RP-1), AND MIL-F-25524A (THERMALLY STABLE)

Fuel Designation, ANPF No	Gamma Dens, ergs/gm Carbon	Distillation, Temperature, °F at, Initial B P	10 % Evap.	50 % Evap	90 % Evap.	End Point	% Evap at 400°F	Residue, Vol %	Distillation Loss, Vol %	Gravity, °API	Gum, mg/100ml Existent	Gum, mg/100ml Potential	Sulfur, % Total	Sulfur, % Mercaptan	Freezing Point, %	Thermal Value, Heat of Combustion, BTU/lb Gross	Thermal Value, Aniline Gravity Product	Viscosity, cs at, 100°F	Viscosity, cs at, −30°F	Viscosity, cs at, −40°F	Composition, Vol % Aromatics	Composition, Vol % Olefins	Smoke Point, mm.	Corrosion	Water Reaction	Flash Point, °F	Aniline Point, °F
JP-6																											
57-91	0	324	329	338	356	389	-	1.0	0.0	47.9	1.80	2.40	0.028	<0.0001	-80	18639	6658	-	3.66	4.10	9.8	1.6	32.0	Pass 1A	Pass	110	137.8
57-92	0	322	328	340	375	480	-	1.0	0.0	47.3	0.80	1.80	0.200	<0.0001	-78	18626	6527	-	3.94	4.40	11.2	1.2	33.0	Pass 1A	Pass	108	-
RJ-1																											
57-3	0	448	460	484	525	546	-	1.4	0.5	33.7	1.00	3.30	-	0.0003	<-76	-	-	3.22	-	-	3.98	2.43	21.7	Pass 1B	Pass	198	160.2
Thermally Stable																											
57-5	0	346	375	415	473	503	33.5	1.2	0.6	43.1	0.50	0.80	0.067	0.0003	<-76	-	6297	-	9.84	12.4	11.4	1.2	27.7	Pass 1B	Pass	126	146.1
57-96	0	336	-	-	-	424	96.0	1.0	0.0	46.4	1.00	2.40	0.010	0.0013	-78	18620	6473	-	4.16	5.71	10.25	1.8	-	Pass 1A	Pass	119	-
RP-1																											
57-7	0	340	371	416	481	515	35.0	1.4	0.6	43.8	0.40	1.60	0.0567	<0.0001	-50	-	6365	-	9.81	10.32	15.3	1.6	24.7	Pass 1B	Pass	154	147.0
	8.71×10^7	341	373	417	479	509	37.0	0.8	0.2	43.3	0.20	-	0.0565	<0.0001	-45	19259	6320	-	9.05	-	14.4	1.2	25.2	Pass 1B	Pass	118	145.9

TABLE IX

EVALUATION OF JP-6, RJ-1, RP-1, AND THERMALLY STABLE TYPE FUELS IN THE CFR FUEL COKER

Fuel Designation, ANPF No	Run No	Gamma Dose, ergs/gm Carbon		Test Condition	Goodness Rating	Preheater Deposits		Fuel Sample	Gamma Dose on Fuel Sample, ergs/gm Carbon	Viscosity at -30°F, cs	Flash Point, °F	Gravity, °API	Index of Refraction, n_D^{25}
		Static	CFR Coker Tube			Max	Av						
JP-6													
57-91								Base		3.66	110	47.9	1.4350
	72	0	0	400/500/6	50	0	0.00	Dynamic	0	2.65	<88	51.5	1.4346
	86	7.81×10^7	1.08×10^7	400/500/6	81	2	1.00	Static	1.17×10^8	2.17	<80	51.4	1.4295
								Dynamic	8.71×10^7	3.49	<80	51.4	1.4323
	89	8.71×10^7	0	400/500/6	33	2	1.30						
57-92								Base		3.94	108	47.3	1.4370
	73	0	0	400/500/6	215	3	0.85	Dynamic	0	3.82	<84	46.9	1.4371
	133	0	0	400/500/6	165	2	0.54						
	149	8.71×10^7	1.81×10^8	400/500/6	437	4	2.23	Static	2.16×10^8	4.03	104	46.8	1.4366
								Dynamic	1.07×10^8	4.14	96	46.8	1.4369
								Dynamic	1.36×10^8	3.89	104	46.9	1.4370
								Dynamic	1.74×10^8	4.06	106	46.8	1.4368
	186	9.49×10^8	2.03×10^8	400/500/6	135	3	1.84	Static	1.07×10^9	4.33	92	46.5	1.4370
								Dynamic	9.67×10^8	4.28	<76	46.9	1.4371
RJ-1													
57-3								Base		56.55	198	33.7	1.4634
	1	0	0	400/500/4	782	0	0.00						
	2	0	0	450/500/4	875	1	0.31						
	3	0	0	500/500/4	900	2	0.54						
	4	0	0	400/500/6	900	0	0.00						
	5	0	0	450/500/6	900	1	0.08						
	7	0	0	450/500/6	857	0	0.00						
	6	0	0	500/500/6	900	0	0.00						
Thermally Stable													
57-5								Base		9.84	126	43.1	1.4466
	15	0	0	400/500/6	60	0	0.00						
	8	0	0	450/500/6	258	4	1.85						

TABLE IX (cont'd)

EVALUATION OF JP-6, RJ-1, RP-1, AND THERMALLY STABLE TYPE FUELS IN THE CFR FUEL COKER

Fuel Designation, ANPF No	Run No	Gamma Dose, ergs/gm Carbon		Test Condition	Goodness Rating	Preheater Deposits		Fuel Sample	Gamma Dose on Fuel Sample, ergs/gm Carbon	Viscosity at -30°F, cs	Flash Point, °F	Gravity, °API	Index of Refraction, n_d^{25}
		Static	CFR Coker Tube			Max	Av						
57-96								Base		4.16	119	46.4	1.4371
	77	0	0	400/500/6	900	0	0.00	Dynamic	0	3.99	92	46.9	-
	131	0	0	400/500/6	802	0	0.00	Dynamic	0	-	-	46.9	1.4372
	132	8.71×10^7	1.81×10^8	400/500/6	515	2	0.68	Static	1.86×10^8	4.05	116	46.8	1.4376
								Dynamic	9.69×10^7	4.06	98	46.8	1.4381
								Dynamic	1.17×10^8	4.42	110	46.7	-
								Dynamic	1.36×10^8	4.99	106	46.8	1.4370
	170	1.01×10^9	2.03×10^8	400/500/6	708	3	1.46	Static	1.20×10^9	-	112	46.7	1.4375
								Dynamic	1.05×10^9	4.23	82	46.8	1.4372
								Dynamic	1.10×10^9	4.05	94	46.8	1.4376
								Dynamic	1.17×10^9	4.32	106	46.8	1.4375
RP-1 57-7								Base		9.81	154	43.8	1.4474
	16	0	0	400/500/6	396	2	0.62						
	32	8.71×10^7	1.07×10^7	400/500/6	75	0	0.00	Static	9.71×10^7	8.10	< 84	43.0	-
	31	8.71×10^7	2.15×10^6	400/500/6	18	2	0.61						
	33	2.26×10^8	6.84×10^6	400/500/6	45	3	1.69						
	83	8.71×10^8	1.59×10^6	400/500/6	122	3	1.56	Static	8.74×10^8	8.63	128	43.2	1.4479
								Dynamic	8.72×10^8	8.14	< 84	43.3	1.4476

TABLE X

PHYSICAL PROPERTIES OF MISCELLANEOUS FUELS

Fuel Designation	I. T. L. Code	Heat Of Combustion, Gross BTU/lb	Gravity,		Viscosity, cs, at:		
			°A P I	Specific	-40°F	0°F	100°F
PLF 960	219	18029	14.1	0.9717	-	-	-
PLF 961	220	19538	32.1	0.8651	-	-	-
PLF 962	221	17916	13.1	0.9784	-	-	-
PLF 963	222	19579	32.2	0.8645	-	-	-
PLF 964	223	19208	31.9	0.8662	-	-	-
PLF 965	224	19556	32.6	0.8621	-	-	-
HTF 1	225	19374	27.8	0.8884	15.96	7.53	2.14
HTF 2	226	18719	18.6	0.9429	Solid	1571.8	15.34
HTF 13	227	19761	42.1	0.8152	Solid	8.20	1.99
HTF 14	228	18656	28.0	0.8870	Solid	23.02	1.70
HTF 15	229	19683	33.6	0.8569	106.1	22.57	3.40
HTF 16	230	19417	28.9	0.8823	2366.0	189.3	8.82
HTF 24	231	19742	41.8	0.8163	Solid	8.92	2.08
HTF 28	232	17916	11.8	0.9872	Solid	85.63	4.54
HTF 30	233	18146	14.2	0.9711	14.92	6.27	1.69
HTF 31	234	19545	27.7	0.8887	Solid	Solid	3.05
K 25 - C	235	19404	27.2	0.8914	25.17	9.66	2.27
F 57 - 15	236	19702	40.3	0.8235	11.95	5.09	1.50
F 57 - 16	237	19870	47.8	0.7890	5.34	2.83	0.90
F-8	238	19906	51.8	0.7719	3.41	1.98	0.88

TABLE XI

PHYSICAL PROPERTIES OF AIRCRAFT TURBINE ENGINE LUBRICANTS ACCORDING TO MIL-L-7808C SPECIFICATION TESTS

Lubricant Designation,		Base Type Oil	Gamma Dose, Static, ergs/gm Carbon	Viscosity, cs at		Pour Point, °F	Flash Point, °F	Fire Point, °F	Foaming Tendency	Evap at 400°F, %	SOD Corrosion Loss, mg/in²	Corrosion, Loss in weight at 400°F, mg/in²		Swelling of Synthetic Rubber, "H" Stock, %	Compatibility	Corrosion And Oxidation Stability, 72 Hours at 347°F								
																Change in Weight, mg/in²					Appearance of Metals	Viscosity change, % at 100°F	Neutralization Number, mg KOH/gm		
Number	Fluid Type Mil Spec			210°F	100°F							Silver	Copper			Al Alloy	Mg Alloy	Steel	Silver	Copper			Initial	Final	Change
ANP 25	7808	Ester	5.91×10^8	3.32	12.83	<-80	430	495	Pass	16.2	-	0.7	1.6	-	Pass	0.08	-2.94	0.10	0.09	-10.12	Fail	41.0	4.88	3.54	-1.34
ANP 55	7808	Ester	4.46×10^8	5.07	19.53	<-80	455	515	Pass	12.3	-	0.6	1.2	-	Pass	0.00	0.01	-0.01	-0.01	-00.16	Pass	1.4	0.80	1.40	0.60
ANP 56	9236	Min.	0	10.61	103.0	- 5	400	435	Pass	28.5	1.4	0.7	1.5	7.9	Pass	0.02	0.02	0.04	0.02	0.00	Pass	36.3	0.03	1.47	1.44
			2.64×10^9	10.12	96.00	0	375	410	-	31.4	-	-	-	-	-	0.11	0.12	0.06	0.22	0.11	Pass	50.0	0.02	0.21	0.19
			6.80×10^9	9.94	93.01	- 5	315	365	-	34.1	-	-	-	-	-	0.13	0.14	0.26	0.15	-0.02	Pass	47.7	0.00	4.21	4.12
			2.64×10^{10}	10.19	93.73	- 5	245	330	-	33.4	-	-	-	-	-	0.02	0.01	0.00	0.00	-1.98	Pass	420.4	0.03	5.70	5.67
ANP 57	9236	Min.	0	10.76	106.3	- 5	395	435	Pass	28.4	1.1	0.6	1.0	1.5	Pass	0.02	0.02	0.02	0.05	-0.46	Pass	55.4	0.02	2.60	2.58
			2.62×10^9	10.72	106.3	0	355	400	-	30.8	-	-	-	-	-	0.02	-0.01	-0.03	-0.01	-0.05	Pass	+85.7	0.01	3.89	3.88
			6.62×10^9	10.97	111.2	0	335	370	-	29.5	-	-	-	-	-	0.00	0.00	0.00	0.00	-1.18	Pass	134.7	0.00	5.42	5.42
			2.63×10^{10}	12.39	132.1	- 5	285	360	-	31.7	-	-	-	-	-	0.00	0.02	0.00	0.02	-0.88	Pass	127.3	0.03	4.67	4.64
ANP 58	9236	Min.	0	7.54	56.3	5	385	415	Pass	-	7.2	0.9	2.4	1.2	Pass	0.01	0.02	0.01	-0.01	-0.14	Pass	98.8	0.01	4.39	4.38
			2.61×10^9	7.45	56.1	5	370	395	-	36.3	-	-	-	-	-	0.00	0.00	0.01	0.01	-0.12	Pass	86.0	0.01	4.03	4.02
			8.71×10^9	7.66	59.05	5	330	370	-	37.0	-	-	-	-	-	0.02	0.02	0.04	0.04	-0.29	Pass	129.2	0.02	5.75	5.73
			2.63×10^{10}	9.03	77.20	- 5	270	365	-	37.1	-	-	-	-	-	-0.02	0.24	-0.16	0.14	0.21	Pass	185.1	0.28	4.74	4.42
ANP 59	9236	Min.	0	7.42	55.3	- 5	390	420	Pass	-	1.7	0.9	2.8	6.1	Pass	0.01	0.02	0.00	-0.01	0.01	Pass	15.26	0.01	0.16	0.15
			2.61×10^9	7.12	52.06	5	355	385	-	36.2	-	-	-	-	-	0.01	0.02	0.00	0.04	0.00	Pass	27.8	0.02	0.57	0.55
			9.23×10^9	6.79	48.66	5	305	365	-	39.1	-	-	-	-	-	0.05	0.09	0.11	0.15	-0.06	Pass	39.6	0.01	2.98	2.97
			2.62×10^{10}	7.02	50.56	0	225	320	-	37.7	-	-	-	-	-	0.02	0.02	0.01	0.00	-1.40	Pass	84.3	0.07	4.27	4.20
ANP 60	9236	Olefin Polym.	0	11.09	117.8	-	355	380	Pass	-	1.2	0.8	0.7	2.0	Pass	0.06	0.05	0.02	0.01	-0.10	Pass	347.9	0.03	7.60	7.57
			2.64×10^9	10.48	110.3	-30	345	355	-	49.1	-	-	-	-	-	0.00	0.01	0.01	0.00	-0.07	Pass	198.8	0.04	5.25	5.21
			8.71×10^9	10.01	103.9	-30	315	330	-	59.7	-	-	-	-	-	0.02	0.18	0.01	0.02	-0.03	Pass	212.0	0.03	5.89	5.86
			2.60×10^{10}	10.93	121.4	-25	240	310	-	58.1	-	-	-	-	-	0.01	0.17	0.04	0.07	6.02	Pass	245.6	0.51	7.16	7.11

TABLE XI (cont'd)

PHYSICAL PROPERTIES OF AIRCRAFT TURBINE ENGINE LUBRICANTS ACCORDING TO MIL-L-7808C SPECIFICATION TESTS

Lubricant Designation,		Base Type Oil	Gamma Coss, Static, ergs/gm Carbon	Viscosity, cs at		Pour Point, °F	Flash Point, °F	Fire Point, °F	Foaming Tendency	Evap at 400°F, %	SOD Corrosion Loss, mg/in²	Corrosion, Loss in weight at 400°F, mg/in²		Swelling of Synthetic Rubber, "H" Stock, %	Compatibility	Corrosion And Oxidation Stability, 72 Hours at 347°F									
																Change in Weight, mg/in²					Appearance of metals	Viscosity change, % at 100°F	Neutralization Number, mg KOH/gm		
Number	Fluid Type Mil Spec			210°F	100°F							Silver	Copper			Al Alloy	Mg Alloy	Steel	Silver	Copper			Initial	Final	Change
ANP 61	9236	Olefin Polym.	0	10.85	113.0	-35	340	370	Pass	59.5	0.5	0.5	0.8	8.3	Pass	-0.07	0.08	0.00	0.14	0.07	Pass	11.0	0.01	0.12	0.11
			8.71×10^9	-	-	-	-	-	-	53.3	-	-	-	-	-	-	-	-	-	-	-	-	-	-	-
			2.60×10^9	9.39	89.39	-35	315	350	-	55.1	-	-	-	-	-	0.01	0.02	0.01	0.02	0.02	Pass	24.2	0.03	0.06	0.03
			1.02×10^{10}	7.54	63.21	-40	270	295	-	63.1	-	-	-	-	-	0.00	0.01	0.02	0.02	-0.04	Pass	71.2	0.03	2.59	2.56
			2.64×10^{10}	6.08	41.53	-55	140	255	-	62.8	-	-	-	-	-	0.02	0.04	0.04	0.02	-0.09	Pass	160.3	0.072	5.49	5.42
ANP 62	25336	Min.	0	5.05	26.1	-60	345	360	Fail	71.3	26.0	1.9	8.1	10.4	Pass	-0.03	0.05	0.02	0.05	0.05	Pass	7.0	0.36	0.90	0.54
			2.66×10^9	4.00	21.92	-50	315	335	-	78.7	-	-	-	-	-	0.14	0.14	0.11	0.13	0.38	Pass	12.5	0.27	1.44	1.17
			8.68×10^9	4.20	23.69	-65	305	335	-	76.2	-	-	-	-	-	0.15	0.16	0.01	0.05	-1.74	Pass	15.8	0.38	5.28	4.90
			2.61×10^{10}	5.39	39.20	-50	330	360	-	68.0	-	-	-	-	-	0.00	0.00	-0.20	0.00	-0.10	Pass	-3.6	0.12	0.41	0.29
ANP 63	Nuclear	Ester	0	-	17.59	<-75	430	485	Pass	14.5	0.2	0.6	2.1	27.3	Pass	0.02	0.00	6.02	0.01	-0.03	Pass	0.4	0.22	1.61	1.39
			2.55×10^9	3.76	14.47	<-75	365	470	-	23.2	-	-	-	-	-	0.00	-0.06	-0.02	0.07	-7.32	Fail	52.0	1.34	7.21	5.87
			8.80×10^9	3.96	15.82	<-75	305	460	-	21.6	-	-	-	-	-	-0.02	-1.80	-0.01	-0.04	-21.79	Fail	101.8	2.92	8.08	5.16
			2.61×10^{10}	5.49	25.94	<-80	205	440	-	26.2	-	-	-	-	-	0.00	-38.58	-1.86	0.00	-1.18	Fail	228.4	7.17	11.85	4.68
ANP 64	Nuclear	Min.	0	-	83.7	20	500	570	Fail	3.0	0.6	1.1	2.6	5.2	Pass	0.28	0.15	0.00	0.00	0.00	Pass	25.1	0.01	0.71	0.70
			2.60×10^9	10.37	88.84	20	495	565	-	2.6	-	-	-	-	-	0.04	0.04	0.07	0.07	-0.01	Pass	28.9	0.02	2.44	2.42
			8.71×10^9	11.34	100.6	20	505	570	-	4.3	-	-	-	-	-	0.48	0.43	0.16	0.17	-0.35	Pass	34.0	0.01	4.80	4.79
			2.53×10^{10}	14.68	144.6	25	465	560	-	6.3	-	-	-	-	-	0.01	0.01	0.01	0.01	0.01	Pass	63.1	0.03	5.11	5.08
ANP 65	9236	Min.	0	10.50	63.84	-	450	475	Pass	27.3	0.1	6.2	75.0	1.0	Pass	0.06	0.10	0.11	0.39	-0.28	Pass	28.6	1.58	2.78	1.20
			8.71×10^8	7.71	52.33	-30	440	470	-	16.3	-	-	-	-	-	0.07	0.01	0.02	0.39	-3.35	Pass	99.0	1.54	3.91	2.37
			8.80×10^9	7.51	55.26	-20	425	455	-	19.6	-	-	-	-	-	0.01	0.01	0.02	0.10	-0.92	Fail	GEL	0.94	6.47	5.53
			2.62×10^{10}	9.11	72.41	-20	385	455	-	20.1	-	-	-	-	-	0.00	0.02	0.12	0.25	0.08	Pass	32.1	0.59	3.86	3.27
ANP 66	9236	Min.	0	-	40.36	-	-	-	Pass	17.1	0.3	3.5	29.4	1.6	Fail	0.28	0.16	0.13	0.37	-3.48	Fail	8.1	1.42	4.92	3.50
			2.62×10^9	6.23	42.00	-20	400	455	-	21.1	-	-	-	-	-	0.24	0.19	0.21	-0.52	0.33	Pass	7.7	1.09	3.04	1.95
			8.88×10^9	6.61	46.51	-20	400	455	-	23.4	-	-	-	-	-	0.10	0.07	0.04	0.29	-2.32	Pass	91.8	0.81	5.24	4.43
			2.60×10^{10}	8.0	60.15	-20	390	445	-	22.6	-	-	-	-	-	0.01	0.01	0.02	0.21	-1.88	Pass	85.0	0.70	5.44	4.74
ANP 68	7808	Ester	0	3.35	14.20	<-75	450	505	-	13.1	-	-	-	-	-	0.15	4.77	0.06	0.09	-4.76	Fail	14.0	2.59	2.31	-0.28
ANP 74	7808	Ester	0	6.50	24.76	<-75	465	520	-	10.0	0.3	-	-	-	Pass	0.01	0.02	0.02	0.01	0.02	Pass	0.2	0.08	0.92	0.84

TABLE XI (cont'd)

PHYSICAL PROPERTIES OF AIRCRAFT TURBINE ENGINE LUBRICANTS ACCORDING TO MIL-L-7808C SPECIFICATION TESTS

Lubricant Designation,		Base Type Oil*	Gamma Dose, Static, ergs/gm Carbon	Viscosity, cs at		Pour Point, °F	Flash Point, °F	Fire Point, °F	Foaming Tendency	Evap at 400°F, %	S.O.D Corrosion Loss, mg/in²	Corrosion, Loss in weight at 400°F, mg/in²		Swelling of Synthetic Rubber, "H" Stock, %	Compatibility	Corrosion And Oxidation Stability, 72 Hours at 347°F									
Number	Fluid Type Mil Spec			210°F	100°F							Silver	Copper			Change in Weight, mg/in²					Appearance of metals	Viscosity change, % at 100°F	Neutralization Number, mg KOH/gm		
																Al Alloy	Mg Alloy	Steel	Silver	Copper			Initial	Final	Change
ANP 75	25336	Syn.*	0	-	15.10	<-75	455	510	Pass	6.4	3.4	0.00	1.5	21.5	Pass	0.00	0.00	0.0	0.0	0.4	Pass	32.3	1.13	1.76	0.63
ANP 76	9236	Ester	0	-	41.65	-55	490	535	Pass	6.3	3.1	0.01	3.5	34.2	Fail	0.00	0.00	0.0	0.0	0.7	Pass	173.7	0.01	0.40	0.40
ANP 77	25336	Syn.*	0	3.52	13.16	<-75	445	510	Fail	7.1	0.08	0.00	3.1	24.2	Pass	0.00	0.00	0.0	0.0	-0.4	Pass	226.0	0.18	0.78	0.60
ANP 78	9236	Ester	0	-	63.59	-45	555	620	Fail	1.6	16.3	0.00	-0.7	20.2	Fail	0.00	0.00	0.0	0.0	-0.1	Pass	6.9	0.09	0.09	0.00
ANP 79	9236	Ester	0	4.31	18.46	<-75	420	485	Pass	18.7	0.2	1.0	1.0	28.8	Pass	0.00	0.00	0.0	0.0	-0.1	Pass	-25.6	0.01	0.36	0.36
ANP 80	9236	Ester	0	5.42	29.06	-60	465	535	Pass	5.9	1.0	-0.3	-1.3	31.3	Fail	0.00	0.00	0.0	0.0	-0.2	Pass	14.9	0.01	0.52	0.52
GTO 38	7808	Ester	0	-	-	-	-	-	-	-	-	-	-	-	-	-	-	-	-	-	-	-	-	-	-
GTO 303	7808	Ester	0	4.6	17.26	<-75	410	495	Pass	15.4	3.0	0.8	1.6	29.6	Pass	0.00	0.00	0.0	0.0	-0.11	Pass	3.8	0.10	18.05	17.90
GTO 307	7808	Syn.*	0	-	12.82	-	-	-	-	-	-	-	-	-	-	-	-	-	-	-	-	-	0.55	-	-
GTO 309	7808	Ester	0	-	13.10	-	-	-	-	-	-	-	-	-	-	-	-	-	-	-	-	-	0.11	-	-
GTO 313	7808	Ester	0	3.35	17.19	<-75	425	490	Pass	15.3	0.00	5.81	2.21	29.3	Pass	0.01	0.02	0.04	0.09	0.23	Fail	14.2	0.08	11.86	11.78
GTO 513	7808	Syn.*	0	-	-	-	-	-	-	-	-	-	-	-	-	-	-	-	-	-	-	-	0.76	-	-
GTO 519	7808	Syn.*	0	-	-	-	-	-	-	-	-	-	-	-	-	-	-	-	-	-	-	-	0.76	-	-
GTO 578	7808	Ester	0	-	15.18	-	-	-	-	-	-	-	-	-	-	-	-	-	-	-	-	-	0.15	-	-

*Information not available to Inland Testing Laboratories

TABLE XII

OXIDATION AND CORROSION STABILITY TEST, 48 HOURS AT 500°F ACCORDING TO MIL-L-9236A

Lubricant Designation	Weight Loss, mg/cm^2						Appearance of Metals	Viscosity Change, %		Neutralization No. mg KOH/gm	
	Steel	Aluminum	Magnesium	Titanium	Silver	Copper		100°F	210°F	Initial	Final
ANP 75	0.0	0.0	*	0.0	0.0	-3.2	Fail	4.3	-	1.13	4.87
ANP 76	0.0	0.0	-7.3	0.0	0.0	0.1	Fail	2056.1	-	< 0.01	3.52
ANP 77	-0.1	0.0	-33.0	0.0	0.1	0.0	Fail	25.3	-	0.18	7.00
ANP 78	-1.6	0.0	-25.6	0.0	0.0	0.1	Fail	-81.0	-	0.09	14.26
ANP 79	-11.2	0.0	*	0.0	0.0	-0.7	Fail	-	716.9	< 0.01	54.39
ANP 80	-3.9	0.0	-23.2	0.0	-0.1	-0.2	Fail	-	366.3	< 0.01	27.24

*Completely dissolved.

TABLE XIII

PHYSICAL PROPERTIES OF HIGH TEMPERATURE AIRCRAFT TURBINE ENGINE LUBRICATING OILS ACCORDING TO MIL-L-9236A SPECIFICATION TESTS

Lubricant Designation	Base Oil Type	Viscosity cs			Pour Point °F	Flash Point °F	Fire Point °F	Autogenous Ignition Temperature, °F	Evaporation at 400°F %	Neutralization Number mg KOH/gm
		100°F	210°F	400°F						
ANP 69	Ester	38.54	6.83	1.79	-75	485	565	788	3.02	0.08
ANP 70	Polyglycol	64.67	11.09	2.86	-50	530	585	770	4.22	0.01
ANP 71	Mineral	137.7	12.65	2.26	10	530	575	739	3.08	0.01
ANP 72	Ester	152.4	18.32	3.47	-35	560	625	-	1.44	9.10
ANP 73	Mineral	285.3	21:91	3.32	-5	565	620	794	0.80	0.01

TABLE XIV

EVALUATION OF LUBRICANTS IN PANEL COKING TESTS

Lubricant Designation	Run No	Gamma Dose Ergs/gm Carbon		Coking Tendency		Oil Consumption, gm	Lubricant Sample	Gamma Dose on sample, ergs/gm Carbon	Viscosity at 100 °F, cs	Neutralization Number, mg KOH/gm	Flash Point, °F	Fire Point, °F	Specific Gravity	Index of Refraction, n_d^{25}	Evaporation at 400 °F, %
		Static	Dynamic	Panel Temp, °F	Coke, mg										
ANP 25							Base	-	12.83	4.88	430	495	0.9150	1.4504	16.20
	75	5.91×10^8	0	600	21.9	200	Dynamic	5.91×10^8	13.61	28.68	-	-	0.9150	1.4509	-
ANP 55							Base	-	19.53	0.80	455	515	-	1.4509	12.16
	74	4.46×10^8	0	600	15.2	130									
	215	4.46×10^8	1.67×10^8	600	38.7	310	Static	6.02×10^8	-	0.85	-	-	0.9153	1.4514	-
							Dynamic	6.13×10^8	-	0.84	-	-	0.9163	1.4512	-
ANP 56							Base	-	103.00	0.03	400	435	-	-	28.50
	11	0	0	600	571.4	100									
	32	2.64×10^9	0	600	351.5	160									
	57	8.62×10^9	0	600	145.5	65									
	39	2.64×10^{10}	0	600	89.7	140									
ANP 57							Base	-	106.3	0.02	396	435	-	-	28.40
	1	0	0	600	541.8	115									
	17	2.62×10^9	0	600	831.6	100									
	58	8.62×10^9	0	600	451.8	55									
	40	2.63×10^{10}	0	600	207.9	120									
ANP 58							Base	-	56.30	0.01	385	415	-	-	-
	2	0	0	600	196.8	195									
	19	2.61×10^9	0	600	225.9	225									
	59	8.71×10^9	0	600	262.3	140									
	41	2.63×10^{10}	0	600	227.8	205									
ANP 59							Base	-	55.30	0.01	390	420	-	-	-
	3	0	0	600	263.7	265									
	23	2.61×10^9	0	600	117.4	290									
	60	9.23×10^9	0	600	60.1	190									
	92	9.23×10^9	0	600	102.8	175	Static	9.23×10^9	49.64	0.01	-	-	0.8446	1.4714	-
							Dynamic	9.23×10^9	158.1	0.37	-	-	0.8699	1.4815	-
	42	2.62×10^{10}	0	600	121.4	255									
ANP 60							Base	-	117.8	0.03	355	380	-	-	-
	4	0	0	600	118.2	205									
	22	2.64×10^9	0	600	22.9	240									
	61	8.71×10^9	0	600	61.8	170									
	93	8.71×10^9	0	600	68.6	285									
	44	2.60×10^{10}	0	600	175.7	224									

TABLE XIV (cont'd)

EVALUATION OF LUBRICANTS IN PANEL COKING TESTS

Lubricant Designation	Run No.	Gamma Dose, Ergs/gm Carbon		Coking Tendency		Oil Consumption, ml	Lubricant Sample	Gamma Dose on sample, ergs/gm Carbon	Viscosity at 100 °F, cs	Neutralization Number, mg KOH/gm	Flash Point, °F	Fire Point, °F	Specific Gravity	Index of Refraction, n_D^{25}	Evaporation at 400 °F, %
		Static	Dynamic	Panel Temp, °F	Coke, mg										
ANP 61							Base	-	113.0	0.01	340	370	-	-	89.50
	10	0	0	600	2.7	190									
	222	9.50×10^9	1.80×10^8	600	87.7	400	Static	9.51×10^9	75.29	< 0.01	-	-	0.8348	1.4670	-
							Dynamic	9.68×10^9	591.6	0.09	-	-	-	1.4749	-
	18	2.60×10^9	0	600	54.1	240									
	68	1.02×10^{10}	0	600	43.1	250									
	47	2.64×10^{10}	0	600	6.7	253									
	72	2.64×10^{10}	0	700	743.9	165									
	53	2.64×10^{10}	1.40×10^8	600	6.7	370	Static	2.65×10^{10}	41.71	3.12	-	-	0.8347	1.4657	57.91
							Dynamic	2.65×10^{10}	414.2	0.23	-	-	0.8619	1.4790	28.30
	70	2.65×10^{10}	1.27×10^8	700	414.5	500	Dynamic	2.65×10^{10}	458.8	3.58	-	-	0.8673	1.4814	31.30
ANP 62							Base	-	26.10	0.36	345	360	-	-	71.30
	5	0	0	600	52.1	420									
	25	2.66×10^9	0	600	44.9	470									
	64	8.68×10^9	0	600	46.6	315									
	31	2.61×10^{10}	0	600	39.4	345									
ANP 63							Base	-	17.59	0.22	430	485	-	1.4509	14.50
	6	0	0	600	63.2	265									
	217	5.87×10^7	1.68×10^8	600	61.5	40	Static	2.11×10^8	-	14.08	405	-	0.9242	1.4522	11.10
							Dynamic	2.27×10^8	-	32.53	-	-	0.9324	1.4510	-
	25	2.55×10^9	0	600	15.7	260									
	55	2.55×10^9	1.40×10^8	600	23.1	220	Static	2.67×10^9	14.42	1.33	-	-	-	1.4516	-
							Dynamic	2.69×10^9	17.79	1.60	-	-	0.9238	1.4581	-
	78	2.59×10^9	1.67×10^8	600	47.3	370	Static	2.74×10^9	16.15	1.54	455	485	-	1.4524	-
							Dynamic	2.76×10^9	16.60	1.68	-	-	0.9110	1.4525	-
	214	2.69×10^9	1.67×10^8	700	1026.0	440	Static	2.84×10^9	-	4.06	-	-	0.9242	1.4522	-
							Dynamic	2.86×10^9	-	8.93	-	-	0.9324	1.4510	-
	65	8.80×10^9	0	600	110.1	145									
	38	2.61×10^{10}	0	600	97.0	225									
ANP 64							Base	-	83.70	0.01	500	570	-	-	3.00
	7	0	0	600	482.2	65									
	204	5.20×10^7	1.67×10^8	600	1047.8	230	Static	2.05×10^8	84.85	0.06	525	585	0.8658	1.4806	3.30
							Dynamic	2.19×10^8	187.8	1.24	-	-	0.8872	1.4875	-
	26	2.60×10^9	0	600	293.1	40									
	66	8.71×10^9	0	600	351.0	10									
	67	8.71×10^9	0	700	899.3	100									
	52	2.53×10^{10}	0	600	96.2	8									

TABLE XIV (cont'd)

EVALUATION OF LUBRICANTS IN PANEL COKING TESTS

Lubricant Designation	Run No	Gamma Dose, Ergs/gm Carbon		Coking Tendency		Oil Consumption, ml	Lubricant Sample	Gamma Dose on sample, ergs/gm Carbon	Viscosity at 100 °F, cs	Neutralization Number, mg KOH/gm	Flash Point, °F	Fire Point, °F	Specific Gravity	Index of Refraction, n_d^{25}	Evaporation at 400 °F, %
		Static	Dynamic	Panel Temp, °F	Coke, mg										
ANP 65							Base	-	63.84	1.58	450	475	-	-	27.30
	8	0	0	600	459.4	90									
	27	8.71×10^8	0	600	39.4	190									
	28	8.71×10^8	0	700	1069.1	600									
	62	8.80×10^9	0	600	42.1	80									
	54	2.62×10^{10}	0	600	135.7	35									
ANP 66							Base	-	40.36	1.42	-	-	-	-	17.10
	9	0	0	600	597.9	220									
	29	2.62×10^9	0	600	59.0	210									
	63	8.88×10^9	0	600	32.6	115									
	56	2.60×10^{10}	0	600	12.6	105									
	73	2.60×10^{10}	0	700	352.9	380									
ANP 68							Base	-	14.20	2.59	450	505	-	1.4540	13.11
	50	0	0	600	60.7	240									
ANP 69							Base	-	38.54	0.08	485	465	-	1.4574	3.02
	220	8.71×10^7	1.67×10^7	600	31.6	90	Static	1.13×10^8	38.60	0.46	495	560	0.8982	1.4581	2.70
							Dynamic	2.54×10^8	66.11	28.81	-	-	0.9189	1.4615	-
	12	0	0	700	478.2	490									
	45	0	0	700	268.7	368									
	50	0	1.40×10^8	700	406.1	250									
	105	1.68×10^9	2.30×10^8	700	205.9	430	Static	1.75×10^9	37.07	0.61	520	575	0.8988	1.4581	3.98
							Dynamic	1.92×10^9	71.96	8.15	-	-	0.9245	1.4635	-
	71	8.97×10^7	1.27×10^8	700	130.0	410	Static	1.86×10^8	38.82	0.29	-	-	0.9029	1.4586	3.28
							Dynamic	2.17×10^8	65.42	5.88	-	-	-	1.4630	-
	230	8.88×10^9	1.90×10^8	700	289.3	380	Static	8.94×10^9	42.67	1.66	440	-	0.8998	1.4589	-
							Dynamic	9.07×10^9	94.04	9.97	-	-	0.9290	1.4652	
ANP 70							Base	-	64.67	0.01	530	585	-	1.4504	4.22
	13	0	0	700	37.5	700									
	35	0	1.04×10^8	700	126.2	460									
	77	3.27×10^8	1.67×10^8	700	79.9	670	Static	4.61×10^8	65.03	-	-	-	0.9880	-	-
							Dynamic	4.94×10^8	73.15	0.66	-	-	0.9950	1.4522	3.10
	203	8.36×10^7	1.67×10^8	700	48.9	660	Static	2.37×10^8	66.52	0.08	510	595	0.9863	1.4501	2.90
							Dynamic	2.51×10^8	77.41	0.70	-	-	0.9972	1.4531	-
	221	8.70×10^9	1.80×10^8	700	151.6	555	Static	8.76×10^9	80.26	0.10	480	575	0.9891	1.4520	-
							Dynamic	8.89×10^9	104.1	3.58	490	565	1.0600	1.4576	-

TABLE XIV (cont'd)

EVALUATION OF LUBRICANTS IN PANEL COKING TESTS

Lubricant Designation	Run No	Gamma Dose Ergs/gm Carbon		Coking Tendency		Oil Consumption, ml	Lubricant Sample	Gamma Dose on sample, ergs/gm Carbon	Viscosity at 100 °F, cs	Neutralization Number, mg KOH/gm	Flash Point, °F	Fire Point, °F	Specific Gravity	Index of Refraction, 25 n_d	Evaporation at 400 °F, %
		Static	Dynamic	Pane. Temp, °F	Coke, mg										
ANP 71							Base	-	137.7	0.01	530	575	-	1.4837	3.08
	16	0	0	700	1307.2	205									
	49	0	1.40×10^8	700	911.9	270	Static	1.27×10^8	138.1	1.47	535	565	0.8784	1.4843	2.90
							Dynamic	1.40×10^8	357.8	1.87	-	-	-	1.4926	-
	106	1.06×10^9	1.00×10^8	700	769.2	715	Static	1.11×10^9	140.3	0.02	-	-	0.8541	1.4848	2.69
							Dynamic	1.15×10^9	150.5	2.36	-	-	0.8850	1.4905	-
	223	$8.97 \times 10^{9*}$	1.90×10^8	700	346.9	90	Static	9.28×10^9	151.8	< 0.01	525	-	-	1.4850	1.95
							Dynamic	1.00×10^{10}	293.3	0.09	-	-	-	1.4906	-
ANP 72							Base	-	152.4	9.10	560	625	-	1.4608	1.44
	14	0	0	700	3310.0	55									
	43	0	1.40×10^8	700	2829.3	60	Static	1.27×10^8	1351.0	1.84	-	-	1.0036	1.4619	0.90
							Dynamic	1.40×10^8	372.7	10.81	-	-	1.0493	1.4790	-
	100	1.55×10^9	1.18×10^8	700	451.5	290									
	225	1.03×10^{10}	1.18×10^8	700	4717.5	90	Static	1.04×10^{10}	283.2	14.08	-	-	-	1.4634	3.20
							Dynamic	1.05×10^{10}	GEL	9.69	-	-	-	1.4765	-
ANP 73							Base	-	285.3	0.01	565	620	-	1.4822	0.80
	218	3.15×10^7	1.68×10^8	600	137.5	40	Static	1.86×10^8	283.3	< 0.01	-	-	0.8709	1.4829	-
							Dynamic	2.00×10^8	492.2	7.55	-	-	0.8889	1.4860	1.80
	36	0	1.04×10^8	700	1356.2	130									
	15	0	0	700	23.2	60									
	202	2.82×10^7	2.30×10^8	700	470.0	100	Static	7.58×10^7	284.9	0.03	-	-	0.8725	1.4827	2.60
							Dynamic	2.58×10^8	1382.0	3.24	-	-	0.9052	1.4940	-
	101	1.05×10^9	1.18×10^8	700	36.0	140	Dynamic	1.17×10^9	1645.4	3.71	-	-	0.9040	1.4928	-
	224	8.41×10^7	1.68×10^8	700	48.4	150	Static	8.45×10^9	312.6	0.01	560	620	-	1.4835	0.52
							Dynamic	8.58×10^9	1308.0	2.84	580	630	-	1.4940	-
ANP 74							Base	-	24.76	0.08	465	520	-	1.4498	9.95
	37	0	0	600	48.3	250									
	46	0	1.40×10^8	600	19.1	100	Static	1.27×10^8	23.74	0.16	-	-	0.9094	1.4509	7.63
							Dynamic	1.40×10^8	27.92	0.40	-	-	0.9004	1.4509	-
	205	3.18×10^8	1.67×10^8	600	32.2	180	Static	4.49×10^8	18.91	0.34	475	535	0.9082	1.4511	-
							Dynamic	4.85×10^8	20.74	-	-	-	0.9070	1.4509	-
	226	9.46×10^9	1.40×10^8	700	227.2	660	Static	9.51×10^9	24.35	7.58	435	-	-	1.4581	-
							Dynamic	9.60×10^9	29.42	9.61	-	-	-	1.4610	-

*Post Irradiated after dynamic test 8.80×10^8 ergs/gm carbon.

TABLE XIV (cont'd)

EVALUATION OF LUBRICANTS IN PANEL COKING TESTS

Lubricant Designation	Run No	Gamma Dose, Ergs/gm Carbon		Coking Tendency		Oil Consumption, ml	Lubricant Sample	Gamma Dose on sample, ergs/gm Carbon	Viscosity at 100 °F, cs	Neutralization Number, mg KOH/gm	Flash Point, °F	Fire Point, °F	Specific Gravity	Index of Refraction, n_d^{25}	Evaporation at 400 °F, %
		Static	Dynamic	Panel Temp, °F	Coke, mg										
ANP 75							Base	-	15.10	1.13	455	510	-	1.4515	6.35
	82	0	0	600	85.0	285	Dynamic	0	15.69	1.78	470	510	0.9087	1.4511	-
	94	0	0	700	2007.7	805									
	206	8.36×10^7	1.67×10^8	600	68.7	190	Static	2.34×10^8	14.53	1.45	470	505	0.9040	1.4509	7.90
							Dynamic	2.51×10^8	16.01	1.68	-	-	0.9050	1.4513	-
	83	1.04×10^8	1.67×10^8	600	92.9	325	Static	2.53×10^8	14.75	1.55	-	-	0.9139	1.4510	1.85
							Dynamic	2.71×10^8	15.84	1.97	-	-	0.9119	1.4516	-
	219	$8.71 \times 10^{7*}$	2.87×10^8	700	1415.3	520	Dynamic	$5.74 \times 10^{8*}$	-	19.53	620	495	0.9200	1.4539	-
	200	1.31×10^9	1.18×10^8	700	218.1	380	Static	1.36×10^9	15.67	1.19	375	465	0.9236	1.4515	13.05
							Dynamic	1.43×10^9	17.22	13.06	-	-	0.9282	1.4516	-
ANP 76							Base	-	41.65	< 0.01	490	535	-	-	6.34
	84	0	0	600	46.7	105	Static	0	-	-	-	-	0.9117	-	-
							Dynamic	0	64.34	0.22	-	-	1.0060	1.4610	-
	95	0	0	700	39.8	317									
	85	8.34×10^7	1.67×10^8	600	30.0	340	Static	2.34×10^8	42.41	0.04	495	555	0.9798	1.4604	5.75
							Dynamic	2.51×10^8	62.41	0.37	-	-	1.0580	1.4605	-
	201	1.50×10^9	1.18×10^8	700	67.2	220	Static	1.58×10^9	42.76	0.91	-	-	0.9751	1.4590	-
							Dynamic	1.62×10^9	95.93	3.82	490	560	1.0263	1.4641	7.65
	227	9.58×10^9	1.90×10^8	700	35.0	340	Static	9.64×10^9	46.40	3.19	410	-	0.9841	1.4606	2.70
							Dynamic	9.77×10^9	140.0	6.70	-	-	1.4430	1.4715	-
ANP 77							Base	-	13.16	0.18	445	510	-	-	-
	79	0	0	600	4.1	220	Dynamic	0	13.65	0.22	-	-	0.9188	1.4500	-
	96	0	0	700	890.4	345									
	86	8.34×10^7	1.67×10^8	600	17.0	110	Static	2.34×10^8	13.20	1.29	445	505	-	1.4508	6.95
							Dynamic	2.51×10^8	13.72	1.08	-	-	-	1.4505	-
	208	6.27×10^7	1.67×10^8	600	14.6	140	Static	2.14×10^8	13.25	1.02	-	-	0.9157	1.4507	9.00
							Dynamic	2.30×10^8	13.84	0.65	-	-	0.9177	1.4500	-
	107	1.44×10^9	1.18×10^8	700	1219.7	325	Static	1.51×10^9	15.11	5.57	410	495	0.9251	1.4512	-
							Dynamic	1.56×10^9	16.20	6.01	-	-	0.9275	1.4516	-
	228	8.71×10^9	1.90×10^8	700	603.9	275	Static	8.77×10^9	16.28	10.23	-	-	-	1.4533	-
							Dynamic	8.90×10^9	-	17.62	-	-	0.9427	1.4584	-

*Post Irradiated after dynamic test 2.00×10^8 ergs/gm carbon.

TABLE XIV (cont'd)

EVALUATION OF LUBRICANTS IN PANEL COKING TESTS

Lubricant Designation	Run No	Gamma Dose, Ergs/gm Carbon		Coking Tendency		Oil Consumption, ml	Lubricant Sample	Gamma Dose on sample, ergs/gm Carbon	Viscosity at 100 °F, cs	Neutralization Number, mg KOH/gm	Flash Point, °F	Fire Point, °F	Specific Gravity	Index of Refraction, n_d^{25}	Evaporation at 400 °F, %
		Static	Dynamic	Panel Temp, °F	Coke, mg										
ANP 78							Base	-	63.59	0.09	555	620	-	1.4566	1.55
	97	0	0	600	16.7	25	Dynamic	0	-	-	-	-	1.2490	-	-
	80	0	0	700	22.6	130									
	87	8.34×10^7	1.67×10^8	600	8.8	90	Static	2.34×10^8	61.24	0.16	-	-	1.0126	1.4565	1.05
							Dynamic	2.51×10^8	100.4	2.91	-	-	1.3100	1.4581	-
	88	7.32×10^7	1.67×10^8	700	28.3	210	Static	2.25×10^8	61.73	0.21	585	640	1.0118	1.4621	2.11
							Dynamic	2.40×10^8	188.5	3.60	-	-	1.4410	1.4566	-
	209	6.27×10^7	1.67×10^8	600	13.7	10	Static	2.14×10^8	61.98	0.13	545	625	1.0105	1.4569	-
							Dynamic	2.30×10^8	82.75	1.04	-	-	1.0188	1.4565	-
	212	1.74×10^6	1.67×10^8	600	26.6	200	Static	1.55×10^8	-	0.56	-	-	1.1330	1.4518	-
							Dynamic	1.70×10^8	-	3.57	-	-	1.0423	1.4618	-
	229	9.19×10^9	1.20×10^8	700	51.6	260	Static	9.29×10^9	80.10	3.18	530	-	-	1.4574	3.25
							Dynamic	9.31×10^9	469.9	7.55	420	485	-	1.4498	18.72
ANP 79							Base	-	18.46	< 0.01	420	485	-	1.4498	18.72
	90	0	0	600	15.7	155									
	108	0	0	700	55.6	515									
	89	9.93×10^7	1.50×10^8	600	15.1	240	Static	2.39×10^8	-	-	-	-	0.9664	-	-
							Dynamic	2.49×10^8	-	-	-	-	0.9970	-	-
	210	8.36×10^7	1.67×10^8	600	49.5	180	Static	2.34×10^8	18.64	0.12	440	485	0.9642	1.4500	1.80
							Dynamic	2.51×10^8	25.81	0.09	-	-	0.9736	1.4518	-
	216	8.38×10^7	1.68×10^8	600	30.3	310	Static	2.34×10^8	-	0.11	425	-	0.9710	1.4496	15.15
							Dynamic	2.52×10^8	-	< 0.01	-	-	0.9826	1.4516	-
	99	0*	1.67×10^8 *	700	221.2	470	Static	4.07×10^8*	26.71	2.14	430	505	0.9647	1.4513	12.80
							Dynamic	4.18×10^8	35.39	2.88	-	-	0.9787	1.4528	-
	102	1.80×10^9	1.18×10^8	700	145.4	550	Static	1.81×10^9	19.13	0.12	425	495	0.9671	1.4494	12.00
							Dynamic	1.92×10^9	49.76	2.38	-	-	0.9998	1.4555	-
	232	8.68×10^9	1.80×10^8	700	152.0	450	Static	8.73×10^9	24.59	3.84	345	-	-	1.4515	13.20
							Dynamic	8.86×10^9	122.4	5.58	-	-	1.0200	1.4634	5.85

*Post Irradiated after dynamic test 2.51×10^8 ergs/gm Carbon.

TABLE XIV (cont'd)

EVALUATION OF LUBRICANTS IN PANEL COKING TESTS

Lubricant Designation	Run No	Gamma Dose, Ergs/gm Carbon		Coking Tendency		Oil Consumption, ml	Lubricant Sample	Gamma Dose on sample, ergs/gm Carbon	Viscosity at 100 °F, cs	Neutralization Number, mg KOH/gm	Flash Point, °F	Fire Point, °F	Specific Gravity	Index of Refraction, n_d^{25}	Evaporation at 400 °F, %
		Static	Dynamic	Panel Temp, °F	Coke, mg										
ANP 80							Base	-	29.06	< 0.01	465	535	-	1.4556	-
	91	0	0	600	10.7	250									
	109	0	0	700	65.6	390	Dynamic	0	81.50	2.42	-	-	1.0202	1.4623	-
	104	5.80×10^7	1.18×10^8	700	178.6	200									
	211	8.36×10^7	1.67×10^8	600	4.3	310	Static	2.34×10^8	-	0.24	-	-	0.9970	1.4546	-
							Dynamic	2.51×10^8	-	3.04	-	-	0.9965	1.4540	-
	213	8.36×10^7	1.67×10^8	700	119.2	360	Static	2.34×10^8	-	0.24	-	-	1.0044	1.4558	-
							Dynamic	2.51×10^8	28.99	3.04	-	-	1.0278	1.4616	-
	98	1.67×10^8	1.67×10^8	600	16.8	100	Static	3.12×10^8	29.84	0.06	-	-	0.9979	1.4540	4.05
							Dynamic	3.34×10^8	32.57	0.12	-	-	0.9934	1.4544	-
	231	1.37×10^{10}	2.00×10^8	700	201.0	330	Static	1.38×10^{10}	42.04	3.40	415	-	-	1.4571	4.60
							Dynamic	1.39×10^{10}	185.1	4.11	-	-	1.0381	1.4666	-
GTO 313							Base	-	17.19	0.08	425	490	-	-	15.30
	33	0	0	600	19.4	205									
	110	0	0	700	1830.2	595									
GTO 373							Base	-	-	0.76	-	-	-	-	-
	111	0	0	700	2240.0	650									
	20	0	0	600	17.7	295									
	76	0	0	600	7.2	160									
GTO 519							Base	-	22.68	0.76	-	-	-	-	-
	21	0	0	600	8.1	250									
	81	0	0	600	29.2	205									

TABLE XV

EVALUATION OF LUBRICANTS IN THE WADC DEPOSITION TESTER

Lubricant Designation	Run No	Gamma Dose, Ergs/gm Carbon		Deposit Weight, gms		Deposition Number	Oil Consumption, ml	Oil Out Temp, °F		Pump Pressure Increase in 12 hrs, PSI	Oil Sample	Viscosity at 100 °F, cs	Neutralization Number, mg KOH/gm	Flash point, °F	Fire point, °F	Specific gravity	Index of refraction, n_d^{25}	Evaporation at 400 °F, %
		Static	Dynamic	Coke	Sludge			1 hr	12 hr									
ANP 25											Base	12.83	3.54	430	495	0.9150	1.4504	16.20
	46	5.91×10^8	0	0.120	1.350	2.550	70	447	453	0.20	Dynamic	27.93	33.34	-	-	-	1.4573	-
	86	5.91×10^8	1.77×10^8	0.185	0.890	2.740	120	425	425	0.75	Dynamic	28.09	33.34	-	-	-	-	-
ANP 55											Base	19.53	0.80	455	515	-	1.4509	12.26
	44	4.46×10^8	0	0.525	0.490	5.740	100	450	400	0.25	Dynamic	43.19	2.68	-	-	-	1.4641	-
	47	4.46×10^8	0	0.210	0.600	2.700	135	438	443	0.05	Dynamic	25.93	27.22	-	-	0.9383	1.4599	-
	85	4.46×10^8	1.54×10^8	0.255	0.725	3.280	100	433	417	0.15	Static	17.75	0.93	455	505	0.9073	1.4507	7.20
											Dynamic	33.83	23.44	-	-	0.9493	1.4605	-
ANP 56											Base	103.0	0.03	400	435	-	-	28.50
	21	2.64×10^9	0	0.435	6.645	10.995	110	435	394	2.40	Dynamic	34.33	4.51	-	-	-	-	-
ANP 58											Base	56.3	0.01	385	415	-	-	-
	24	2.63×10^{10}	0	0.215	0.700	2.800	180	430	415	0.40	Dynamic	80.71	6.70	-	-	-	-	-
ANP 39											Base	55.3	0.01	390	420	-	-	-
	66	9.23×10^9	0	0.800	4.130	12.150	130	430	329	4.25	Static	48.71	0.01	-	-	0.8458	1.4714	-
											Dynamic	147.1	4.26	-	-	0.8751	1.4801	
ANP 60											Base	117.8	0.03	355	380	-	-	-
	62	0	0	0.205	0.690	2.740	200	420	370	0.80	Dynamic	915.7	5.24	-	-	0.8959	1.4844	-
	22	2.64×10^9	0	0.700	0.890	7.890	135	412	395	0.00	Dynamic	311.7	0.68	-	-	-	-	-
ANP 61											Base	113.0	0.01	340	370	-	-	59.50
	48	0	0	0.250	0.050	2.550	140	425	430	0.25	Dynamic	338.9	3.12	-	-	-	-	-
	76	0	1.76×10^8	0.360	0.870	4.470	135	430	380	0.40	Static	108.1	<0.01	-	-	0.8351	1.4679	-
											Dynamic	227.4	3.40	365	410	-	1.4727	-
	93	9.49×10^9	9.00×10^7	0.220	1.000	3.200	90	430	420	0.45	Static	75.67	<0.01	370	-	0.8350	1.4668	55.70
											Dynamic	280.1	14.40	350	380	0.8729	1.4755	-
	41	1.02×10^{10}	0	0.225	1.050	3.300	160	451	435	0.50	Dynamic	328.5	0.47	-	-	-	1.4769	-
	43	2.64×10^{10}	0	0.070	0.655	1.355	170	431	440	0.10	Dynamic	205.8	0.96	-	-	-	1.4744	
	27	2.64×10^{10}	0	0.055	0.552	1.102	155	440	444	0.15	Dynamic	332.6	3.48	-	-	0.8745	1.4760	

TABLE XV (cont'd)

EVALUATION OF LUBRICANTS IN THE WADC DEPOSITION TESTER

Lubricant Designation	Run No	Gamma Dose, Ergs/gm Carbon		Deposit Weight, gms		Deposition Number	Oil Consumption, ml	Oil Out Temp, °F		Pump Pressure Increase in 12 hrs, PSI	Oil Sample	Viscosity at 100 °F, cs	Neutralization Number, mg KOH/gm	Flash point, °F	Fire point, °F	Specific gravity	Index of refraction, n_d^{25}	Evaporation at 400 °F, %
		Static	Dynamic	Coke	Sludge			1 hr	12 hr									
ANP 62											Base	26.10	0.36	345	360	-	-	71.30
	20	2.66×10^9	0	0.700	3.660	10.660	100	438	418	0.25	Dynamic	39.94	2.72	-	-	-	-	-
	38	8.68×10^9	0	0.317	5.320	8.490	225	411	410	0.20	Dynamic	40.89	3.49	-	-	-	1.4830	-
	31	2.61×10^{10}	0	1.980	2.145	21.945	40	411	429	0.35	Dynamic	GEL	6.22	-	-	GEL	1.4880	-
	84	2.61×10^{10}	1.70×10^8	1.180	1.550	13.350	65	428	418	0.55	Static	39.69	0.02	310	360	0.8782	1.4841	64.02
											Dynamic	GEL	7.46	-	-	-	1.4229	-
ANP 63											Base	17.59	0.22	430	485	-	1.4509	14.50
	110	0	2.90×10^8	0.220	0.660	2.860	45	390	387	0.00	Static	13.23	0.22	430	455	0.9165	1.4496	-
											Dynamic	17.43	13.02	-	-	0.9319	1.4522	-
	19	2.55×10^9	0	0.190	0.590	2.490	90	422	460	0.05	Dynamic	47.07	41.30	-	-	-	-	-
	25	2.55×10^9	0	0.130	0.660	1.960	45	437	450	-0.05	Dynamic	39.17	35.48	-	-	-	-	-
	39	8.80×10^9	0	0.335	0.635	4.185	100	450	445	0.15	Dynamic	56.20	41.30	-	-	-	-	-
	83	8.80×10^9	1.76×10^8	0.180	0.550	2.350	80	435	430	0.15	Static	16.14	3.10	310	470	0.9166	1.4524	18.70
											Dynamic	30.13	20.86	-	-	0.9457	1.4590	-
	63	2.61×10^{10}	0	0.420	0.772	4.972	250	451	435	0.25	Dynamic	15.37	15.88	-	-	0.9140	1.4581	-
ANP 64											Base	83.70	0.01	500	570	-	-	3.00
	65	0	0	0.060	1.825	2.425	120	444	365	0.70	Static	73.12	0.03	-	-	0.8650	1.4805	-
											Dynamic	209.0	6.50	-	-	0.8958	1.4870	-
	80	0	1.54×10^8	0.580	0.840	6.640	70	400	358	0.40	Static	82.31	0.02	530	580	0.8657	1.4802	2.70
											Dynamic	351.8	6.18	-	-	0.9072	1.4920	-
	78*	0	1.77×10^8	0.350	1.475	4.975	90	385	360	0.05	Static	83.33	0.02	-	-	0.8634	1.4803	2.40
											Dynamic	100.6	1.04	-	-	0.8737	1.4815	-
	40	8.71×10^9	0	0.155	0.733	2.283	75	425	405	0.40	Dynamic	527.6	7.78	-	-	0.9112	1.4885	-
	30	2.53×10^{10}	0	0.210	1.045	3.145	100	430	344	0.85	Dynamic	1954.0	7.33	-	-	0.9199	1.5017	-
ANP 65											Base	63.84	1.58	450	475	-	-	27.30
	36	8.80×10^9	0	0.950	24.295	33.795	60	446	265	2.40	Dynamic	GEL	6.53	-	-	GEL	-	-
ANP 66											Base	40.56	1.42	-	-	-	-	17.10
	37	8.88×10^9	0	0.330	0.965	4.265	55	428	429	0.20	Dynamic	GEL	7.94	-	-	GEL	1.4880	-
	32	2.60×10^{10}	0	0.270	0.917	3.617	110	418	442	0.15	Dynamic	490.6	7.35	-	-	-	1.4945	-
ANP 68											Base	14.20	2.59	450	505	-	1.4540	13.11
	42	0	0	0.445	1.485	5.935	90	436	401	1.00	Dynamic	16.41	9.38	-	-	-	-	-
	79	0	1.77×10^8	0.250	1.060	3.560	50	420	398	1.10	Static	12.24	2.78	-	-	0.9150	1.4542	-
											Dynamic	16.11	8.32	-	-	0.9255	1.4542	-

*Test interrupted 1-1/2 hrs. to repair coupling

TABLE XV (cont'd)

EVALUATION OF LUBRICANTS IN THE WADC DEPOSITION TESTER

Lubricant Designation	Run No	Gamma Dose, Ergs/gm Carbon		Deposit Weight, gms		Deposition Number	Oil Consumption, ml	Oil Out Temp, °F		Pump Pressure Increase in 12 hrs, PSI	Oil Sample	Viscosity at 100 °F, cs	Neutralization Number, mg KOH/gm	Flash point, °F	Fire point, °F	Specific gravity	Index of refraction, n_d^{25}	Evaporation at 400 °F, %
		Static	Dynamic	Coke	Sludge			1 hr	12 hr									
ANP 69																		
											Base	38.54	0.08	485	565	-	1.4574	3.02
	23	0	0	0.150	0.800	2.300	70	417	429	0.10	Dynamic	71.19	17.72	-	-	-	-	-
	53	0	1.76×10^8	0.270	0.650	3.350	105	420	440	0.10	Static	37.84	0.16	-	-	-	1.4585	-
											Dynamic	85.15	21.00	-	-	-	1.4649	-
	73	1.05×10^9	1.77×10^8	0.165	0.715	2.370	150	425	442	0.20	Static	38.85	0.40	-	-	0.8986	1.4580	4.19
											Dynamic	106.5	23.56	-	-	0.9427	1.4629	-
	101	1.30×10^{10}	1.76×10^8	0.145	0.685	2.140	80	395	395	0.20	Static	55.09	3.04	405	-	-	1.4594	6.35
											Dynamic	140.3	22.62	-	-	0.9053	1.4689	-
ANP 70																		
											Base	64.67	0.01	530	585	-	1.4504	4.22
	16	0	0	0.090	0.700	1.600	95	410	413	0.00	Dynamic	55.21	3.13	-	-	-	-	-
	18	0	0	0.200	0.790	2.790	125	402	417	-0.15	Dynamic	63.88	2.38	-	-	-	1.4555	-
	57	1.09×10^9	1.80×10^8	0.855	0.560	0.110	160	375	375	0.15	Dynamic	60.91	2.12	-	-	-	-	-
	50	0	1.76×10^8	0.190	0.730	2.630	175	443	425	0.00	Dynamic	55.43	1.92	-	-	-	1.4531	-
	92	8.71×10^9	1.76×10^8	0.240	0.820	3.220	110	366	380	-0.05	Static	64.26	0.05	465	570	0.9899	1.4519	5.20
											Dynamic	80.04	6.44	-	-	0.9979	1.4534	1.90
ANP 71																		
											Base	137.7	0.01	530	575	-	1.4837	3.08
	26	0	0	0.130	0.825	2.125	15	440	415	0.20	Dynamic	1510.0	8.07	-	-	-	-	-
	70	9.75×10^8	1.03×10^8	0.020	0.720	0.920	40	350	370	-0.05	Static	139.9	0.05	530	575	-	1.4846	2.70
											Dynamic	98.00	0.07	-	-	-	1.4828	-
	74	1.83×10^9	1.52×10^8	0.110	1.370	2.470	130	455	380	0.80	Static	-	< 0.01	-	-	0.8764	1.4855	1.88
											Dynamic	1932.0	8.56	-	-	0.9290	1.4831	-
	94	8.97×10^9	1.52×10^8	0.170	0.580	2.280	100	440	429	0.25	Static	150.5	0.01	490	-	-	1.4850	2.05
											Dynamic	379.4	6.73	-	-	-	1.4950	-
ANP 72																		
											Base	152.4	9.10	560	625	-	1.4608	1.44
	26	0	0	0.300	1.400	4.400	45	400	323	0.60	Dynamic	1180.0	18.80	-	-	-	-	-
	72	1.26×10^9	1.77×10^8	0.710	0.570	7.670	200	405	345	0.50	Static	150.7	9.60	-	-	-	1.4609	-
											Dynamic	470.3	16.85	-	-	-	1.4655	-

TABLE XV (cont'd)

EVALUATION OF LUBRICANTS IN THE WADC DEPOSITION TESTER

Lubricant Designation	Run No	Gamma Dose, Ergs/gm Carbon		Deposit Weight, gms		Deposition Number	Oil Consumption, ml	Oil Out Temp, °F		Pump Pressure Increase in 12 hrs, PSI	Oil Sample	Viscosity at 100 °F, cs	Neutralization Number, mg KOH/gm	Flash point, °F	Fire point, °F	Specific gravity	Index of refraction, n_d^{25}	Evaporation at 400 °F, %
		Static	Dynamic	Coke	Sludge			1 hr	12 hr									
ANP 73											Base	285.3	0.01	565	620	-	1.4822	0.80
	17	0	0	0.020*	1.280	1.480	65	420	390	0.15	Dynamic	667.8	5.91	-	-	-	-	-
	52	0	1.76×10^8	0.130	0.160	1.460	90	420	375	0.80	Static	286.8	0.01	-	-	-	1.4840	0.98
											Dynamic	2947.0	5.91	-	-	0.9179	1.4982	-
	71	1.05×10^9	1.77×10^8	0.155	0.970	2.520	150	445	242	1.70	Static	284.6	<0.01	-	-	-	1.4827	2.48
											Dynamic	1299.0	3.55	-	-	-	1.4866	-
	95	1.02×10^{10}	1.76×10^8	2.460	1.240	25.870	40	220	108	-2.20	Static	286.5	<0.01	405	-	-	1.4820	-
											Dynamic	-	7.04	-	-	-	1.4942	-
	102	1.02×10^{10}	1.75×10^8	0.380	N.A.**	N.A.**	120	480	393	-0.90	Static	307.2	0.01	535	-	-	1.4833	-
											Dynamic	-	7.15	-	-	0.9168	1.4946	-
ANP 74											Base	24.76	0.08	465	520	-	1.4498	9.95
	122	0	0	0.140	0.700	2.100	50	433	449	-0.15	Dynamic	20.48	15.55	-	-	-	1.4529	-
	81	2.33×10^8	1.77×10^8	0.680	0.580	7.380	120	440	410	-0.10	Static	18.71	0.40	450	520	0.9073	1.4510	7.10
											Dynamic	38.32	27.51	-	-	0.9512	1.4606	-
	96	9.54×10^9	8.80×10^7	0.290	0.770	3.670	130	450	435	0.90	Static	-	2.42	410	-	-	1.4518	-
											Dynamic	74.66	34.28	-	-	-	1.4716	-
ANP 75											Base	15.10	1.13	455	510	-	1.4515	6.35
	51	0	0	0.642	1.100	7.520	70	418	395	0.20	Dynamic	15.42	9.88	-	-	-	1.4522	-
	54	0	1.77×10^8	0.510	0.290	5.390	50	390	390	0.15	Static	15.36	1.30	450	500	-	1.4511	8.85
											Dynamic	15.51	8.26	-	-	0.9170	1.4521	-
	75	1.74×10^9	1.76×10^8	0.120	0.540	1.740	75	435	420	0.50	Static	14.07	1.86	-	-	0.9110	1.4507	-
											Dynamic	14.56	4.93	-	-	0.9129	1.4500	-
ANP 76											Base	41.65	<0.01	490	535	-	-	6.34
	56	0	0	0.315	1.590	4.740	95	385	375	0.90	Dynamic	47.60	2.97	-	-	0.9852	1.4612	-
	55	0	1.77×10^8	0.380	0.945	4.745	50	450	440	0.25	Static	41.55	0.06	-	-	-	1.4604	6.10
											Dynamic	44.59	4.92	-	-	-	1.4588	-
	90	0	8.80×10^7	0.260	0.640	3.240	50	390	410	0.00	Static	42.21	0.08	480	540	0.9800	1.4597	6.25
											Dynamic	49.95	16.01	-	-	0.9894	1.4612	-
	97	9.58×10^9	8.80×10^7	0.120	0.480	1.680	70	410	422	0.30	Static	45.96	3.14	405	-	0.9841	1.4607	-
											Dynamic	62.65	6.78	-	-	-	1.4581	-

*Heater Potting Compound Flaked out in Test

**Not Available

TABLE XV (cont'd)

EVALUATION OF LUBRICANTS IN THE WADC DEPOSITION TESTER

Lubricant Designation	Run No.	Gamma Dose, Ergs/gm Carbon		Deposit Weight, gms		Deposition Number	Oil Consumption, ml	Oil Out Temp., °F		Pump Pressure Increase in 12 hrs., PSI	Oil Sample	Viscosity at 100 °F, cs	Neutralization Number, mg KOH/gm	Flash point, °F	Fire point, °F	Specific gravity	Index of refraction, n_d^{25}	Evaporation at 400 °F, %
		Static	Dynamic	Coke	Sludge			1 hr	12 hr									
ANP 77											Base	13.16	0.18	445	510	-	-	7.10
	64	0	0	0.115	0.835	1.985	120	385	418	0.05	Static	12.35	0.20	440	515	0.9169	1.4505	8.33
											Dynamic	13.02	4.25	-	-	-	1.4497	-
	69	0	1.77×10^8	0.100	0.454	1.454	40	380	380	0.15	Static	12.89	1.06	450	510	0.8987	1.4512	7.10
											Dynamic	13.56	1.16	-	-	0.9075	1.4510	-
	77	1.45×10^9	1.76×10^8	0.180	0.810	2.610	105	418	398	0.35	Static	13.37	0.03	435	500	0.9204	1.4505	7.70
											Dynamic	14.74	3.87	-	-	-	1.4506	-
ANP 78											Base	63.59	0.90	555	620	-	1.4566	1.55
	138	0	0	0.050	0.299	0.799	50	435	424	-0.10	Dynamic	-	0.25	-	-	-	-	-
	58	0	1.77×10^8	0.190	0.640	2.540	100	418	429	-0.10	Static	59.74	0.10	-	-	1.0107	1.4565	2.15
											Dynamic	85.84	5.86	-	-	1.2200	1.4585	-
	89	0	1.92×10^8	0.100	0.700	1.700	50	420	415	0.05	Static	-	0.20	545	-	1.0176	0.4564	2.75
											Dynamic	61.97	1.25	-	-	1.0169	1.4561	-
	98	9.14×10^9	1.10×10^8	0.070	0.690	1.390	80	425	403	0.50	Static	76.75	3.09	360	-	-	1.4573	-
											Dynamic	205.9	11.35	-	-	1.0519	1.4634	-
ANP 79											Base	18.46	< 0.01	420	485	-	1.4498	18.72
	60	0	0	0.100	0.690	1.690	130	440	441	0.40	Dynamic	63.12	12.14	-	-	-	1.4602	-
	59	0	1.77×10^8	0.120	0.665	1.865	160	440	432	0.20	Static	18.09	0.06	-	-	-	1.4498	-
											Dynamic	73.09	10.22	-	-	1.1820	1.4590	-
	99	9.32×10^9	1.10×10^8	0.090	0.460	1.360	105	430	445	0.30	Static	23.33	4.34	-	-	0.9745	1.4510	-
											Dynamic	61.29	9.26	-	-	1.0012	1.4560	-
ANP 80											Base	29.06	< 0.01	465	535	-	1.4556	5.85
	61	0	0	0.285	0.760	3.610	70	430	430	0.00	Dynamic	-	-	-	-	0.9976	-	-
	68	0	1.77×10^8	0.250	0.790	3.290	20	410	370	0.10	Static	29.27	0.06	470	535	-	1.4559	4.57
											Dynamic	32.39	1.69	-	-	-	1.4555	-
	91	-	1.02×10^8	0.090	0.410	1.310	50	412	415	-0.05	Static	17.72	0.15	480	540	0.9940	1.4553	4.30
											Dynamic	34.12	3.70	-	-	0.9999	1.4562	-
	100	1.37×10^{10}	1.10×10^8	0.120	0.550	1.750	80	418	412	-0.25	Static	39.50	3.60	370	-	-	1.4568	10.95
											Dynamic	50.33	2.28	-	-	1.0132	1.4573	-

TABLE XV (cont'd)

EVALUATION OF LUBRICANTS IN THE WADC DEPOSITION TESTER

Lubricant Designation	Run No	Gamma Dose, Ergs/gm Carbon		Deposit Weight, gms		Deposition Number	Oil Consumption, ml	Oil Out Temp., °F		Pump Pressure Increase in 12 hrs, PSI	Oil Sample	Viscosity at 100 °F, cs	Neutralization Number, mg KOH/gm	Flash point, °F	Fire point, °F	Specific gravity	Index of refraction, n_d^{25}	Evaporation at 400 °F, %
		Static	Dynamic	Coke	Sludge			1 hr	12 hr									
GTO 38											Base	11.37	0.73	-	-	-	-	-
	33	0	0	0.383	3.335	7.165	100	420	408	6.25	Static	13.79	3.42	-	-	-	1.4535	-
											Dynamic	14.91	11.08	-	-	-	-	-
GTO 307											Base							
	10	0	0	0.020	0.251	0.451	90	400	388	6.60	Dynamic	12.82	0.55	-	-	-	-	-
												15.33	16.77	-	-	-	-	-
GTO 309											Base	13.10	0.11	-	-	-	1.4560	-
	88	0	0	0.150	1.690	3.190	115	438	428	1.65	Dynamic	16.63	16.32	-	-	-	-	-
	34	0	0	0.300	2.450	5.450	100	412	425	5.65	Dynamic	17.66	19.73	-	-	-	-	-
GTO 313	7	0	0	0.220	1.110	3.310	50	400	445	0.00	Dynamic	18.75	28.15	-	-	-	-	-
	8	0	0	0.200	1.080	3.080	80	392	396	0.10	Dynamic	18.12	28.43	-	-	-	-	-
	9	0	0	0.220	1.090	3.290	55	425	433	-0.05	Dynamic	19.45	32.63	-	-	-	-	-
	11	0	0	0.050	1.165	1.665	65	425	423	-0.10	Dynamic	18.33	12.43	-	-	-	-	-
	45	0	0	0.100	0.650	1.650	90	412	422	0.10	Dynamic	17.97	11.93	-	-	-	-	-
	67	0	0	0.130	1.010	2.310	60	400	401	0.20	Dynamic	18.26	11.03	-	-	0.9262	-	-
	87*	0	0	0.415	0.620	4.770	125	425	430	0.35	Dynamic	24.86	33.81	-	-	0.9492	1.4547	-
	88*	0	4.46×10^8	1.210	0.730	12.830	135	430	435	0.20	Static	-	00.26	-	-	0.9158	1.4512	-
											Dynamic	21.20	27.03	-	-	0.9451	1.4565	-
GTO 373											Base	-	0.76	-	-	-	-	-
	12	0	0	0.230	2.440	4.740	30	407	421	1.60	Dynamic	15.05	15.06	-	-	-	-	-
GTO 519											Base	22.68	0.76	-	-	-	-	-
	15	0	0	0.350	0.600	4.100	135	410	400	0.00	Dynamic	23.28	19.59	-	-	-	-	-
GTO 578											Base	15.18	0.15	-	-	-	-	-
	87	0	0	0.290	1.220	4.120	60	447	430	0.40	Dynamic	19.85	19.00	-	-	-	-	-

* 25 hr. Deposition Test

TABLE XVI

PHYSICAL PROPERTIES OF JET ENGINE LUBRICATING OILS ACCORDING TO MIL-O-6081B

Lubricant Designation	Gamma Dose, ergs / gm Carbon	Index Of Refraction, n_d^{25}	Viscosity at 100°F, cs.	Pour Point, °F	Flash Point, °F	Fire Point, °F	Copper Corrosion, at 212 °F	Evoporation at 400°F, %
Grade 1005:								
MLO 56-766	0	1.4899	5.14	<-80	255	260	Pass 1A	94.5
MLO 56-767-1	8.71×10^8	1.4905	4.92	<-80	235	270	Pass 1A	94.5
MLO 56-767-2	8.71×10^8	1.4905	4.91	<-80	245	260	Pass 1A	93.3
MLO 56-768-1	2.61×10^9	1.4903	4.93	<-80	245	265	Pass 1A	93.9
MLO 56-768-2	2.61×10^9	1.4905	4.94	<-80	245	265	Pass 1A	94.9
MLO 56-769-1	8.71×10^9	1.4907	4.96	<-80	250	270	Pass 1A	92.5
MLO 56-769-2	8.71×10^9	1.4905	4.95	<-80	230	255	Pass 1A	92.1
MLO 56-770-1	2.61×10^{10}	1.4914	5.41	<-80	245	275	Pass 1A	91.3
MLO 56-770-2	2.61×10^{10}	1.4915	5.49	<-80	235	265	Pass 1A	89.8
MLO 56-771-1	8.71×10^{10}	1.4952	7.87	<-80	225	270	Pass 1A	81.2
MLO 56-771-2	8.71×10^{10}	1.4945	7.41	<-80	230	255	Pass 1A	82.8
Grade 1010:								
ANPO-177	0	1.4728	10.25	-80	310	340	Pass 1A	96.7
MLO 56-773-1	8.71×10^8	1.4727	10.27	-80	320	330	Pass 1A	97.2
MLO 56-774-1	2.61×10^9	1.4735	10.35	<-80	305	335	Pass 1A	96.6
MLO 56-774-2	2.61×10^9	1.4734	10.36	<-80	335	350	Pass 1B	96.8
MLO 56-775-1	8.71×10^9	1.4738	9.47	<-80	310	330	Pass 1B	93.3
MLO 56-775-2	8.71×10^9	1.4735	10.90	<-80	335	345	Pass 1B	93.1
MLO 56-776-1	2.61×10^{10}	1.4762	13.01	<-80	270	325	Pass 1B	87.1
MLO 56-776-2	2.61×10^{10}	1.4759	12.75	<-80	270	325	Pass 1B	86.8
MLO 56-777-1	8.71×10^{10}	1.4804	25.75	<-65	230	315	Pass 1B	70.1
MLO 56-777-2	8.71×10^{10}	1.4806	26.29	<-65	230	315	Pass 1B	69.5

*Irradiated at Materials Testing Reactor, gamma radiation canal, National Reactor Testing Station, Idaho Falls, Idaho.

TABLE XVII

PHYSICAL PROPERTIES OF AIRCRAFT RECIPROCATING (PISTON) ENGINE LUBRICATING OILS ACCORDING TO MIL-L-6082 B

Lubricant Designation	Neutralization Number mg KOH/gm	Neutrality (Qualitative)	Precipitation Number ml/10 ml	Free and Corrosive Sulfur, Rating	Specification Number mg KOH/gm	Gravity, ° API	Flash Point, °F	Fire Point, °F	Pour Point, °F	Conradson Carbon Residue, % by wt
Shell 1100	0.01	Pass	0	1A	1.6	28.4	515	580	-20	0.323
ANP 1*	< 0.01	Pass	0	1A	1.9	29.1	480	515	0	0.135

*Irradiated in SPT II Reactor, Dose 9.10×10^8. Data from Convair GTR SPT No. 2 Report.

as received, the lubricant taken from the reservoir at the end of the test, and the lubricant taken from the test section at the end of the run.

The evaluation of repeatability for the Model "C" Panel Coker and the Deposition Tester will now be discussed.

The repeatability of the Deposition test results with lubricant GTO-313 can be expressed in two parts: One for the unmodified rig, and the other for the modified rig in the radiation cell. The following values are based on correlation runs, not all of which are included in the tables. The average deposition number obtained with the modified rig (4 runs) was 2.2 ± 0.7, with an average deviation of 26 percent and a maximum deviation of 52 percent. The average deposition number obtained with the unmodified rig (5 runs) was 2.9 ± 0.6, with an average deviation of 20 percent and a maximum deviation of 32 percent.*

The repeatability of the panel coker test is within 20 percent of the mean.** Duplicate determinations made during this study gave results that are within these limits.

---

*Private communication. These values may be compared with those of the Propulsion Laboratory, Wright Air Development Center. D.N. = 2.7 ± 0.5 for the modified method effective 1 April 1958. Before this time the value was 3.2 ± 0.5.

**Reference 28, p 227.

The repeatability of all mechanical evaluation rigs will continue to be studied and, as new data are forthcoming, more accurate figures will be obtained.

C. Greases

The data for greases consist of results obtained in the Pope Grease Tester, Table XVIII, used according to CRC Method L-35. The greases tested were:

MLG-58-374

MLG-58-355

MLG-58-363

Specification tests were not performed, and an evaluation of repeatability is not possible due to the lack of a sufficient number of identical runs. The discussion of these materials will be postponed to future reports when more data become available.

TABLE XVIII

HIGH TEMPERATURE PERFORMANCE OF GREASE IN ANTIFRICTION BEARINGS

According to Federal Test Method Standard No. 791-333T

Grease Designation	Gamma Flux, R/hr	Gamma Dose, ergs/gm Carbon	Bearing Load, (lb) Radial	Bearing Load, (lb) Thrust	Test Speed, rpm	Test Temp., °F	Type of Failure	Hours to Failure	Condition of Bearing	Condition of Grease
MLG-58-374	0	0	15	5	10,000	600	Motor Overload	20.1	Noisy, Jammed, and Dry	Dry and Powdery
	0	0	15	5	10,000	600	Over Temperature	33.5	Noisy, Jammed, Dry, and Broken Separator	Dry and Powdery
MLG-58-355	0	0	15	5	10,000	600	Belt Slippage	60.0	Noisy	Black Gummy Sludge
	3.27×10^5	8.80×10^9	15	5	10,000	600	Motor Overload	200.8	Severe Vibration Last Hour of Test	Gummy Sludge
MLG-58-363	0	0	15	5	10,000	600	Motor Overload	152.5	Jammed	Grayish Sludge
	0	0	15	5	10,000	600	Over Temperature	7.3	Jammed	Gummy Sludge

SECTION IV

DISCUSSION OF RESULTS

The effect of radiation on the behavior of fuels and lubricants must be assessed in a combined environment where the interactions of temperature, mechanical stress, and radiation will simultaneously affect the material under investigation.[16]

The data obtained in this study are in agreement with the theory of O. Sisman[26] that the use of the environments separately does not satisfactorily predict performance. Assuming adequate correlation between the rigs and the gas turbine, it is expected that a number of the fuels and lubricants examined should be satisfactory for use in an airborne reactor.

The following section will assess the effect of radiation on fuels and lubricants. This discussion will be presented in two major parts: (1) Fuels, and (2) Lubricants. Each major part will present the effects of static irradiation alone, the effects of static preirradiation and subsequent mechanical evaluation, the effects of mechanical evaluation in a radiation environment, and a relative performance rating of the materials that appear promising for use in a radiation environment.

A. Fuels

Other investigators have shown that organic materials when irradiated may degrade, polymerize or cross link[5, 7, 8, 15]. The rates of these radiation-induced reactions are difficult to evaluate for a material as complex in structure as a fuel. However, certain properties delineated by the specifications such as viscosity at -30°F, initial boiling point, flash point, and gum are rather sensitive to the effects of radiation and may be used to indicate trends. Degradation should lower the values of these properties while polymerization should result in an increase. Cross linking may also cause an increase in the values similar to polymerization except that changes in gum content and viscosity at -30°F should tend to be greater.

1. Effects of Static Irradiation

Variation of several properties of fuels become evident after static exposure to gamma radiation.[6, 22] Most of the measured properties change, although no significant over-all trends are discernible (Table XIX).

TABLE XIX

EFFECTS OF STATIC IRRADIATION ON FUELS

Fuel Designation ANPF No.	Gamma Dose, ergs/gm carbon	Initial Boiling Point, °F Value	Change	Existent Gum mg/100 ml Value	Change	Viscosity at 30°F, cs Value	Change	Gravity °API Value	Change	Flash Point °F Value	Change
57-2	0	331	-	-	-	4.90	-	46.9	-	120	-
	2.61×10^9	330	-1	-	-	4.54	-0.46	46.9	0.0	116	-4
57-58	0	317	-	1.0	-	7.18	-	44.2	-	118	-
	2.61×10^9	332	+15	3.5	+2.5	7.16	-0.02	44.0	-0.2	110	-8
57-59	0	317	-	1.5	-	7.39	-	44.1	-	118	-
	8.71×10^8	174	-143	1.5	0.0	6.80	-0.59	43.9	-0.2	74	-44

Of particular interest is the fact that during static irradiation several fuels formed a precipitate which was observed as a dark brown to light tan residue in the irradiation container. This precipitate was observed with ANPF 57-55, 57-62, 57-63, 57-93, and 57-112. This same precipitate was noted during dynamic testing in a radiation environment but was not formed when these fuels were tested without radiation. Fuels, such as ANPF 57-62 and 57-112, showed relatively high "goodness" ratings in the "cold" coker and failed in the "hot" coker. Thus, it is suggested that the formations of the precipitate is a direct cause of filter plugging and could therefore be a criterion for a screening test for fuels to be used in a radiation environment.*

2. Mechanical Evaluation - CFR Fuel Coker

The CFR Fuel Coker evaluates the filter clogging and deposit forming tendencies of fuels. Filter clogging and the formation of deposits in an engine is a result of fuel decomposition during the transfer of fuel from the reservoir (fuel tank) to the engine proper. In this investigation, fuel decomposition, as determined by the "goodness" rating,** is caused by elevated temperatures and

---

*Precipitates were also observed by investigators at Southwest Research Institute, Reference 11.

**Since the "goodness" rating method was in effect at the start of the program, all results in this report are on this basis. The new reporting procedure is being followed at present.

mechanical stresses, and is generally enhanced in a radiation environment. Preirradiation followed by mechanical evaluation shows no obvious trends.

The "goodness" rating of a fuel is determined by measuring the change in pressure drop across a filter and is a result of accumulated decomposition products. The change in filter pressure drop is plotted as a function of time on an empirical scale such that the change after 300 minutes essentially determines the rating, Figure 5.

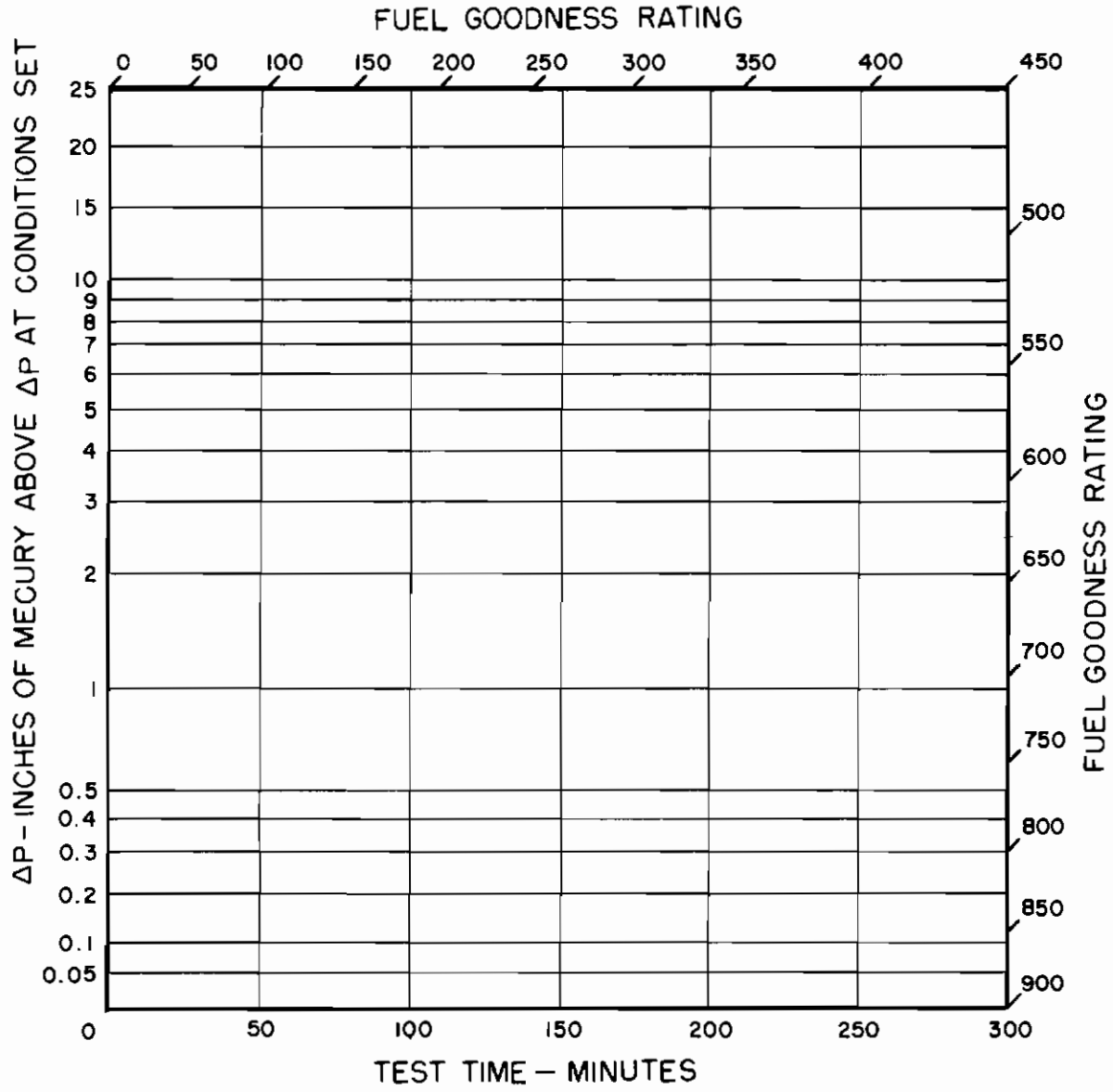

Figure 5. Relationship between "Goodness" Rating and Pressure Drop-Time

Increasing the operating temperature of the preheater and filter can affect the "goodness" rating of a fuel as shown in Table XX. Preirradiation of a fuel and subsequent evaluation in the CFR Fuel Coker may cause changes in "goodness" rating as shown in Table XXI. Similar effects were noted by other investigators. (22)

During mechanical evaluation of fuels in a radiation environment, it was noted, in most cases, that the "goodness" rating tends to decrease while the preheater deposit increases. However, in some cases, irradiation has little if any effect on the value of the "goodness" rating. This is illustrated with fuels ANPF 57-76, 57-105, 57-107, 57-115, and 57-120.

It is of interest to note that preirradiation may serve to hide adverse radiation effects which might be observed during mechanical evaluation in a radiation environment. For instance, ANPF 57-55 exhibits a decrease in "goodness" rating from 765 to 592 for a "hot" coker test with preirradiation to 7.81×10^7 ergs/gm carbon in the coker fuel reservoir. Preirradiation to 1.07×10^9 ergs/gm C and subsequent mechanical evaluation in a radiation environment results in a "goodness" rating of 750.

It is also of interest to note that mechanical evaluation in a nonradiation environment after preirradiation gives decidedly different results than mechanical evaluation in a radiation environment. For example, the fuel ANPF 57-77 irradiated to a total dose of 1.93×10^8 ergs/gm carbon during mechanical evaluation gives a "goodness" rating of 721. The same fuel irradiated to 2.02×10^8 ergs/gm carbon and subsequently evaluated in a nonirradiation environment gives a "goodness" rating of 324.

The effects discussed above clearly indicate that (1) preirradiation serves to alter a test fuel so that subsequent tests are run essentially on a "new" fuel, and (2) static irradiation and subsequent mechanical evaluation in a nonradiation environment cannot predict the behavior of a fuel under the combined effect of mechanical, thermal, and radiation stresses.

Further information can be obtained by examination of the changes in physical properties of fuels after mechanical testing. The measured physical parameters, such as viscosity at -30°F, flash point, index of refraction, and API gravity appear to have little direct

TABLE XX

EFFECT OF TEMPERATURE ON THE BEHAVIOR OF FUELS IN THE CFR FUEL COKER

Behavior of Fuel	Fuel Designation	Operating Conditions, °F Preheater/Filter	Goodness Rating Value	Goodness Rating Change
Decrease in Goodness Rating	57-2	350/450	766	-
		400/500	245	-521
	56-6	300/400	744	-
		350/450	54	-690
	57-51	300/400	900	-
		400/500	715	-185
	57-58	300/400	900	-
		400/500	49	-851
	57-63	300/400	900	-
		400/500	98	-802
	57-99	300/400	900	-
		400/500	55	-845
Thermally Stable	57-50	300/400	742	-
		400/500	750	+8
	57-52	300/400	875	-
		400/500	900	+25
	57-53	300/400	522	-
		400/500	653	+131
	57-54	300/400	773	-
		400/500	782	+9
	57-61	300/400	900	-
		400/500	900	0
	57-62	300/400	900	-
		400/500	900	0

TABLE XXI

EFFECT OF PREIRRADIATION ON THE BEHAVIOR OF FUELS IN THE CFR FUEL COKER

Fuel Designation ANPF	Gamma Dose, Static ergs/gm Carbon	Goodness Rating Value	Change
57-77	0	507	-
	2.02×10^8	324	-183
57-78	0	405	-
	1.27×10^8	541	+136
57-80	0	485	-
	8.01×10^7	235	-250
	8.90×10^8	95	-390
57-86	0	875	-
	8.79×10^7	120	-755
57-76	0	92	-
	7.23×10^7	137	+45

correlation with radiation dose. However, when marked changes in "goodness" rating occur, corresponding changes take place in one or more of the above parameters (Figure 6).

To better assess the effects of radiation on a fuel, it would be of interest to know the changes that occur in the CFR Fuel Coker during a test run. These changes were followed by use of a function dR/dt which was derived to measure the decomposition rate of a fuel through the filter plugging rate (Appendix VII).

Fuel decomposition products may affect the rate of fuel decomposition as they accumulate. Thus, as the test run progresses, deposits will form, and the effects measured by the pressure drop across the filter will depend largely on the CFR system itself including the fuel under test. Only at zero time is it possible to relate the observed effects to the behavior of the fuel alone by this approach. A stable fuel should therefore be one which shows a low $\left(\frac{dR}{dt}\right)_o$ value and little variation of $\left(\frac{dR}{dt}\right)$ with time. Table XXII presents values of $\left(\frac{dR}{dt}\right)_o$ for the fuels studied during this investigation.

TABLE XXII

INITIAL DECOMPOSITION RATE OF FUELS IN THE CFR FUEL COKER

Fuel Designation ANPF	Run No.	Condition	Gamma Dose ergs/gm Carbon Static	Gamma Dose ergs/gm Carbon Dynamic	Goodness Rating	$(\frac{dR}{dt_o}) \times 10^3$	Group No.
56-6	14	300/400/6	0	0	744	1.4	II
	34	300/400/6	1.74×10^8	5.75×10^6	40	100.0	IV
	11	350/450/6	0	0	50	66.7	IV
	12	350/450/6	0	0	58	75.0	IV
57-86	174	300/400/6	8.79×10^7	0	120	31.6	IV
	167	300/400/6	8.71×10^7	1.81×10^8	337	12.3	IV
	196	300/400/6	0	0	840	0.2	I
57-95	135	300/400/6	0	0	841	0.9	I
	166	300/400/6	8.71×10^7	1.81×10^8	842	0.3	I
	169	300/400/6	1.08×10^9	2.03×10^8	213	4.5	III
57-110	52	300/400/6	0	0	900	0.0	I
	178	300/400/6	8.71×10^7	2.03×10^8	240	19.4	IV
57-112	96	300/400/6	7.81×10^7	1.52×10^8	578	9.7	IV
	173	300/400/6	9.75×10^8	2.03×10^8	300	8.9	IV
	194	300/400/6	1.04×10^9	2.03×10^8	390	1.8	II
57-2	9	350/450/6	0	0	775	1.0	I
	10	350/450/6	0	0	765	1.1	II
	24	350/450/6	1.34×10^7	3.49×10^7	272	700.0	IV
	17	400/500/6	0	0	70	6.7	III
	18	400/500/6	0	0	420	6.1	III
57-50	43	300/400/6	0	0	742	0.5	I
	192	400/500/6	0	0	750	1.8	II
	195	400/500/6	8.71×10^7	2.03×10^8	840	0.9	I
57-51	44	300/400/6	0	0	900	0.0	I
	185	400/500/6	0	0	715	0.8	I
	190	400/500/6	8.71×10^7	2.03×10^8	900	0.0	I

TABLE XXII (cont'd)

INITIAL DECOMPOSITION RATE OF FUELS IN THE CFR FUEL COKER

Fuel Designation ANPF	Run No.	Condition	Gamma Dose ergs/gm Carbon Static	Gamma Dose ergs/gm Carbon Dynamic	Goodness Rating	$\left(\frac{dR}{dt_o}\right)\times 10^3$	Group No.
57-52	45	300/400/6	0	0	875	0.7	I
	165	400/500/6	0	0	900	0.0	I
	176	400/500/6	8.71×10^{7}	2.03×10^{8}	900	0.0	I
57-53	46	300/400/6	0	0	522	1.9	II
	158	400/500/6	0	0	653	1.2	II
	184	400/500/6	8.71×10^{7}	2.03×10^{8}	900	0.0	I
57-54	47	300/400/6	0	0	773	0.5	I
	49	400/500/6	0	0	782	0.4	I
	136	400/500/6	1.12×10^{8}	1.18×10^{8}	856	0.2	I
	99	400/500/6	3.71×10^{8}	9.84×10^{7}	420	1.2	II
	104	400/500/6	2.71×10^{9}	1.31×10^{8}	900	0.0	I
	177	400/500/6	1.02×10^{10}	2.03×10^{8}	803	0.8	I
57-55	48	400/500/6	0	0	765	0.8	I
	138	400/500/6	1.07×10^{9}	1.81×10^{8}	750	1.1	II
57-56	50	400/500/6	0	0	857	0.2	I
	100	400/500/6	7.81×10^{7}	1.04×10^{8}	900	0.0	I
	140	400/500/6	2.93×10^{9}	1.81×10^{8}	900	0.0	I
57-57	51	400/500/6	0	0	500	2.2	III
	102	400/500/6	7.81×10^{7}	1.04×10^{8}	750	0.6	I
	143	400/500/6	1.49×10^{9}	1.81×10^{8}	827	0.5	I
57-58	20	300/400/6	0	0	900	0.0	I
	26	300/400/6	1.34×10^{7}	6.37×10^{7}	340	10.5	IV
	35	400/500/6	0	0	49	4.2	III
57-59	23	300/400/6	0	0	900	0.0	I
	28	300/400/6	1.48×10^{7}	4.36×10^{7}	303	5.6	III
	36	400/500/6	0	0	900	0.0	I

TABLE XXII (cont'd)

INITIAL DECOMPOSITION RATE OF FUELS IN THE CFR FUEL COKER

Fuel Designation ANPF	Run No.	Condition	Gamma Dose ergs/gm Carbon Static	Gamma Dose ergs/gm Carbon Dynamic	Goodness Rating	$\left(\frac{dR}{dt}\right)_0 \times 10^3$	Group No.
57-60	25	300/400/6	0	0	802	0.3	I
	193	300/400/6	2.83×10^9	2.03×10^8	555	1.5	II
	37	400/500/6	0	0	900	0.0	I
	60	400/500/6	3.90×10^7	4.47×10^7	310	3.7	III
57-61	27	300/400/6	0	0	900	0.0	I
	38	400/500/6	0	0	900	0.0	I
	61	400/500/6	8.80×10^7	9.06×10^6	72	15.2	IV
57-62	29	300/400/6	0	0	900	0.0	I
	38a	400/500/6	0	0	900	0.0	I
	63	400/500/6	8.80×10^7	3.14×10^7	230	22.7	IV
57-63	30	300/400/6	0	0	900	0.0	I
	39	400/500/6	0	0	98	27.1	IV
	64	400/500/6	8.80×10^7	2.45×10^7	38	60.0	IV
57-76	62	400/500/6	0	0	92	23.8	IV
	142	400/500/6	0	0	327	7.0	III
	187	400/500/6	7.23×10^7	0	137	7.4	IV
	106	400/500/6	7.81×10^7	6.28×10^7	297	5.8	III
57-77	78	400/500/6	0	0	507	2.4	III
	97	400/500/6	8.71×10^7	6.01×10^7	390	2.7	III
	108	400/500/6	7.81×10^7	1.09×10^8	721	1.2	II
	200	400/500/6	2.02×10^8	0	324	2.3	III
	157	400/500/6	1.98×10^9	1.81×10^8	570	1.3	II
57-78	79	400/500/6	0	0	405	14.5	IV
	109	400/500/6	7.81×10^7	6.89×10^7	320	3.1	III
	188	400/500/6	1.77×10^8	0	541	2.1	III
57-79	80	400/500/6	0	0	100	23.7	IV
	110	400/500/6	7.81×10^7	2.61×10^7	134	2.7	III

TABLE XXII (cont'd)

INITIAL DECOMPOSITION RATE OF FUELS IN THE CFR FUEL COKER

Fuel Designation ANPF	Run No.	Condition	Gamma Dose ergs/gm Carbon Static	Dynamic	Goodness Rating	$\left(\frac{dR}{dt_o}\right) \times 10^3$	Group No.
57-80	82	400/500/6	0	0	485	19.9	IV
	111	400/500/6	5.88×10^7	1.09×10^8	660	3.6	III
	175	400/500/6	8.01×10^7	0	235	6.9	III
	155	400/500/6	8.90×10^8	0	95	18.2	IV
	152	400/500/6	9.87×10^8	1.81×10^8	98	100.0	IV
57-81	137	400/500/6	0	0	484	1.0	I
	114	400/500/6	4.36×10^7	1.09×10^8	900	0.0	I
	154	400/500/6	1.26×10^9	1.81×10^8	826	0.3	I
57-89	183	400/500/6	8.71×10^7	2.03×10^8	900	0.0	I
57-90	71	400/500/6	0	0	477	4.1	III
	171	400/500/6	8.71×10^7	2.03×10^8	353	2.8	III
57-93	74	400/500/6	0	0	826	1.0	I
	180	400/500/6	8.71×10^7	2.03×10^8	765	0.8	I
57-94	75	400/500/6	0	0	165	18.6	IV
	134	400/500/6	0	0	92	20.7	IV
	151	400/500/6	8.71×10^7	1.81×10^8	257	8.5	IV
47-97	139	300/400/6	0	0	458	2.3	III
	40	400/500/6	0	0	534	1.1	II
	67	400/500/6	3.45×10^8	5.40×10^6	54	142.9	IV
57-98	41	400/500/6	0	0	855	0.2	I
	81	400/500/6	1.56×10^8	2.70×10^7	200	9.2	IV
	92	400/500/6	1.17×10^7	7.40×10^7	900	0.0	I
57-99	42	300/400/6	0	0	900	0.0	I
	88	300/400/6	7.81×10^7	7.36×10^7	578	5.5	III
	144	400/500/6	0	0	55	35.6	IV

TABLE XXII (cont'd)

INITIAL DECOMPOSITION RATE OF FUELS IN THE CFR FUEL COKER

Fuel Designation ANPF	Run No.	Condition	Gamma Dose ergs/gm Carbon Static	Dynamic	Goodness Rating	$\left(\frac{dR}{dt}\right)_o \times 10^3$	Group No.
57-100	153	400/500/6	0	0	670	2.0	II
	93	400/500/6	7.81×10^7	7.36×10^7	814	0.6	I
	168	400/500/6	1.35×10^9	2.03×10^8	708	0.8	I
57-101	117	400/500/6	0	0	900	0.0	I
	116	400/500/6	8.71×10^7	1.09×10^8	827	0.5	I
	145	400/500/6	1.35×10^9	1.81×10^8	103	17.4	IV
	148	400/500/6	1.40×10^9	1.81×10^8	81	48.1	IV
57-102	147	400/500/6	0	0	752	0.6	I
	94	400/500/6	7.81×10^7	7.36×10^7	842	0.6	I
57-103	118	400/500/6	0	0	654	1.5	II
	119	400/500/6	7.84×10^7	1.09×10^8	900	0.0	I
	179	400/500/6	1.17×10^9	2.03×10^8	900	0.0	I
57-104	146	400/500/6	0	0	532	1.9	II
	95	400/500/6	7.8×10^7	1.09×10^8	457	1.5	II
57-105	120	400/500/6	0	0	827	0.3	I
	122	400/500/6	2.07×10^8	1.09×10^8	900	0.0	I
	159	400/500/6	1.04×10^9	1.81×10^8	826	0.6	I
57-106	121	400/500/6	0	0	900	0.0	I
	127	400/500/6	8.62×10^7	1.81×10^8	900	0.0	I
57-107	123	400/500/6	0	0	900	0.0	I
	124	400/500/6	7.84×10^7	1.09×10^8	900	0.0	I
	162	400/500/6	2.02×10^9	1.81×10^8	900	0.0	I
57-108	125	400/500/6	0	0	815	0.4	I
	128	400/500/6	7.80×10^7	1.81×10^8	900	0.0	I
	164	400/500/6	2.05×10^9	1.81×10^8	765	0.7	I

TABLE XXII (cont'd)

INITIAL DECOMPOSITION RATE OF FUELS IN THE CFR FUEL COKER

Fuel Designation ANPF	Run No.	Condition	Gamma Dose ergs/gm Carbon Static	Dynamic	Goodness Rating	$\left(\frac{dR}{dt}\right)_o \times 10^3$	Group No.
57-109	129	400/500/6	0	0	825	0.2	I
	130	400/500/6	1.50×10^8	1.81×10^8	665	1.8	II
	172	400/500/6	2.05×10^9	2.03×10^8	900	0.0	I
57-111	53	400/500/6	0	0	187	14.9	IV
57-113	55	300/400/6	0	0	520	2.6	III
	181	300/400/6	8.71×10^7	2.03×10^8	543	0.8	I
57-115	141	400/500/6	8.71×10^7	1.81×10^8	900	0.0	I
	156	400/500/6	1.09×10^9	1.81×10^8	900	0.0	I
	182	400/500/6	9.06×10^9	2.03×10^8	440	2.8	III
57-120	198	400/500/6	0	0	900	0.0	I
	199	400/500/6	8.71×10^7	2.03×10^8	900	0.0	I
57-121	65	400/500/6	7.81×10^7	2.89×10^7	213	10.7	IV
57-91	72	400/500/6	0	0	50	86.4	IV
	86	400/500/6	7.81×10^7	1.08×10^7	81	86.7	IV
	89	400/500/6	8.71×10^7	0	33	171.4	IV
57-92	133	400/500/6	0	0	165	15.3	IV
	149	400/500/6	8.71×10^7	1.81×10^8	437	3.1	III
	186	400/500/6	9.49×10^8	2.03×10^8	135	15.3	IV
57-7	16	400/500/6	0	0	396	3.0	III
	32	400/500/6	8.71×10^7	1.07×10^7	75	26.7	IV
	33	400/500/6	2.26×10^8	6.84×10^6	45	33.3	IV
57-5	15	400/500/6	0	0	60	10.0	IV
	8	400/500/6	0	0	258	6.2	III

TABLE XXII (cont'd)

INITIAL DECOMPOSITION RATE OF FUELS IN THE CFR FUEL COKER

Fuel Designation ANPF	Run No.	Condition	Gamma Dose ergs/gm Carbon Static	Gamma Dose ergs/gm Carbon Dynamic	Goodness Rating	$(\frac{dR}{dt})_o \times 10^3$	Group No.
57-3	1	400/500/4	0	0	782	1.0	I
	2	450/500/4	0	0	875	0.3	I
	3	500/500/4	0	0	900	0.0	I
	4	400/500/6	0	0	900	0.0	I
	7	450/500/6	0	0	857	0.1	I
	6	500/500/6	0	0	900	1.0	I
57-96	131	400/500/6	0	0	802	0.8	I
	132	400/500/6	8.71×10^7	1.81×10^8	515	4.5	III
	170	400/500/6	1.01×10^9	2.03×10^8	708	1.2	II

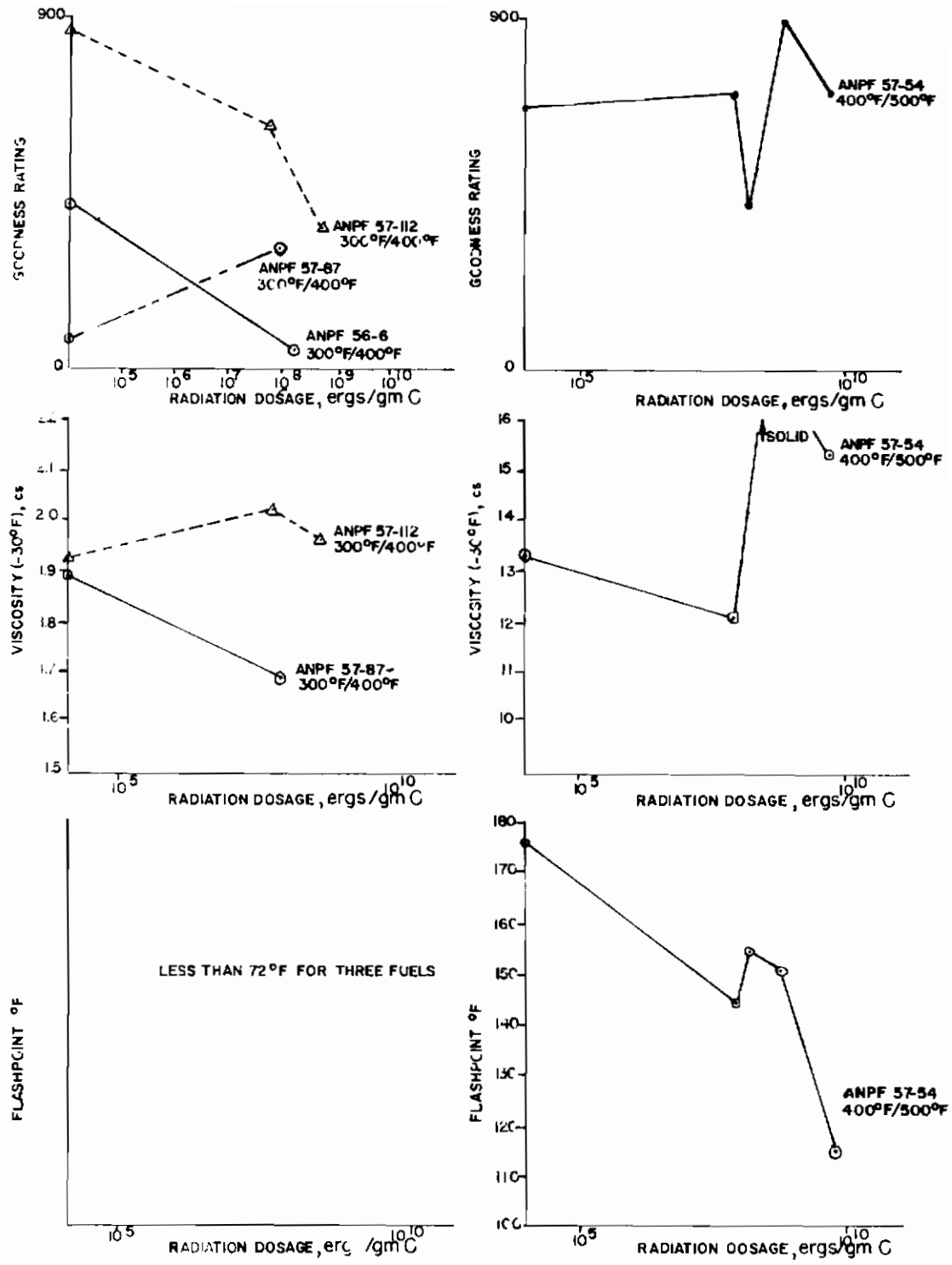

Figure 6. Changes in Properties of Fuels During Mechanical Tests in a Radiation Environment

Figure 7 shows the effect of radiation on ANPF 57-84. It is indicated that radiation is not only detrimental to the decomposition rate of the fuel itself but, in addition, very seriously increases the filter plugging tendency of the decomposition products. Figure 8 shows how the decomposition of ANPF 57-100 is affected by radiation. Even though the fuel itself seems to become more stable toward thermal shock imposed by the system, it appears that the fuel decomposition products have an increasingly adverse effect on fuel stability as the fuel is exposed to greater doses of radiation.

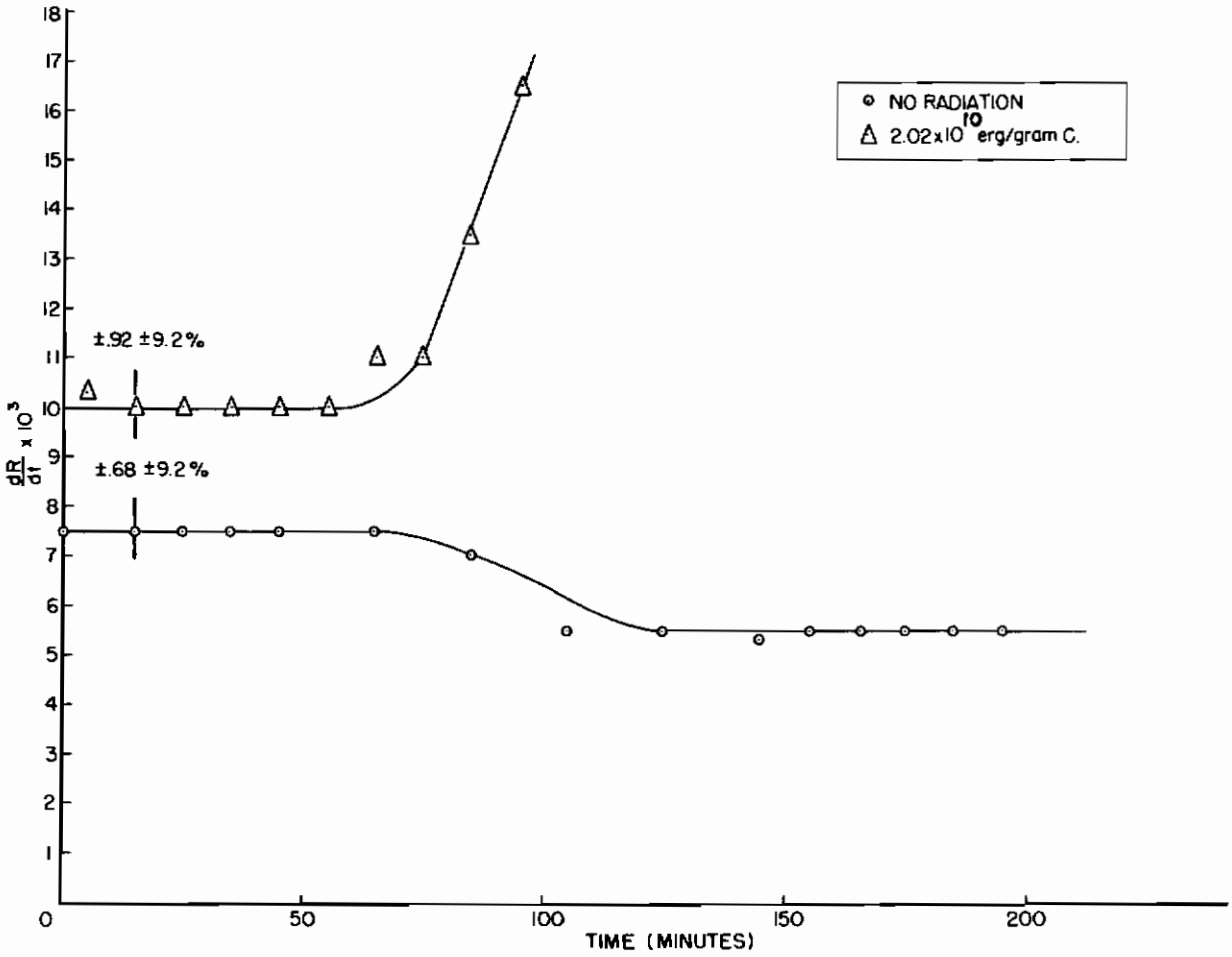

Figure 7. Decomposition Rate of ANPF 57-84 in the CFR Fuel Coker

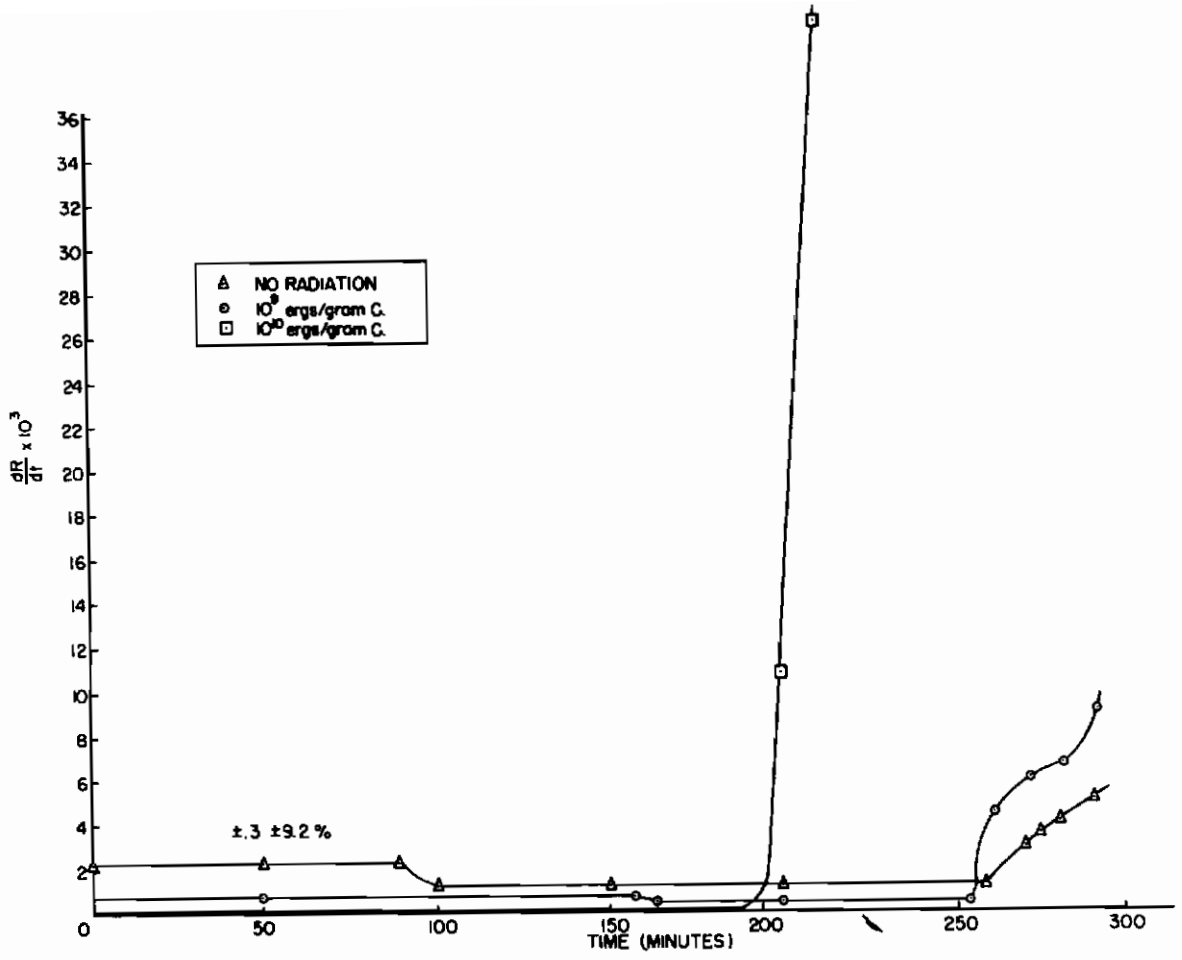

Figure 8. Decomposition Rate of ANPF 57-100 in the CFR Fuel Coker

3. Relative Performance of Fuels

Ten fuels were chosen from those studied as showing the least change in performance and thus the most promise for application in an airborne reactor. The following criteria were applied in this selection:

(1) In the screening test, the increase in differential pressure shall not exceed 11.5 inches of mercury.

(2) In mechanical evaluation in a radiation environment, the preheater rating shall not exceed Code 2.

Table XXIII lists the fuels meeting these requirements. They are tabulated in order of the increasing differential pressure observed with mechanical evaluation in a radiation environment.

B. Lubricants

Lubricants may degrade, polymerize or cross-link as a result of radiation. Here too, as in the case of fuels, following the course of these individual reactions would be rather involved. Many of the lubricants are complex in structure, and even though some are relatively pure chemicals, they are high in molecular weight and give varied products on decomposition.

Parameters delineated by the various lubricant specifications are available to detect over-all trends. Thus, viscosity and flash point should decrease with degradation and increase with polymerization or cross-linking. The neutralization equivalent should increase with increasing radiation dose indicating increased susceptibility to oxidation, although the reverse may occur if acids are removed by volatilization or further reaction. Changes in index of refraction should occur with changes in chemical structure: the formation of double bonds should cause an increase while formation of shorter chain lengths should cause a decrease. Cross-linking and cyclization should cause an increase. The corrosion and oxidation test should detect changes in deposit forming and corrosive tendencies of a lubricant.

1. Static Irradiation

The changes in the properties of various lubricants upon static irradiation are shown in Tables XI and XVI. Although no general trends are discernible, individual lubricants exhibited significant changes in properties. Examples of such changes are given in Table XXIV. The lack of general trends is fully in accord with the findings of other investigators.(6, 19, 20)

Some interesting changes have occurred in the corrosion and oxidation test. The purpose of this test is twofold. First, it gives some information on the behavior of an oil after extended exposure to catalysts at high temperature, and secondly, it gives some information on the behavior of metals in the presence of the partially oxidized oil. These effects are assessed by determining the change in neutralization number and viscosity of the oil and, also, by determining the change in weight of the metal specimens after the high temperature exposure. The neutralization number change is indicative of the extent of oxidation. By a slight modification of the present procedure as described in Appendix III, metal weight losses can be determined and the amount of deposits formed can be ascertained.

TABLE XXIII

FUELS EXHIBITING GREATEST RADIATION STABILITY IN THE CFR FUEL COKER

Fuel Designation, ANPF	Fuel Type	Test Temperature °F	ΔP, inches Hg.* No Radiation	ΔP, inches Hg.* 9×10^7 ergs/gmC (Approximate)	Maximum Preheater Deposits CRC Code No Radiation	Maximum Preheater Deposits CRC Code 9×10^7 ergs/gmC (Approximate)	Remarks
57-95	JP-4	300/400	0.08**	0.15	0**	1	
57-112	JP-4	300/400	0.0	4.60	0	1	
57-120	JP-5	400/500	0.0	0.0	1	2	API Gravity, 53.1 Flash Point, 130°F
57-107	JP-5	400/500	0.0	0.0	1	2	Failed Water Reaction
57-51	JP-5	400/500	0.9	0.0	1	2	Viscosity at -30°F, 23.06 cs Aromatics, 50% Explosiveness, 100% Flash Point, 82°F
57-105	JP-5	400/500	0.2	0.0	0	2	Smoke Point, 19 mm
57-56	JP-5	400/500	0.1	0.0	2	2	Flash Point 110°F
57-102	JP-5	400/500	0.6	0.15	1	0	API Gravity, 55.8 Flash Point, 122°F
57-57	JP-5	400/500	11.15	0.6	2	0	Freezing Point, -35°F Olefins, 7.1% Flash Point, 138°F Failed Water Reaction
57-96	Thermally Stable	400/500	0.15**	9.4	0**	2	

*At 300 minutes
**Average of two determination

TABLE XXIV

EFFECT OF STATIC IRRADIATION ON LUBRICANTS

Lubricant Designation ANP	Lubricant Base Type	Gamma Dose ergs/gm carbon	Viscosity; cs, at 100°F		Flash Point °F		Neutralization No. mg KOH/gm	
			Value	Change	Value	Change	Value	Change
56	Mineral	0	103.0	-	400	-	0.03	-
		2.64×10^{10}	93.7	-9.3	245	-155	0.03	0.00
61	Olefin Polym.	0	10.8	-	340	-	0.01	-
		2.64×10^{10}	6.1	-4.7	140	-200	0.07	+0.06
62	Mineral	0	26.1	-	345	-	0.36	-
		2.66×10^{9}	21.9	-4.2	315	-30	0.27	-0.00
		8.68×10^{9}	23.7	-2.4	305	-40	0.38	+0.02
		2.61×10^{10}	39.2	+13.1	330	-15	0.12	-0.24
63	Ester	0	17.6	-	430	-	0.22	-
		2.55×10^{9}	14.5	-3.1	365	-65	1.34	+1.12
		8.80×10^{9}	15.8	-1.8	305	-125	2.92	+2.70
		2.61×10^{10}	25.9	+8.3	205	-225	7.17	+6.95
66	Mineral	0	40.4	-	400	-	1.42	-
		2.60×10^{10}	60.2	+19.8	390	-10	0.70	-0.72

The results of this modified procedure on four irradiated oils are given in Table XXV. Data obtained by the standard method are provided for comparison. It should be noted that the revised procedure does not give any weight gains. The quantities of metal corrosion and of coke deposition are separately assessed and the extent and type of metal attack determined. It is now discernible that copper is attacked in all cases, and that lubricant ANP 63 becomes increasingly corrosive to magnesium alloy with increasing radiation dose.

2. Mechanical Evaluation

The mechanical evaluation of lubricants was carried out in (1) the Model C Panel Coker, (2) The WADC Deposition Tester, (3) The WADC High Temperature Bearing Head, and (4) The CRC Grease Tester. The results from the first two machines will be discussed in detail. Bearing Test results will be presented in the next progress report. The data obtained on the latter tester during the reporting period are presented in Section III. Insufficient runs are available to ascertain any trends.

The formation of varnish, sludge, and coke is the result of a complex process involving oxidation and polymerization of the lubricant. In a general way, these products can be considered as a dehydrogenated high molecular weight material. Some of the factors controlling the amount of deposits formed are: the composition of the original material, the presence ofcatalysts, the temperature at which the material is tested, the quantity of radiation received by the material, and the evaporation rate of the material.

a. Model C Panel Coker

The panel coking test evaluates a lubricant for its coking tendencies. It can also be used to predict oil consumption. These properties are measured as a function of temperature and time (Appendix IV). The discussion of panel coking tests is divided into three parts. The first part will discuss the effect of temperature on the lubricant, the second the effect of radiation, and third will be a presentation of a possible method for determining the heat of formation of coke for a lubricant from available data.

The amount of coke formed during the 600°F panel coking tests without irradiation varied from 2.7 mg for ANP-61 to 597.9 mg for ANP-66. Increasing the panel temperature to

TABLE XXV

COMPARISON OF STANDARD AND REVISED CORROSION AND OXIDATION TEST

Lubricant ANP Designation	Gamma Dose, Static ergs/gmC	Behavior of Metal Specimens				
			Change in weight, mg/cm^2			
		Metal	Standard	Revised	Coke	Microscopic Examination of Cleaned Area
58	2.61×10^9	Steel	+0.01	-0.01	0.02	Uniform very slight etch
		Silver	+0.01	-0.01	0.02	Uniform very slight etch
		Aluminum Alloy	0.0	-0.01	0.01	Pitted
		Magnesium Alloy	0.0	-0.01	0.01	No significant obs.
		Copper	-0.12	-0.68	0.56	Severe attack under coke
60	2.64×10^9	Steel	+0.01	-0.01	0.02	Crystals coke, rust
		Silver	0.0	0.0	0.0	Minute oxide covering
		Aluminum Alloy	0.0	-0.02	0.02	Pitted
		Magnesium Alloy	+0.01	-0.65	0.66	Crystals, severe etch
		Copper	-0.07	-1.14	.07	Severe etch under coke
63	2.55×10^9	Steel	-0.02	-0.01	trace	Uniform etch, some rust
		Silver	-0.07	-0.07	0.0	No significant obs.
		Aluminum Alloy	-0.06	-0.04	0.0	No significant obs.
		Magnesium Alloy	-0.06	-0.05	trace	No significant obs.
		Copper	-7.32	-15.59	8.27	Pitted, severe etch
63	8.80×10^9	Steel	-0.01	-0.03	0.02	Varnish removed
		Silver	-0.04	-0.06	0.02	No significant obs.
		Aluminum Alloy	-0.02	-0.02	0.0	No significant obs.
		Magnesium Alloy	-1.30	-1.94	0.64	Severe attack under coke
		Copper	-21.79	-21.79	0.0	

TABLE XXV (cont'd)

COMPARISON OF STANDARD AND REVISED
CORROSION AND OXIDATION TEST

Lubricant ANP Designation	Gamma Dose, Static ergs/gmC	Metal	Behavior of Metal Specimens: Change in weight, mg/cm^2 Standard	Revised	Coke	Microscopic Examination of Cleaned Area
63	2.61×10^{10}	Steel	-1.86	-1.91	0.05	Etched
		Silver	0.0	-0.02	0.02	Slight uniform etch
		Aluminum Alloy	0.0	0.0	0.0	No significant obs.
		Magnesium Alloy	-38.58	-45.21	6.63	Coupon disintegrated
		Copper	-1.18	-1.38	0.20	Localized severe etch
64	2.53×10^{10}	Steel	+0.01	0.0	0.01	Thin varnish layer
		Silver	+0.01	-0.02	0.03	Etched
		Aluminum Alloy	+0.01	-0.01	0.02	Erosion
		Magnesium Alloy	+0.01	0.0	0.01	Crystalline deposit
		Copper	+0.01	-1.38	1.39	Severe etching

700°F generally resulted in greater amounts of coke formation, with variation of 22.6 mg for ANP-78 to the extremes of 2007.7 mg for ANP-75 and 2240.0 mg for GTO-373. The lubricant ANP-76 showed a slight decrease in coke formation, i.e., from 46.7 mg to 39.8 mg with an increase in temperature from 600 to 700°F.

The oil consumption during the panel coking test also varied. Oil consumption may be considered as a measure of the rate of lubricant evaporation. This evaporation is due to low molecular weight constituents which are present in the original material or which may be formed during the test. The oil consumption in an 8 hour panel coking test at 600°F, with no irradiation, varied from 25 ml for ANP-78 to 420 ml for ANP-62. A temperature increase to 700°F caused an increase in oil consumption, with variation, from 130 ml for ANP-78 to 805 ml for ANP-75.

Since the coke formation and the oil consumption vary both with temperature and radiation dose, and since the evaporation leaves behind the high molecular weight constituents which are available to further polymerize with more coke formation, an additional parameter could be considered. This parameter is the amount of coke formed per quantity of oil consumed. Since the amount of coke formed is dependent on the residence time of the original and makeup lubricant on the panel, it will vary as the quantity of additional makeup lubricant increases. This permits the introduction of a concentration term for the coke formation, namely $[\text{coke}]$, i.e., the mg of coke formed per ml of oil consumed. As an illustration, Table XXVI shows the variation of coke, oil consumption, and the quantity of coke formed per ml of oil consumed for the lubricants ANP-75 through ANP-80. For increased temperature, the coke concentration $[\text{coke}]$ increases for ANP-75, 77, and 80. It decreased for ANP-76 and 78 and remains approximately constant for ANP-79. Those lubricants which increase in $[\text{coke}]$ with increase in temperature suggest more polymerization than decomposition; similarly, those which decrease in $[\text{coke}]$ with increase in temperature suggest more decomposition than polymerization.

It is of interest to check the repeatability of the panel coking test using the coke concentration for lubricant ANP-79. Since radiation caused little or no change in the lubricant at the 600°F panel coking test, these runs were selected to

TABLE XXVI

EFFECT OF RADIATION ON COKE CONCENTRATION IN THE PANEL COKING TEST

Lubricant ANP Designation	Run No.	Gamma Dose Ergs/gm Carbon		Coking Tendency		Oil Consumption	Coke
		Static	Dynamic	Panel Temp(°F)	Coke(mg)	(ml)	(mg/ml)
75	82	0	0	600	85.0	285	0.30
	94	0	0	700	2007.7	805	2.51
	206	8.36×10^7	1.67×10^8	600	68.7	190	0.36
	83	1.04×10^8	1.67×10^8	600	92.9	325	0.31
	219	8.71×10^7	2.87×10^8	700	1415.3	520	2.72
	200	1.31×10^9	1.18×10^8	700	218.1	380	0.57
76	84	0	0	600	46.7	105	0.45
	95	0	0	700	39.8	317	0.13
	85	8.34×10^7	1.67×10^8	600	30.0	340	0.10
	207	9.41×10^7	1.68×10^8	600	302.0	50	6.04
	201	1.50×10^9	1.18×10^8	700	67.2	220	0.31
	227	9.85×10^9	1.90×10^8	700	35.0	340	0.10
77	79	0	0	600	4.1	220	0.02
	96	0	0	700	890.4	345	2.58
	86	8.34×10^7	1.67×10^8	600	17.0	110	0.15
	208	6.27×10^7	1.67×10^8	600	14.6	140	0.10
	107	1.44×10^9	1.18×10^8	700	1219.7	325	3.75
	228	8.71×10^9	1.90×10	700	603.9	275	2.20

TABLE XXVI (cont'd)

EFFECT OF RADIATION ON COKE CONCENTRATION IN THE PANEL COKING TEST

Lubricant ANP Designation	Run No.	Gamma Dose Ergs/gm Carbon		Coking Tendency		Oil Consumption (ml)	Coke (mg/ml)
		Static	Dynamic	Panel Temp(°F)	Coke(mg)		
78	97	0	0	600	16.7	25	0.67
	80	0	0	700	22.6	130	0.17
	87	8.34×10^7	1.67×10^8	600	8.8	90	0.10
	88	7.32×10^7	1.67×10^8	700	28.3	210	0.13
	209	6.27×10^7	1.67×10^8	600	13.7	10	1.37
	212	1.74×10^6	1.67×10^8	600	26.6	200	0.13
	229	9.19×10^9	1.20×10^8	700	51.6	260	0.20
79	90	0	0	600	15.7	155	0.10
	108	0	0	700	55.6	515	0.11
	89	9.93×10^7	1.50×10^8	600	15.1	240	0.06
	210	8.36×10^7	1.67×10^8	600	49.5	180	0.28
	216	8.38×10^7	1.68×10^8	600	30.3	310	0.10
	99	0	1.67×10^8	700	221.2	470	0.47
	102	1.80×10^9	1.18×10^8	700	145.4	550	0.26
	232	8.68×10^9	1.80×10^8	700	152.0	450	0.34
80	91	0	0	600	10.7	250	0.04
	109	0	0	700	65.6	390	0.17
	104	5.80×10^7	1.18×10^8	700	178.6	200	0.89
	211	8.36×10^7	1.67×10^8	600	4.3	310	0.01
	213	8.36×10^7	1.67×10^8	700	119.2	360	0.33
	98	1.67×10^8	1.67×10^8	600	16.8	100	0.17
	231	1.37×10^{10}	2.00×10^8	700	201.0	330	0.61

calculate repeatability. An average [coke] value of 0.14 mg/ml with a mean deviation of about 60 percent is shown in Table XXVII. This compares reasonably with the value for coke formation.(28)

TABLE XXVII

REPEATABILITY OF THE PANEL COKING TEST WITH LUBRICANT ANP-79

	(Coke) (mg/ml)	Deviation
	0.10	-0.04
	0.06	-0.08
	0.28	+0.14
	0.10	-0.04
Average	0.14	0.08

As was previously stated, the effect of radiation on lubricants is a complex interaction. This interaction can lead to more coke formation (polymerization), oil consumption (decomposition), or a combination of the two reactions. The formation of the final products will depend not only on the quantity of irradiation but equally, if not more important, on the amount of preirradiation (static irradiation) on the lubricant and, also, the subsequent amount of dynamic irradiation during the panel coking test. Although this study was designed to test large numbers of lubricants, it is possible to determine some of these interactions with particular lubricants. A comparison will be made to determine the effect of preirradiation (static) with no dynamic irradiation on the lubricant, the effect of increasing the amount of static irradiation, the effect of dynamic irradiation with no static irradiation, and, finally, the effect of combined static and dynamic irradiation. The effect of the combination of temperature and radiation on the lubricant will also be discussed.

The effect of preirradiation prior to subsequent mechanical evaluation in the Panel Coker is summarized in Table XXVIII using lubricants ANP 61, 65, and 66 as examples.

The panel coking tests on lubricant ANP-55, with a dynamic irradiation of 1.67×10^8 ergs/gm carbon, showed an increase

TABLE XXVIII

EFFECTS OF PREIRRADIATION ON BEHAVIOR OF LUBRICANTS IN THE MODEL C PANEL COKER AT 600°F

Lubricant Designation ANP	Gamma Dose, Static ergs/gm Carbon	Coke Formation mg		Oil Consumption, ml		Coke Concentration, mg/ml	
		Value	Change	Value	Change	Value	Change
61	0	2.7	-	190	-	0.014	-
	2.60×10^{9}	54.1	+51.4	240	+50	0.225	+0.211
	1.02×10^{10}	43.1	+40.4	250	+60	0.173	+0.159
	2.64×10^{10}	6.7	+4.0	253	+63	0.027	+0.013
65	0	459.4	-	90	-	5.10	-
	8.71×10^{8}	39.4	-420.0	190	+100	0.207	-4.893
	8.80×10^{9}	42.1	-417.3	80	-10	0.526	-4.574
	2.62×10^{10}	135.7	-323.7	35	-55	3.87	-1.23
66	0	597.9	-	220	-	2.72	-
	2.62×10^{9}	59.0	-538.9	210	-10	0.281	-2.439
	8.88×10^{9}	32.6	-565.3	115	-105	0.283	-2.437
	2.60×10^{10}	12.6	-585.3	105	-115	0.120	-2.600

in coke formation and in oil consumption, with no change in coke concentration compared to the same test without irradiation. Although the test on lubricant ANP-74, with dynamic irradiation of 1.4×10^{8} ergs/gm carbon, showed no change in coke concentration, there was a decrease in the coke formation and the oil consumption.

It is of interest to determine whether there is a difference between preirradiation and testing of a lubricant as compared to preirradiation and testing with dynamic irradiation, with both total quantities of irradiation being approximately equal. An illustration of this comparison can be found by examining the data for lubricant ANP-61, Table XXIX. This seems to strongly suggest that different results can be obtained by preirradiation alone compared to preirradiation followed by dynamic irradiation.

The heat of formation of coke (Appendix VIII) viscosity, and quantity of coke for lubricants ANP-75 through 80, have been determined and are presented in Table XXX. From the

TABLE XXIX

COMPARISON OF COMBINED AND SEPARATE ENVIRONMENTS LUBRICANT ANP-61 IN THE MODEL C PANEL COKER

Temperature °F	Gamma Dose ergs/gm Carbon		Coke Formation, mg		Oil Consumption ml		Coke Concentration mg/ml	
	Static	Dynamic	Value	Change	Value	Change	Value	Change
600°	0	0	2.7	-	190	-	0.014	-
	2.64×10^{10}	0	6.7	+4.0	253	+63	0.027	+0.013
	2.64×10^{10}	1.4×10^{8}	6.7	+4.0	370	+180	0.018	+0.004
700°	2.54×10^{10}	0	743.9	-	165	-	4.48	-
	2.65×10^{10}	1.27×10^{8}	414.5	-329.4	500	+335	0.828	-3.652

TABLE XXX

HEAT OF COKE FORMATION (MODEL C PANEL COKER)

Lubricant Designation	Heat of Coke Formation (kcal)	Coke formed, mg 600°F	Coke formed, mg 700°F	Viscosity, cs at 100°F
ANP-75	+29	85	2007	15.10
ANP-76	-17	47	40	41.65
ANP-77	+66	4	890	13.16
ANP-78	-19	16	22	63.59
ANP-79	+13	16	56	18.46
ANP-80	+20	11	66	29.06

heat of coke formation, it appears that ANP-76 and ANP-78 are similar, and that there is similarity between ANP-79 and 80. It is very interesting to note that the two lubricants with negative heats of coke formation are the most viscous of the lubricants and also show the lowest change in coke formation between tests run at 600°F and at 700°F.

b. WADC Deposition Tester

The WADC Deposition Tester evaluates the relative resistance of lubricants to oxidation and thermal shock. Results are described in terms of a deposition number, which is obtained

from the weight of coke deposited on an aluminum heater and the weight of sludge deposited on a filter screen. The lubricant undergoing test is continually circulated and makeup oil is automatically added as consumption occurs.

Static irradiation and subsequent mechanical evaluation may result in increases or decreases in deposition number. In some cases, maxima or minima are observed in the relation of deposition number to static irradiation dose (Table XXXI).

TABLE XXXI

EFFECT OF STATIC IRRADIATION ON DEPOSITION NUMBER OF LUBRICANTS

Lubricant Designation ANP	Base Oil Type	Gamma Dose ergs/gm Carbon	Deposition Number Value	Change
60	Olef.	0	2.74	-
	Polym.	2.64×10^{9}	7.89	+5.15
61	Olef.	0	2.55	-
	Polym.	1.02×10^{10}	3.30	+0.75
		2.64×10^{10}	1.36	-1.19
64	Mineral	0	2.42	-
		8.71×10^{9}	2.83	+0.41
		2.53×10^{10}	3.14	+0.72

The variation of the deposition number during mechanical evaluation is indicated in Table XXXII.

In the case of lubricants ANP-61 and 64, Tables XXXI and XXXII, it is of interest to compare the changes in Deposition Number occurring during mechanical evaluation after static irradiation and those occurring during mechanical evaluation in a radiation environment. In each case, marked differences are apparent. These differences are borne out by the corresponding physical and chemical changes (Table XV). For example, the neutralization number of lubricant ANP-64 varies directly as the deposition number during static irradiation. An inverse relation is observed during mechanical evaluation in a radiation environment. The same behavior is observed with respect to the viscosity.

TABLE XXXII

EFFECT OF RADIATION ON THE BEHAVIOR OF LUBRICANTS IN THE WADC DEPOSITION TESTER

Lubricant Designation, ANP	Base Oil Type	Gamma Dose ergs/gm Carbon	Value	Change
61	Olef. Polym.	0	2.55	-
		1.76×10^8	4.47	+1.92
64	Mineral	0	2.42	-
		1.54×10^8	6.64	+4.22
		1.77×10^8	4.97	+2.55
68	Ester	0	5.94	-
		1.77×10^8	3.56	-2.38

To assess the effects of radiation on the behavior of oils in the deposition tester, it was felt that the sludge and coke formation should be considered in the light of oil consumption. For this reason, the Deposition Number per ml oil consumed (DN/ML) is suggested as a means to evaluate Deposition Test data.

At different radiation levels, the parameter DN/ML for ANP-64 behaves in a fashion similar to the viscosity and the neutralization number, Table XXXIII. It is particularly interesting to note that the statically irradiated material subjected to cold dynamic testing shows less drastic change for the DN/ML function with increasing dose than the material subjected to hot dynamic testing. To adequately evaluate the indicated trends, it would be necessary to obtain complete data for accurate curves so that comparisons may be made.

In general, it appears that the Deposition Number increases with increasing radiation. Frequently, increased oil consumption offsets the increase in total deposition so that the Deposition Number/ml oil consumed tends to behave in a fashion similar to that observed for "goodness" ratings of fuels, i.e., maxima and minima appear in the plots of this parameter vs. radiation dose, Figure 9.

TABLE XXXIII

EFFECT OF RADIATION ON THE BEHAVIOR OF LUBRICANT ANP 64 IN THE WADC DEPOSITION TESTER

Gamma Dose ergs/gm C		Deposit Wt. gms		Deposition No.	Oil Consumption ml	DN/ML		Viscosity cs 100°F		Neutralization Number mg KOH/gm	
Static	Dynamic	Coke	Sludge			Value	Change	Value	Change	Value	Change
0	0	0.06	1.83	2.43	120	0.0202	-	73.1	-	0.03	-
8.71×10^{9}	0	0.12	0.73	2.28	75	0.0305	+0.0103	527.6	+454.5	7.78	+7.75
2.53×10^{10}	0	0.21	1.05	3.15	100	0.0315	+0.0113	1954.0	+1880.9	7.33	+7.70
0	1.54×10^{8}	0.58	0.84	6.64	70	0.0949	+0.0747	351.8	+278.7	6.18	+6.15
0	1.77×10^{8}	0.35	1.48	4.98	90	0.0553	+0.0351	100.6	+27.5	1.04	+1.03

To further assess the value of this parameter, the repeatability of the DN/ML function was determined using the data obtained for GTO 313. The average value for the parameter was found to be 0.0515. The average deviation from the mean was found to be ±0.019, the maximum deviation being 0.0360. The repeatability is ±40 percent which corresponds favorably with that of the Deposition Number (see page 50).

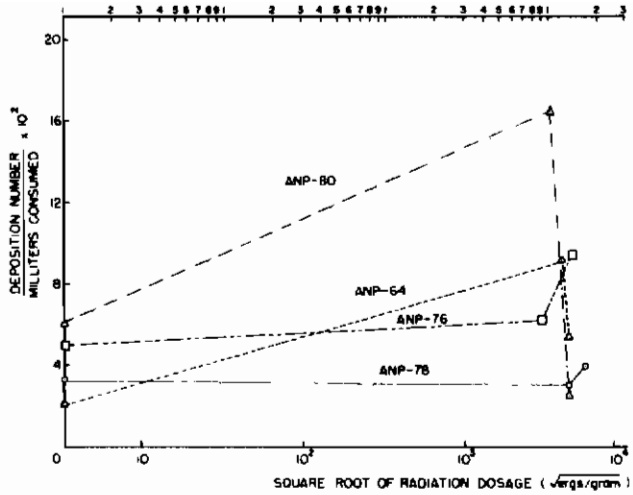

Figure 9. Behavior of Lubricants in the WADC Deposition Tester in a Radiation Environment

c. Relative Rating of Lubricants

Tests in the Model "C" Panel Coker were conducted at temperatures of 600°F and 700°F. Tables XXXIV and XXXV

TABLE XXXIV

OILS EXHIBITING LOWEST DEPOSIT FORMING TENDENCIES
600°F MODEL C PANEL COKER TEST

ANP Identification	Deposits, mg Without Radiation	Deposits, mg With Radiation	Maximum Observed Deposits Radiation Level ergs/gm C	Maximum Observed Deposits mg
80	10.7	4.3	3.34×10^8	16.8
77	4.1	14.6	2.51×10^8	17.0
79	15.7	15.1	2.51×10^8	49.5
74	48.3	19.1	0	48.3
78	16.7	26.6	1.70×10^8	26.6
76	46.7	30.0	0	46.7
63	63.2	61.5	0	63.2
61	2.7	87.7	9.68×10^9	87.7

TABLE XXXV

OILS EXHIBITING LOWEST DEPOSIT FORMING TENDENCIES
700°F MODEL C PANEL COKER TEST

ANP Identification	Deposits, mg Without Radiation	Deposits, mg With Radiation	Maximum Observed Deposits Radiation Level ergs/gm C	Maximum Observed Deposits mg
78	22.6	28.3	9.31×10^9	51.6
76	39.8	67.2	1.62×10^9	67.2
70	37.5	126.2	8.88×10^9	151.6
80	65.6	178.6	1.39×10^{10}	201.0
79	55.6	221.2	1.67×10^8	221.2

list the oils giving less than 80 mg of deposits at each of the two temperatures without radiation. Following initial selection for inclusion in the table, the oils were then listed in order of increasing deposit formation in the radiation environment. Because a number of the lubricants did not receive similar doses at high levels of radiation, the comparison was made at the lowest dose on the dynamic sample from the test in the radiation cell. This dose was approximately 10^8 ergs/gm carbon, except for ANP-61 which received about 10^{10} ergs/gm carbon. Also appearing in the tables are the maximum coke formation for each oil, and the radiation level at which this maximum was observed. In some instances, maximum deposits occurred without radiation.

The oils which appear in both Table XXXIV and Table XXXV are those which, having shown good performance at 600°F, were then tested at 700°F and showed good performance at the high temperature. Lubricant ANP-70 was not tested at 600°F.

The oils appearing in Table XXXVI are those which exhibited the best performance in the WADC Deposition Tester. Initial selection of the oils was based on a Deposition Number of 5.0 or less resulting from tests without radiation. The oils are arranged in order of increasing Deposition Number at the lowest level of total radiation which was approximately 10^8 ergs/gm carbon. The maximum observed Deposition Number was at the

TABLE XXXVI

OILS EXHIBITING LOWEST DEPOSIT FORMING TENDENCIES
WADC DEPOSITION TESTER

ANP Identification	Deposition Number Without Radiation	Deposition Number With Radiation	Maximum Deposition Number Radiation Level ergs/gm C	Maximum Deposition Number D.N.
71	2.12	0.92	1.98×10^9	2.47
80	3.61	1.31	0	3.61
77	1.98	1.45	1.63×10^9	2.61
73	1.48	1.46	1.04×10^{10}	25.87
79	1.69	1.86	1.77×10^8	1.86
78	0.80	2.54	1.77×10^8	2.54
70	2.20	2.63	1.72×10^9	9.11
76	4.74	3.24	1.77×10^8	4.74
69	2.30	3.35	1.76×10^8	3.35
61	2.55	4.47	1.76×10^8	4.47

radiation dose shown for each oil.

The oils appearing in Table XXXVII are those which are common to Table XXXVI and Table XXXIV and/or Table XXXV.

The relative rating of the lubricants is based on their performance in the WADC Deposition Tester and they follow the same order as listed in Table XXXVI. These lubricants performed well at doses of at least 10^8 ergs/gm carbon, and a number performed well at doses as high as 10^{10} ergs/gm carbon. Comments in Table XXXVII indicate results of 350°F engine tests where these data are available.

TABLE XXXVII

RELATIVE RATING OF LUBRICATING OILS

ANP Identification	Deposition Number	Comments
80	1.31	Only major change is in 700°F Panel Coker Passed 350°F Engine Test
79	1.86	Major change occurs in 700°F Panel Coker
78	2.54	Failed in 350°F Engine Test
70	2.63	Failed 350°F Engine Test
76	3.24	Failed 350°F Engine Test
61	4.47	

The following oils were not considered in the relative ratings (Table XXXVII) but are worthy of further evaluation:

(1) ANP-25, irradiated prior to receipt. No test results available without radiation.

(2) ANP-63, Deposition Number is not available without radiation.

(3) ANP-69, no 600°F Panel Coker Test without radiation.

(4) ANP-71, no 600°F Panel Coker Test.

The following oils have not yet been evaluated and are not considered in the relative ratings: GTO 309, 313, 373, 519, and 578.

ANP-77 was not included in Table XXXVII although it appears in Tables XXXIV and XXXVI because its uncontrolled foaming tendency resulted in failure in the 350°F engine test.

SECTION V

SUMMARY AND CONCLUSIONS

The evaluation of 79 fuels and 41 lubricants in dynamic test equipment has clearly demonstrated the need to assess the effects of mechanical, thermal, and radiation stresses simultaneously. That is, the results obtained by testing a material in a combined environment are not always the same as results obtained by alternate exposure of the material to the environments separately. Mechanical tests in a radiation environment often affect the materials under evaluation more severely and at lower doses than the same tests conducted in a nonradiation environment on preirradiated samples.

A number of materials performed well in the radiation environment. Ten fuels and six lubricants with the best performance characteristics were chosen for further investigation and potential use in an aircraft nuclear propulsion system. At radiation doses up to at least 10^{10} ergs/gram carbon, the majority of these materials show satisfactory performance in dynamic test equipment.

A. Fuels

The properties of fuels show little change after exposure to doses up to 10^{8} ergs/gram carbon of gamma radiation under static conditions; however, as the dose is increased beyond 10^{9} ergs/gram carbon, the values of parameters such as flash point, initial boiling point, and viscosity at -30°F will usually decrease, while the gum content will increase.

The results of mechanical evaluation in the CFR Fuel Coker show that the formation of deposits in this device is a useful parameter for comparing the behavior of fuels. The goodness rating, which is a measure of the thermal stability of a fuel, will generally decrease with increasing temperature, but a number of the fuels tested showed no change up to the maximum operating temperature used during this program. Preirradiation and subsequent mechanical evaluation may give either an increase or decrease in the goodness rating. In many instances, when the goodness rating is plotted against the radiation dose, a maximum or minimum in the curve appears.

Mechanical evaluation in a radiation environment shows that the effect of radiation alone on various properties of the fuels required by the

specification tests is not sufficient to predict trends. For example, in the combined environment of radiation and those produced by the CFR Fuel Coker, the viscosity at -30°F will usually increase, whereas radiation applied separately does not produce this effect. Preirradiation and subsequent mechanical evaluation may often show an improvement or no change in the goodness rating. When the same evaluation is conducted in a radiation environment, these fuels may show either a decrease in goodness rating or a rapid failure. In some instances, these failures have been associated with fuels that form a precipitate during or after static irradiation.

Preliminary investigation has shown that the effect of radiation on fuels can be assessed by following the time-rate of change of filter pressure drop in the CFR Fuel Coker. In most instances, radiation increases the rate of filter plugging. Preirradiation and subsequent dynamic evaluation cannot be used to predict performance, for in many instances it improves the fuel.

A number of fuels perform well in the CFR Fuel Coker operating in a radiation environment at doses up to 10^{10} ergs/gram carbon. These fuels are listed in Table XXIII and should be satisfactory for use in conjunction with an airborne reactor.

B. Lubricants

Static irradiation, as in the case of fuels, does not affect lubricants until a static dose of about 10^{9} ergs/gram carbon is reached. Beyond this dose, the flash point and viscosity usually decrease. The neutralization number will usually increase, as will the tendency toward metal corrosion and increasing deposit formation.

The Model C Panel Coker and the WADC Deposition Tester measure the tendency of lubricants to form coke and, in the latter case, to form sludge. Both dynamic test machines provide suitable parameters for comparing the behavior of lubricants.

The Model C Panel Coker showed that increasing temperature usually increases the amount of coke formed. Preirradiation and subsequent mechanical evaluation may cause an increase or decrease in the amount of coke formed. When the test is conducted in a radiation environment, more severe coke formation usually occurs. In some instances at 700°F, the coke formation decreases. The heat of formation of coke was calculated from the data for a series of lubricants. It is interesting to note that

negative heats of formation correspond to viscous lubricants which showed the lowest change in coke formation with temperature. A coke concentration term was introduced. This is the ratio of coke formed to oil consumed. Although high coke formation and high oil consumption are individually of interest, the ratio permits further comparison of trends.

The WADC Deposition Tester was used to determine the Deposition Number of lubricants. Preirradiation caused an increase or decrease in this parameter; in some cases, the Deposition Number passed through either a maximum or minimum with increasing radiation dose. Evaluation in the radiation environment usually caused either an increase or a small change in the Deposition Number. When the Deposition Number is considered in conjunction with oil consumed (DN/ML), other trends become evident. Thus, DN/ML behaves the same as the viscosity and inversely as the neutralization number.

A number of lubricants that perform well in the Model C Panel Coker, and WADC Deposition Tester in the radiation environment at doses up to 10^{10} ergs/gram carbon, are listed in Table XXXVII. These lubricants might be satisfactory for use in conjunction with an airborne reactor.

SECTION VI

FUTURE PROGRAM

The major objective of this program is to evaluate the performance in a radiation environment of fuels, hydraulic fluids, and lubricants developed by other Air Force contractors. As pertinent data is obtained, it should then be possible to establish criteria for specifications covering these materials to be used in a radiation environment.

The program to date has been a "crash" type screening effort that has resulted in the selection of a number of fuels and oils which are considered promising for use in an airborne reactor. However, it is now necessary to investigate more carefully the behavior of these materials and, also, to study the reasons for good performance in dynamically radiated test machinery. To accomplish these purposes the following items will be incorporated into the future program:

(1) More precise determinations of test results will be obtained using at least duplicate runs and, preferably, the number of determinations required for statistical significance.

(2) The effects of dose rates will be investigated.

(3) Complete specification testing will be undertaken, where possible, before and after dynamic evaluation in a radiation environment to determine if ensuing changes in properties may affect engineering design.

(4) Different base stocks comprising both mineral and synthetic fluids will be evaluated.

(5) The effect of additives in different base stocks will be evaluated.

In addition to the evaluation of fuels and oils, increased emphasis is being placed on hydraulic fluids, greases, and dry film lubricants. It is anticipated, from preliminary results, that suitable materials will be forthcoming in the near future.

APPENDIX I

CHEMISTRY AND PETROLEUM LABORATORY

The chemistry laboratory used in support of this project is located at the Cook Technological Center, Morton Grove, Illinois, and was designed and financed by the Cook Electric Company. The facility is extensively equipped for the physical, chemical, and mechanical evaluation of fuels and lubricants, particularly for the requirements in the specifications listed in Table I.

The staff consists of 16 engineers and scientists representing the fields of mechanical engineering, metallurgy, lubrication engineering, physical and organic chemistry, and physics. Trained technicians are available to support technical personnel in the performance of the varied tests.

The laboratory is shown schematically in Figure 10, and views of the interior are shown in Figure 1. The fireproof building has 8000 square feet of floor space and is adjacent to the radiation cell laboratory. The two laboratories are housed in separate buildings and are connected by a passageway. Each laboratory is air-conditioned by a separate system to minimize contamination.

The isolated radiochemical laboratory is located as far as possible from sources of radiation. Another part of the laboratory used for hazardous projects is a special cell constructed to withstand explosions. This cell incorporates a detection and automatic washdown system as well as blowout windows.

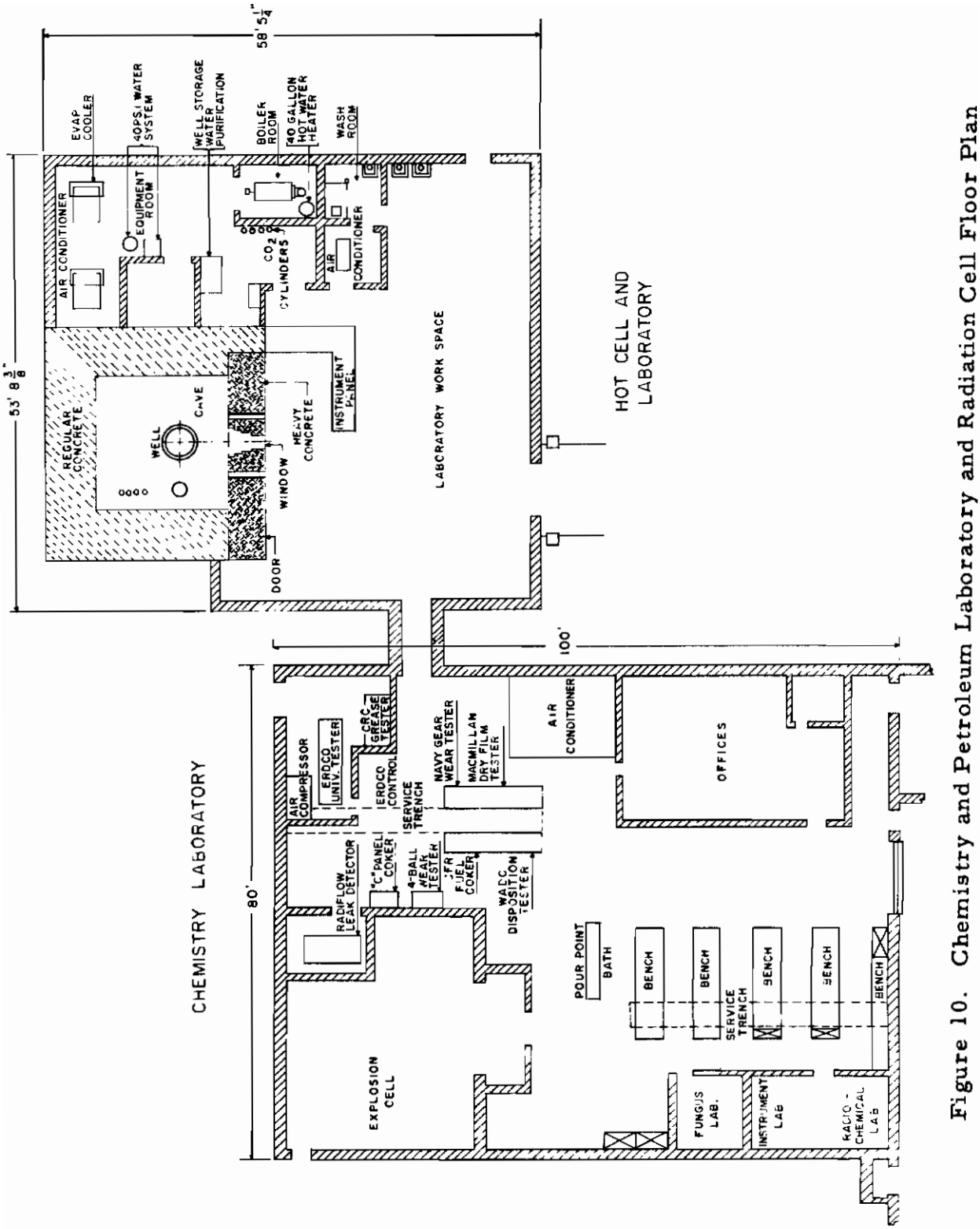

Figure 10. Chemistry and Petroleum Laboratory and Radiation Cell Floor Plan

APPENDIX II

GAMMA-RADIATION FACILITY

The gamma-radiation facility is an integral part of the testing program described in this study. It was designed and privately financed by the Cook Electric Company and was constructed to accommodate large dynamic test equipment. Considerable equipment and facilities were built into the cell to make it versatile and completely safe in operation. This discussion concerns the shielding requirements, construction, equipment, and safety features. The source loading, cell operation, and dosimetry are presented in Appendices V and VI.

Among the most important considerations in the building of the Cobalt 60 facility was the determination of the shielding required to safeguard personnel from radiation.

The front wall of the cell is constructed of magnetite concrete with a density of 4.5 g/cc; the side, backwalls, and the ceiling are constructed of ordinary concrete and the viewing window is lead glass. For purposes of the shielding calculations, a point source of 100,000 curies of Cobalt 60 was assumed. The maximum permissible flux, I, on the operator side of the source was set at 2 mr/hr.

The flux level 4 feet from the unshielded source was calculated using the relation

$$I_o = \frac{0.868\ CEN \times 10^6}{d^2}$$

where

I_o = source intensity (mr/hr)

C = curie level

EN = average energy times number of particle emergent per disintegration (for Cobalt 60, there are 2 gamma quanta)

d = distance of the measuring instrument from the source.

Based on this calculation of I_o, the number of half thicknesses, n, required to reduce I_o to I was calculated using the relation

$$n = 3.33 \log, \frac{I_o}{I}$$

This leads to the value n = 25.547. Assuming a 20 percent buildup factor, the half thickness of magnetite concrete is 1.8 inch, which gives a minimum front wall thickness of 45.9 inches. The actual wall thickness is 48 inches to insure an adequate safety margin.

The thickness of ordinary concrete with a half-thickness value of 2.3 that is required to reduce the radiation level on the operator side to 2 mr/hr is 62 inches. The side and back walls of the facility are actually 68.0 inches thick and the roof is 54 inches thick. Thus, an adequate safety margin is maintained everywhere except on the roof. Even on the roof it is possible to work for 20 hours before a dose of 100 mr is reached.

To further insure safety of operation, calculations were carried out assuming misplacement of the 100,000 curie point source 1 foot from the wall. These calculations led to radiation levels below the allowable limit of 2 mr/hr for all sides of the source except the roof, where source misplacement is extremely unlikely.

The physical dimensions of the source chamber are 16 feet wide by 16 feet long by 15-1/2 feet high. The walls were poured in location in prefabricated forms. The entire structure is reinforced with 3/4 inch steel rods placed 8 inches apart. The foundation for the cave extends 8 feet down insuring that no sag can occur. The source well is located 4 feet from the front face, approximately in the center of the front wall. The well is 4 feet in diameter and 24 feet deep, providing 22 feet of water shield when the source is submerged. The source itself is a hollow cylinder, 3 slugs thick, 14 inches high, and 23 inches in diameter (see Figure 11). The source is raised and lowered on a mechanical elevator device provided with a magnetic clutch (see Figure 12). The weight of the source is counterbalanced to lower the source to the bottom of the well in case of power failure.

The radiation shielding window is a 48 inch thickness of solid slabs of glass. The complete unit is composed of a standard 36 inch assembly, to which was added another 11 inch thickness on the cold side. The 11 inch panel was added for several reasons: not only does it provide additional shielding value, making the complete assembly equivalent to the front wall, but it alters the refractive index sufficiently to increase the viewing angle to 11 degrees over the 7 degree advantage already provided by the larger

assembly. The spaces between the glass are filled with a high grade optical quality oil to minimize fringing and annoying optical effects produced by light transmittance through glass interfaces.

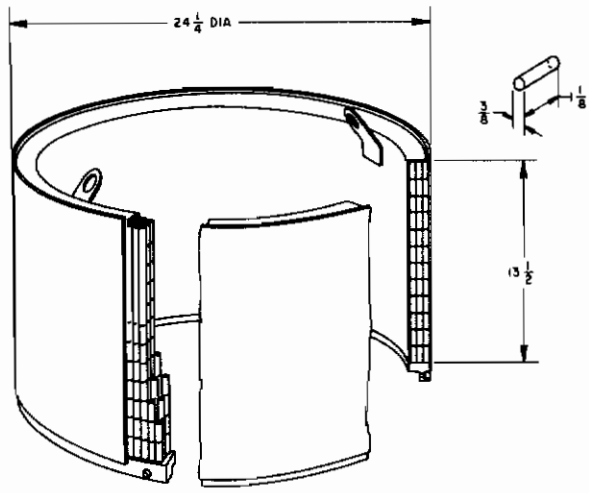

Figure 11. Cobalt 60 Source

The front face of the cell contains the 48 inch thick lead glass viewing window, the door, four 4 inch diameter plugged access ports, two larger diameter access ports, and a pair of Argonne Type 8 master slave manipulators. The rear wall contains five 4 inch diameter access ports while the ceiling contains two. In addition, provisions are made for pumping liquids through pipes embedded in the foundation. There are several dozen such high pressure lines which run under the foundation into a side room.

The door of the cell has its own traction motor which is connected to a series of interlocking switches so that opening or closing the door can only be accomplished under safe conditions (Figure 3). It consists of a 1/4 inch sheet steel frame filled with magnetite concrete which was poured with the door in location.

The entire facility is built and operated on a fail safe basis. The source's electrical operating controls (Figure 13) are set so that the door cannot be opened unless a microswitch is tripped. Conversely, the source cannot be raised unless a switch on the door is in a proper position. Two men are required to operate the door closing controls to minimize possibility of accidents. A 15 second time delay between the initial activation of the source elevating mechanism and actual source elevation is provided to allow activation of the "Scram" mechanism in the cave. During this 15 second period, a siren sounds in the cave.

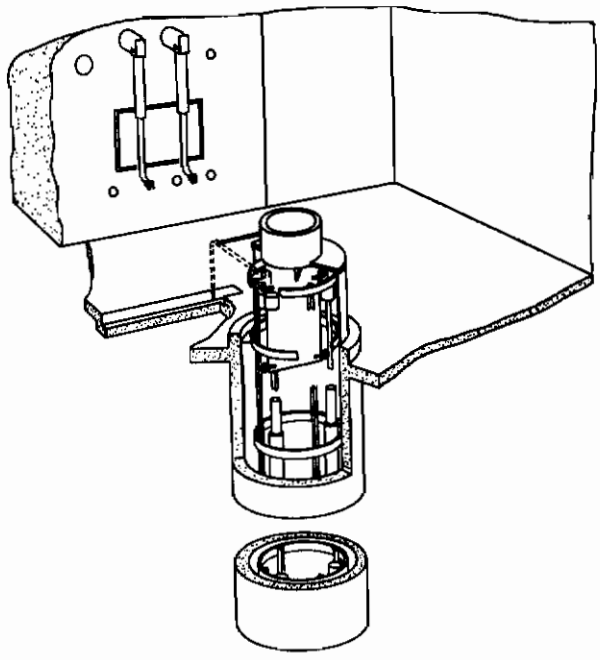

Figure 12. Source Elevator

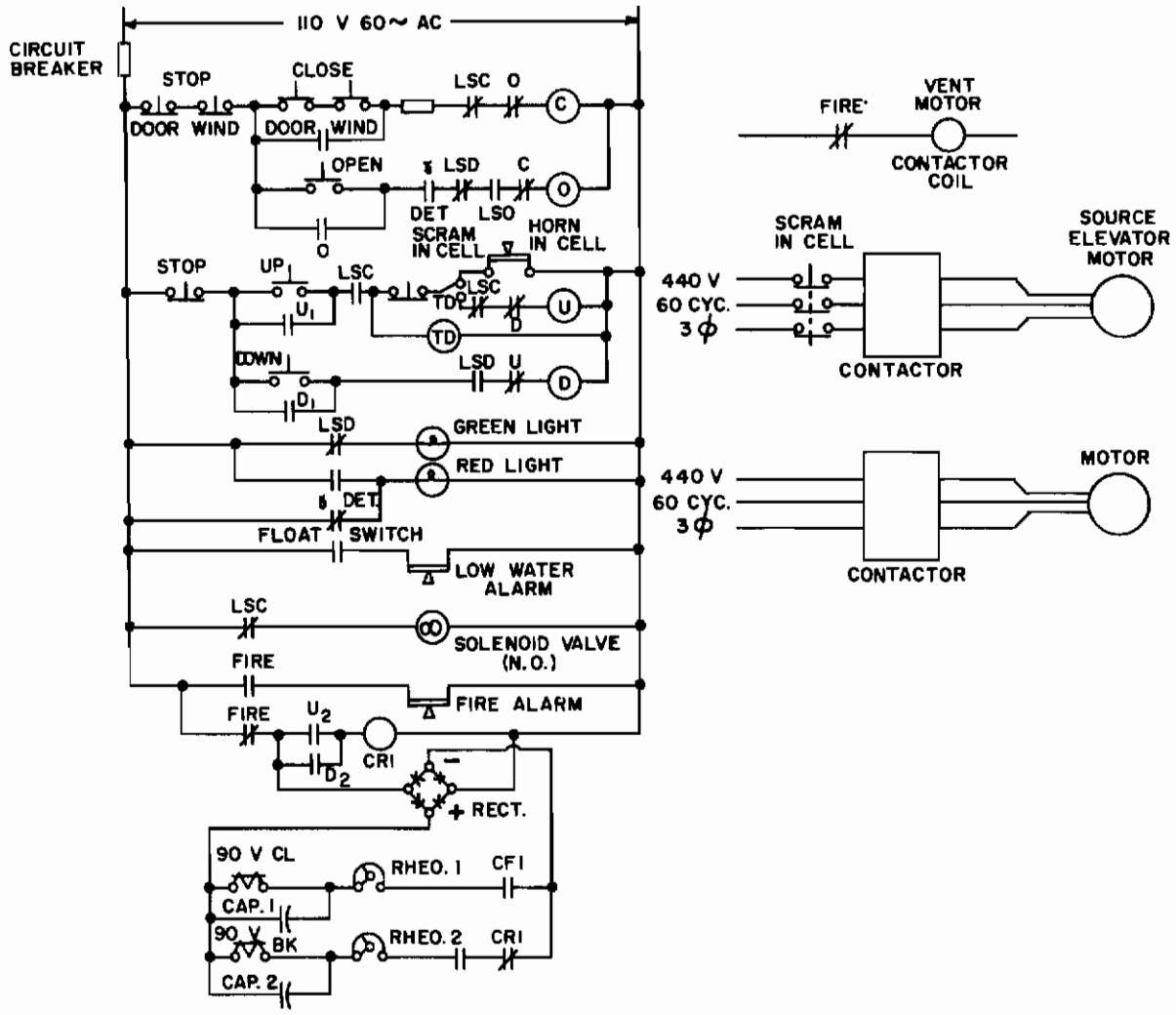

Figure 13. Cobalt 60 Cell Wiring Diagram

A separate air-conditioning system keeps the cave pressure slightly negative with respect to the external facilities. This air-conditioning circulating system operates through absolute filters, exhausting one third of the cell air each minute. A separate CO_2 foam fire extinguishing system is installed in the cave to immediately quench any potential fire.

To further insure safe source operation, all access ports as well as the door are stepped to allow no linear radiation path from the cave to the external facilities. Furthermore, a radiation monitor is connected to the interlock circuit so that the door cannot be opened unless the radiation level in the cave is safe.

A de-ionizer continuously removes dissolved minerals from the source storage well to prevent electrolytic effects and to prevent residual

radiation buildup in case of leaks.

Should any maintenance be required in the main source well, a dry well, equipped with a 4 foot thick magnetite concrete plug, is provided in the cave to allow source storage while maintenance is in progress.

In addition to the large auxiliary dry storage hole, there are four smaller dry storage holes with 2-1/2 foot thick plugs to allow storage of smaller quantities of radioactive materials.

To give the cell operations a maximum flexibility, a 5 ton crane with universal travel is installed in the cell, and a 10 ton crane is installed on the loading platform of the external 3000 square foot laboratory facility. These cranes, together with the master-slave manipulators, allow operators to move any type of equipment virtually anywhere in the Cobalt 60 facility. Special conduits provide 110 volts, 220 volt electricity, and water to the facility. Flood lights provide for maximum vision of source and cell operations.

It is interesting to note that upon first operation of the source no leaks were detected. The entire facility was found to be sound from both the point of view of safety and of mechanical operation.

APPENDIX III

LABORATORY TEST METHODS

The following presents the test methods used to determine the values of the parameters tabulated in Section III.

Fuels

Test	Method
Corrosion	FTMS No. 791, No. 5309.1
Distillation	ASTM D-86
Explosiveness	FTMS No. 791, No. 1151.1
Flash Point	FTMS No. 791, No. 1102.7
Freezing Point	FTMS No. 791, No. 1411.3
Gravity, API	ASTM D-287
Gum, Existent	ASTM D-381
Gum, Potential	ASTM D-873
Olefins and Aromatics	ASTM D-1319
Reid Vapor Pressure	ASTM D-323
Smoke Point	ASTM D-1322
Smoke Volatility Index	ASTM D-1322
Sulfur, Mercaptan	ASTM D-1219
Sulfur, Total	ASTM D-90
Thermal Value	FTMS No. 791, No. 25023
Viscosity	ASTM D-445

Lubricants

Test	Method
Compatibility	MIL-L-7808, Para. 4.5.9 MIL-L-25336, Para. 4.5.9
Conradson Carbon Residue	ASTM D-189
Corrosion, Copper	FTMS No. 791, No. 5309.1
Evaporation	MIL-L-7808, Para. 4.5.11 ASTM D-972
Fire Point	ASTM D-92
Flash Point	ASTM D-92
Foaming Tendency	ASTM D-892
Gravity, API	ASTM D-287
Neutralization Number	ASTM D-664
Oxidation - Corrosion*	FTMS No. 791, No. 5308.4
Pour Point	ASTM D-97
Saponification Number	ASTM D-94
Shell Four Ball Wear	ML 201/1/53
SOD Lead Corrosion	MIL-L-7808, Para. 4.5.13 MIL-L-25336, Para. 4.5.13
Spontaneous Ignition Temperature	ASTM D-286
Sulfur, Free and Corrosive	ASTM D-130
Swelling of Synthetic Rubber	MIL-L-7808, Para. 4.5.8 MIL-L-25336, Para. 4.5.8
Viscosity	ASTM D-445

*Also see Special Tests

Special Test

Corrosion and Oxidation Test

The corrosion and oxidation test was carried out in accordance with the standard procedure. After completion of the test, the metal coupons were suspended in a MIL-C-25107 cleaner at 120°F for 1 hour, then water-rinsed. This was followed by a rinse of iso-propyl alcohol and of benzene. After air drying, the coupons were reweighed in the normal fashion. The results of this revised procedure were compared with those obtained by using the standard procedure.

In addition to the normal visual examination, the metal coupons were carefully examined under a microscope at 100X magnification before and after the modified cleaning procedure.

APPENDIX IV

MECHANICAL TEST SYSTEMS

Detailed descriptions of the mechanical test systems used in the evaluation of fuels and lubricants in a radiation environment are given in this section. This description includes the objective, methods, and parameters for the following rigs:

(1) The CFR Fuel Coker

(2) The WADC Deposition Tester

(3) The Model "C" Panel Coker

(4) The WADC High Temperature Bearing Tester

(5) The CRC Grease Tester

Modifications necessary for operation in a radiation environment are covered.

A. CFR Fuel Coker

The CFR Fuel Coker is a test apparatus to determine the thermal stability of gas turbine engine fuels. The evaluation is based on the degree of solid deposits and filter plugging that result from the flow of fuel over a heated aluminum tube and through a heated filter element.

For simplicity, the CFR Fuel Coker Test Rig may be arbitrarily divided into a test section and a support section. The test section consists of the components that apply thermal stress to the fuel. The support section consists of the associated plumbing, electrical connections, and the control and recording equipment.

The components comprising the test section are the preheater assembly and the filter furnace. The preheater simulates hot sections of a fuel system where deposits may form and collect. The filter furnace contains a sintered element which will collect as well as form additional solid decomposition products. The degree of clogging (deposit buildup) is recorded by changes in differential pressure across the filter.

The fuel to be tested is pumped at the specified rate and pressure through the annular space formed by concentric aluminum tubes (the preheater assembly). The inner tube is heated so that the fuel leaving this space is at a specified temperature. The fuel then flows through a sintered stainless steel filter of controlled porosity which is maintained at a prescribed temperature*. Figure 14 is a schematic representation of the flow pattern.

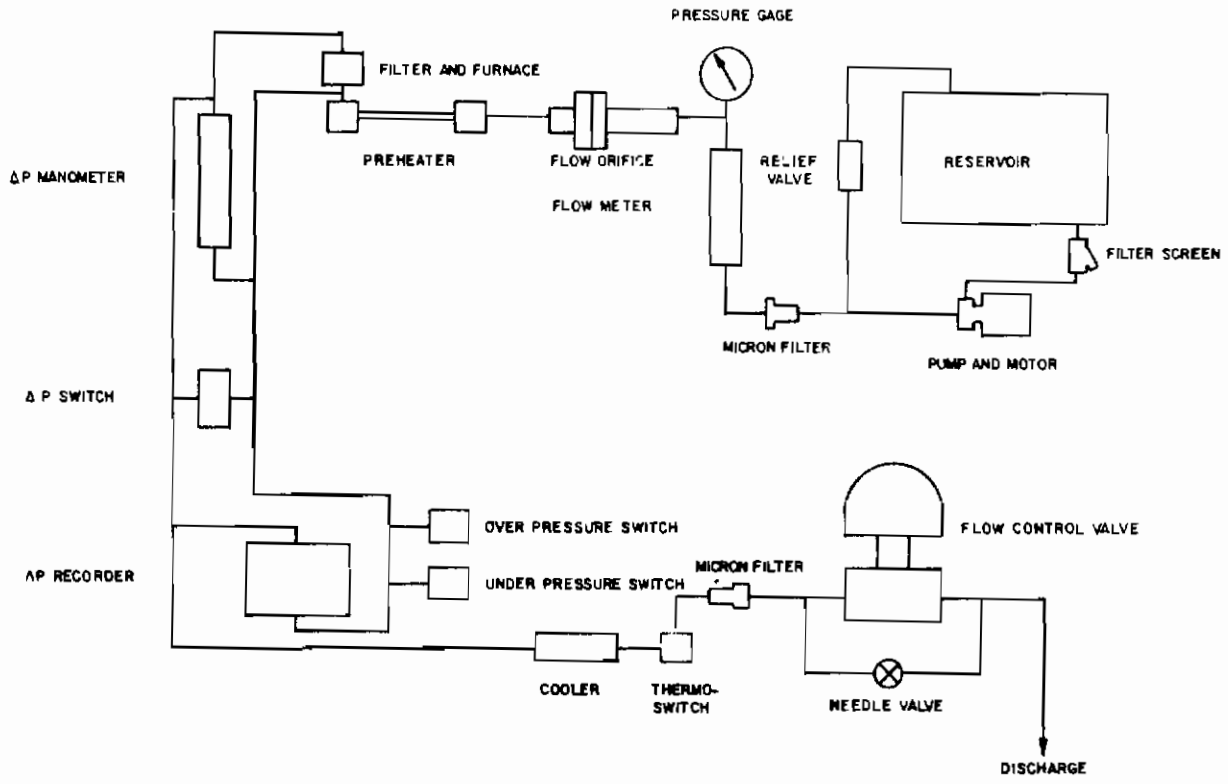

Figure 14. CFR Fuel Coker - Flow Diagram

The relative power required to achieve and maintain the thermal conditions is controlled and recorded. Differential pressure across the filter is monitored and recorded. The discharge of fuel is weighed and recorded to ascertain the exact flow rate. Test duration is nominally 5 hours. This period is shortened if differential pressure reaches 25 inches Hg before expiration of the 5 hours. Upon completion of the test period, the aluminum tube and filter are visually evaluated as to color and area covered.**

*See applicable Military Specification for temperature and flow rate.
**FTMS No. 791, Method 3464-T

The study of the effect of radiation on fuels entailed the use of two test rigs, one for nonradiation testing, and the second for dynamic radiation testing. For nonradiation work the standard unit was used; the second required modification.

Modification of the CFR Fuel Coker for use in the irradiation facility was accomplished by removing the test section and positioning it next to the source, with the pump, pressure relief valve and manometer, while keeping all other supporting equipment in a nonradiation area. The flow pattern in the rig was altered by positioning the rotameter and flow orifice between the flow control valve and the preceding filter rather than keeping them in their position before the preheater. This alteration permits the flow to be controlled from outside the radiation area without subjecting the controlling equipment to possible damage. Schematic representation of the modified equipment is shown in Figure 15.

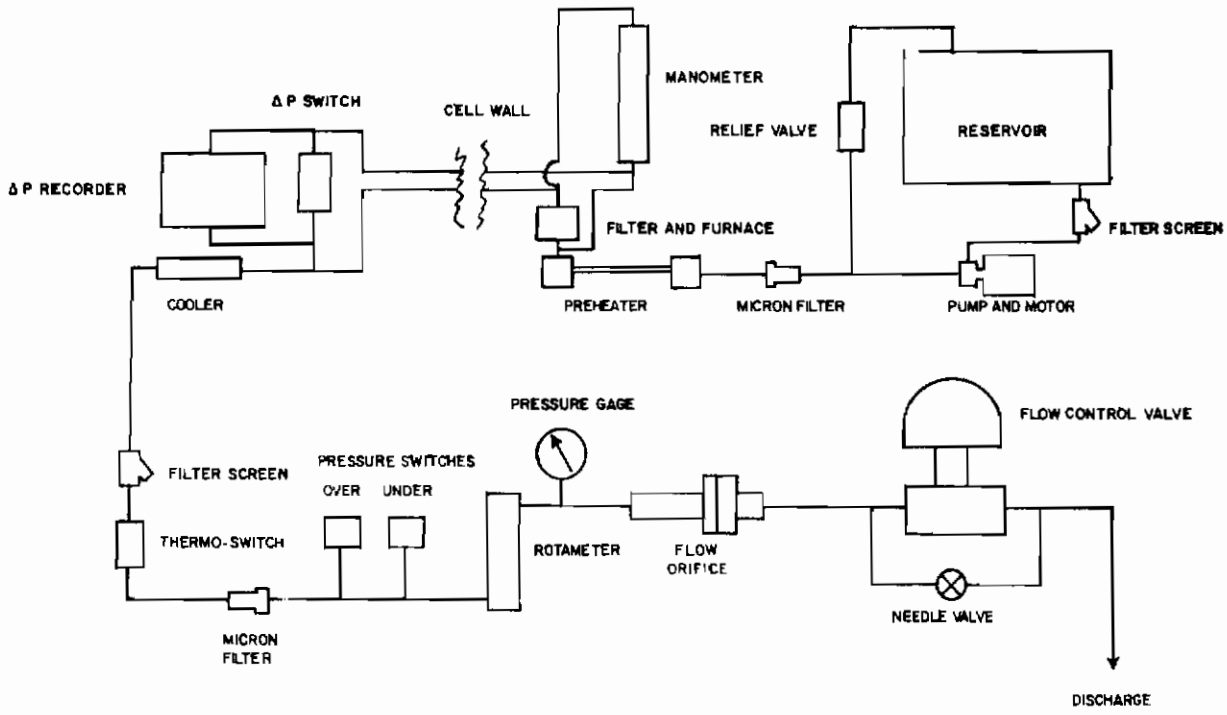

Figure 15. CFR Fuel Coker - Modified Flow Diagram

A fuel reservoir tank (approximately 6 gallons capacity) constructed of stainless steel is used for radiation of the fuel sample prior to flow through the test section. The reservoir is shaped in the form of an arc of a hollow cylinder. This configuration permits maximum and more uniform radiation flux through the fuel prior to test. Relative positions of the source, reservoir, and test section are shown in Figure 16.

Comparison of results in the modified and unmodified rigs demonstrate that the accuracy of the test was not impaired by the change in relative position of the components or by the additional lengths of required tubing. This comparison is given in Table XXXVIII.

B. Model "C" Panel Coker

The Model "C" Panel Coker is an apparatus developed for use in determining the tendency of gas turbine engine lubricants to develop solid decomposition products when in contact with a metal surface at high temperature.(17)

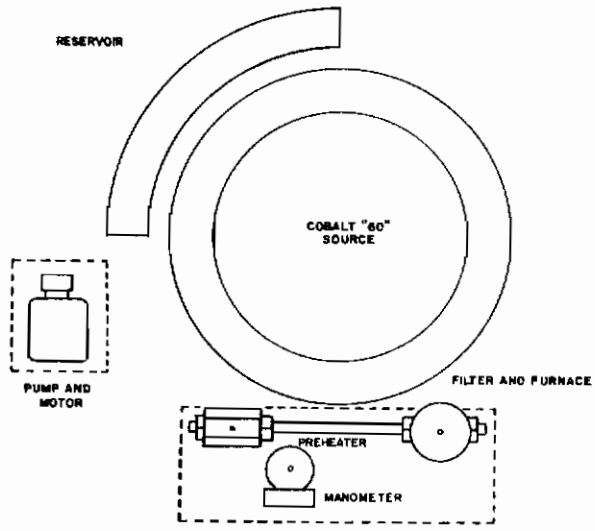

Figure 16. Test Section of CFR Fuel Coker in Radiation Cell

TABLE XXXVIII

EFFECT OF MODIFICATION ON THE PERFORMANCE OF THE CFR FUEL COKER

Run No.	Rig No.	Fuel Tested	Rig Modified	Preheater Temp, °F	Filter Temp, °F	Goodness Rating	p, inch Hg	Time of test, minutes
9	82	ANPF 57-2	No	350	450	775	0.45	300
21	82	ANPF 57-2	Yes	350	450	758	0.55	300
10	81	ANPF 57-2	No	350	450	765	0.50	300

Flow Rate is 6 pph

The equipment consists of an oil reservoir connected by a feeder tube to an oil sump. A spinner with wire whiskers is rotated in the sump, splashing oil upon a heated aluminum test panel. The weight of deposits accumulated on the panel in a specified interval of time is a measure of the coking tendency of the lubricant under test. At present, this test is required for lubricants qualifying for military specifications MIL-C-8188, MIL-L-7808, MIL-L-9236, and MIL-L-25336.

The standard test is of 8 hours duration, with a spinner speed of 1000 rpm. Test panel temperature is as specified in the applicable military specification. Test oil level in the sump is constant and is adjusted according to the procedure outlined in the "Detailed Handbook".[28] Oil consumed during the test is recorded.

The Model "C" Panel Coker used in radiation work was modified by increasing the reservoir capacity to 1000 ml. The spinner drive motor was protected from direct radiation by 2 inches of lead. Extension of the control and instrument lines into the radiation-free area provided remote operation and monitoring of the test.

The test section of this apparatus, consisting of the oil sump, spinner, test panel, reservoir, and supporting equipment, was placed adjacent to the Cobalt 60 source (Figure 17). The positioning was adjusted so the test panel and oil sump would be in a region of high flux density (see dosimetry section).

The Model "C" Panel Coker was used principally as a screening device to determine which of the submitted lubricants should be subjected to more thorough examinations.

C. WADC Deposition Tester

The objective of this test is to determine the solid deposit and sludge forming tendencies of lubricating oils in contact with high temperature metal surfaces in the presence of humidified air.[18] The test is performed by

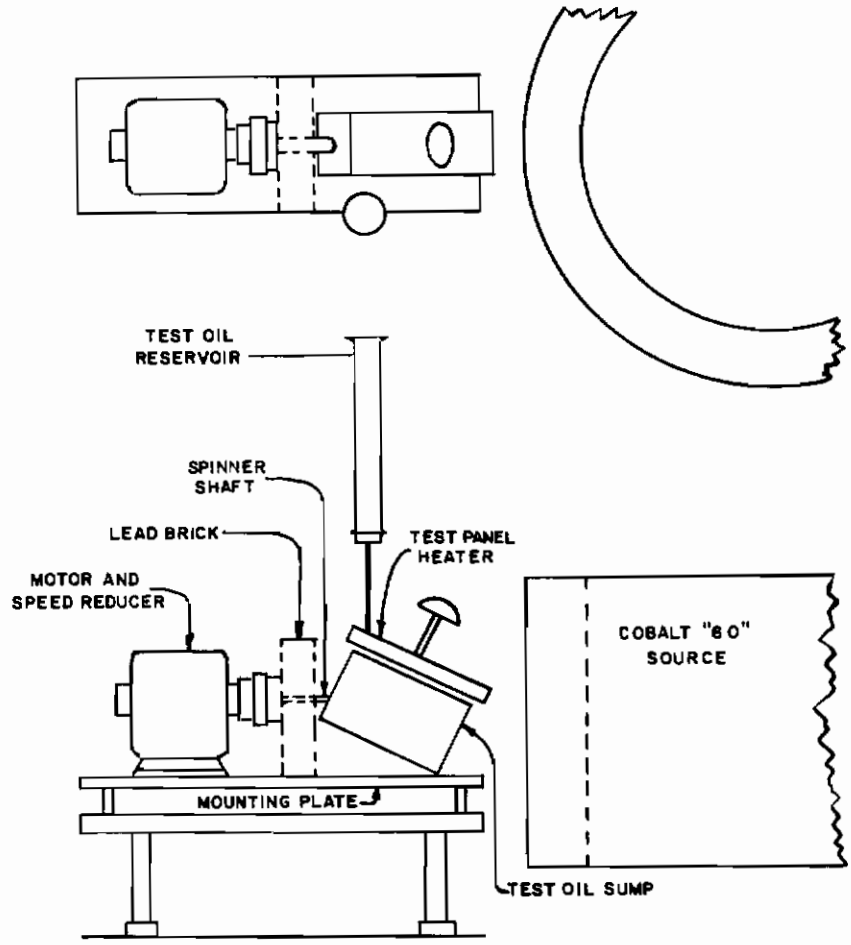

Figure 17. Model C Panel Coker in Radiation Cell

circulating a sample of oil over a heated aluminum tube and through a stainless steel filter for a specified period of time. At the end of this time, the solid deposits and sludge are visually evaluated and their weights determined. In addition, physical and chemical changes in the lubricant are measured. Figure 18 is a photograph of the WADC Deposition Tester. An extra test section appears to the right of the standard rig.

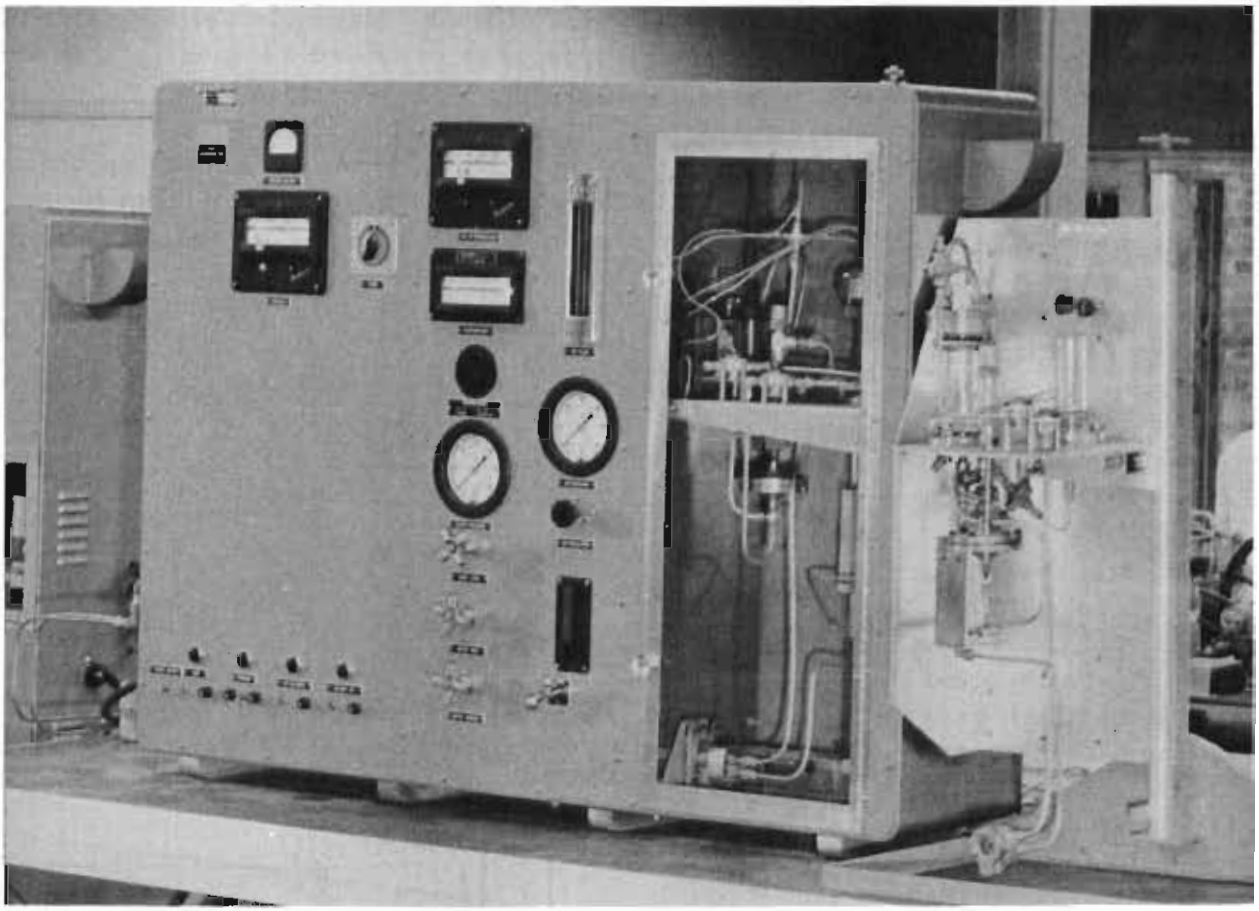

Figure 18. WADC Deposition Tester

The sample of lubricant is pumped through a 100 mesh stainless steel screen and to the top of the annular cavity formed by an inner heated aluminum cylinder and an outer glass tube. Humidified air is allowed to bubble up from the bottom of this space, aerating the gravity driven oil. The oil then flows through a heat exchanger and returns to the pump. The flow pattern is shown schematically in Figure 19.

The standard test is of 12 hour duration. During the test the following variables are controlled:

Oil-In Temperature	300°F
Coking Tube Temperature	590°F
Air Flow Rate	300 ml/min
Test Section Air Temperature	120°F
Aerated Oil Level, Below Top of Coking Glass	1-1/2 inch

Oil flow rate is adjusted to 300 ml/min of standard oil at 280°F as prescribed by the "Detailed Handbook".[28] The controlled variables are noted and recorded at 30 minute intervals. At these intervals the following uncontrolled conditions are also recorded: temperature of the oil leaving the coking head, oil pressure at the filter inlet, oil remaining in the makeup reservoir, and voltage required to maintain the temperature of the coking tube.

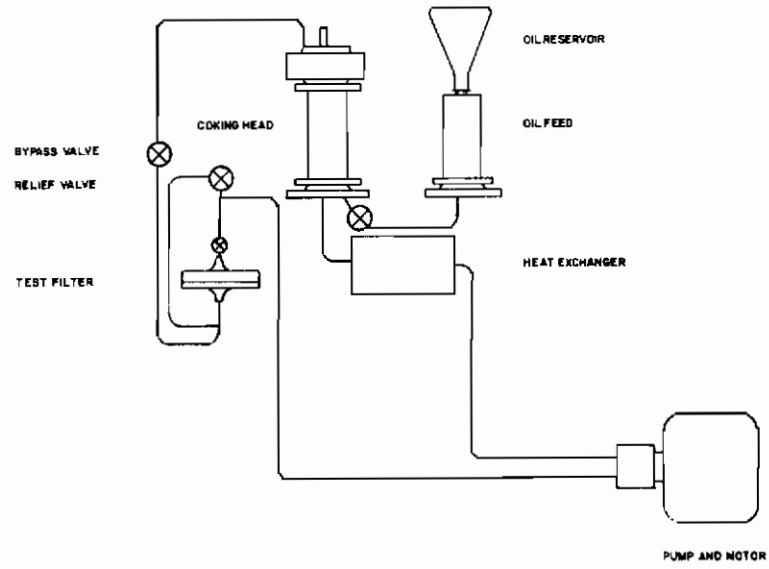

Figure 19. WADC Deposition Tester-Flow Diagram

Modification of the WADC Deposition Test Sections for use in a radiation environment were kept to a minimum in order to preserve base line data. The air saturator was removed from the cabinet and mounted on the test section rack. A cart was constructed to support the test section rack and also the pump, motor, and drive assembly, which were removed from the cabinet. The heat exchanger was mounted horizontally below the shelf on the rack to reduce the over-all height of the test section (Figure 20). Air temperature in the modified rig was not controlled.

The necessary hydraulic and electrical connections were extended to the control console, which was positioned in a radiation-free area to allow remote operation and monitoring of the test.

It was discovered in early testing in the radiation environment that the teflon used as a gasket material between the glass and abutting metal parts of the WADC Deposition Tester would not be satisfactory.

A number of elastomers and gasket materials such as asbestos and impregnated asbestos were studied to determine suitability for use in the combined environment of lubricant, heat, and radiation.* Silastic 50-24-480, supplied by Dow-Corning Corporation, showed the best performance in the Deposition Rig and was chosen as the gasket material.

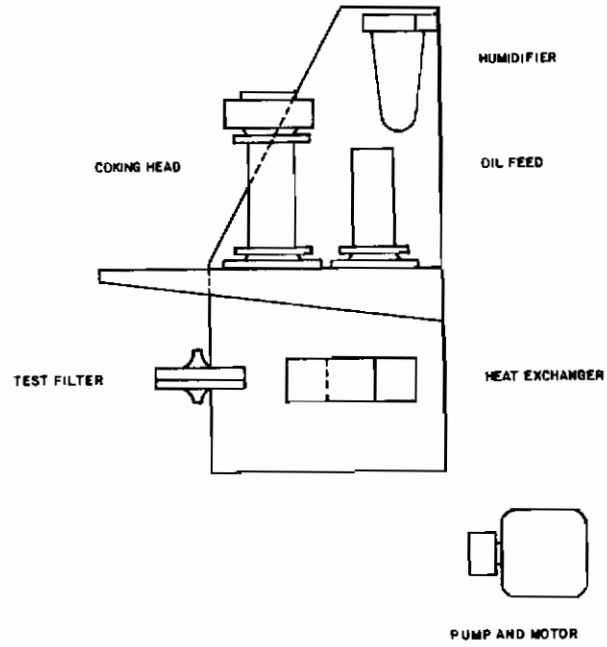

Figure 20. WADC Deposition Tester - Modified Test Section

D. WADC High Temperature Bearing Tester

The objectives of this test are the determination of performance and deterioration characteristics of lubricating oils intended for gas turbine engine bearing application.

The test is performed by circulating a sample of the lubricant to be tested, under controlled flow and temperature conditions, over a 100 mm roller bearing. The rotational speed and outer race temperature of the bearing are controlled, as is the radial load on the bearing. Viscosity and acidity of the test oil is determined at intervals. Evaluation of the solid deposits formed on the test bearing and housing following the test gives indication of the deposit forming tendency of the lubricant.

---

*The following companies cooperated in this investigation:

Crane Packing Company, 6400 Oakton Street, Morton Grove, Illinois

Dow-Corning Corporation, Midland, Michigan

B.F. Goodrich Chemical Company, 3135 Euclid Avenue, Cleveland 15, Ohio

The equipment used in this test is the "Ryder Gear Erdco Universal Tester" drive and support section with the "WADC High Temperature Bearing Head" test section. This equipment is capable of producing rotational speeds up to approximately 12,500 rpm, radial bearing loads up to approximately 1000 pounds, and bearing temperatures, measured at the outer race, up to approximately 700°F. The oil to be tested may be preheated to produce a temperature up to approximately 500°F at the test oil jet, depending on the tendency of the lubricant to form deposits on the test oil heaters and the desired oil flow rate. The test oil flow is variable from zero to approximately 4 lb/min. Figure 21 is a schematic representation of the test oil system.

For radiation work the universal drive and support section were placed permanently in the radiation cell with the necessary hydraulic and electrical connections made to the control console in the work area outside the cell. The WADC Bearing Heads were modified for radiation studies by removing excess metal from the front of the test section. The test oil jet was mounted on the periphery of the front cover to reduce the source-to-bearing dimension. Standard seals between the support and test sections were replaced by graphite-faced stainless steel bellows type seals. Figure 22 shows the modified heads.

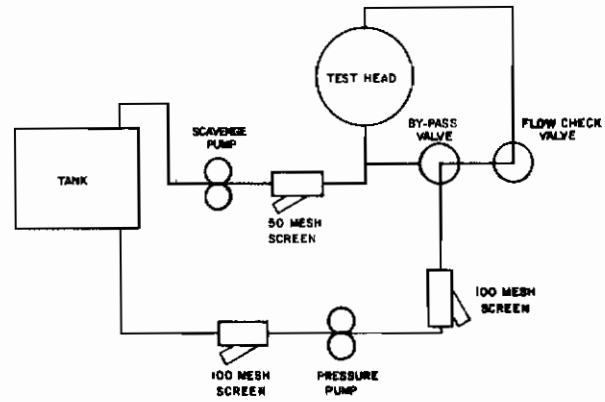

Figure 21. WADC High Temperature Bearing Tester - Test Oil System

The test utilizes 100 mm roller bearings rotated at 10,000 ± 100 rpm and with a radial load of 500 pounds. Test bearing thermocouples are located at approximately 105, 225, and 345 degree position clockwise from top center, Figure 22, as viewed from the front of the head. The junction at 345 degrees energizes a galvonometer type position-proportioning controller. The remaining two bearing junctions indicate temperature on an 18 point potentiometer. Temperature of the bearing at the 345 degree position is maintained at 500 ± 10°F.

The test oil system has a capacity of 2 gallons. Test oil flow is adjusted to 1.0 ± 0.1 lb/min, and the temperature of the oil entering the test head is 335 ± 5°F. Air, saturated with moisture at ambient temperature, enters the test head at 600 cc/min.

At 30 minute intervals, the following test conditions are recorded; elapsed hours, bearing load, bearing temperature, bulk oil temperature, test oil-in temperature, and test oil-out temperature. Also recorded at this time are bearing speed, saturated air flow, and differential pressure across the graphite seal. The condition of the drive and support section is noted by measuring and recording temperatures and pressures at strategic points.

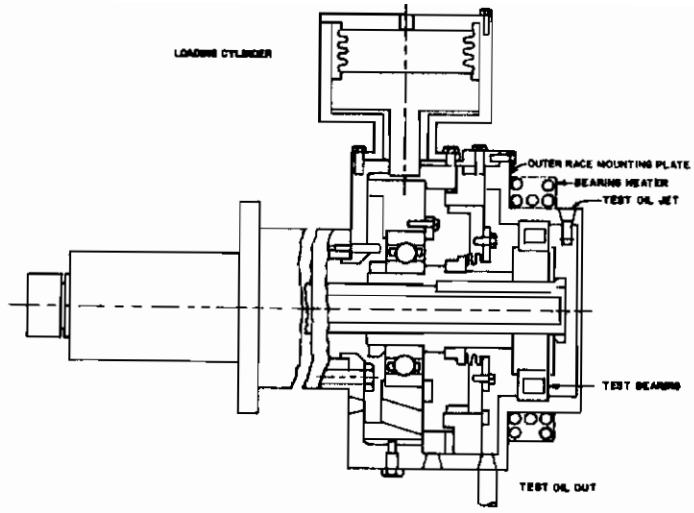

Figure 22. Modified WADC High Temperature Bearing Tester

The bearing test is conducted for 50 hours of running time. A 1 minute sample of test oil is withdrawn at each 10 hour interval for viscosity and neutralization number determinations. Test oil flow rate is also checked at this time. At the end of the 50 hour test, the front and back parts of the test bearing and supporting structure are photographed and visual examination is made to determine solid deposits.

E. CRC Grease Tester

The objective of this test is to evaluate the suitability and performance of greases for antifriction bearings at elevated temperatures at shaft speeds to 10,000 rpm.

The equipment consists of a test spindle,* spindle oven, and drive motor assembly (Figure 23). The spindle design is such that a "Z" spring produces a 5 pound thrust load on the test bearing. Radial load is applied to the spindle pulley by means of a spring supported motor cradle applying tension to the drive belt and is adjusted to 15 pounds.

The grease to be tested is packed into two bearings of S.A.E. No. 204 size fabricated of heat-resistant materials. The bearings are assembled

*Pope Machinery Corp., Grease Test Spindle P-6301A-HT-SP

into the test spindle and rotated by hand to distribute the lubricant and check the assembly. Power is applied to the motor and heaters to bring the temperature at the outer race up to test condition within 1-1/2 hours. This temperature is held within ±3°F, while the test is running.

The test is run in series of four cycles, each cycle consisting of 20 hours running and 4 hours shutdown with a 72 hour shutdown over weekends. The run is continued until failure occurs. Failure is defined as any of the following conditions: a 300 percent increase in spindle power, locking of the test bearing, or a 20°F increase over test temperature.*

Modification of the test section for use in the radiation environment was accomplished by decreasing the oven size and removing excess metal from around the test bearing (Figure 24). The modified test section was mounted on a wheeled table for maximum portability. During test, the equipment is positioned adjacent to the gamma source, and control is from a remote console. Figure 23 shows the relative positions of the grease tester and the Cobalt 60 source.

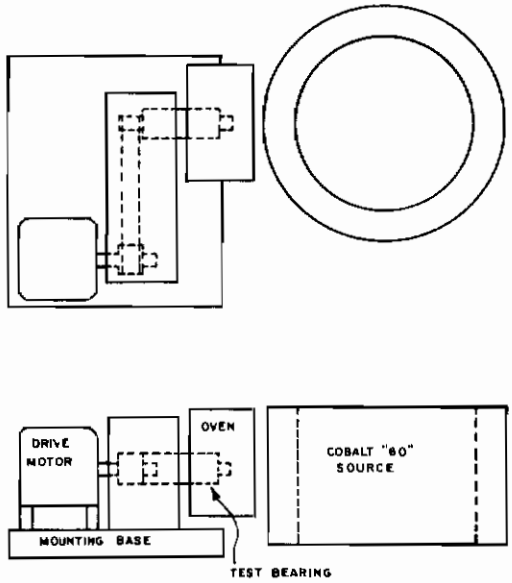

Figure 23. CRC Grease Tester in Radiation Cell

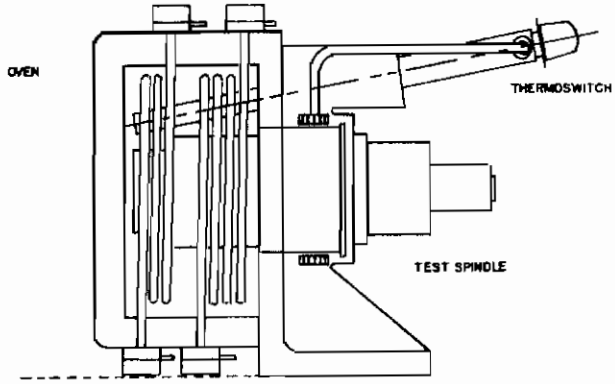

Figure 24. CRC Grease Tester Modified Test Section

*FTMS No. 791, Method 333-T

APPENDIX V

DOSIMETRY - INSTRUMENTATION

A prime requisite for obtaining data in a radiation environment is accurate dosimetric measurements. This section presents the results of studies leading to instrumentation and techniques for measuring dose and dose rate.

A. Modification and Design of the Graphite Ionization Chamber

The graphite CO_2 ionization chamber that is used for Cobalt 60 dosimetry is a variation of the one used at Oak Ridge National Laboratories for gamma-flux measurements in the bulk shielding facilities reactor[1] (see Figure 25). The only change that was made in the chamber design was the reduction of the graphite wall thickness from 0.777 centimeter to 0.239 centimeter. This change is discussed under Item 3 below.

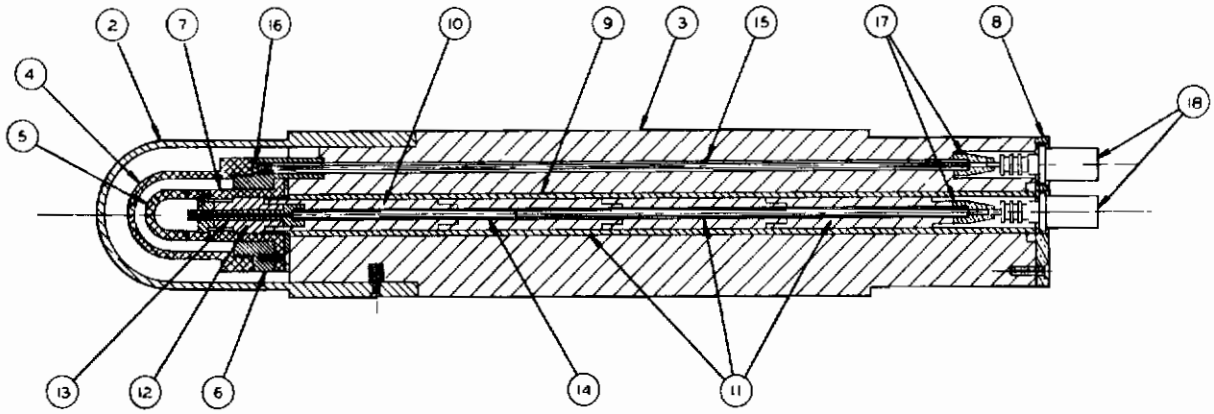

2. Electrode shield - polystyrene
3. Body - polystyrene
4. High voltage electrode - graphite
5. Collector electrode - graphite
6. Electrode insulator - teflon
7. Guard electrode - graphite
8. Connector plate - brass
9. Guard electrode lead - 24S aluminum
10, 11, 12. Collector electrode insulators - polystyrene
13. Collector electrode positioning pin - 24S aluminum
14. Collector electrode lead 24S aluminum
15. High voltage connector lead to - 24S aluminum
16. Electrical contact pin
17. High voltage and signal lead adaptor pins
18. High voltage and signal connectors

Figure 25. Graphite Ionization Chamber for Cobalt 60 Facility

The ionization chamber was designed, as nearly as possible, according to the Bragg -Gray principles. A statement of these principles follows:[13]

(1) The thickness of the wall material must be greater than the range of the secondary particles in the wall material.

(2) The cavity dimensions must be less than the average range of the secondary particles of the gas in the cavity.

(3) The incident radiation must not be appreciably attenuated in passing through the chamber.

The following is a short analysis of the chamber's ability to satisfy the Bragg-Gray principles.

(1) The formula given for the practical range of secondary particles in a substance is $Rp = 412 \times E_o^n$, where Rp is reported in mg/cm^2, E_o = energy of the incident gamma radiation in Mev, and $n = 1.265 - 0.0954 \ln E_o$.[2] This equation is valid for energies of E_o between 0.01 and 2.5 Mev. For simplicity of calculations, the average energy of the Cobalt 60 gamma rays will be taken to be 1.25 Mev.

$Rp = (412)(1.302) = 537 \text{ mg/cm}^2$

The density of graphite is 2.25 g/cm^2

Rp = 0.2385 cm or 0.094 inch

The actual graphite thickness is 0.095 inch, which makes the wall slightly thicker than the range of the most energetic secondary particles in the wall. The wall thickness of the Oak Ridge chamber was calculated for 3.5 Mev fission product gamma rays and was 0.777 cm.

(2) By application of the practical range formula above, a value of 268.8 cm for the range of secondary particles in the CO_2 contained in the chamber cavity is obtained. The actual interelectrode distance of 0.802 cm adequately fulfills the second principle.

(3) To satisfy the third principle, the attenuation factor is calculated for a 1.25 Mev gamma-ray beam passing through 0.2385 cm of graphite. This is done in the following manner:

λ = attenuation factor = $1 - e^{-\mu x}$ where the attenuation factor equals the fractional part of the gamma-ray beam that is modified or attenuated in the wall material

μ = absorption coefficient = $n\Sigma$, where n = number of atoms per mole, and Σ = total atomic cross section

x = thickness of the wall material multiplied by density of wall material

n = 5.01×10^{22} atoms/mole, $\Sigma = 1.15 \times 10^{-24}$ cm^2

μ = 0.0575 cm^2/gram

λ = 1.0 - 0.97 = 0.03

The 1.25 Mev gamma-ray beam is modified by only 3 percent in passing through the graphite walls. This satisfies principle (3).

B. Calculation of Absorbed Energy per Gram of Graphite Equivalent to 1 Roentgen

To ascertain the photon energy limitations of the Inland Testing Laboratories graphite CO_2 ionization chamber, calculations were made to determine the range of photon energies over which the absorbed energy in graphite corresponds to 1 roentgen.[13] The two sources of reference used in compiling the data were from Hine and Brownell, "Radiation Dosimetry", and from Davisson and Evans[10] to obtain the absorption cross-section values for varying photon energies. These data are shown in Table XXXIX.

1. Procedure

The photon energy range covered by the study varied from 20 Kev to 10 Mev. From values obtained for absorption cross section and photon flux for varying photon energies, the absorbed energy for the graphite was calculated.

2. Discussion

A plot of the absorbed energy of graphite as a function of photon energy, Figure 26, obtained from the data of Table XXXIX, indicates that the ion chamber will resemble an "air" chamber for all photons from 100 Kev to 2 Mev. This adequately covers all primary, as well as secondary photons produced by albedo of Cobalt 60 energies discussed in Section VI.

TABLE XXXIX

GAMMA ENERGIES AS A FUNCTION OF ABSORBED ENERGY IN GRAPHITE

Photon Energy E (Mev)	0.02	0.06	0.20	0.40	0.60	1.0	2.0	5.0	10.0
Abs. Cross-Sec (σ) barns	0.0205	0.051	0.088	0.098	0.098	0.093	0.077	0.051	0.035
Abs. Coef (μ) $cm^2/gm \times 10^{-2}$	0.627	1.54	2.66	2.95	3.06	2.79	2.34	1.55	1.09
Photon Flux $N(hv) \times 10^8$ cm^2-hr	54.6	304	97.1	44.4	29.5	18.7	11.2	5.92	3.49
Abs. Energy (rd) erg/gm-hr	1.08	44.9	83.1	83.6	86.5	85.0	84.6	73.5	58.6

Sample Calculation

$$Rd = E\gamma N(hv) \quad 1.6 \times 10^{-6} \qquad 5 \text{ (Equation 1)}$$

$$= (0.02 \times 54.6 \times 10^8 \times 0.627 \times 10^{-2}) \quad 1.6 \times 10^{-6}$$

= 1.08 erg/gm-hr absorbed energy in graphite for 0.02 Mev photons

Note: The absorbed energy equivalent for air indicated by Hine and Brownell is 83.8 ergs per gm roentgen as of the 1956 publication.[13]

C. Operational Characteristics for the Inland Testing Laboratories Chamber

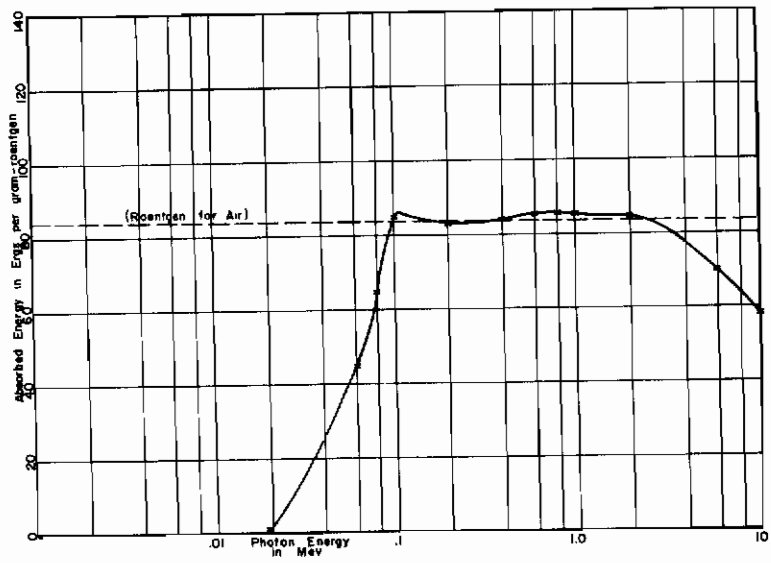

Figure 26. Absorbed Energy in Graphite as a Function of Photon Energy

The current resulting from the ionization of a gas in any chamber is a function of applied voltage, and, for any given radiation intensity, there is a minimum voltage required. As the voltage difference between the electrodes of an ionization chamber is increased from a low to a high value, the current collected increases linearly at low voltages, and, at continuing increased voltage, the current collected approaches asymptotically the saturation current for a given radiation intensity. The efficiency of current collection is denoted as the ratio of the measured current to the ideal saturation current.*

For the Inland Testing Laboratories ionization chamber it was essential to determine the above characteristics of minimum voltage requirements for a saturation current and the collection efficiency by theoretical calculations and verification of the results by experimentation.

1. Theoretical

There are theoretical expressions that may be derived to calculate the saturation curve for plane-parallel, cylindrical, and spherical ionization chambers. The geometric design of the Inland Testing Laboratories ionization chamber, shown in Figure 25, is a combination of the characteristics of both spherical and cylindrical chambers. The basic equation of Hine and Brownell,** for calculating the voltage required for current saturation of plane-parallel chambers,

---

*Reference 13, p 163

**Reference 13, pp 165-6

is stated to be applicable to cylindrical geometries. Since the Inland Testing Laboratories ionization chamber has both a cylindrical and a spherical geometry, it was necessary to determine if either geometry is applicable at saturation current. The equation for plane-parallel geometry is:

$$V = M\left(\frac{d^2\sqrt{q}}{\varepsilon}\right) \tag{2}$$

where:

V = applied voltage

M = the constant characteristic of the gas at a given temperature and pressure (15.9)

d = electrode spacing (cm)

q = charge (esu/cm^3 -sec)

ε = a function of the charge, the electrode gap separation, and the applied voltage

The electrode spacing d is the gap between the electrodes of the ion chamber and is expressed by

$$d = K(a - b) \tag{3}$$

where:

a = inside radius of outside electrode

b = outside radius of inside electrode

K = geometric constant

The equations of Hine and Brownell for determining K for spherical and cylindrical geometry are:[13]

$$K(\text{spherical}) = \sqrt{\left[1/3\ (a/b + 1 + b/a)\right]} \tag{4}$$

$$K(\text{cylindrical}) = \sqrt{\left[\frac{a/b + 1}{a/b - 1}\ \frac{\ln (a/b)}{2}\right]} \tag{5}$$

The K value for the spherical and cylindrical geometries of the Inland Testing chamber was calculated using the constants for the chamber.

a = 1.10 cm (inside radius of outside electrode)

b' = 0.85 cm (outside radius of inside electrode)

M = 15.9

$$K_{spherical} = \sqrt{1/3\,(1.295 + 1 + 0.773} = 1.01$$

$$K_{cylindrical} = \sqrt{\frac{(1.295 + 1)}{(1.295 - 1)}\,\frac{\ln 1.295}{2}} = 1.004$$

The electrode gap d for the two geometries was:

d(spherical) = 0.253 cm

d(cylindrical) = 0.251 cm

The calculations demonstrate that the cylindrical and spherical portions of the Inland Testing Laboratories ion chamber have essentially the same electrode spacing.

In order to carry out the calculation of Equation (2) for a selected dose rate, it is necessary to assume a collection efficiency of 99 percent. Then, from the generalized saturation curve of Hine and Brownell,* $\varepsilon = 0.1$. The theoretical minimum voltage necessary for three dose rates is given in Table XL.

The results indicate that a minimum potential of 240 volts is required to maintain ionization current saturation for dose rate of 2×10^6 R/hr.

2. Experimental

Based upon the above equations the experimental determination of the saturation current was conducted for various radiation dose

---

*Reference 13, p 166, Figure 7.

rates. A variable negative voltage power supply ranging from 0 to 300 volts was used. The potential applied to the ion chamber was increased in increments of 5 volts for each dose rate position. The voltage was increased until a constant ionization current was obtained. The data are presented in Table XLI.

TABLE XL

APPLIED POTENTIAL AS A FUNCTION OF DOSE RATE

Dose Rate R/hr	Dose Rate Ergs/gmC/hr	Calculated Minimum Voltage
2.0×10^6	1.74×10^8	240
6.0×10^5	5.23×10^7	131
1.1×10^4	9.58×10^5	17.7
3.4×10^3	2.96×10^5	9.94
2.6×10^3	2.26×10^5	8.62

TABLE XLI

IONIZATION CURRENT AS A FUNCTION OF APPLIED VOLTAGE

Current, amperes x 10^7 at Various Dose Points, ergs/gmC

Applied Voltage, Volts	5.23×10^7	2.96×10^5	2.26×10^5
5	0.31	0.008	0.0189
10	0.68	0.015	0.0448
15	1.01	0.0169	0.0515
20	1.29	0.0172	0.0545
25	1.56	0.0175	0.056
30	1.85	0.0175	0.056
35	2.02	-	-
40	2.20	0.0175	0.0575
45	2.38	-	-
50	2.45	-	0.0580
60	2.70	0.0177	-
80	2.95	0.0177	0.0585
100	3.10	0.0178	-
120	3.10	0.0179	0.0585
150	3.20	0.0179	0.0585
210	3.21	0.0179	0.0585
300	3.22	0.0179	0.0585

A plot of the data of Table XLI, shown in Figure 27, demonstrates vividly the dependency of collection current upon applied voltage. It is apparent that the minimum voltage required to produce current saturation at 6 x 10^5 R/hr is at least 140 volts. For lower dose rates correspondingly less voltage is required for saturation current.

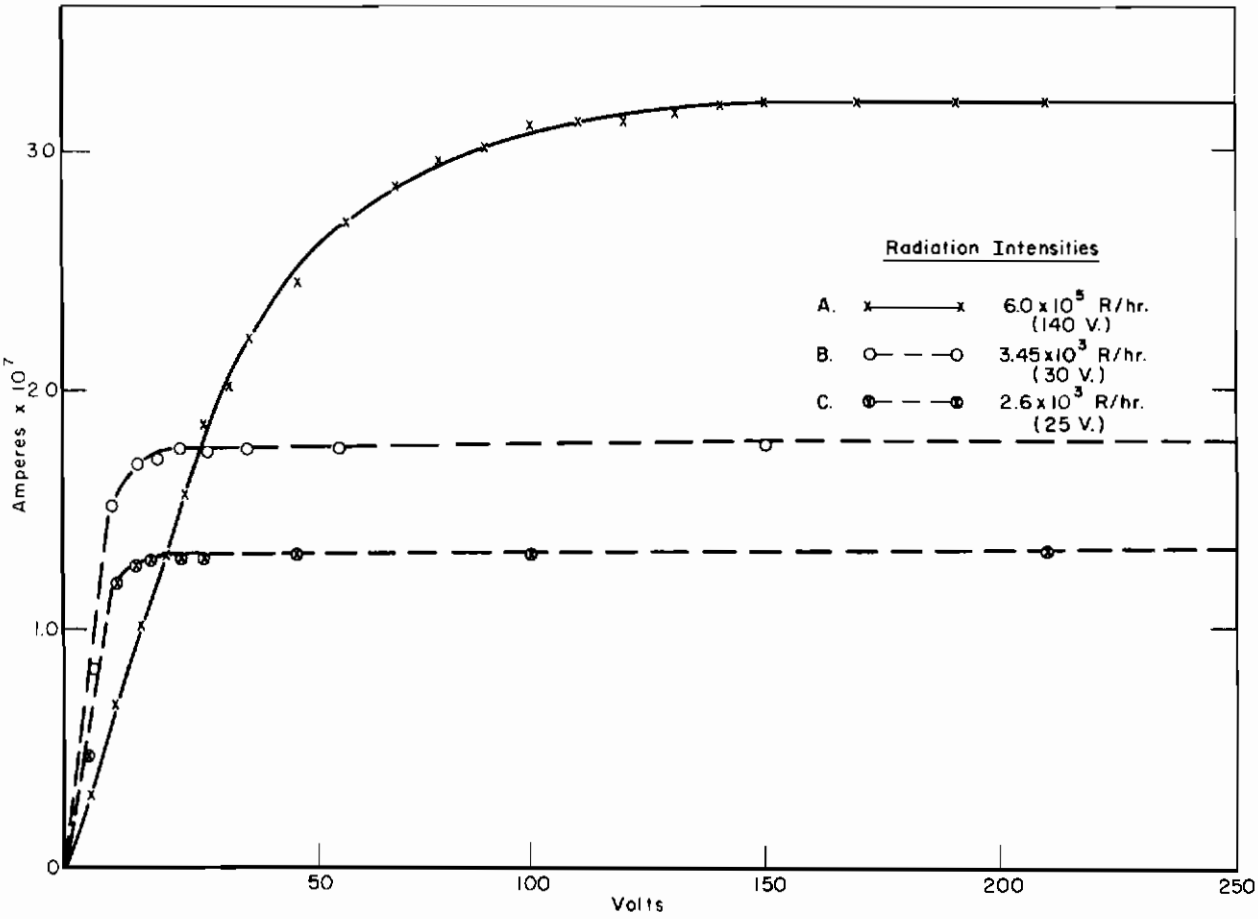

Figure 27. Saturation Current for Graphite Ionization Chamber at Various Radiation Intensities

3. Collection Efficiency

The ratio of the measured current to the ideal saturation current defines the collection efficiency for any chamber. From the generalized saturation curve of Hine and Brownell the collection efficiency (f) is given by [13]

$$f = \frac{2}{1 + \sqrt{1 + \varepsilon^2}} \qquad (6)$$

For a dose rate of 6×10^5 R/hr, from Figure 27, V = 140 volts of current saturation. Rearranging Equation (2) and solving for

$$\varepsilon = \frac{m\,(d^2\sqrt{q}\,)}{V} \qquad (7)$$

then $$\varepsilon = \frac{16\,(0.25)^2}{140}\sqrt{\frac{6 \times 10^5}{3.6 \times 10^3}}$$

$$\varepsilon = 0.0923$$

Finally, the collection efficiency is

$$f = \frac{2}{1 + \sqrt{1 + (0.0920)^2}}$$

$$f = 0.998$$

The results of the above study for the Inland Testing Laboratories chamber indicate a collection efficiency of near ideal saturation. Also, the experimentally determined voltage of 6×10^5 R/hr is in good agreement with the theoretically calculated voltage previously determined for this dose rate. Therefore, it may be concluded that the ionization currents measured with the Inland Testing Laboratories chamber approach the ideal saturation current within 99 percent.

D. Calibration of the Inland Testing Laboratories Ionization Chamber

After the range of photon energies had been determined with respect to the absorbed energy of the graphite corresponding to 1 roentgen, and after the operational characteristics of the ionization chamber had been determined, it was essential to calibrate the chamber. This required a theoretical expression of gamma dose rate in terms of ionization current equivalent to 1 R/hr. To satisfy the validity of the theoretical calculations, the ion chamber was calibrated with a known source and the experimental chamber constant was compared with the theoretical value.

1. Theoretical

The radiation unit, roentgen, is directly proportional to the gamma dose rate, $(N(h_\nu)$, and the energy, E_γ, of the photons.[4] This relationship is expressed as:

$$R \approx E_\gamma N\ (h_\nu) \tag{8}$$

To express this relationship in terms of charge per unit volume equivalent to one R/hr, the current (I_γ) and the charge developed per unit volume per hour $\frac{(dq)}{(dt)}$ in an ionization chamber can be expressed as:

$$\frac{dq}{dt} = \frac{1.602 \times 10^{-19}}{3.6 \times 10^{3}} \quad \frac{E_\gamma N (h_\nu) \mu m \rho}{w} \tag{9}$$

$$I_\gamma = \frac{dq}{dt} \times V \tag{10}$$

where:

$\frac{dq}{dt}$ = charge per hour per unit volume

I_γ = current (amps) developed in chamber equivalent to 1 R/hr

E = photon energy

$N(h_\nu)$ = photons/cm^2-sec

μ_m = mass absorption coefficient of carbon dioxide in cm^2/gm

ρ = density of carbon dioxide in gm/cm^3 at STP

w = energy required to form ion pair in carbon dioxide in Mev/ion pair

V = volume of ionization chamber

1 ion pair = 1.602×10^{-19} coulombs

Since the $\frac{dq}{dt}$ and also the I_γ terms contain the density of carbon dioxide, these terms must be corrected for the pressure and temperature at which the chamber was used. The correction factor can be expressed as

$$I_C = I_\gamma \frac{P_c T_a}{P_a T_c} \quad (11)$$

where P_c and T_c are measured pressure and temperature and P_a and T_a are standard pressure and temperature.

The values for the terms used in Equations 9 and 10 that are specific for the Inland Testing Laboratories ionization chamber are:

$E = 1.25$ Mev = average energy per photon for Cobalt 60

$N(h_\gamma) = 1.63 \times 10^9$ photons/cm^{2}sec

$\mu_m = 2.67 \times 10^{-2}$ cm^2/gm

$\rho = 1.97 \times 10^{-3}$ gm/cm^3 at STP

$w = 3.43 \times 10^{-5}$ Mev/ion pair

$v = 3.9124$ cm^3

sec/hr $= 3.6 \times 10^3$

Upon substitution of these values into Equation 10, the theoretical chamber constant is:

$I_\gamma = 5.47 \times 10^{-13}$ amps equivalent to 1 R/hr at STP

The correction factor for the temperature and pressure at which the chamber is used was obtained by using Equation 11.

$$I_c = 5.47 \times 10^{-13} \frac{29.29}{29.92} \frac{273}{295} \quad (12)$$

Thus, the theoretical chamber constant becomes $I_c = 4.96 \times 10^{-13}$ amperes which is equivalent to 1 R/hr. A temperature of 22°C (273°A) and pressure of 29.29 inches were used to correlate the theoretical value to the experimental value.

2. Experimental

To verify the validity of the theoretical ionization chamber constant, arrangements were made with the Argonne Cancer Research

Hospital of the University of Chicago for use of their standard kilocurie Cobalt 60 source. This source had been calibrated by use of National Bureau of Standard Victoreen R meter reading 16.8 R/min at a distance of 81.6 cm.

The Inland Testing Laboratories graphite CO_2 ionization chamber was positioned at seven different accurately measured distances from the source. The chamber was located each time such that its center was in the exact middle of the gamma beam emerging from the columnator. Carbon dioxide gas was allowed to flow through the graphite chamber at a rate of no more than three bubbles per second in order to maintain atmospheric pressure after a previous 10 minute flushing. A potential of at least 750 volts was applied to insure current saturation. The Keithley Model 410 micromicroammeter was used to measure the ionization current of the chamber collected. Each current measurement was checked for accuracy by use of the inverse square law at each position as compared with the NBS calibrated value at the 81.6 cm position. This was necessary in order to determine any influence of albedo on the dose rate at the selected positions.

The dose rate on the chamber at each selected position was calculated by inverse squares using values of the above mentioned NBS calibrated position. The dose rate, ionization current, and the chamber constant are given in Table XLII. Finally, the data for the ionization current in amperage vs. dose rate in roentgens per hour were plotted to obtain the linear calibration curve shown in Figure 28. The use of this graph will be discussed.

TABLE XLII

VARIATION OF IONIZATION CURRENT WITH DOSE RATE

Distance from Source (cm)	Dose Rate* (R/hr)	Ionization** Current (amps x 10^9)	Chamber Constant (amps x 10^{13} ≒ 1R/hr	Deviation from Mean
43.3	3578	1.86	5.20	0.08
69.5	1391	0.71	5.10	0.02
81.6	1008	0.53	5.26	0.14
95.1	744	0.39	5.24	0.12
119.1	467	0.23	4.93	0.19
189.0	188	0.094	5.00	0.12
286.1	81.8	0.042	5.13	0.01
		Average	5.12	±0.10

*1R/hr≒87.1 ergs/gmc/hr

**Atmospheric pressure = 29.29 inches Temperature = 22°C

The ordinate represents the measured ion current, and the abscissa represents the dose rate in R/hr. The exponents are determined by the use of the insert. The nonprime letters in the insert correspond to ion chamber exponents while the prime letters correspond to dose rate exponents. The proper ion chamber current exponent is located in the body of the insert, thus determining the proper cycle to use, i.e., (1), (2), etc. The dose rate is then located on the chart in one of the prime letter cycles, and the exponent is determined by reading the intersection of the corresponding prime letter and cycle in the insert.

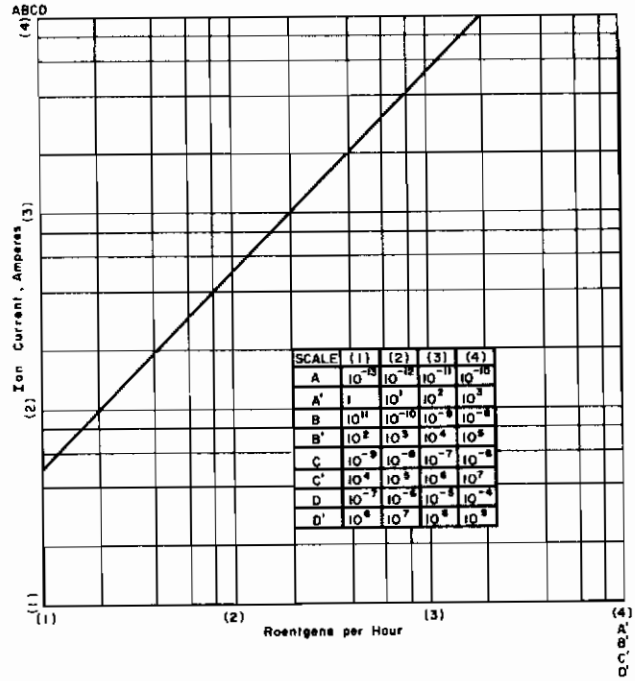

SCALE	(1)	(2)	(3)	(4)
A	10^{-13}	10^{-12}	10^{-11}	10^{-10}
A'	1	10^{1}	10^{2}	10^{3}
B	10^{11}	10^{-10}	10^{-9}	10^{-8}
B'	10^{2}	10^{3}	10^{4}	10^{5}
C	10^{-9}	10^{-8}	10^{-7}	10^{-6}
C'	10^{4}	10^{5}	10^{6}	10^{7}
D	10^{-7}	10^{-6}	10^{-5}	10^{-4}
D'	10^{6}	10^{7}	10^{8}	10^{9}

Figure 28. Calibration Plot for Graphite Ionization Chamber

To illustrate, assume a measured ionization current of 4.0×10^{-8} amps. This exponent value has a nonprime letter of C and a cycle number of (2). The number 4.0 is then found on the second ordinate cycle, and the dose rate value, (8.0) is obtained by the value of this number on the abscissa. The exponent for the dose rate value is obtained by noting the abscissa cycle which the number falls in, i.e. (1).

The exponent is obtained by reading the value of C' under cycle (1), which is 10^{4}. Therefore, the dose rate for an ionization current of 4.0×10^{-8} amperes is 8.0×10^{4} R/hr.

From Table XLII, the average experimental chamber constant is $5.12 \pm 0.10 \times 10^{-13}$ amperes = 1 R/hr. This value compares very favorably with the theoretical value of 5.47×10^{-13} amperes, which provides additional confidence in the validity of the chamber constant.

E. Supplementary Methods of Dosimetry

Although the Inland Testing Laboratories graphite CO_2 ionization chamber will continue to be used as the basic standard for radiation dosage in terms of ergs per gram carbon, the need for supplemental methods of dosimetry was recognized. In this connection, the use of cobalt glass, ceric-cerous, and ferric-ferrous chemical dosimetry were given consideration. Although some of these studies are still in a developmental stage, the results for cobalt and ferric-ferrous chemical dosimetry indicate excellent agreement with the graphite ion chamber results.

1. Cobalt Glass Dosimetry

The Nuclear Effects Group of the U. S. Army Quartermaster Food and Container Institute in Chicago cooperated in the program of dosimetry utilizing cobalt glass as the radiation receptor. The glass was obtained from the Bausch and Lomb Optical Company, Rochester, New York. The specifications of the dosimeter are as follows:

Melt = F0261

Dimensions = 15 x 6 x 1.5 mm

Composition of glass = 62.5 percent SiO_2, 20.8 percent B_2O_3, 10.6 percent Na_2O, 6 percent Al_2O_3

To this is added 0.1 percent Co_3O_4 which serves as the radiation sensitive component. Each ampule of the cobalt glass was calibrated by the National Bureau of Standards with a known Cobalt 60 source.

A rack of styrofoam was constructed to contain the cobalt glass dosimeters in the desired position with respect to the Inland Testing Laboratories Cobalt 60 source. With this support rack located as indicated in Figure 29, the source was raised in order to effect exposure of the dosimeters. Upon completion of the irradiation, the source was lowered and the dosimeters read for optical density (absorbence) by use of a Beckman Model DU spectrophotometer. The comparative data for cobalt glass and the ion chamber were taken at three different levels within the source cylinder at the center position. The results are presented in Table XLIII. As can be noted, there is excellent agreement between the readings, although no definite conclusions can be drawn since a statistically significant number of comparisons are not available.

2. Ferric-Ferrous Chemical Dosimetry

The ferric-ferrous iron dosimetry was accomplished by preparing a solution composed of 0.001 normal $FeSO_4$, 0.8 normal H_2SO_4, and 0.001 normal NaCl. After exposure to radiation, the concentration of the ferric ions is determined by using a Beckman DU spectrophotometer. The dose rate on the dosimeters were calculated from the concentration of ferric ions and the time of exposure. The results obtained with iron dosimeters and with the ion chamber are presented in Table III for comparison. The results show good agreement between the two methods of dosimetry, and iron dosimetry may be used justifiably with confidence.

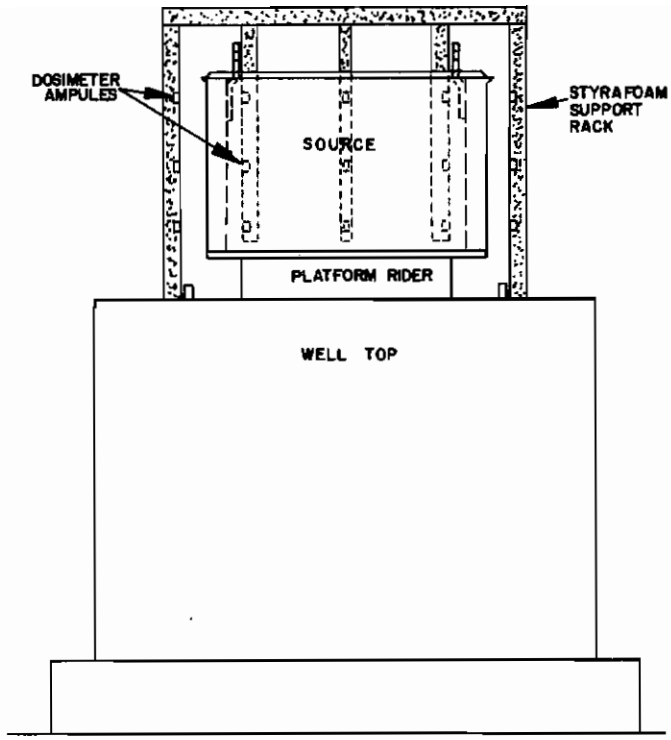

Figure 29. Dosimetry of Cobalt 60 Source

3. Advantage of Supplemental Dosimetry

Both cobalt and iron dosimetry have one natural advantage over ion chamber dosimetry. The large size of the ion chamber prohibits its use in close, restricted locations, such as found in and on the test equipment located in the irradiation facility. Both cobalt and iron dosimeters, on the other hand, are small and may be conveniently located at positions unreachable by the ion chamber. This fact alone assures their importance as a supplementary dosimetry method.

TABLE XLIII

COMPARISON OF DOSE RATE
COBALT GLASS AND ION CHAMBER

Dosimeter	Dose Rate (ergs/gmC/hr)x10^{-3}		
Ionization Chamber	5.01	5.92	5.31
Cobalt Glass	5.00	5.99	5.30

APPENDIX VI

DOSIMETRY - APPLICATION

This section presents a detailed account of the applications of dosimetry at the Inland Testing Laboratories radiation facility. These applications are varied and include all phases of work from the initial albedo and background characteristics to the determination of dose rates on dynamic test equipment.

A. Total Albedo and Background Characteristics for the Cobalt 60 Irradiation Cell

With the completion of the Inland Testing Laboratories Cobalt 60 facility, the albedo and background characteristics for the irradiation cell were determined. Albedo is a function of the absorption coefficient of any given material. Therefore, the lower the atomic number of the element or elements, the less is the absorption for gamma rays.[13, 27] A high percentage of the gamma rays that suffer Compton interaction will be reflected back as albedo radiation at a lower energy than the incident photon. This "backscatter" radiation becomes broadly maximum at an energy of 213 Kev.[23]

As mentioned above, the emergent energy spectrum shows a backscatter peak in the region of 150 to 250 Kev, Figure 30, which does not

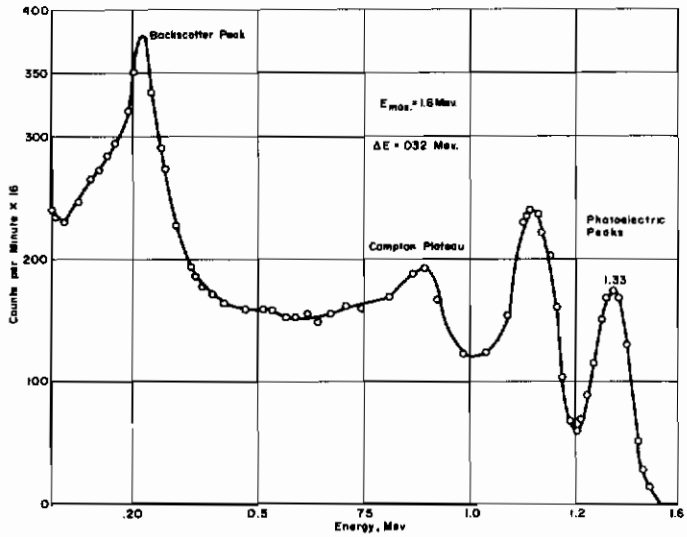

Figure 30. Spectrum of Cobalt 60

vary greatly with incident angle or energy. Perkins et al, using Monte Carlo type calculations[23] have determined the albedo for concrete and aluminum.

The intensity of the albedo is a function of the quantity as well as the density of the material.* A comparison of the albedo and the Cobalt 60 photons is shown in Figure 30. The "backscatter" peak represents the photons of a narrow range of energies that suffer a particular Compton scattering from the surrounding material. Conversely, the greater the atomic number the lower the albedo due to more complete absorption of the incident photons. Ideally, as the absorption coefficient approaches infinity, the albedo will approach zero.[13] Since all known materials have a finite absorption coefficient, it is important in dosimetry to determine the albedo properties for materials around a source of radiation.

Albedo measurements were taken at three different locations within the irradiation cell. Since unobstructed air most closely approaches the properties of an infinite absorber, an albedo measurement for comparison was taken in an unobstructed location, Figure 31.

The P. R. Bell type single-channel pulse height analyzer, equipped with a NaI(Tl) scintillation crystal, and phototube were used to take the spectral measurements, Figure 40. A cone of lead 2 inches in base diameter was placed over the face of the NaI crystal for shielding against the incident gamma photons. A Cobalt 60 source of approximately 7 mc activity was placed directly over the lead shield. The entire assembly was vertically placed and located in the irradiation cell at three different positions: over the source well, adjacent to the surface of the magnetite concrete wall, and also adjacent to the west wall of ordinary concrete (Figures 32 and 33). A 25 foot length of coaxial cable connected the phototube assembly with the analyzer located outside the cell. For the outside air measurements the phototube assembly was suspended approximately 20 feet in

Figure 31. Location of Albedo Measurement for Air

*Rathbun, E.R., Private Communications, Cook Research Laboratories, 1957

Figure 32. Location of Albedo Measurement over Source Well

Figure 33. Location of Albedo Measurement for Cell Wall

the air, Figure 31, in an open field at least 80 feet from all obstructions.

Differential counts were taken at 2 percent intervals over a gamma-ray spectral range of 1.6 Mev.

In addition to the albedo measurements, a differential background count was taken within the irradiation cell to determine the normal radiation background characteristics inherent in the structural material of the cell.

Referring to the spectral plots of differential counts for the albedo study at the various locations mentioned above, Figure 34 - 37, it is noted that in every case, a peak of emergent energy photons is obtained in the spectral region of 150 to 250 Kev. It is of interest to point out that these data support the calculations by Perkins et al.[23]

The intensity of the albedo taken over the source well, at a point approximately in the geometric center of the room, Figure 34, is more than

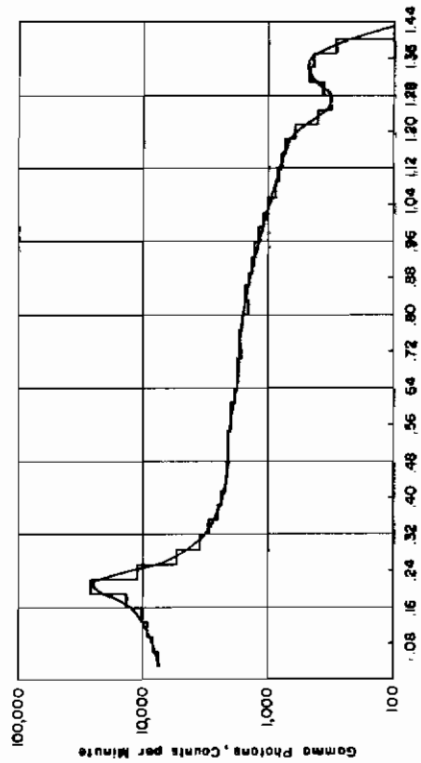

Figure 36. Albedo for Air

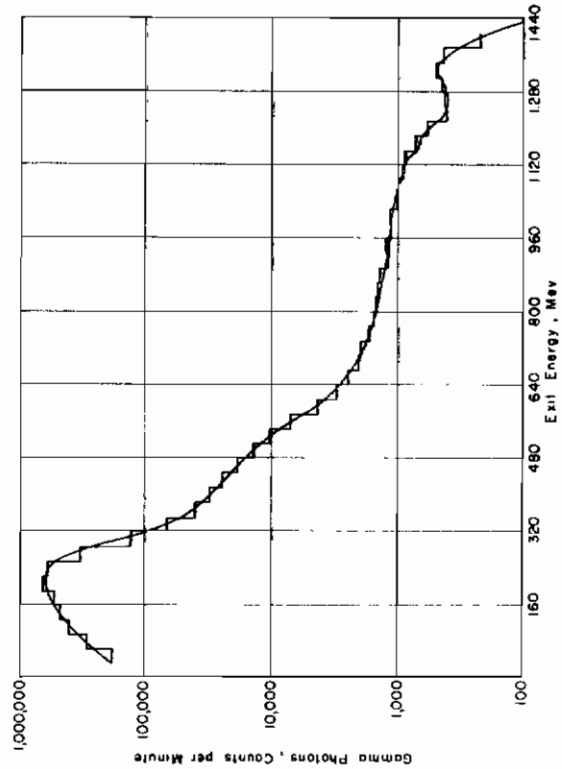

Figure 37. Albedo for Concrete Wall of Cell

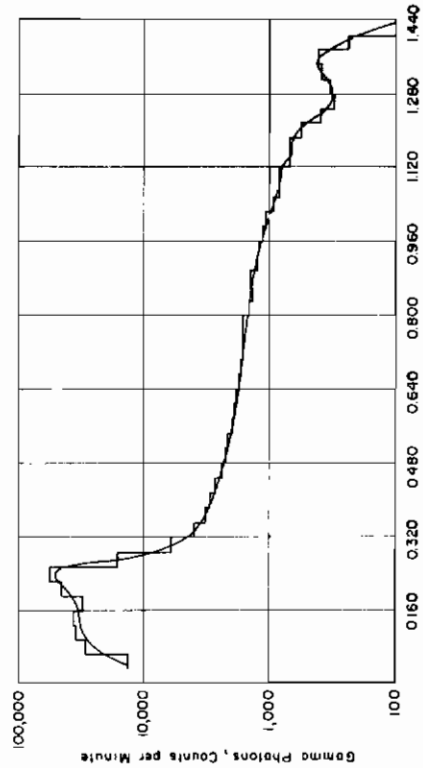

Figure 34. Albedo Over Source Well

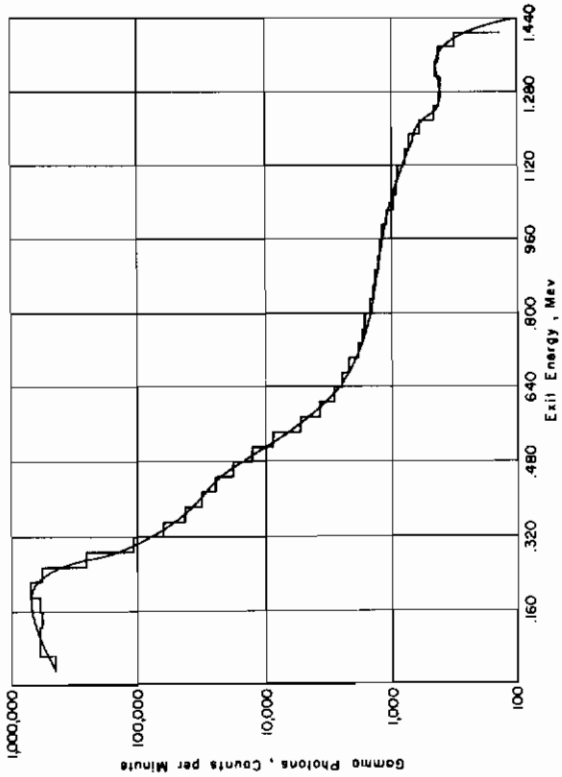

Figure 35. Albedo of Magnetite Concrete Wall of Cell

twice the intensity of the "control" albedo for air, Figure 36. As this is the normal location for the Cobalt 60 irradiator, the data represented in Figure 34 are representative of the albedo characteristics of the Cobalt 60 irradiator at this location, differing only in intensity.

In order to demonstrate the different absorption characteristics of magnetite concrete and ordinary concrete, two additional albedo measurements were made at locations adjacent to these respective walls. As is noted from Figure 37, the intensity of total albedo at the concrete wall is greater than that obtained adjacent to the magnetite concrete wall, by a factor of 1.2, Figure 35. This adequately demonstrates the higher absorption coefficient of magnetite concrete over ordinary concrete. The albedo at different locations within the cell is contained in Table XLIV. The data adequately demonstrate that high albedo tends to produce a higher absorbed dosage for a given subject material. This is due to the fact, as mentioned previously, that low energy photons will produce a higher absorbed dosage due to a greater number of photon interactions.

TABLE XLIV

ALBEDO ABSORBED ENERGY, MEV

Location	At 180 Kev	Total
Outside - Open Air	4,890	47,171
Over Source Well	12,700	78,534
Magnetite Wall	133,000	694,487
Concrete Wall	139,500	753,285

Background counts were run for control purposes at each of the locations in the irradiation cell mentioned above, as well as outside. The data are included in Table XLIV.

The background count outside is approximately twice that for inside the irradiation cell as might be expected. Also, the background counts at the two wall surfaces are significantly lower than that over the well due to the better shielding effect for the crystal by the walls at these locations. The background count over the source well is considered more representative of the activity inherent in the room due to the central location of the phototube in the room.

From the data of Table XLV, the total absorbed dosage due to the background activity in the room is less than 0.005 mrad/hr in sodium iodide.

TABLE XLV

BACKGROUND ACTIVITY

Location	Backscatter Peak, Kev	Intensity, counts per minute		Absorbed Energy, Mev		Dose Rate mrad/hrx10^3
		Backscatter Peak	Total	Backscatter Peak	Total	
Outside, Open Air	224	163	3121	37	576	5.54
Over Source Well	160	188	1882	30	446	4.28
Magnetite Wall	160	163	1485	26	415	4.00
Concrete Wall	128	176	1457	22	390	3.75

B. Theoretical Source Configuration Calculations (Optimum Configuration)

The following calculations are intended to show the spatial distribution of the Cobalt 60 source elements in the form of a hollow cylinder that will maximize the dose rate at a distance of 3 inches from the cylinder wall. The calculations will take into account the self-absorption of the source elements; however, the source will be considered to be in "free space", i.e., the effects of any surrounding structures such as the cell walls, the source well, etc., will be neglected. In actuality, the walls of the radiation shield and the source well have an albedo for gamma rays and these reflected gamma rays also contribute to the dose rate at the point of interest. Because of the added complexity, the contribution of reflection from the various structures in the cell will be ignored.

Self-absorption affects the radiation intensity outside the source in two ways, (1) Compton scattering reduces the energy of the primary gamma photons, (2) the photoelectric effect results in total absorption of the gamma photons within the structure of the source material. Pair production does not need to be considered in the calculation because the cross section for pair production at the average Cobalt 60 gamma-ray energy (1.25 Mev) is negligibly small.

The closed form formula for the gamma-ray intensity, ϕ, on the midplane of a hollow cylinder of inner radius R_I and outer radius R_o at a point, P, outside the cylinder will first be given. If the general form derived by Rockwell[25] for a disk source is integrated over a coordinate perpendicular to the disk and the lower limit for the radial integration is changed, the intensity for a hollow cylinder is obtained and is given by

$$\phi = \frac{S_v}{2\pi} \int_0^{h/2} \int_0^{2\pi} \int_{R_I}^{R_o} \frac{\exp\left[-\bar{\mu}(z^2 + r^2 + d^2 - 2rd\cos\alpha)^{1/2} \right]}{(z^2 + r^2 + d^2 - 2\,rd\cos\alpha)} r\, dr\, d\alpha\, dz \qquad (1)$$

where

S_v = the volume activity (photons/in^3-sec)

h = the height of the cylinder

z = the distance above or below the midplane of an elemental disk forming the cylinder

d = the distance from the central axis of the cylinder to the point P

r = the radial distance from the center of the cylinder to the elemental source volume

α = the polar angle in planes perpendicular to the axis of the cylinder

$\bar{\mu}$ = $\mu_s(R_o - R_I) / (R_o + a)$ where μ_s = the absorption coefficient of the source and a is the distance of the point P from the outside wall of the cylinder

The above integral is not amenable to any straightforward integration techniques in closed form; however, it can be shown when the point P lies outside the cylinder or when $d^2 > R_o^2 - z^2$, that ϕ can be expanded in the following way:

$$\phi(P) = \frac{S_v}{2} \int_0^{h/2} dz \sum_{n=0}^{\infty} \frac{R_o^{2n+2} - R_I^{2n+2}}{2^n (n+1)} \sum_{j=0}^{n} \frac{d^{2j}}{2^j (n-j)! (j!)^2}$$

$$D^{n+j} \left(\frac{e^{-\bar{\mu} r}}{r^2} \right) \Bigg| \; r = \sqrt{z^2 + d^2} \qquad (2)$$

where $D^{n+j} (e^{-\bar{\mu} r / r^2})$ is the (n+j)th derivative of $(e^{-\bar{\mu} r}/r^2)$, evaluated at the value, $r = \sqrt{z^2 + d^2}$.

Ordinarily, a factor B(Z), called the buildup factor, should multiply the integral above, but it will be presently shown that the buildup factor can be made an intrinsic part of the calculation under certain conditions. In the usual calculation for Cobalt 60 gamma rays, the attenuation or absorption coefficient is taken to be the total Compton scattering coefficient. This means that every gamma ray which has been scattered is initially considered lost to the beam, but since Compton scattered gamma rays do contribute to the dose rate in large angle geometries such as this one, the intensity which is now too low is increased by a factor called the buildup factor to account for the scattered gamma rays.

For the present calculation, a coefficient called the true absorption coefficient [10, 13] will be used. The true absorption coefficient is calculated from the cross section for the photon energy acquired by the recoil electrons and therefore truly absorbed. The weighted value for the true absorption coefficient is 0.320 in.$^{-1}$, using weight factors of 40 percent by volume of cobalt and 60 percent by volume of aluminum. This value is based on the actual cobalt dimensions of 0.25 inch diameter and 1 inch length encapsulated in aluminum with final dimensions of 0.625 inch diameter and 1.125 inch length. Using the same weighting factors, the weighted value for the total Compton scattering coefficient is 0.710 in.$^{-1}$. Both of these values hold for a gamma-ray energy of 1.25 Mev.

The reason for using the true absorption coefficient will be apparent from the following discussion. If most of the Cobalt 60 gamma rays do not suffer more than three or four Compton scatterings, and, hence, if the source cylinder wall is not much greater than three or four mean-free paths for Compton scattering, the true absorption coefficient will not vary by much

more than 10 percent for most of the gamma rays traversing the cylinder wall, whether they be the primary gamma photons or the modified (scattered) photons.[10, 13] This will be true over a range of gamma-ray energies from approximately 0.20 to 2.0 Mev.[13] The result is an exponential variation of the energy lost per collision by photons of varying energy. This can be translated into an exponential absorption of the energy in the gamma-ray flux as it traverses the cylinder wall. Thus, the necessity for distinguishing photons of different energies vanishes, and only the rate at which energy is being absorbed by the source need be considered. The self-absorption, therefore, can be accounted for on the basis of the average energy absorbed in the source by Compton scattering. The contribution to the energy absorption by the photoelectric process for gamma-ray energies 0.20 Mev to 2.0 Mev is less than 10 percent of that for the Compton scattering process for both cobalt and aluminum, so that it may be neglected.

The angular direction of the scattered gamma rays after each scattering can be neglected, because, for a truly homogenous cylindrical source, as many gamma rays will be scattered into an angular cone from various parts of the source as there will be scattered into any other angular cone. This follows from the fact that if the cylindrical source is bisected by a plane parallel to its axis, the gamma flux crossing the plane in one direction is equal to the gamma flux crossing the plane in the opposite direction, if the source is truly homogenous.

What has just been said of energy absorption in cobalt and aluminum can also be said of energy absorption in air in the range 0.20 to 2.0 Mev. This fact is important in obtaining the dose rate in roentgens per hour in the air. Therefore, for the most desirable Cobalt 60 source configuration, it is of interest to obtain the maximum energy flux at P. The dose rate R_D at the point P is then:

$$R_D(P) = \frac{\mu_a{}^{air} E_o \phi(\bar{\mu}_a)}{D_R} \qquad (3)$$

where $\mu_a{}^{air}$ and $\bar{\mu}_a$ = the true absorption coefficients for air and the source elements, respectively, for $0.20 \leq E \leq 2.0$ Mev

E_o = the initial gamma-ray energy

D_R = 83.8 ergs/gram of air (definition of the roentgen)

ϕ = the gamma-ray intensity in photons/in^2-sec

The numerical results presented in Table XLVI for the dose rates at a point that is always 3 inches from the outside wall of the cylinder on the midplane were computed by an IBM 650 computer. In all configurations the source volume is considered constant: the 7000 slugs of the proposed source yield a volume of 873.6 in^3. Calculations show that if the slugs are packed in contact with one another, the "dead" volume will not be more than 10 percent of the total hollow cylinder volume.

The following is a list of constants used in the calculations:

TABLE XLVI

DOSE RATES AS A FUNCTION OF SOURCE WALL THICKNESS AND HEIGHT

Dose Rate, Roentgens*/Hr x 10^{-5} for Number of Slugs in Wall Thickness, n

Height (in.)	n = 2	3	4	5	6
14	3.00	4.61	5.72	6.35	-
16	3.62	5.35	6.43	6.91	-
18	4.20	5.98	6.95	7.30	-
20	4.73	6.47	7.31	7.53	7.31
22	5.19	6.85	7.54	7.60	7.28
24	5.56	7.11	7.64	7.59	7.18
26	-	7.28	7.68	7.50	7.04
28	-	7.36	7.65	7.36	6.86
30	-	7.40	7.56	7.28	6.66

*1R = 87.1 ergs/gmC

Source Strength = 62,000 curies

Number of photons = 7.4×10^{10}/curie-sec

Energy of primary gamma rays = 1.25 Mev

Source volume (allowing for 10 percent "dead" volume) = 950 in^3

Mean true absorption coefficient ($0.20 \leq E \leq 2.0$ Mev) for source elements weighted for cobalt and aluminum = 0.0320 in^{-1}

True absorption coefficient = 0.028 cm^2/gm for air at STP

Diameter of slugs = 3/8 inch

Height of slugs = 1-1/8 inch

From the values of the dose rates, a hollow cylinder of wall thickness, 4 slugs and height 26 inches, yields the highest dose rate for the given source volume. This cylinder has an inner radius of 3.64 inches and an outer radius of 4.99 inches. The reason for not choosing this configuration for the final source design will be discussed later. Calculations were performed for configurations up to and including 6 slugs thick. Because the mean-free path for Compton scattering of unmodified Cobalt 60 gamma rays is 1.41 inches, the validity of the assumptions made becomes less for wall thicknesses greater than approximately 4 inches.

C. Accepted Source Dimensions

The data of Table XLVI indicate that a source configuration of 4 slugs thick will produce the greatest dose rate at a point on the midplane 3 inches from the source. However, for practical purposes, a source of 3 slugs thick will show less variation in the dose rate along a plane for equipment located 3 inches from the cylinder even though there is a lower intensity at this point. The sample calculations below will verify this statement.

Example:

Consider a piece of material 36 inches in length to be irradiated by a 62,000 curie Cobalt 60 source. The problem is to determine which of two configurations, n = 3 slugs thick and h = 14 inches, or n = 4 slugs thick and h = 26 inches, shows the least variation in dose rate across the horizontal length of the material. In order to simplify the calculations, the piece of material may be considered to be a plane 36 inches long lying perpendicular to the midplane at a point 3 inches from the outside wall of the cylinder, Figure 38. A line from the center of the cylinder drawn along a radius of the cylinder bisects the plane at the specified point P. The following dimensions are given:

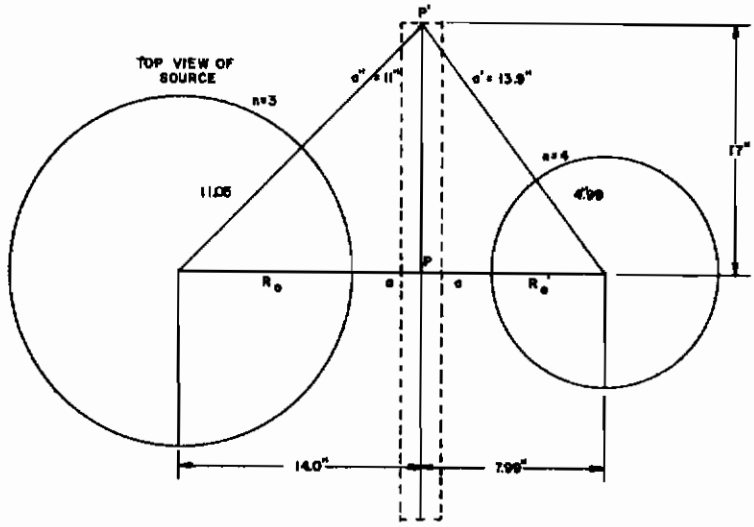

Figure 38. Comparative Source Dimensions

n = 3 slugs	n = 4 slugs
a = 3 inches	3 inches
h = 14 inches	26 inches
R_o = 11.05 inches	4.99 inches
R_I = 10.03 inches	3.64 inches
Intensity at P: 4.61×10^5 R/Hr	7.68×10^5 R/hr

From the properties of right triangles, the quantities below are easily calculated.

$a'' + R_o$ = 22.0 inches

a'' = 11.0 inches to point P'

$a' + R_o$ = 18.9 inches

a' = 13.9 inches to point P'

With the above values of a' and a'', the dose rate at P' for each of the above configurations may be calculated according to the method given previously. They are:

$R_D(P', n3) = 1.87 \times 10^5$ R/hr $\qquad$ $R_D(P', n4) = 1.96 \times 10^5$ R/hr

The ratio of the dose rate at 3 inches away to the dose rate at point P' is 2.46 for n = 3 and 3.92 for n = 4. The variation of the n = 4 configuration is about 1.6 times as great as that of the n = 3 configuration along the horizontal dimension of the given plane. Hence, to obtain a more uniform dose rate over sizable planar objects, it is necessary to use a configuration that is not optimum according to the calculations. A second advantage is that equipment may be placed closer around the n = 3 configuration due to the larger perimeter of the cylinder. A third advantage of the n = 3 configuration is the utilization of the hollow cavity within the cylinder to preirradiate lubricants and fuels. The inner diameter of the n = 3 configuration is 20.0 inches, whereas the inner diameter of the n = 4 configuration is 7.2 inches.

1. Theoretical Isodose-Rate Contours for the Chosen Configuration

To verify the method used to calculate the dose rates, computations to determine the isodose-rate contours were made for a configuration whose dimensions were very close to those of the actual source. In the actual source the total volume of the source slugs was somewhat

less than that used in the calculations for the optimum configuration, for not all the 7000 slugs were used. The total source strength was measured to be 49,811 curies at the end of October, 1957. In the theoretical calculations of the isodose-rate contours, the total volume was that of the 7000 slugs originally intended for the source design but the total source strength was adjusted to 49,811 curies. The dimensions of the actual source differed from those used in the theoretical calculations by 5 percent. In Table XLVII, a is the radial distance

TABLE XLVII

OBSERVED AND CALCULATED ISODOSE PLOT CONTOURS

a (inches)	RD (R/hr) x 10^{-5}* Calculated	Observed	Percent Difference from Observed
3	4.19	4.2	-0.2
11	1.71	1.6	+6.9
23	0.710	0.560	+26.8
39.8	0.317	0.283	+12.0

*1R = 87.1 ergs/gmC

from the outside wall of the cylinder to the observation point. The observed values were measured by a graphite ion chamber. Although the reduced source strength amounts to a correction of -19.7 percent, a correction of +10 percent was added to account for the neglected terms of the expansion series in the calculation; since only two terms in the series were taken for the computation. Thus, the net correction was -9.7 percent for each calculated value. Actually, the error introduced into the calculation by neglecting the terms beyond the second in the series becomes smaller as the observation point moves farther and farther from the source. The correction, therefore, for the most remote isodose-rate contours should be less than those for the close-in contours.

2. Experimental Verification of the Theoretical Calculations

To provide experimental verification of the method used to determine the optimum configuration, small scale configurations were

constructed of low activity slugs. The dimensions of the slugs are the same as those used in the actual source, namely, 3/8 inch diameter by 1-1/8 inches in length. Both types of slugs are enclosed in an aluminum capsule. Although there are only 2,135 slugs with a total volume of 265 cubic inches, various configurations could be made. Because the activity of the slugs was too low to be determined accurately, the following scheme was used to check the calculated values for the configurations with the measured ones. The dose rates in Equation 3 in Section A may be written in the following manner.

$$R_D(P) = \frac{\mu_a^{air} E_o S_v K_{nh}}{2 D_R} \qquad (4)$$

where K_{nh} = a geometrical factor depending on the wall thickness, n slugs, and the height of the cylinder h,

and S_v = volume specific activity.

All the other symbols are defined as before. A reference configuration may be used for comparison purposes. When a ratio is formed of the dose rates for any two configurations, all other factors, including that of the specific activity, cancel out except for the factor K_{nh}, which is independent of the specific activity. Hence, by comparing the ratio of the measured intensity of any other configuration to the reference source, the ratio of the corresponding calculated values may be checked. This follows from the relationship:

$$\frac{R_D(nh)}{R_D(ref.)} = \frac{K_{nh}}{K_{ref.}} \qquad (5)$$

If the ratios of the measured intensity of a number of given configurations check well with the calculated ratios, the original configuration calculations will have been confirmed.

The techniques of configuration construction and intensity measurements are shown in Figures 39 and 40. The slugs were assembled into various cylindrical configurations as shown in Figure 39. Each configuration was constructed according to the dimensions given in Table XLVIII. The intensity of each cylinder so constructed was measured by use of a NaI(Tl) scintillation crystal and the P.R. Bell-type differential pulse height analyzer shown in Figure 40. The NaI(Tl) crystal and phototube were placed at a point on the midplane located

Figure 39. Low Activity Assembly of Cobalt 60 Configuration

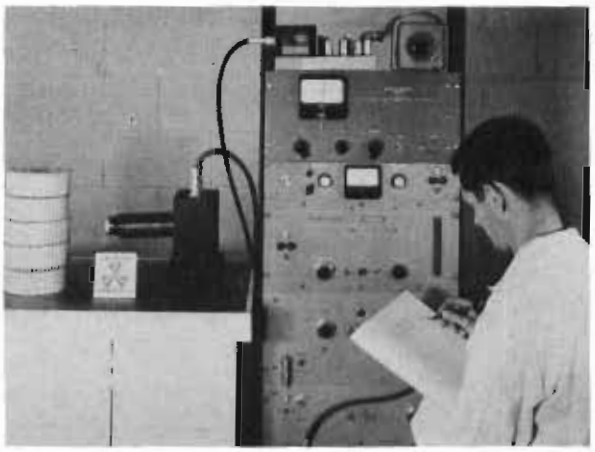

Figure 40. Intensity Measurement of the Cobalt 60 Configuration

TABLE XLVIII

RATIOS OF CALCULATED AND MEASURED INTENSITIES

n	h (in.)	Measured R_D (10^{-4} Mev/min)	Knh (in.)	$\frac{R_D(nh)}{R_D(ref)}$	$\frac{Knh}{K_{ref}}$
2	11.5	5.98	0.478	0.75	0.82
2	16.0	7.30	0.539	0.91	0.92
3	13.5	7.78	0.565	0.97	0.97
3	18.0	8.03	0.584	1.00	1.00
3	24.8	6.48	0.538	0.81	0.92
4	11.5	7.93	0.557	0.99	0.96
4	16.0	8.60	0.579	1.07	0.99
4	18.0	6.99	0.565	0.87	0.97

3 inches from the cylinder. Differential count-rates of 1 minute duration were taken at intervals corresponding to progressive increments equal to 2 percent of the spectrum. The voltage channel width used on the pulse height analyzer is 2 percent of the maximum range of 80 volts for the spectrum. The instruments were calibrated with a standard Cobalt 60 source so that 80 volts correspond to 1.6 Mev.

The ratio of the measured intensities was compared to the calculated values according to Equation (5). For simplicity of calculation, the NaI(Tl) crystal dose rates are expressed in Mev/min in Table XLVIII. The dose rates were obtained by numerically integrating the intensity spectrum measured for each configuration. In Table XLVIII, the configuration of wall thickness 3 slugs and height 18.0 inches was arbitrarily selected as the reference source to which all other configurations were compared. The calculated ratios agree favorably with the measured intensity ratios, for the estimated accuracy of the data is of the order of 10 percent. Likewise, the trends in the ratios as one goes from configuration to configuration have been generally verified. However, because the estimated error is of the same order as the variation in the values of the ratios, the only good check point between the calculated and the measured ratios is that for the configuration n = 2 and h = 11.5 inches. Unfortunately, time has not permitted the extension of this study to other configurations.

Figure 41 contains gamma spectral scans of the photon energies for two source configurations. Graph No. 1 presents the spectrum for a configuration whose wall is 4 slugs thick, and graph 2 shows a configuration 2 slugs thick. It will be noted that doubling the wall thickness has the effect of increasing the intensity of the low energy 128 Kev peak by a factor of 1.5. That is, the backscatter peak over the range of 0.128 to 0.32 Mev represents 20 percent of the total dose rate of the n = 4 source configuration, while the backscatter peak for the

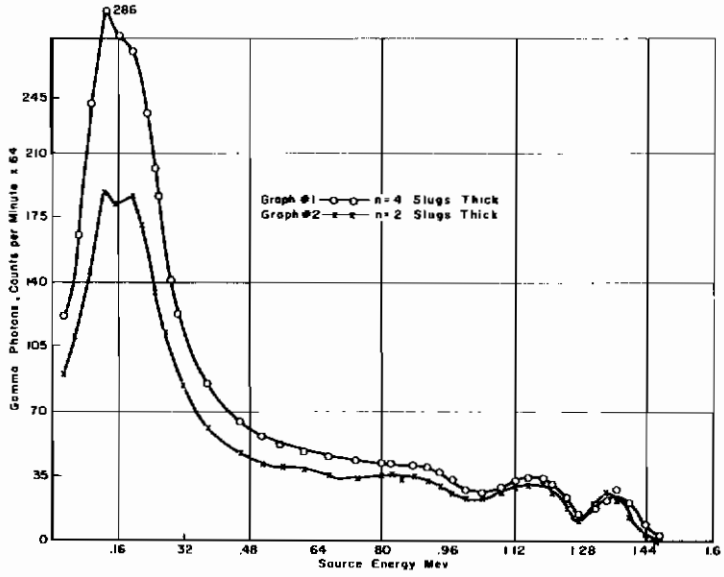

Figure 41. Gamma Spectrum I - Source Configuration

n = 2 configuration contributes 18 percent to the total dose rate. A similar effect is observed for configurations 3 and 4 slugs thick of the same height, Figure 42. In this case, the low energy intensity is increased by a factor of 1.1 for n = 4 over n = 3. In this case, the back-scatter peak contributes 20 percent of the total dose rate for the n = 4 configuration while this region represents 19 percent of the total for the n = 3 configuration.

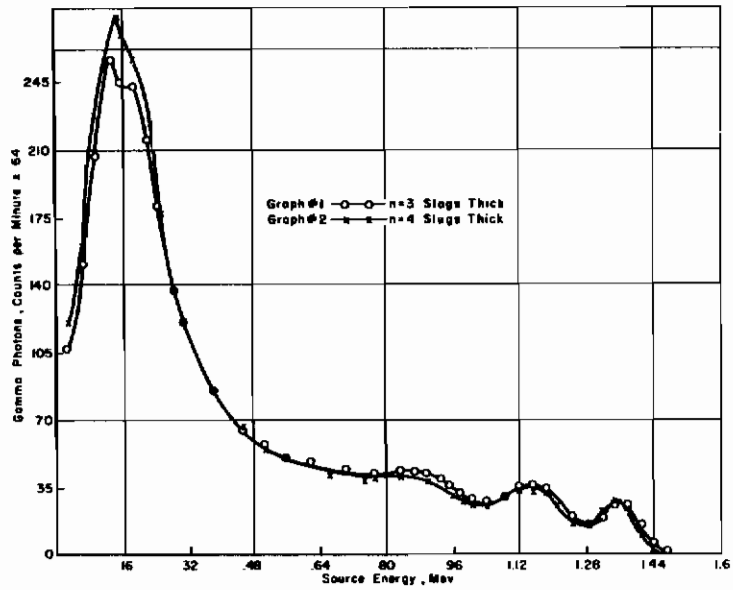

Figure 42. Gamma Spectrum II - Source Configuration

D. Assay of the Cobalt 60 Slugs and Assembly of the Inland Testing Laboratories Irradiation Source

The Cobalt 60 slugs supplied by the AEC of Canada were produced by reactor neutron reaction at Chalk River, Canada, and are of low specific activity. As the total activity for each slug estimated by AEC of Canada was based upon neutron flux and exposure time, it was essential that a representative sample of the Cobalt slugs be assayed for an accurate value of the total activity available for the irradiation source. The method of assay used was based upon the principle of M. C. Atkins of the Material Laboratory, Wright Air Development Center[3] with modifications to meet the needs of the Inland Testing Laboratories irradiation facility. The assay and assembly of the irradiation source was carried out as a composite operation.

Procedure

The Inland Testing Laboratories ionization chamber and the Kiethley Model 410 micromicroammeter were used in the assay of the Cobalt 60 source.

In order to reduce the background to a practical level for assay, the ion chamber and assay tube were located within a 1 square foot chamber constructed of 8 inches of lead brick, Figure 43, with the center of the ion

chamber located exactly 1 foot from the assay tube, Figure 44. The assay chamber was located within the irradiation cell at a convenient location for easy insertion and removal of the assay tube from the chamber, Figure 45.

It was determined that 95 slugs representatively selected from the entire amount of 7000 would be sufficient to determine the activity with 1 percent error. Since the assay was carried out in conjunction with the loading of the Nucledyne source container, every seventieth slug was taken for assay. The slugs were inserted into the assay tube by means of the Argonne Type Model 8 master-slave manipulators, Figure 45. Upon completion of the intensity reading, the assay tube was removed from the assay chamber, emptied and returned to the chamber ready for the next reading. Each assay reading was preceded by a background reading with the difference representing the assayed radiation intensity of the slug. Slugs were arranged in the Nucledyne source container designed to accommodate a column of 14 slugs in height and 3 slugs thick with outside diameter of 24 inches. The entire operation was carried out by use of the remote manipulators. When the loading of the source container was completed, there were 314 slugs remaining. Due to unavoidable dead volume space between the loaded slugs, it was impossible to include these slugs within the container. Therefore, the final assembled operational source

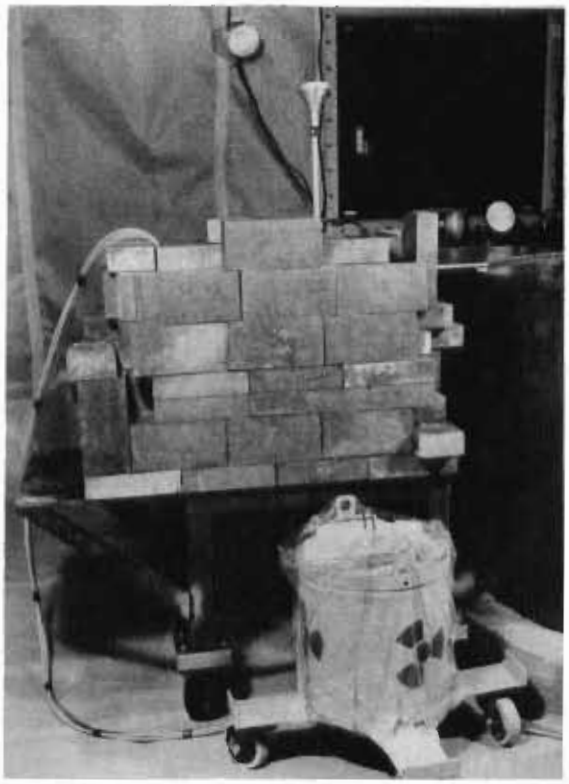

Figure 43. Assay Measurement Chamber - Outside View

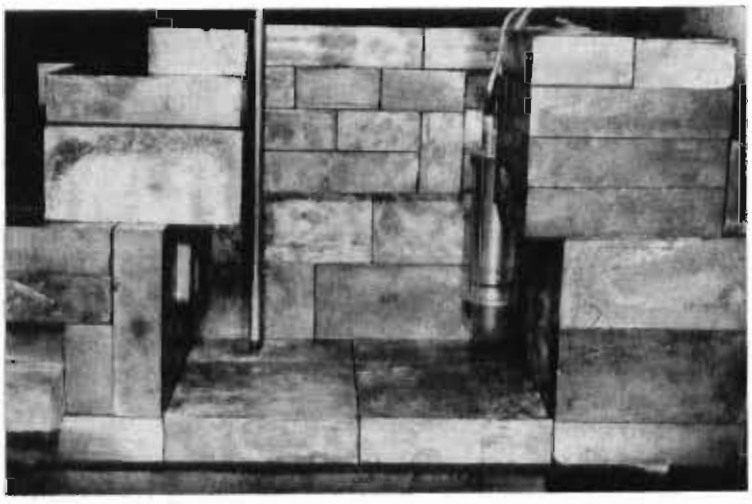

Figure 44. Assay Measurement Chamber - Inside View

contains a total of 6686 slugs. The remainder are reserved in a sealed container within the storage well and may be used as a low intensity source.

Due to albedo contribution to the total reading for each slug within the assay chamber, it was necessary to select one of the assayed slugs for an open air reading. The albedo contribution to the ion chamber reading in the open air would be negligible, and, therefore, the measured intensity would be more representative of the actual activity present within the slug. By use of the ratio of the outside assay to chamber assay value, a factor is obtainable for converting all slug assay values to "true" activity.

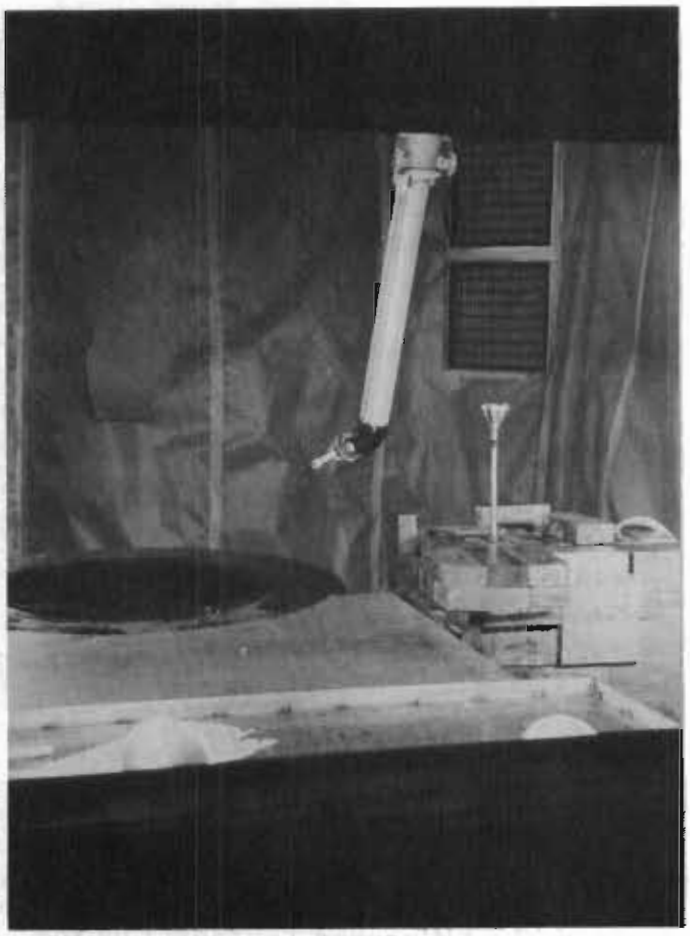

Figure 45. Assay Measurement Chamber - In Radiation Cell

For this purpose, an 18 foot derrick was built to support the slug capsule, Figure 46. The source could then be raised by remote handling cables to the top of the derrick and the intensity measured with the Inland Testing Laboratories chamber located at a measured distance from the source. The derrick was mounted atop the irradiation cell over one of the utility ports in the roof. By use of the remote manipulators and cave crane, the reference source was removed from its storage well, Figure 47, and transferred to the derrick cables. The source was then raised into position by remote handling methods, with the building serving as a shield for personnel. Four separate radiation intensity measurements at different distances were taken for greater accuracy. The average activity calculated from the individual radiation intensity values, as measured at the selected distances of 6 inches and 1, 2, and 4 feet, was used as a standard reference for all chamber assay values.

The results for the assay of the Cobalt 60 source are given in Table XLIX. The first column of this table refers to the number of the slug that

TABLE XLIX

COBALT 60 ASSAY

Slug No.	Total Current (amps)x10^{11}	Background Current (amps)x10^{11}	Net Current of slug (amps)x10^{11}	$(R/hr)_1$* 5.12×10^{-13} amp 1 R/hr	Press. inches Hg.	$(R/hr)_2$ (Press. & Temp. Corrected)	Curies (C_2) C_2= R/hr x 0.070796)	Curies (C_3) C_3= C_2 x decay	Curies (C_4) C_4= C_3 x 0.7583
1	8.0	0.108	7.89	154	29.91	151	10.69	10.71	8.12
2	8.1	0.102	8.00	156	29.91	153	10.83	10.85	8.23
3	8.8	0.098	8.70	170	29.91	166	11.75	11.77	8.92
70	8.1	0.088	8.01	156	29.91	153	10.83	10.85	8.23
140	7.8	0.037	7.76	152	29.84	149	10.55	10.57	8.01
210	7.6	0.078	7.52	147	29.84	144	10.19	10.21	7.74
280	8.3	0.075	8.22	161	29.84	158	11.19	11.21	8.50
350	9.4	0.072	9.33	182	29.84	179	12.67	12.69	9.62
420	9.2	0.080	9.12	178	29.85	175	12.39	12.43	9.43
490	12.0	0.072	11.93	233	29.85	229	16.21	16.26	12.33
560	9.5	0.051	9.45	185	29.85	181	12.81	12.85	9.74
630	11.5	0.060	11.44	223	29.85	219	15.50	15.55	11.79
700	7.5	0.065	7.43	145	29.89	142	10.05	10.08	7.64
770	8.5	0.060	8.44	165	29.89	162	11.47	11.50	8.72
840	9.0	0.058	8.94	175	29.89	171	12.11	12.15	9.21
910	9.1	0.05	9.05	177	29.89	173	12.25	12.29	9.32
980	9.5	0.04	9.46	185	29.83	182	12.88	12.92	9.80
1050	4.5	0.04	4.46	87	29.83	85	6.02	6.04	4.58
1120	2.5	0.10	2.40	47	29.83	46	3.26	3.27	2.48
1190	5.0	0.08	4.92	96	29.83	94	6.65	6.67	5.06
1260	5.0	0.08	4.92	96	29.77	94	6.65	6.67	5.06
1330	5.0	0.07	4.93	96	29.77	94	6.65	6.67	5.06
1400	5.5	0.08	5.42	106	29.77	104	7.36	7.38	5.60
1470	4.35	0.08	4.27	83	29.77	82	5.80	5.82	4.41
1540	5.9	0.075	5.82	114	29.93	112	7.93	7.95	6.03
1610	4.8	0.07	4.73	92	29.93	90	6.37	6.39	4.84

*1R = 87.1 ergs/gmC

TABLE XLIX (cont'd)

COBALT 60 ASSAY

Slug No.	Total Current (amps)x10^{11}	Background Current (amps)x10^{11}	Net Current of slug (amps)x10^{11}	$(R/hr)_1$* 5.12x10^{-13} amp 1 R/hr	Press. inches Hg.	$(R/hr)_2$ (Press. & Temp. Corrected)	Curies $(C_2)C_2$= R/hr x 0.070796)	Curies $(C_3)C_3$= C_2 x decay	Curies $(C_4)C_4$= C_3 x 0.7583
1680*	4.45	0.35	4.10	80	29.93	78	5.52	5.54	4.20
1750	4.5	0.35	4.15	81	29.93	79	5.59	5.61	4.25
1820	5.75	0.33	5.42	106	29.96	104	7.36	7.38	5.60
1890	4.25	0.32	3.93	77	29.96	75	5.31	5.33	4.04
1960	4.8	0.32	4.48	88	29.96	86	6.09	6.11	4.63
2030	6.6	0.32	6.28	123	29.96	120	8.50	8.53	6.47
2100	6.75	0.315	6.43	126	29.99	123	8.71	8.74	6.63
2170	6.3	0.31	5.99	117	29.99	114	8.07	8.35	6.33
2240	6.25	0.31	5.94	116	29.99	113	8.00	8.28	6.28
2310	6.25	0.315	5.93	116	29.99	113	8.00	8.28	6.28
2380	7.25	0.305	6.94	136	30.10	132	9.34	9.67	7.33
2450	7.95	0.32	7.63	149	30.16	145	10.27	10.63	8.06
2520	6.2	0.32	5.88	115	30.10	112	7.93	8.21	6.22
2590	5.2	0.32	4.88	95	30.10	92	6.51	6.74	5.11
2660	5.4	0.32	5.08	99	30.18	96	6.80	7.04	5.34
2730	5.3	0.32	4.98	97	30.18	94	6.65	6.88	5.22
2800	7.8	0.32	7.48	146	30.18	142	10.05	10.40	7.89
2870	6.2	0.33	5.87	115	30.18	112	7.93	8.21	6.23
2940	5.55	0.33	5.22	102	30.09	99	7.01	7.25	5.50
3010	7.2	0.33	6.87	134	30.09	130	9.20	9.52	7.22
3080	6.6	0.34	6.26	122	30.09	119	8.42	8.71	6.60
3150	8.5	0.33	8.17	160	30.09	156	11.04	11.43	8.67
3220	8.5	0.33	8.17	160	30.00	156	11.04	11.43	8.67
3290	6.35	0.335	6.01	117	30.00	114	8.07	8.35	6.33
3360	8.2	0.34	7.86	154	30.00	150	10.62	10.99	8.33
3430	5.5	0.36	5.14	100	30.00	98	6.94	7.18	5.44
3500	6.4	0.37	6.03	118	30.05	115	8.14	8.42	6.38

*1R ≎ 87.1 ergs/gmC

TABLE XLIX (cont'd)

COBALT 60 ASSAY

Slug No.	Total Current (amps)x10^{11}	Background Current (amps)x10^{11}	Net Current of slug (amps)x10^{11}	$(R/hr)_1$* $5.12x10^{-13}$ amp 1 R/hr	Press. inches Hg.	$(R/hr)_2$ (Press. & Temp. Corrected)	Curies $(C_2)C_2$= R/hr x 0.070796	Curies $(C_3)C_3$= C_2 x decay	Curies $(C_4)C_4$= C_3 x 0.7583
3570	5.1	0.37	4.73	92	30.05	90	6.37	6.59	5.27
3640	7.7	0.37	7.33	143	30.05	139	9.84	10.18	8.14
3710	6.1	0.37	5.73	112	30.05	109	7.72	7.99	6.39
3780	4.9	0.36	4.54	89	30.19	86	6.09	6.30	5.04
3850	6.2	0.36	5.84	114	30.10	111	7.86	8.13	6.50
3920	6.3	0.36	5.94	116	30.19	113	8.00	8.28	6.62
3990	5.4	0.35	5.05	99	30.19	96	6.80	7.04	5.63
4060	8.5	0.35	8.15	159	30.37	153	10.83	11.21	8.97
4130	7.1	0.36	6.74	132	30.37	127	8.99	9.30	7.44
4200	8.5	0.36	8.14	159	30.37	153	10.83	11.21	8.97
4270	8.8	0.36	8.44	165	30.37	159	11.26	11.65	9.32
4340	7.5	0.36	7.14	139	30.45	134	9.49	9.82	7.86
4410	8.6	0.38	8.22	161	30.45	155	10.97	11.35	9.08
4480	4.68	0.38	4.30	84	30.45	81	5.73	5.93	4.74
4550	8.39	0.37	8.02	157	30.45	151	10.69	11.06	8.85
4620	5.80	0.36	5.44	106	30.48	102	7.22	7.47	5.98
4690	7.05	0.36	6.69	131	30.48	126	8.92	9.23	7.38
4760	5.6	0.35	5.25	103	30.48	99	7.01	7.25	5.80
4830	5.1	0.35	4.75	93	30.48	89	6.30	6.52	5.22
4900	7.15	0.35	6.80	133	30.47	128	9.06	9.38	7.50
4970	8.5	0.34	8.16	159	30.47	153	10.83	11.21	8.50
5040	6.2	0.34	5.86	114	30.47	109	7.72	7.99	6.06
5110	9.9	0.36	9.54	186	30.47	179	12.67	13.11	9.94
5186	5.45	0.35	5.10	100	30.47	96	6.80	7.04	5.34
5250	10.0	0.33	9.67	189	30.47	182	12.88	13.33	10.11
5320	10.0	0.33	9.67	189	30.46	182	12.88	13.33	10.11
5390	10.5	0.33	10.17	199	30.46	191	13.52	13.99	10.61

*1R ≎ 87.1 ergs/gmC

TABLE XLIX (cont'd)

COBALT 60 ASSAY

Slug No.	Total Current (amps)x10^{11}	Background Current (amps)x10^{11}	Net Current of slug (amps)x10^{11}	$(R/hr)_1$* 5.12×10^{-13} amp 1 R/hr	Press. inches Hg.	$(R/hr)_2$ (Press. &Tem Corrected)	Curies $(C_2)C_2$= R/hr x 0.070796	Curies $(C_3)C3$= C_2 x decay	Curies $(C_4)C_4$= C_3 x 0.7583
5460	10.0	0.32	9.68	189	30.46	182	12.88	13.33	10.11
5530	8.6	0.30	8.30	162	30.46	156	11.04	11.43	8.67
5600	9.8	0.30	9.50	186	30.46	179	12.67	13.11	9.94
5670	8.58	0.32	8.26	161	30.46	155	10.97	11.35	8.61
5740	7.9	0.30	7.60	148	30.46	142	10.05	10.40	7.89
5810	10.0	0.30	9.70	189	30.46	182	12.88	13.33	10.11
5880	8.1	0.30	7.80	152	30.46	146	10.34	10.70	8.11
5950	10.5	0.28	10.22	200	30.46	192	13.59	14.06	10.66
6020	10.3	0.25	10.05	196	30.46	188	13.30	13.76	10.43
6080	10.4	0.25	10.15	198	30.46	190	13.45	13.92	10.56
6160	10.0	0.25	9.75	190	30.46	183	12.96	13.47	10.17
6230	8.0	0.24	7.76	152	30.46	146	10.34	10.70	8.11
6300	8.5	0.235	8.26	161	30.46	155	10.97	11.35	8.61
6370	8.3	0.22	8.08	158	30.46	152	10.76	11.14	8.45
6790	8.3	0.205	8.09	158	30.46	152	10.76	11.14	8.45

*1R ≎ 87.1 ergs/gmC

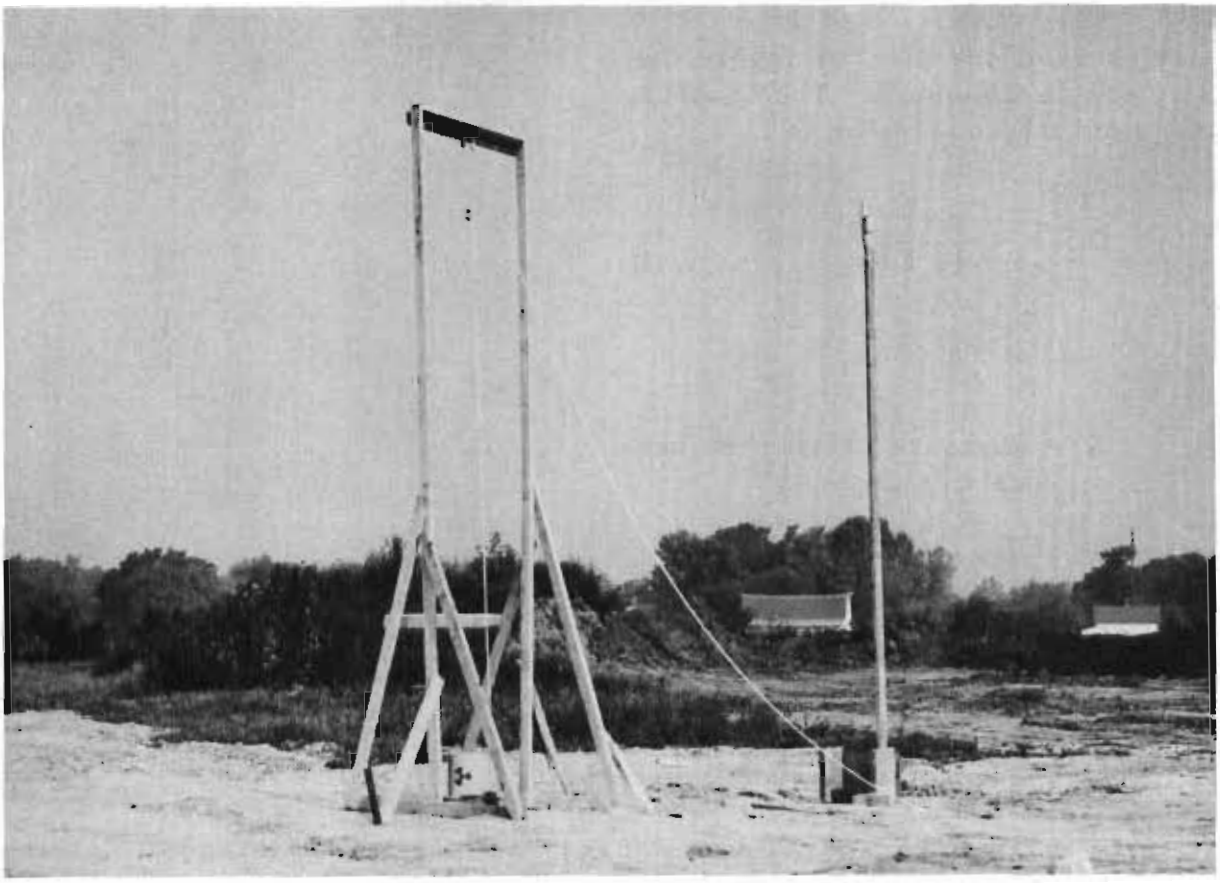

Figure 46. Open Air Measurement of Reference Source

was being assayed in the assembling of the source. Column 2, 3, and 4 refer to ionization currents measured with the Keithley 410 micromicroammeter. Column 5 is the conversion of the ionization current to equivalent dose rate using the experimental conversion factor discussed in Appendix V. Column 6 is the pressure reading at the time of the assay The temperature remained at 22°C during the entire assay. Column 7 is the correction term for pressure.

The general pressure correction factor is

$$(R/hr)_2 = (R/hr)_1 \frac{(29.29)}{P} \qquad (13)$$

where P is the measured pressure in inches of mercury. The temperature correction was not used since the temperature during the assay was the same temperature used for the chamber constant.

The conversion of dose rate to curies using the inverse square law is given in Column 8. The equation used for the conversion is

$$C_2 = \frac{RX^2}{5.64\ EN} \qquad (14)$$

where

X = distance of ion chamber from source

R = dose rate in R/hr

E = 1.25 Mev = the average energy of the Cobalt 60 photons

N = 2, the total number of Cobalt 60 photons per disintegration

5.64 = the inherent definition of the roentgen.

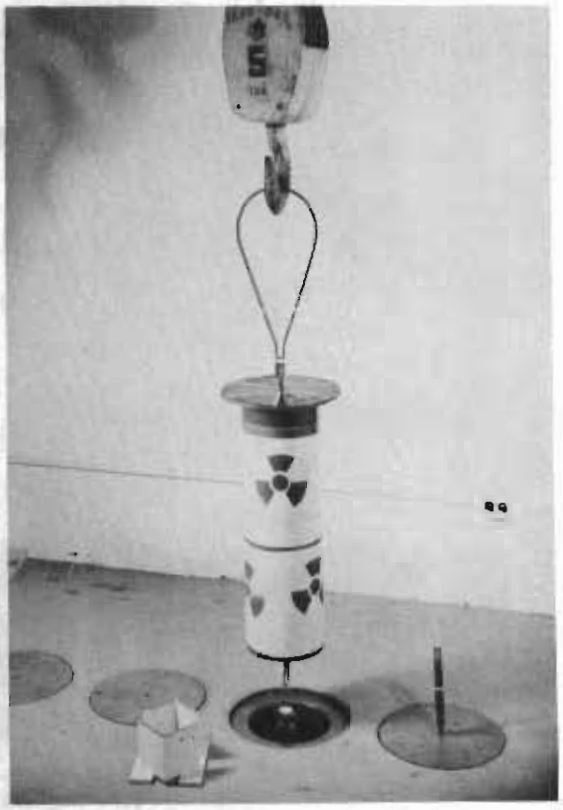

Figure 47. Storage of Reference Source

The constant contains the term 7.07×10^4 Mev/cm^3 of standard air which is based on a recent value of 34 ev of absorbed energy per ion pair as recommended by the International Commission for Radiological Units.

With the ionization chamber placed 1 foot from the Cobalt 60 slug, Equation (14) may then be written:

$$C_2 = 0.070796(R/hr) \qquad (15)$$

The activity per slug corrected for decay since shipment is given in Column 9. The decay correction factor was obtained from data given in Table L. The Cobalt 60 slugs from shipments 1, 2, 3 contained a total of 4900 slugs and were randomly placed in the source. An average decay period of 99 days was assumed for these shipments. The decay was calculated by the expression

$$C_D = C_e^{(+0.00035813)N} \qquad (16)$$

TABLE L

DECAY CORRECTION FOR COBALT 60 SOURCE AT TIME OF ASSAY

Order of Shipment	Date Shipped	Number of Slugs	Date Measured	Number of Days of Decay	Decay Correction e + (0.00035813) Days
4	9/13/57	1-350	9/19/57	6	1.002
	9/13/57	351-910	9/20/57	7	1.003
	9/13/57	911-1470	9/21/57	8	1.003
	9/13/57	1471-2030	9/22/57	9	1.003
	9/13/57	2031-2100	9/23/57	10	1.004
3	7/26/57	2100	9/23/57	99	1.035
2	6/11/57	1050	to	99	1.035
1	4/29/57	1750	9/26/57	99	1.035

N = number of days decay

0.00035813 = the decay constant for Cobalt 60.

Column 10 contains the corrected term to obtain a curie value in open air. This correction was made by comparing the curie value of slug No. 6790 in open air and then in the assay assembly. Table LI shows the curie value of slug No. 6790 at various distances in open air from the ionization chamber. The average curie value for slug No. 6790, as determined in the lead chamber, was 11.14. The correction factor for the assay in open air is

$$C_4 = C_3 \frac{8.43}{11.14} = C_3 (0.758)$$

On summing the curie values of the 95 slugs in Column 10, one obtained a total activity of 707.97 curies. Thus, the average activity per slug is 7.45 curies. Therefore, for the 7000 slugs, the total value is 52,150

TABLE LI

THE CURIE VALUE OF SLUG NO. 6790 IN OPEN AIR

Distance (ft)	Current (amps x 10^{11})	Dose-Rate (R/hr)*	Dose-Rate** $(R/hr)_C$	Curies	Curies*** (Decay Corrected)	Deviation (from mean)
0.5	24.7	482	468.9	8.29	8.44	0.01
1.0	6.0	117	113.8	8.05	8.20	0.23
2.0	1.63	31.8	30.9	8.75	8.91	0.48
4.0	0.375	7.32	7.1	8.01	8.18	0.25
					Av. 8.43	±0.24

*1R ≑ 87.1 ergs/gmC

**$(R/hr)_C = (R/hr) \frac{29.29}{29.06} \frac{T}{295}$

$= (R/hr)\ (0.973)$

*** Decay factor for 48 days

$$C_D = C_e^{+(0.00035813)\ 48}$$

$= C \times 1.018$

curies. The limits of error were then determined as follows.

The standard deviation, σ, is

$$\sigma = \left[\frac{\sum_{i=1}^{95} (Xi - \bar{X})^2}{95-1} \right]^{\frac{1}{2}}$$

where Xi is the curie value of the i th unit and $\bar{X}$ is the mean value. The

quantity $\sum_{i=1}^{95} (Xi - \bar{X})^2$ in the above equation may be expressed as

$$\sum_{i=1}^{95} (Xi - \bar{X})^2 = \sum_{i=1}^{95} Xi^2 - \frac{\left(\sum_{i=1}^{95} Xi\right)^2}{95}$$

Upon calculation of these quantities one obtains

$$\sum_{i=1}^{95} (Xi - \bar{X})^2 = 5,654.73 - \frac{(707.97)^2}{95}$$

or

$$\sum_{i=1}^{95} (Xi - \bar{X})^2 = 378.71$$

and thus, the standard deviation becomes

$$\sigma = 2.007$$

The standard error of the mean, σ_X, was estimated to be

$$\sigma_X = \frac{\sigma}{\sqrt{95}} = \frac{2.007}{\sqrt{95}} = 0.206$$

Further, with 95 percent probability, it may be asserted that the true mean is

$$\bar{X} \pm \frac{2\sigma}{\sqrt{95}} = 7.45 \pm 0.41$$

Thus, the value of 7.45 curies is the true mean with a 95 percent probability of not being in error more than ± 5.5 percent. Table LII summarizes the placement of the 7000 Cobalt slugs and the curie values associated with them.

E. Isodose Plots for the Operational Inland Testing Laboratories Cobalt 60 Facility

When the loading of the source container was completed, it was necessary to accurately determine the radiation dose rates of the source, and also the dose rates at various operational locations within the empty Inland Testing Laboratories irradiation facility.

Data were gathered and plotted to obtain an isodose reference of the empty Cobalt 60 source. This isodose reference, which determines radiation dose rates for the irradiation of materials, was also used to check the source configuration calculations discussed in Section B of this Appendix.

TABLE LII

TOTAL ACTIVITY OF THE COBALT 60 SOURCE

Number of Slugs	Total Activity Curies
7000	52,150
6686*	49,810.7
314**	2,339.3

*The number of slugs in the Nucledyne operational source container.

**The number of slugs excess and reserved in the auxiliary container.

Isodose Plots

To obtain an isodose plot, distances were accurately measured in 1 foot intervals from the center of the source cylinder to the walls of the cell. Ion chamber measurements were recorded at each point marked on the cell floor plan and at elevation levels from the floor up to 8-3/4 feet in intervals of 1 foot (Figures 48 and 49). The ion chamber was located at each position by careful use of the cave crane. Ionization chamber currents were read with the Kiethley 410 micromicroammeter and were then converted to roentgen per hour. To obtain accurate isodose plots of the dose rate data, two separate references plots were prepared considering dose rates for lines of constant height from the floor, Figure 49, and lines of constant vertical distance from the source. These two plots were then used to prepare isodose plots of the source at the vertical front and side midplane positions. This method of plotting permits preparation of a three-dimensional isodose plot for every square foot of the irradiation cell around the source, Figure 50.

The isodose plots presented in Figure 49 were obtained in the Cobalt 60 radiation facility before placement of any machinery in the cell. The placement of heavy machinery in the cell can alter the isodose plots due to the absorption effect of metallic parts and shielding material. To determine the general effects of heavy machinery on the isodose plots, dose rate measurements were made at several points before and after installation of the Erdco

Figure 48. Isodose Measurement - Inside Cell View

metal in the Erdco Tester. The general effect of introducing the Erdco Universal tester in the radiation facility was, however, to decrease the dose rate.

From the isodose plots of the Inland Testing Laboratories Cobalt 60 source, the dose rate varies from 0.02 megaroentgen at 8 feet from the source to 1.1 megaroentgens at a point 2 inches from the inside source wall at the midplane. The highest dose rate detected outside the source cylinder is 0.61 megaroentgen at a point 1 inch from the outside wall.

Universal Tester, Figure 51. The measurements at these points are shown in Table LIII. From these values it can be seen that the dose rate values from the isodose lots are valid only to about 1 foot from the outside of the source container, and that beyond that point supplementary dosimetry is necessary to determine the exact dose rate.

It is of interest to note that at points near the Erdco the dose rates were increased by the placement of the Tester. This is explained by considering the scattering produced by

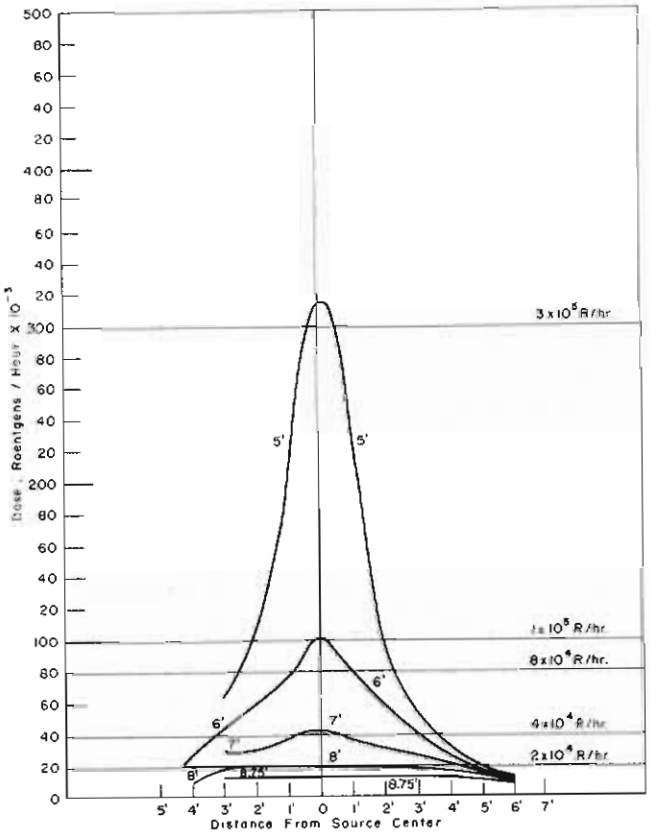

Figure 49. Isodose Lines of Constant Height - Cobalt 60 Source

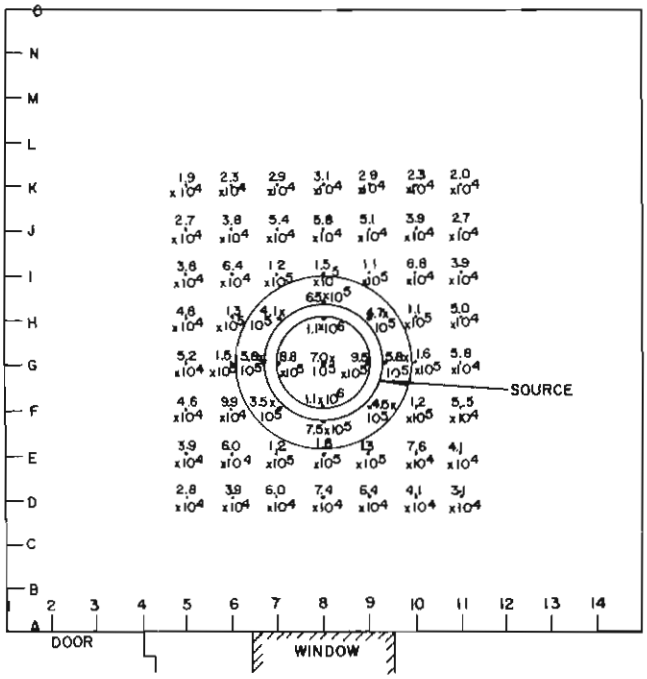

Each Ordinate Unit is Equal to One Foot
Date of Measurement—October 31, 1957

Figure 50. Source Dose Points at Four Foot Level

In order to obtain the highest dose rate possible for static material irradiation, an aluminum platform insert, Figure 52, was designed for use with the source. Materials located on this platform insert receive a radiation dose of no less than 0.7 megaroentgen and as high as 1.1 megaroentgens for materials located close to the inside source cylinder. Further, the platform insert in no way impairs the outside working space around the source. The accurate dimensions of the Cobalt 60 source and supporting equipment are shown in Figure 52.

E. Radiation Intensity on Test Rigs

The physical size of the Inland Testing Cobalt 60 facility, as described in Appendix I, permits the simultaneous operation of several test rigs, Figure 53. The dose rates on the various components of the test sections for the test rigs were determined, where feasible, with the graphite CO_2 ionization chamber. Ferric-ferrous chemical dosimetry was used where the size of the ion chamber prevented its use. When chemical dosimetry was used, the validity of the results was determined by comparison of several chemical dosimetry values with ion chamber values.

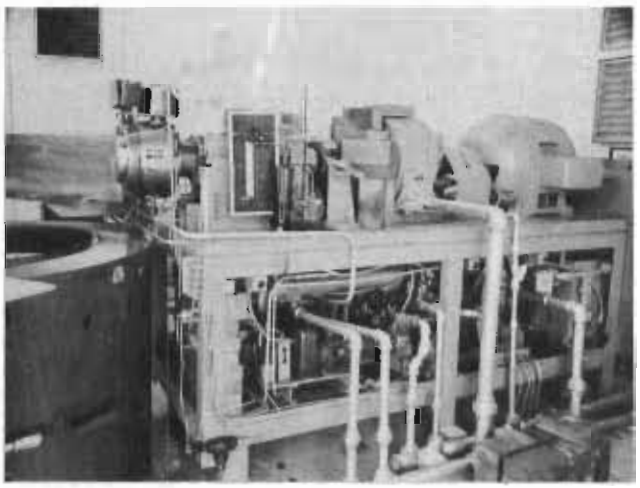

Figure 51. ERDCO Universal Tester - Modified WADC High Temperature Bearing Head in Radiation Cell

TABLE LIII

ISODOSE CHECK POINTS (BEFORE AND AFTER INSTALLATION OF ERDCO UNIVERSAL TESTER)

Check Point*	Height ft	Dose Rate Before Erdco Installation R/hr	Before Erdco Installation erg/gmC/hr	After Erdco Installation R/hr	After Erdco Installation ergs/gmC/hr
G-10	4	1.60×10^5	1.39×10^7	1.72×10^5	1.50×10^7
I-13	3	1.60×10^5	1.39×10^7	1.22×10^5	1.06×10^7
E-8	3	1.32×10^5	1.15×10^7	1.78×10^5	1.55×10^7
I-8	3	9.90×10^4	8.62×10^6	1.50×10^5	1.31×10^7
I-5	3	3.40×10^4	2.96×10^6	2.52×10^4	2.19×10^6
I-5	4	3.75×10^4	3.27×10^6	3.15×10^4	2.74×10^6
M-5	3	1.10×10^4	9.58×10^5	5.25×10^3	4.57×10^5
M-10	3	1.20×10^4	1.04×10^5	4.75×10^2	4.14×10^4
M-10	4	1.25×10^4	1.09×10^5	3.10×10^3	2.70×10^5

*Points are as indicated in Figure 50. Center of Erdco is approximately at J-11.

The modifications of the test rigs for dynamic testing of fuels and lubricants in the Inland Testing Laboratories Cobalt 60 cell are discussed in Appendix IV.

1. CFR Fuel Coker

The CFR Fuel Coker evaluates the thermal stability of gas turbine engine fuels. The fuel coker was modified to place the test section consisting of the pump, preheater filter assembly, and manometer in a radiation area, see Figure 16. The pump and motor are shielded by lead bricks to increase operational life in a radiation environment.

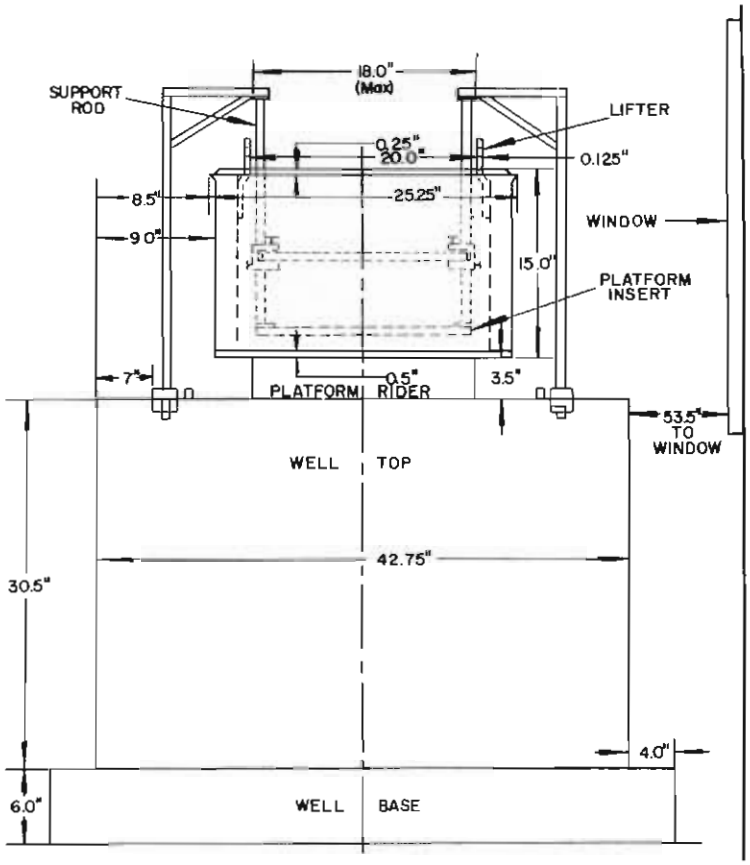

Figure 52. Cobalt 60 Source and Support Equipment

The manometer, preheater, and filter were placed on a jig board for portability. The preheater tube is positioned 4 inches above the base of the source container and the middle of the tube is 1 inch from the source, while the lateral ends of the tube are approximately 4 inches from the source container. The dose rates on the test section components are given in Table LIV.

The fuel reservoir tank was constructed in the form of an arc of a hollow cylinder 14 inches high. The front face of the reservoir is about 1 inch from the face of the source container. Ferric-ferrous chemical dosimetry was conducted on the front and rear face of the reservoir, and ion chamber measurements were made in the center of the tank. The dose rates on the CFR Fuel Coker reservoir are given in Table LV.

The dose rate value for the CFR Fuel Coker preheater tube was obtained by averaging the center and the lateral dose rate values. Due to the

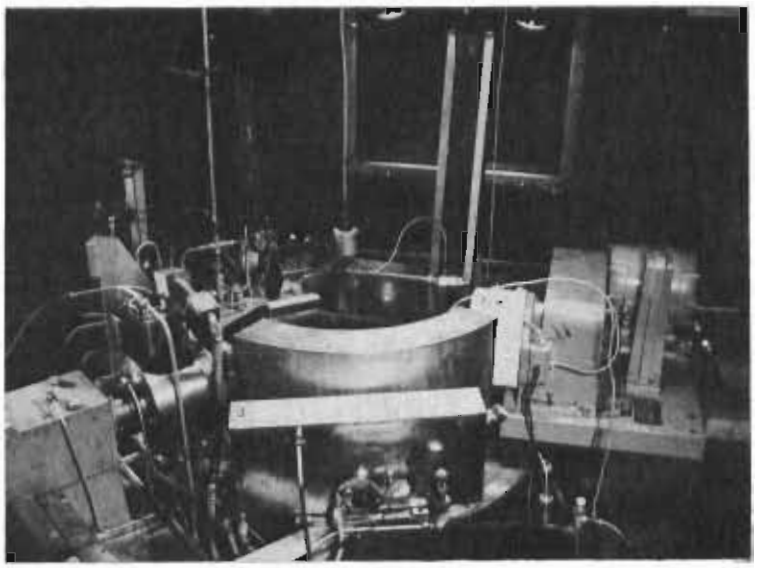

Figure 53. Test Rigs in Radiation Cell

TABLE LIV

DOSE RATES ON COMPONENTS OF THE CFR FUEL COKER

Component	R/hr	Ergs/gmC/hr
Filter furnace	3.41×10^5	2.97×10^7
Center preheater tube	5.02×10^5	4.37×10^7
Left lateral preheater tube	4.42×10^5	3.85×10^7
Right lateral preheater tube	4.43×10^5	3.85×10^7

TABLE LV

DOSE RATES ON THE CFR FUEL COKER RESERVOIR

Position*	R/hr	Ergs/gmC/hr
Front face	4.98×10^5	4.34×10^7
Front face	5.04×10^5	4.39×10^7
Front face	5.91×10^5	5.15×10^7
Center	3.6×10^5	3.13×10^7
Center	4.15×10^5	3.61×10^7
Center	4.2×10^5	3.65×10^7
Center	4.4×10^5	3.83×10^7
Center	4.4×10^5	3.83×10^7
Center	4.3×10^5	3.75×10^7
Center	3.6×10^5	3.14×10^7
Rear face	2.97×10^5	2.59×10^7
Rear face	2.99×10^5	2.60×10^7
Rear face	3.0×10^5	2.61×10^7

*Readings taken from left to right in equal length increments

geometry of the tube and its relationship to the source, the use of the universe square law could not validly be applied. The average dose rate valve for the preheater tube was 4.66×10^5 R/hr or 4.05×10^7 ergs/gmC/hr.

The dose rate value for the reservoir was obtained by the average of dose rate values obtained on the front face, rear face, and the middle of the tank. The inverse square law could not be validly applied, and it was assumed that an arithmetic average would closely approximate the true dose rate value. The dose rate on the reservoir tank was calculated to be 4.12×10^5 R/hr or 3.59×10^7 ergs/gm/C/M.

2. WADC Deposition Tester

The deposition tester determines the solid deposit and sludge forming tendencies of lubricating oils in contact with high temperature metal surfaces in the presence of humidified air. The modification of the WADC Deposition Tester for dynamic testing in a radiation environment is discussed in Appendix IV. Ferric-ferrous chemical dosimetry was used to determine the dose rates on the components mounted on the test section rack. The dose rates on the components mounted on the test section rack are given in Table LVI.

TABLE LVI

DOSE RATES ON COMPONENTS OF THE WADC DEPOSITION TESTER

Position or Component	R/hr	Ergs/gmC/hr
Middle Coking Tube	2.77×10^5	2.41×10^7
Bottom of Test Filter	2.27×10^5	1.98×10^7
Bypass Valve	5.69×10^5	4.96×10^7
Bottom of Pressure Relief Bypass Valve	5.20×10^5	4.53×10^7
Outlet End of Oil Cooler	1.44×10^5	1.25×10^7
Inlet End of Oil Cooler	1.93×10^5	1.68×10^7
Oil in Thermocouple Cross	2.64×10^5	2.30×10^7
Top Coking Tube	2.17×10^5	1.89×10^7
Bottom Oil Feeder	1.23×10^5	1.07×10^7
Top Reservoir	7.54×10^4	6.56×10^6

The dose rate values on the coking tube in the WADC deposition tester was calculated to be 2.76×10^5 R/hr or 2.40×10^7 ergs/gmC/hr. This value was obtained by taking the arithmetic average of dose rate values at points on the surface of the coking tube. For example, dose rate values were obtained for the two lateral sides of the midplane of the tube. The values obtained were 2.78×10^5 R/hr (2.42×10^7 ergs/gmC/hr and 2.76×10^5 R/hr (2.40×10^7 ergs/gmC/hr). The average gives a representative dose rate value for the midplane of the coking tube.

3. Model C Panel Coker

The model C Panel Coker evaluates the tendencies of lubricating oils to form solid decomposition products when in contact with a hot metal surface. For radiation testing, the unmodified test rig was raised about 4 inches to make the mounting plate level with the base of the source container, Figure 20. Ferric-ferrous chemical dosimetry was used to determine the dose rate on the test rig and the values are given in Table LVII.

TABLE LVII

DOSE RATES ON THE MODEL C PANEL COKER

Position	R/hr	Ergs/gmC/hr
Top cover	1.44×10^5	1.25×10^7
Front face oil sump	4.14×10^5	3.61×10^7
Left face oil sump	2.86×10^5	2.49×10^7
Right face oil sump	2.41×10^5	2.10×10^7
Reservoir (500 cc level)	7.88×10^4	6.86×10^6

The dose rate value for the Model C Panel Coker sump was obtained by taking the arithmetical average of the dose rate values obtained on the circumference of the oil sump. This value was 2.74×10^5 R/hr (2.38×10^7 ergs/gmC/hr).

4. CRC Grease Tester

The modified CRC Grease Tester is mounted on a wheeled table for portability as described in Appendix IV. During tests the face covering of the oven is about 1 inch from the face of the source container, Figure 23. For dosimetry measurements the oven covering was visually divided into eight quadrants and the dose rates determined at the periphery of each quadrant for the face and also the rear of the oven covering.

The dose rates recorded are given in Table LVIII.

TABLE LVIII

DOSE RATES ON COMPONENTS OF THE CRC GREASE TESTER

Position* (degrees)	Face of Oven Cover		Rear of Oven Cover	
	R/hr	Ergs/gmC/hr	R/hr	Ergs/gmC/hr
0	3.18×10^5	2.77×10^7	1.36×10^5	1.18×10^7
45	4.98×10^5	4.34×10^7	1.72	1.50
90	5.02×10^5	4.37×10^7	1.93	1.68
135	5.69×10^5	4.96×10^7	2.14	1.86
180	5.58×10^5	4.86×10^7	2.34	2.04
225	4.87×10^5	4.24×10^7	1.99	1.73
270	4.28×10^5	3.73×10^7	1.87	1.63
315	3.87×10^5	3.37×10^7	1.53	1.33

*Angular measurement starting at 12:00 o'clock.

The estimated average dose rate on the bearing is 3.27×10^5 R/hr (2.85×10^7 ergs/gmC/hr). This was obtained by averaging the dose rates at the front and the rear face of the oven cover. With the test bearing positioned 2-1/2 inches from the face covering of the

oven, the dose rate on the bearing was estimated by linear interpolation between the face and rear oven cover values. The interpolation was necessitated since calculations using the inverse square law indicated high absorbence in the oven.

5. Erdco Universal Tester

The Ryder Gear Wear Head on the Erdco Universal Tester was modified for dynamic testing of oils in a radiation environment as discussed in Appendix IV. The reservoir was placed on a permanent stand as shown in Figure 51. The front face of the reservoir is approximately 6 inches from the face of the source container, and the bottom of the reservoir is level with the bottom of the source container.

Ferrous-ferric chemical dosimetry measurements were made on the front and rear face of the reservoir. The results are given in Table LIX.

TABLE LIX

DOSE RATES ON THE ERDCO UNIVERSAL TESTER RESERVOIR

Front Face		Rear Face	
R/hr	Ergs/gmC/hr	R/hr	Ergs/gmC/hr
2.43×10^5	2.12×10^7	1.29×10^5	1.12×10^7
3.24×10^5	2.82×10^7	1.55×10^5	1.35×10^7
2.60×10^5	2.26×10^7	1.16×10^5	1.01×10^7

The WADC Bearing Head with the Erdco Universal Tester is used to evaluate the performance and suitability of lubricating oils intended for bearing lubrication in gas turbine engine application. Dose rates on the periphery of the bearing and in the center of the bearing shaft were determined by ferric-ferrous chemical dosimetry. The results are given in Table LX.

The estimated average dose rate on the Erdco reservoir was obtained by linear interpolation of dose rate values obtained on the surface of the reservoir. Since the inverse square law could not be validly applied, the

TABLE LX

DOSE RATES ON COMPONENTS OF THE WADC BEARING HEAD

Position* (degrees).	R/hr	Ergs/gmC/hr
0	2.68×10^5	2.33×10^7
90	2.86×10^5	2.49×10^7
180	3.24×10^5	2.82×10^7
360	2.77×10^5	2.41×10^7
Center	2.44×10^5	2.13×10^7

*Angular measurement starting at 12:00 o'clock.

value was interpolated to be 2.04×10^5 R/hr (1.78×10^7 ergs/gmC/hr).

The estimated dose rate value on the bearing is 2.67×10^5 R/hr (2.33×10^7 ergs/gmC/hr). This was obtained by linear interpolation of the dose rate values obtained for the circumference of the bearing and the value obtained for the center of the bearing shaft. The use of the inverse square law indicated high absorbence and could not validly be used.

APPENDIX VII

DERIVATION AND ANALYSIS OF THE $\frac{dR}{dt}$ FUNCTION*

A clearer understanding of the behavior of fuels in the CFR Fuel Coker under radiation stress can be obtained by calculation of the rate of decomposition. This rate of decomposition must be related to the filter plugging rate, which, in turn, is related to the filter pressure.

The CFR Fuel Coker is a once-through flow system, in which the primary test parameter is the pressure drop across a filter. This pressure drop varies during the test as a result of filter plugging.

For purposes of this discussion, the filter may be considered as the sum of many small capillaries, such that it can be represented by one equivalent capillary of a size producing the same pressure drop as the filter. Since the flow rate through the coker is slow (of the order of 0.5 cc/sec), ideal flow may be assumed.

Accepting these assumptions, one may write the Hagen-Poiseuille equation as

$$v = \frac{\pi r^4}{8\eta} \frac{\Delta P}{l} \qquad (1)$$

where v is the flow rate in cc/sec, r is the radius of the equivalent capillary in cm, l is the length of the equivalent capillary in cm, ΔP is the pressure drop across the capillary in dynes/cm^2, and η is the viscosity of the liquid (fuel) in poises.

A fuel flow rate through the coker is approximately constant throughout the run. Furthermore, the fuel viscosity does not change appreciably.

Accepting a constant fuel flow and viscosity, one may write the relation

---

*This derivation is to assess radiation effects only and is not presented as a new parameter for the CFR Fuel Coker.

$$\frac{\Delta P_i}{\Delta P_o} = \left(\frac{r_o}{r_i}\right)^4 \qquad (2)$$

where the subscript o refers to the conditions at the time "conditions set" are reached, i.e., zero time, and the subscript i refers to conditions after time t.

We may now define a function

$$R = \frac{r_o}{r_i} = \left(\frac{\Delta P_i}{\Delta P_o}\right)^{1/4} \qquad (3)$$

Furthermore, it may be stated

$$r = \text{function (total coke formed)} \qquad (4)$$

Hence, a plot of the function "R" vs. time will yield a slope, $\left(\frac{dR}{dt}\right)$ which shall be assumed to represent the decomposition rate of the fuel. Typical plots of R and $\left(\frac{dR}{dt}\right)$ are shown in Figures 54 and 55. The arrows on the

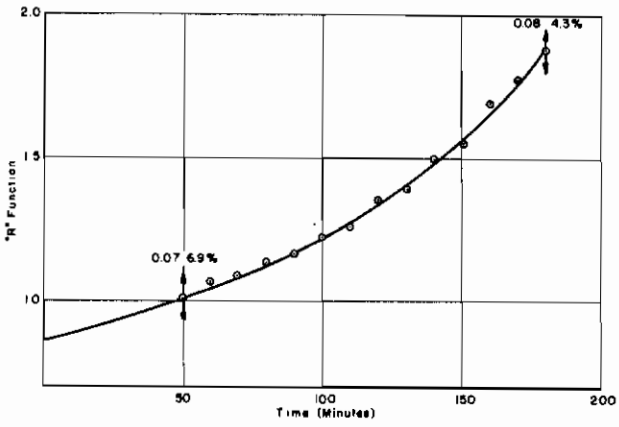

Figure 54. Decomposition Rate of ANPF 57-60 (Irradiated) in the CFR Fuel Coker

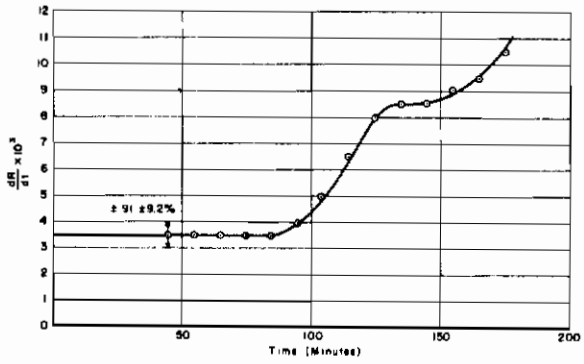

Figure 55. Change in Decomposition Rate of ANPF 57-60 (Irradiated) in the CFR Fuel Coker

curves represent the accuracy of the experimental points. For the R function, a variation of ±7 percent is experimentally observed. The $\left(\frac{dR}{dt}\right)$ function varies by ±10 percent. The repeatability of the R and $\left(\frac{dR}{dt}\right)$ functions cannot be assessed at this time because of the lack of data.

A more rigorous treatment of the R and $\left(\frac{dR}{dt}\right)$ functions is now under consideration.

An increasing $\left(\frac{dR}{dt}\right)$ function may be due to one or both of the following effects. The fuel decomposition products may act as catalysts for further fuel decomposition. The deposition of decomposition products on surfaces may increase the size of the surfaces sufficiently to increase the rate of surface catalyzed decompositions.

A decreasing $\left(\frac{dR}{dt}\right)$ function may be explained by one or more of the following phenomena. Coating of the surfaces in the system may result in lower fuel exposure temperatures, even though the metal system components are still at the set values. Generally, this would result in lower reaction rates. In addition, this coating may also block out a catalytic metal surface, thus again reducing the decomposition rate. Decomposition products may occur that will tend to inhibit further fuel breakdown. Coating of the metal surfaces may reduce the capillary cross section to the point where turbulence may ensue, which, in turn, will affect $\left(\frac{dR}{dt}\right)$.

Fuels can be rated according to $\left(\frac{dR}{dt}\right)_o$ values as follows: Group I contains stable fuels with $\left(\frac{dR}{dt}\right)_o$ values between 0 and 1; Group II contains acceptable fuels that are less stable than those in Group I and which have $\left(\frac{dR}{dt}\right)_o$ values between 1 and 2; Group III contains fuels of borderline stability with $\left(\frac{dR}{dt}\right)_o$ values between 2 and 7; Group IV contains unstable fuels with $\left(\frac{dR}{dt}\right)_o$ values greater than 7. Reference to Figure 56 shows that Group I fuels have "goodness" ratings above 700, and Group II fuels have "goodness" ratings from 400 to 800. Group III fuels have "goodness" ratings no greater than 600, and Group IV fuels have "goodness" ratings below 400.

The value of $\left(\frac{dR}{dt}\right)_o$ can be assessed in 1 hour or less by calculating the ratio $\left(\frac{\Delta P}{\Delta P_o}\right)^{1/4}$ and dividing by the time required to reach ΔP.

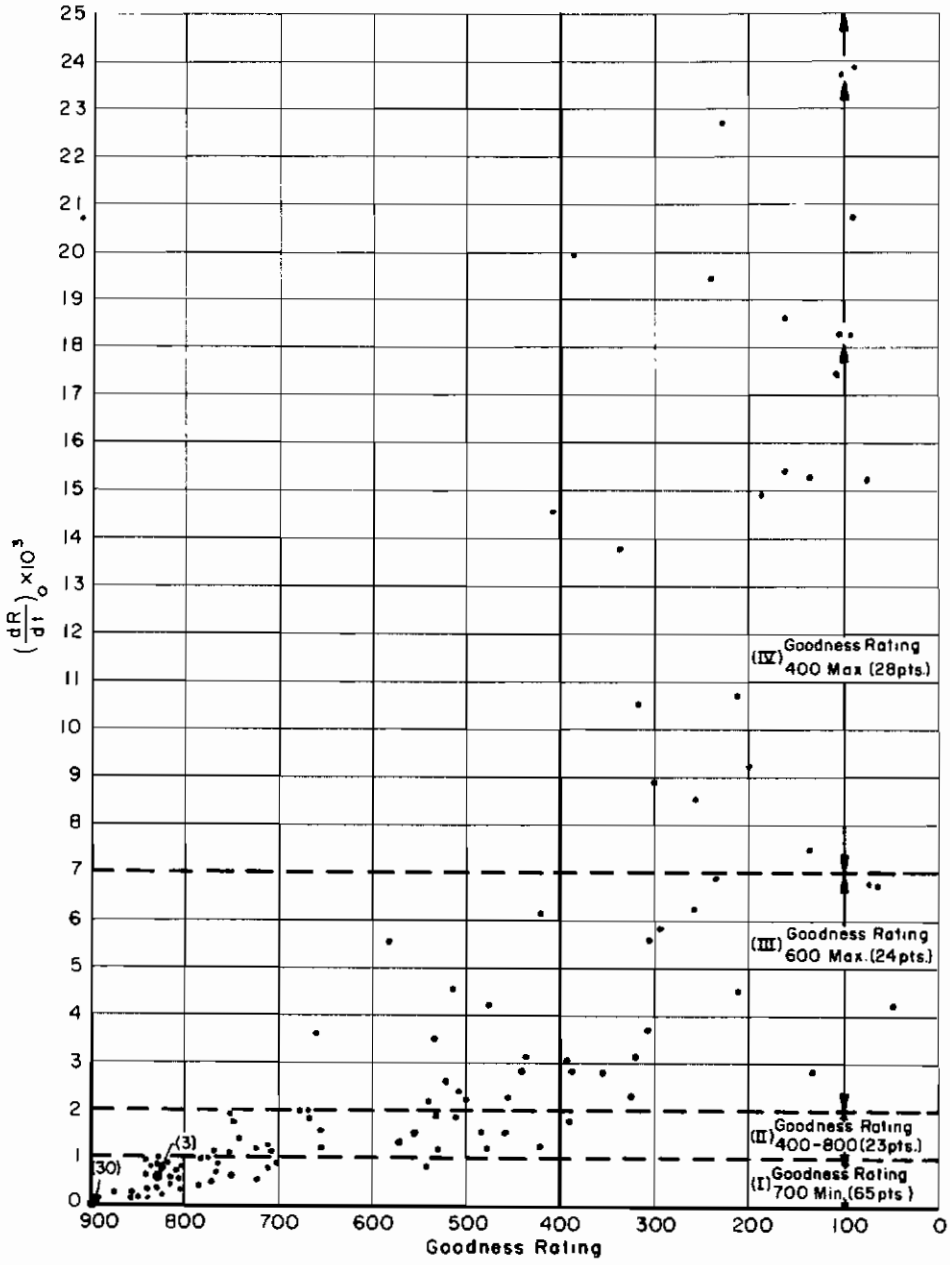

Figure 56. Correlation of $\frac{dR}{dt}_o$ with Goodness Rating

It is essential that ΔP_o, the value of ΔP at "conditions set", be a value other than zero. For experimental runs where $\Delta P_o = 0.0$, a value of ΔP observed within the first 20 minutes may be used as ΔP_o, provided no pressure surges have occurred in the interim.

APPENDIX VIII

HEAT OF FORMATION OF COKE IN THE MODEL C PANEL COKER

To further assess the magnitude of different effects occurring during lubricant breakdown, the following method is presented.

Consider the following reaction

$$C_1 + C_2 \ldots k \text{ coke} \tag{1}$$

Where C_1, C_2, . . . are the concentrations of the various components producing coke.

The kinetic equation for the reaction can be written as

$$\frac{d\left[\text{coke}\right]}{dt} = k \prod_{i=o}^{i=n} C_i^{m_i} \tag{2}$$

Where $\left[\text{coke}\right]$ is the coke formation per ml of oil consumption,

k is the rate constant for the reaction at a given temperature,

C_i is the i^{th} reactant, and

m_i is the order of i^{th} component.

For a finite period of time (8 hours), the reaction may be written as

$$\frac{\Delta\left[\text{Coke}\right]}{\Delta t} = k \prod_{i=o}^{i=n} C_i^{m_i} \tag{3}$$

Taking the log of both sides, one obtains

$$\ln \frac{\Delta\left[\text{Coke}\right]}{\Delta t} = \ln k + \sum_{i=o}^{n} \ln C_i^{m_i} \tag{4}$$

From Arrhenius equation, one has

$$\ln k = - \frac{\Delta H}{RT} + A \tag{5}$$

where

ΔH is the heat of formation,

T is the absolute temperature, and

R and A are constants

Substituting Equation (5) into (4), one obtains

$$\ln \frac{\Delta [\text{Coke}]}{\Delta t} = - \frac{\Delta H}{RT} + A + \sum_{i=o}^{n} \ln C_i^{m_i} \tag{6}$$

or

$$\ln \Delta [\text{Coke}] = - \frac{\Delta H}{RT} + \text{constant} \tag{7}$$

A plot of $\ln \Delta [\text{Coke}]$ vs. $\frac{1}{T}$ should yield a straight line with slope = $- \frac{\Delta H}{R}$

REFERENCES

1. Abele, R K., High Level in Ion Chamber Details, Oak Ridge National Laboratories, Instrumentation and Controls Division, Drawing No. Q-1822-2, September 20, 1956.

2. American Institute of Physics Handbook, McGraw-Hill Book Co., 1957, New York, N.Y., pp 8, 39-40.

3. Atkins, M.C., Design and Use of a 23,000 Curie Cobalt 60 Source for Material Testing, WADC, WCRT TM 56-159, Appendix A.

4. Ballweg, L. H. and Meem, J. L., A Standard Gamma-Ray Ionization Chamber for Shielding Measurements, ORNL 1028, 1951.

5. Beckerley, J. G., Kamen, M.D., and Schiff, L. I., Ann. Rev. Nuclear Science, 5, 221 (1955).

6. Bolt, R.O. and Carroll, J.G., Effects of Radiation on Aircraft Lubricants and Fuels, WADC TR 56-646 Part II, January 31, 1958

7. Charlesby, A., "The Cross-Linking and Degradation of Paraffin Chains by High Energy Radiation", Proc. Roy. Soc., A222, 60 (1954).

8. Collinson, E. and Swallow, A. J., "The Radiation Chemistry of Organic Substances", Chem. Reviews, 55, 477 (1956).

9. Cosgrove, S.L., The Effect of Nuclear Radiation on Lubricants and Hydraulic Fluids REIC Report No. 4, ASTIA AD 154432, April 30, 1958.

10. Davisson, C.M. and Evans, R.D. "Gamma-Ray Absorption Coefficients," Rev. Mod. Phys., 24, 79-107 (1952).

REFERENCES (Cont'd)

11. Droegemueller, E. A. and Clark, John R., Dynamic Gamma-Radiation Effects of Hydrocarbon Fluids Under Thermal, Oxidative, and Mechanical Stress, Vol. IV, Proceedings of the Second Semiannual 125A Radiation Effects Symposium, October 22-23, 1957.

12. Fainman, M. Z. The Behavior of Fuels and Lubricants Under Dynamic Conditions in the Presence of Gamma Radiation, Vol. IV, Proceedings of the Second Semiannual 125A Radiation Effects Symposium, October 22-23, 1957.

13. Hine, G. J. and Brownell, G. L., Radiation Dosimetry, 1956, Academic Press, 25.

14. Kinderman, E. M., Effects of High Energy, High Intensity Electromagnetic Radiation on Organic Liquids, WADC TR 57-465, July 1957.

15. King, J. A. and Rice, W. L. R., The Effect of Nuclear Radiation on Lubricants, ASME-ASLE Lubrication Conference, Atlantic City, N. J., 25, 1956.

16. Krasnow, M. E., Reynolds, O. P., Thistlethwaite, R. L., Vilter, E: J., White, H. G. R., and Mitchell, R. A., Determination of Testing Schemes for ANP Weapon System Materiel, WADC TN 57-185, ASTIA AD 118288, May 1957.

17. Ku, P. M., Aviation Gas Turbine Lubricant Research and Test Method Development, SWRI Report No. AvD 214, November 27, 1956.

18. Ku, P. M. and Johnston, R. K., Aviation Gas Turbine Lubricant Research and Test Method Development, SWRI Report No. AvD 275, September 30, 1957.

19. Mahoney, C. L., Kerlin, W. W., Barnum, E. R., and Sax, K. J., Engine Oil Development, WADC TR 57-177, ASTIA AD 130925, July 1957.

20. Matuszak, A. H., Nuclear Radiation Resistant Turbine Engine Lubricants, WADC TR 57-255, ASTIA AD 131065, September 1957.

21. Neeley, R. J., Variation in Results of Dynamically and Statically Irradiated Aircraft Fluids, Vol. IV, Proceedings of the Second Semiannual 125A Radiation Effects Symposium, October 22-23, 1957.

22. Nixon, A. C., Thorpe, R.E., Minor, H.B., and Lusebrink, T.R., Research on Determination of the Stability of Jet Engine Fuels, WADC TR 53-63, Part IV, January 1958.

23. Perkins, J. F., "Monte Carlo Calculations of Gamma-Ray Albedos of Concrete and Aluminum," J. App. Phys., 26, 655-8 (1955).

24. Rice, W.L.R., Nuclear Radiation Resistant Lubricants, WADC TR57-299, ASTIA AD 118329, May 1957.

25. Rockwell, T., Reactor Shielding Design Manual, 1956: C. Van Nostrand Co. Princeton, N.J., 394.

26. Sisman, O, The Problem of Establishing Specifications for Irradiated Organic Materials, Oak Ridge National Laboratory, Paper No. 198, 1956.

27. Stephenson, R., Introduction to Nuclear Engineering, 1954, McGraw-Hill Book Co., New York, N.Y.

28. Wright Air Development Center, Detailed Handbook on Test Procedures in Support of Turbojet and Turboprop Lubricants WADC, March 1957.